# Are Bering Sea canyons unique habitats within the eastern Bering Sea?

Michael F. Sigler, Christopher N. Rooper, Gerald R. Hoff, Robert P. Stone, Robert A. McConnaughey and Thomas K. Wilderbuer

## Abstract

Some of the largest submarine canyons in the world incise the eastern Bering Sea shelf break, including Bering, Pribilof, Zhemchug, Pervenets and Navarin canyons. In 2012, the North Pacific Fishery Management Council (NPFMC) received testimony from environmental organizations to protect coral, sponge and other benthic habitat of fish and crab species in two of these canyons (Pribilof and Zhemchug). In response to this testimony, the NPFMC requested that the NOAA Alaska Fisheries Science Center analyze the distribution of fishes and benthic invertebrates and the vulnerability of their habitat to fishing activities. We compiled data from the eastern Bering Sea that included trawl survey data on fish and invertebrate distributions and observations of ocean conditions and benthic habitat. These data were analyzed using multivariate techniques to determine if the two canyons are distinguishable from the adjacent continental slope. The potential for fishing effects on coral and sponge was assessed with spatial modeling of historical fishing effort, coral and sponge distributions and an index of their vulnerability to physical damage. Pribilof and Zhemchug canyons do show some distinguishing physical characteristics from the adjacent slope such as lower oxygen and pH and higher turbidity, but none based on biological characteristics (i.e., fish, coral and sponge distributions). These analyses imply that Pribilof and Zhemchug canyons are not biologically unique. Instead the major variables structuring the communities of fish and invertebrates on the eastern Bering Sea slope appear to be depth and latitude rather than submarine canyons. Corals were predicted to occur predominantly along the eastern Bering Sea slope, whereas sea whips were predicted to occur predominantly along the outer continental shelf. Sponges were mixed, with about two-

thirds of their habitat predicted for the outer shelf and the remainder for the slope. One unique feature of the focal canyons is that about one third of the coral habitat predicted for the eastern Bering Sea slope occurs in Pribilof Canyon, an area that comprises only about 10% of the total slope area. Although apparently concentrated there, the average density of coral for Pribilof Canyon (0.28 colonies $m^{-2}$) is much less than the density for the Aleutian Islands (1.23 colonies $m^{-2}$). The physical and biological characteristics of Zhemchug and Pribilof canyons are spatially heterogeneous; coral habitat was more common in some sections of Pribilof Canyon. Higher vulnerability indices were found both within and between canyons and were not unique to Pribilof and Zhemchug canyons. Pelagic trawl, longline and pot gear but not bottom trawl gear overlapped some coral and sponge habitats of the slope including canyons. Substantial overlap does not explain whether effects of fishing were light, medium or high, just that effects likely were greater in overlap areas compared to other areas. Further, the effect for the pelagic trawl fishery will depend on how often and where fishing occurs on bottom.

# Introduction

In 2012, the North Pacific Fishery Management Council (NPFMC) received testimony from environmental organizations for management measures to provide Essential Fish Habitat (EFH) protection to coral, sponge and other benthic habitat of fish and crab species for two of the largest eastern Bering Sea canyons (Pribilof and Zhemchug). Earlier testimony prompted a review of scientific information in 2006 (McConnaughey et al. 2006), which found that canyons are unique geological features but insufficient information was available to judge their importance as EFH. In this paper, we address a 2012 request by the NPFMC to the NOAA Alaska Fisheries Science Center to determine whether these two canyons (Pribilof and Zhemchug) provide unique coral and sponge habitats for managed fish species.

Some of the largest submarine canyons in the world incise the eastern Bering Sea shelf break (Karl et al. 1996, Normarck and Carlson 2003) including Bering, Pribilof, Zhemchug, Pervenets and Navarin canyons (Figure 1). All five canyons are large but their seafloor gradients and shapes differ. Navarin (total volume = 5,400 $km^3$), Pervenets (1,700 $km^3$) and Bering (4,300 $km^3$) canyons have lower seafloor gradients than Pribilof (1,300 $km^3$) and Zhemchug (5,800 $km^3$) canyons (Karl et al. 1996). Navarin and Pervenets canyons resemble gently sloping

amphitheaters; Zhemchug and Pribilof canyons are very elongate parallel to the shelf edge, rugged and steeper; Bering Canyon is V-shaped and gradually widens downslope (Karl et al. 1996). Two other large canyons, St. Matthew (740 $km^3$) and Middle (1,800 $km^3$), lie along the eastern Bering Sea outer shelf, but barely indent the shelf break (Karl et al. 1996). Roughly 20% of the shelf edge between Alaska and the Equator is interrupted by steep, narrow and abrupt submarine canyons (Hickey 1995). An estimated 290 submarine canyons are found along the western coast of North America and are spaced an average of 30-35 km apart (Harris and Whiteway 2011).

An along-slope current, the Bering Slope Current, flows northwest along the slope of the eastern Bering Sea (Stabeno et al. 1999) with moderate flow (2 to 18 cm $sec^{-1}$) following the bathymetry and existing primarily in the upper 300 m (Schumacher and Reed 1992). Eddies ranging in size from 40 to 150 km may be imbedded in the flow (Stabeno et al. 1999). Depending on their size and shape, canyons that indent the shelf break can interrupt along-slope currents and thus may create unique physical environments in canyons compared to the adjacent slope. Results from a model of Bering Sea physical oceanography indicate that deep-basin water is moved northward onto the eastern Bering Sea shelf by mesoscale processes along the shelf break; canyons along the shelf break appear to be more prone to eddy activity and, therefore, are associated with higher rates of on-shelf transport (Clement Kinney et al. 2009). Onshelf transport may occur virtually anywhere along the shelf break and preferential transport onto the shelf has been observed at Bering Canyon and west of the Pribilof Islands (Stabeno et al. 1999). The latter occurs as the outer shelf narrows south of St. George Island, accelerating the flow, which then turns northward, becomes shallower and parallels the 100-m contour west of the Pribilof Islands; some weak, northward transport also may occur east of the Pribilof Islands (Stabeno et al. 2008). Tidal motion and topography interact in the Pribilof Canyon where observations show enhancement of the diurnal tidal currents (Kowalik and Stabeno 1999). Other detailed physical oceanography studies of Bering Sea canyons are lacking, in part because measurements in submarine canyons are difficult to make (Hickey 1995); their availability for some other Pacific Coast canyons provide insights into processes that also may occur for Bering Sea canyons. In steep-sided (up to 45 degrees seafloor gradient) and narrow Astoria Canyon, estimated vertical velocities were as great as 50 m $d^{-1}$ (upward) during upwelling and 90 m $d^{-1}$ (downward) during wind relaxation following upwelling events; at depths up to 100 m above the canyon, a cyclonic

circulation pattern occurred, but above that the flow field was undisturbed by canyon topography (Hickey 1997). Sediment deposition rates were high (~60 g $m^{-2}$ $d^{-1}$) in the head of Quinault Canyon but were low (3-6 g $m^{-2}$ $d^{-1}$) elsewhere in the canyon and on the open slope (Baker and Hickey 1986).

Enhanced production often occurs at continental shelf margins like the eastern Bering Sea slope and outer shelf, which have been previously identified as an area of enhanced primary and secondary productivity (the "Bering Sea Greenbelt") (Springer et al. 1996). More recent oceanographic observations (Rho and Whitledge 2007) and estimates derived from satellite observations (Brown et al. 2011) imply that this area of enhanced primary production also includes the middle shelf in addition to the outer shelf and slope. Areas of further concentration may occur in the Bering Sea that are related to eddies. Earlier research found that these eddies transit parallel to the continental slope and are not tied to the canyons (Schumacher and Stabeno 1994). However recent research found that eddy activity in eastern Bering Sea is particularly strong near the major shelf-break canyons during the spring months, likely influencing the spring bloom, and in situ data from an eddy sampled near Pribilof Canyon in 1997 suggest that these eddies can carry water from the outer shelf into the basin (Ladd et al. 2012). Nevertheless enhanced production may occur in canyons under some circumstances. In Kaikoura Canyon, New Zealand, the physical setting appears suitable for trapping particulate organic matter derived from pelagic production and coastal detrital export; benthic biomass and infauna were elevated and fish abundance was higher in the canyon than the adjacent slope (De Leo et al. 2010). The head of Scripps Canyon lies immediately adjacent to the California coast and longshore transport delivers substantial quantities of macrophyte detritus from macroalgae which strong tidal and gravity currents distribute through much of the canyon system (Vetter and Dayton 1999).

Our analysis addresses five questions posed by the NPFMC, which we simplified as: 1) Are the canyons unique habitats?; 2) Are the canyons homogeneous habitats?; 3) What are the fish associations with habitat features?; 4) What is the vulnerability of the canyons?; 5) Are benthic habitats vulnerable? Our paper is organized into three topics: 1) Physical habitat characteristics (questions 1 and 2); 2) Fish, crab, coral and sponge distributions and associations (question 3); and 3) Overlap of fishing and vulnerable habitats (questions 4 and 5). All of the questions are addressed within the context of the eastern Bering Sea geographic area. The terms

habitat and benthic habitat often are used interchangeably and can include both physical (e.g., sediment) and biological (e.g., coral) structure. In this paper, we distinguish physical and biological habitats and for the overlap analysis, focus on the overlap of fishing with coral and sponge habitats.

# Methods

## Data

Available information that describes eastern Bering Sea seafloor and ocean habitat includes bathymetry (depth and seafloor gradient), sediment (grain size and sorting) and oceanographic information such as temperature, current speed and productivity. The bathymetry information covers the eastern Bering Sea shelf and slope and has been assembled from National Ocean Service "smooth sheets" based on digitized soundings collected from historical surveys by hydrographic ships (S. Lewis, Alaska Regional Office-NMFS, personal communication). A smooth sheet is the final, neatly drafted, accurate plot of a hydrographic survey using verified or corrected data. These data are mostly from historical mapping efforts and have better coverage in shallow waters of the eastern Bering Sea shelf and slope. We transformed the depth data to a continuous coverage on a fine scale (100 m x 100 m) grid of the eastern Bering Sea shelf and slope using inverse distance weighting implemented in ArcGIS software (ESRI 2009). The Spatial Analyst package in ArcGIS was then used to compute maximum seafloor gradient at each grid point (maximum gradient among adjacent eight grid cells, expressed as rise divided by the run multiplied by 100 and expressed as a percentage. The seafloor gradient and bathymetry information were then aggregated into a regular 1 x 1 km grid for further analysis.

Two measurements of sediment type were used in these analyses, grain size and sediment sorting. The sediment information is stored in the Eastern Bering Sea Sediment Database (EBSSED) (McConnaughey and Smith 2000) and was supplemented with data from the National Geophysical Data Center Sea Floor Sediment Grain Size database (http://ngdc.noaa.gov/geosamples/metadata.jsp?g=G00127). The sediment information describes grain size and sorting for the top-most 10 cm of seafloor. Mean grain size is expressed as "phi" which is a negative $\log_2$-transform of grain size in millimeters (e.g., large "phi" indicates fine

grains). Because the usual sampling tools are bottom grabs and corers, the sediment information does not distinguish boulder or bedrock habitat and as a result, this habitat type is implicitly excluded from our analysis. Sediment sorting is defined as the standard deviation of phi in each sediment sample. The grain size and sorting values from the sediment data were kriged into a continuous coverage on a 1 x 1 km grid of the eastern Bering Sea shelf and slope using ordinary kriging (Venables and Ripley 2002). For kriging this data set, an exponential model was the best fit to the semi-variogram of both grain size and sorting values and was used for interpolation.

Measurements of bottom temperature have been collected routinely since 1996 during standard bottom trawl surveys for fish and crab of the eastern Bering Sea shelf and slope (Hoff and Britt 2011, Lauth 2011). Standard surveys of the continental shelf have been conducted annually during June-July 1982-2012. Shelf survey stations are located at the mid-point of 37 x 37-km grid cells for depths of 30-200 m. Standard surveys of the upper continental slope were conducted during June-July 2002, 2004, 2008, 2010 and 2012. Each year, the slope survey was conducted by randomly sampling 200 stations from approximately 350 possible stations. The slope survey covers depths of 200-1,200 m and the latter marks the depth limit of our analyses. The bottom temperature data from all survey years were kriged using a spherical semi-variance model to create an interpolated surface of bottom temperatures that represent the long-term average of summer conditions in the eastern Bering Sea. Additional types of oceanographic measurements, including oxygen, turbidity, pH and light were collected only during the 2012 slope survey. Bottom salinity was collected on both the eastern Bering Sea shelf and slope during 2012 surveys.

Two other sources of oceanographic information (ocean currents and ocean productivity) were included in our analysis. A model-based reconstruction of ocean currents from 1975 to 2010 is available for the eastern Bering Sea from the Northeast Pacific (NEP) “Regional Ocean Modeling System” (ROMS) (e.g., Danielson et al. 2011). Major eastern Bering Sea currents are the Bering Slope Current which follows the shelf break and the Alaska Coastal Current which follows the Alaska coastline; mid-shelf currents are sluggish. Currents vary both in time (e.g., shelf circulation and transport across the shelf break are influenced by seasonal patterns in wind direction (Danielson et al. 2012)) and space (e.g., stronger currents occur south of St. George Island where the shelf narrows (Stabeno et al. 2008)). For our analysis, the values were averaged because long-term current patterns likely influence spatial patterns of long-lived benthic species

including deepwater coral and sponge. The long-term average current data were available on a regular grid (10 x 10 km) and were transformed to a 1 x 1 km grid using inverse distance weighting because there was no indication of non-random spatial structure in semi-variogram plots.

Satellite-based measurements of ocean productivity (ocean color) from 2003 to 2011 are available for the eastern Bering Sea from the Sea-viewing Wide Field-of-view Sensor (SeaWiFS) Project (Behrenfeld and Falkowski 1997). The monthly average data for May to September of each year on a regular grid (11.9 x 18.5 km) was downloaded from Oregon State University's Ocean Productivity website (http://www.science.oregonstate.edu/ocean.productivity/) for the years 2003-2011. For each grid cell, these data were averaged across months within each year and then averaged across all years. We averaged over all years rather than taking annual values because months often were poorly sampled or sampled not at all due to cloud cover. There was no indication of non-linear spatial structure in the regularly spaced data points, so average productivity was interpolated using inverse distance weighting into a continuous coverage on a 1 km x 1 km grid.

The standard bottom trawl surveys of the eastern Bering Sea shelf and slope (Hoff and Britt 2011, Lauth 2011) also describe fish and invertebrate (e.g., coral) distributions and are the primary source of data for these taxa in our study (http://www.afsc.noaa.gov/RACE/groundfish/survey_data/default.htm). We analyzed data for both the shelf and slope surveys from 2002, 2004, 2008, 2010 and 2012, which are the years standard slope surveys have been conducted. For these analyses, records were only used if trawl performance was satisfactory and if the distance fished, geographic position, average depth and water temperature profile were recorded. Trawl tows were deemed satisfactory if the net opening was within a predetermined normal range, the gear maintained contact with the seafloor, and the net suffered little or no damage during the tow. Data from a total of 2,696 bottom-trawl tows were used (1,777 from the shelf survey and 919 from the slope survey). All fish and invertebrates captured during a survey tow were sorted to the lowest taxonomic level practical, typically species, and the total weight in the catch was determined. Catch per unit effort (CPUE, number $ha^{-1}$) for each taxonomic group was calculated using the area swept computed from the net width for each tow multiplied by the distance towed recorded with GPS. In addition, longline surveys cover the eastern Bering Sea slope (http://www.afsc.noaa.gov/abl/mesa/mesa_sfs_lsd.htm).

Fourteen stations are sampled every other year. Data from a total of 84 longline sets for the years 2001, 2003, 2005, 2007, 2009 and 2011 were available. All fish and invertebrates captured during a longline set were sorted to the lowest taxonomic level practical and the total weight in the catch was determined. Catch per unit effort (CPUE, number hook$^{-1}$) for each taxonomic group was calculated.

Other data sets were considered but not used in our analysis. Small areas of the seabed and associated fauna have been observed visually (Brodeur 2001, Busby et al. 2005, Hoff 2010, Rooper et al. 2010, Miller et al. 2012) and tabular data of habitat classification are available from these studies. However these samples are limited mostly to canyon habitat. Measures of habitat type derived from acoustic backscatter ('Q-values') have been reported for the Bering Sea shelf (McConnaughey and Syrjala 2009) but not for the slope. The lack of comparative values for either of these data sources prevents their use in our overall habitat analyses, though we complete some analysis of the visual observations. Coral and sponge data are collected by observers in fisheries observer programs; however identification has not been a high priority historically and only limited training has been provided for that purpose. The spatial resolution is variable, depending on gear type, fishing practices and haul duration. The data may be useful for presence validation but not absence validation, unless significant data filtering based on assumptions about sampling and operations, is done. Other surveys using acoustics and surface trawls sample pelagic but not benthic habitat and so were not analyzed.

## Analyses of physical habitat characteristics

We distinguish three major physical habitats in our analysis: shelf, canyon and non-canyon slope. The shelf is further divided into three oceanographic domains based on the usual location of oceanic fronts during summer (inner < 50 m, middle 50-100 m, outer 100-180 m) (Coachman 1986). We made one change in these boundaries that affected the seaward, oceanographic boundary of the outer shelf. We substituted the geological boundary between the continental shelf and slope, the shelf break, which is defined as a prominent change in seafloor gradient from low to steeper (pers. comm., David W. Scholl, USGS emeritus). This boundary was chosen using the following approach. Contours were placed on the seafloor gradient map at 0.5, 1, 2, 3 and 5 percent. The contours for 1, 2 and 3 percent generally were close together, indicating that the seafloor gradient is changing rapidly there. In contrast, the contours for 0.5 percent were

distinctly separated from 1, 2 and 3 percent. The contours for 5 percent often were discontinuous and irregular. We chose the 1 percent contour as the shelf-slope boundary because this was the shoreward contour where a prominent change in seafloor gradient occurred (i.e., the distinct separation of 0.5 from 1, 2 and 3 percent). The resultant shelf-slope boundary typically lies at about 200 m except for the northern edge of Bering Canyon and the adjacent slope where the boundary lies at about 500 m. The lateral boundary of a canyon is defined as the intersection of the canyon opening with the continental slope; the canyon lateral boundaries were located at the closest ridge crest on either side of the canyon axis (pers. comm., H. Gary Greene, Moss Landing Marine Laboratories). These two measures were then used to define the boundaries of each canyon in our analysis.

We distinguish five large canyons that intersect the eastern Bering Sea shelf break including three lower seafloor gradient canyons (Navarin, Pervenets and Bering) and two higher seafloor gradient canyons (Pribilof and Zhemchug) (Karl et al. 1996). We do not distinguish two other canyons, St. Matthew and Middle canyons, because they barely indent the shelf break and have only minor morphological expression on the shelf (Karl et al. 1996).

Multivariate analyses were applied to determine whether physical habitat characteristics differ among the five large canyons, the four slope areas lying between the canyons and the three oceanographic domains of the continental shelf (a total of 12 areas). These analyses were completed using data on depth collected annually during trawl surveys, data on salinity, oxygen, turbidity, pH and light collected only during the 2012 trawl survey and other habitat information including seafloor gradient, current, long-term average temperature, productivity and grain size and sorting that were not associated with a specific trawl haul, but potentially are useful in defining habitats. We completed the multivariate analyses using three data groupings (Table 1) because more measurement types were collected in 2012 and also to determine if separately analyzing the slope data affected the results. These three data groupings were Case A: all years (2002, 2004, 2006, 2008, 2010, 2012) data - from both shelf and slope surveys when both surveys occurred; Case B: all years data - from slope survey only; and Case C: 2012 data – from slope survey only (when additional types of oceanographic measurements were collected).

As described in the data section, the seafloor gradient, current, long-term temperature, productivity and grain size and sorting information was compiled on a 1 x 1 km grid. For each trawl survey station, this 1 x 1 km grid (e.g., seafloor gradient in the grid cell where the bottom

trawl tow occurred) was associated with the information collected during the trawl survey (e.g., depth) and then the habitat data were analyzed. For each trawl survey station, there were measurements of depth for all years and measurements of salinity, oxygen, turbidity, pH and light for 2012 only. For the corresponding 1 x 1 km grid cell, there were values of seafloor gradient, temperature, current, productivity and grain size and sorting. Data were normalized (to mean = 0 and SD = 1) by subtracting the mean and dividing by the standard deviation to remove the effect of scale differences among variables.

These habitat variables were used in a principal component analysis (PCA) of the trawl survey stations using the MASS package implemented in R statistical software (Venables and Ripley 2002). Patterns in the PCA were examined graphically to determine if the 12 habitat areas were easily distinguishable and if so, what factors were associated with these differences. The PCA also indicated the habitat variables that contributed the most to the variability of the habitat data set and indicated where strong or weak covariation among habitat variables was apparent.

Each station was located in one of the 12 areas and this classification was tested using quadratic discriminant function analysis (DFA) with the normalized data using the MASS package implemented in R statistical software (Venables and Ripley 2002). The quadratic DFA measures how well group membership is predicted for each habitat area using an optimal combination of quadratic functions. Station groupings were determined using leave-one-out cross-validation of the data. The percentage agreement between the observed classifications and the predicted classifications indicated the degree to which the areas could be discriminated from each other using the habitat variables. Lastly an analysis of similarity (ANOSIM) was completed to test for statistically significant differences among habitat areas using the MASS package implemented in R statistical software (Venables and Ripley 2002). This analysis compares the rank order of dissimilarity values between two or more groups. In this case the groupings were the 12 areas and the dissimilarity matrix was computed from the habitat variables. ANOSIM produces an R-value, which is a test statistic that varies between -1 and 1, and a probability based on random permutation of the groupings. An R-value of 0 indicates random assignment of the data into groups, while an R-value of 1 indicates perfect discrimination between groups was obtained. Statistical significance can be determined by $p<0.05$, but with large sample sizes such as ours, the probability must be viewed in light of the R-value. An R-value close to zero can indicate that the relationship is not meaningful, even if $p < 0.05$.

## Analyses of fish, crab, coral and sponge distributions

Our approach was to examine ecologically important fish and crab species with importance based on density (kg $ha^{-1}$). We selected the top 10 fish and crab species from each survey (shelf trawl survey, slope trawl survey, longline survey) and created a combined list of species to analyze. The combined list consisted of 20 fish and crab species (Table 2) and totaled less than 30 species because some species were on more than one top 10 list. We used the longline survey data only to compile the list, but not for analysis, because only 14 longline survey stations were sampled every other year and the sample years differed for the longline and slope trawl surveys. For coral and sponges, we initially selected several major taxa and also differentiated some notable taxa like *Primnoa* spp. Based on preliminary analyses however we had to pool the taxa further because sample sizes for some taxa were too low for reliable analysis. The resultant three groups were coral (all corals except sea whips and sea pens), sea whip (this group name includes one species of sea whip (*Halipteris willemoesi*) and sea pens, which were uncommon), and sponge (Table 3). All catch data were log (+ constant) transformed prior to analysis. The constant used for each species was one-half of the minimum positive catch (> 0) for that species. Data were normalized (to mean = 0 and SD = 1) by subtracting the mean and dividing by the standard deviation to remove the effect of scale differences among variables for multivariate analyses.

We applied a similar multivariate analysis approach (i.e., PCA, DFA, ANOSIM) to the biota information as we applied to the habitat information except that only slope and outer shelf data were analyzed (Figure 1). We excluded the inner and middle shelf from the analysis because of their consistent difference from the other areas. For the biota analysis, unlike the physical habitat analysis, there was no need to group data and distinguish Cases A, B and C (Table 1) because the same biota information was collected for all survey years. Multivariate analysis (DFA) was applied to determine how well group membership could be predicted for the focal canyons (Zhemchug and Pribilof canyons) and the slope areas lying between the canyons.

In addition to the multivariate analyses, we also used the bottom trawl survey data to test for relationships between physical habitat and biota. We used generalized additive modeling (GAM, Hastie and Tibshirani 1990) fit using the mgcv package in R (Wood 2006) to construct relationships between habitat variables (location, depth, temperature, gradient, current speed, ocean productivity, grain size and sediment sorting) and the density of the top 20 fish and crab

species. A parallel method was used to individually predict the presence or absence of coral, sponge and sea whips. Presence-absence was used in the GAMs for corals and sponges instead of density (CPUE) because the combination of a large number of zero catches and high variability in positive catches where they occurred were difficult to model an appropriate error distribution. Our approach was similar but not identical to other recent predictive modeling of coral distribution (Woodby et al. 2009, Ross and Howell 2013).

The GAMs were constructed for each fish and crab species using the log-transformed catch per unit of effort (LCPUE in kg $ha^{-1}$). A factorial analysis was used to determine the best-fitting model for each species or taxa group, where the full model containing all variables was fit to the data, and then the least significant variable was eliminated and the model refit. LCPUE models were compared using the generalized cross-validation (GCV) criterion (Wood 2006). The elimination of the least significant variable was repeated until no further gain in GCV was attained. This model was then determined to be the best-fitting model for the species. Overfitting of the models was reduced using the ad-hoc method of increasing the penalty on effective degrees of freedom by 1.4 for each degree of freedom used by the smoothing function (Kim and Gu 2004). For LCPUE data, a normal distribution was used in the fitting, while for presence-absence data, a binomial distribution was used. Presence models were compared using the unbiased risk estimator (UBRE) criterion (Wood 2006). For LCPUE data the scale parameter was estimated from the data and for presence-absence data the scale was one. When the best-fitting model was determined for each fish species, the LCPUE was predicted for each 1 x 1 km block in the eastern Bering Sea outer shelf and slope. For the invertebrate groupings, predictions were made for the probability of presence. Summaries of these prediction layers are presented graphically.

To judge the accuracy of the LCPUE models, the model predictions were correlated to the observations using the squared Pearson correlation coefficient. Two methods were used to judge the accuracy of the presence-absence models. For the first method, the area under the curve (AUC) was computed which calculates the probability that a randomly chosen presence observation would have a higher probability of presence than a randomly chosen absence observation using rank data. We used the scale of Hosmer and Lemeshow (2005), where AUC value > 0.5 is estimated to be better than chance, a value > 0.7 is estimated to be acceptable, and values > 0.8 and 0.9 are excellent and outstanding, respectively. The coral, sea whip and sponge

presence-absence models predicted the probability of each group being present, a continuous variable. This was then translated into a prediction of presence-absence using a threshold value for the probability. Since the data set contained many more absences than presences, the resulting models could be biased towards absence (Hosmer and Lemeshow 2005). Thresholds were chosen empirically for translating the probabilities to presence-absence that balanced the number of false positives and false negatives in the predictions. The empirically derived thresholds were about 0.3 and varied slightly depending on data set. This presence-absence information was then used to calculate a contingency matrix and Cohen's Kappa (Fielding and Bell 1997), which is the second method used to judge the accuracy of the predictions.

We used visual survey data for coral and sponge to evaluate their numerical abundances in Pribilof and Zhemchug canyons. In analysis of visual survey data, the term coral includes sea whips and sea pens unlike the analyses of trawl survey data which distinguish sea whips and sea pens from other coral taxa. Data are available from surveys conducted in 2007 (Miller et al. 2012) and 2012 (pers. comm., J. Hocevar, Greenpeace). A total of 23 dives were completed; 7,209 frames were available that covered a total of 30,132 square meters. Transects were located to cover the geographical extent of the canyons, as well as the slope nearby, and were located approximately equidistantly, although a few dives were close together to cover a broader depth range at a location. These video frames were a subset of the entire dive; non-overlapping frames were extracted from each video transect at a constant rate of 1 frame per 30 seconds (Miller et al. 2012). We applied the same method to compute numerical density as Stone (2006) in order to compare Bering canyon densities to those for the Aleutian Islands. In this method, the total number of coral and sponge colonies counted is divided by the total area surveyed (e.g., divide a count of 1,000 colonies by an area surveyed of 2,000 $m^2$ with a result of 0.5 colonies $m^{-2}$). Confidence intervals for these values were estimated by the bootstrap method (Efron and Tibshirani 1993). In our application of the bootstrap method, dives were sampled with replacement within canyon, a density (the bootstrap replicate) was computed and the 95% confidence intervals determined from a distribution of 1,000 bootstrap replicates which was corrected for bias if necessary (bias-corrected percentile method).

## Spatial overlap of fishing and vulnerable habitats

We examined the spatial overlap of fishing and vulnerable habitats by combining the probability of coral, sea whip and sponge presence, fishing effort distributions and an index of susceptibility to damage by fishing. The probability of coral, sea whip, and sponge presence was based on the predictive maps produced by the GAM modeling. Intensive fisheries observer programs for groundfish (National Marine Fisheries Service, Seattle WA, North Pacific Groundfish Observer Program database), and crab (Alaska Department of Fish and Game, Division of Commercial Fisheries, Kodiak, Bering Sea/Aleutian Islands crab observer database) monitor fishing effort in the eastern Bering Sea. Set location and gear type (bottom trawl, pelagic trawl, longline (hook and line), pot) are among the data types recorded. We compiled the number of observed sets during 2002-2011 by gear type on the recorded 1 minute latitude x 1 minute longitude grid and then interpolated (linear) these totals onto the 1 km x 1 km grid used for our other data types.

For the susceptibility index, each coral and sponge taxon was scored for vulnerability to damage from fishing based on visual observations of damage rates from the central Aleutian Islands and the height and rigidity of the specimens (Stone and Alcorn, in press) (Table 3). Large, upright rigid taxa such as Antipatharians and bamboo corals were damaged more often (Stone and Alcorn, in press) so we assigned a score of 3, whereas small, flexible taxa such as plexaurid (*Swiftia pacifica*) and acanthogorgiid gorgonians (*Calcigorgia* spp.) were damaged less often (Stone and Alcorn, in press) so we assigned a score of 1. Primnoid gorgonians (*Plumarella aleutiana*) are of similar size to the plexaurids and acanthogorgiids but generally have a more rigid skeleton and appear to have intermediate vulnerable to disturbance (Stone and Alcorn, in press) so we assigned a score of 2. Sea whips were assigned an intermediate score of two since they are upright and rigid but vary greatly in size from < 5 cm to > 1 m. These scores consider vulnerability to physical damage only and do not consider differences in recovery rates once damage occurs. Only limited information on recovery rates is available to incorporate into our analyses. Coldwater coral and sponge generally are long-lived (decades or centuries) and slow-growing (typically < 2 cm per year), so that any damage likely will have long-lasting effects. The susceptibility scores for each of the three coral and sponge groups were based on the catch-weighted average of the group members' scores, which were 2.93 for coral, 2.93 for sea whip/pen and 2.14 for sponge.

Vulnerability indices were computed for each 1 km x 1 km grid cell by multiplying probability of occurrence of coral, sea whip and sponge presence by the corresponding susceptibility scores and summing across the three coral and sponge groups. The maximum possible value of the vulnerability index is about eight which occurs when the probability of presence is one for all three taxa (1 × 2.93 + 1 × 2.93 + 1 × 2.14). The vulnerability indices were mapped and then summarized for 10 areas (five canyons, four inter-canyon areas and outer shelf). Overlap indices were computed for each 1 km x 1 km grid cell by multiplying these vulnerability indices by the corresponding number of observed fishery sets by gear type. The overlap indices were mapped by gear type and then summarized for the 10 areas. Overlap indices were segregated by gear type because gear effects on benthic invertebrates differ by gear type. Because reliable, quantitative estimates of these differences are not available, we did not compute a single set of overlap indices that combined fishing gears.

# Results

## Habitat characteristics

The eastern Bering Sea is characterized by a broad, flat shelf. The adjacent slope is shallow-gradient seafloor; most (90%) is 10% gradient or less. Most (90%) seafloor gradient of Pervenets, Navarin and Bering canyons is 5% or less and most seafloor gradient of Pribilof and Zhemchug canyons is 10% or less. The maximum seafloor gradients of any 1 x 1 km grid cell in Zhemchug and Pribilof canyons are 45% and 50% respectively. Most (90%) seafloor gradients of the intercanyon areas are 7% or less (Bering-Pribilof), 16% or less (Pribilof-Zhemchug) or 11% or less (Zhemchug-Pervenets, Pervenets-Navarin). The maximum seafloor gradient of any 1 x 1 km grid cell on the slope is 67% for the Pribilof-Zhemchug intercanyon area.

We computed the seafloor area of individual canyons and non-canyon slope based on the canyon definitions described in the methods. Compared to the total seafloor area of the eastern Bering Sea slope, canyons comprise almost half (43%) of the total area (Bering 11%, Pribilof 10%, Zhemchug 10%, Pervenets 5% and Navarin 7%). The relative volumes (Navarin (total volume = 5,400 $km^3$), Pervenets (1,700 $km^3$), Bering (4,300 $km^3$), Pribilof (1,300 $km^3$) and Zhemchug (5,800 $km^3$) canyons (Karl et al. 1996)) often differ from the relative areas due to

morphological differences. For example, the areas of Pribilof and Zhemchug canyons are similar but the volume of Zhemchug Canyon is larger because of the larger opening of this canyon. In addition, our study excludes seafloor depths below 1,200 m (the depth limit of the bottom trawl surveys) and Zhemchug Canyon has more habitat below this depth than Pribilof Canyon. The total seafloor areas of the intercanyon areas comprise over half (57%) of the total slope area (Bering-Pribilof 18%, Pribilof-Zhemchug 20%, Zhemchug-Pervenets 14%, Pervenets-Navarin 4%).

Broad-scale patterns were apparent in the physical characteristics of the eastern Bering Sea. Focusing on the outer shelf and slope, bottom temperature and ocean color were higher southward (Supplement (S) 1, S2). Current speed was lower for the southeastern shelf compared to the slope and the shelf farther north, especially Navarin Canyon (S3). Grain size generally was coarser and more sorted shoreward (S4-5). Oxygen and pH were lower and turbidity higher in Pribilof and Zhemchug canyons (S6-7). Salinity was higher on the slope than outer shelf (S8).

These broad-scale patterns in physical characteristics distinguished the shelf from the slope and the canyons from the adjacent slope areas. The Case A (for case definitions, see Table 1) PCA distinguished inner shelf from middle and outer shelf based on grain size, sediment sorting, temperature and ocean color and distinguished shelf from slope based on depth, seafloor gradient and current (Figure 2). The related DFA indicated that group membership was medium to highly predictable for inner shelf (97% of stations were grouped correctly), middle shelf (90% of stations were grouped correctly), outer shelf (80% of stations were grouped correctly), canyon (79% of stations were grouped correctly) and inter-canyon slope (78% of stations were grouped correctly) (Table 4). Quadratic discriminants of deeper depths, larger seafloor gradients and higher current speeds were characteristics that defined canyons and inter-canyon slope areas from the shelf areas of the eastern Bering Sea. ANOSIM indicated that there were significant differences among the 12 areas of the eastern Bering Sea ($R = 0.557$, $p = 0.001$).

A division segregates the left and right-hand sides of the Case B plot of PCA components 1 and 2 with Pribilof Canyon to the left and Zhemchug Canyon to the right which are distinguished by grain size, sediment sorting and ocean color (Pribilof Canyon) and seafloor gradient and current (Zhemchug Canyon) (Figure 3a). The Case B plot of PCA components 1 and 3 distinguished Pribilof Canyon based on depth and sediment sorting (Figure 3b). Of the two focal canyons, Pribilof and Zhemchug, the related DFA indicated that group membership was

highly predictable for Pribilof Canyon compared to adjacent slope areas where 98% of canyon stations were grouped correctly and all the adjacent slope stations were predicted correctly. Zhemchug Canyon and its surrounding areas were also highly predictable, as 99% of Zhemchug Canyon were predicted correctly and 98% of adjacent slope stations were predicted correctly (Table 5). Sediment sorting distinguished Pribilof Canyon from the rest of the slope and grain size distinguished the two canyons and the intercanyon areas. Zhemchug Canyon also was less productive (lower ocean color) than other slope areas including Pribilof canyon. Depth and temperature were not very useful in discriminating among canyon and inter-canyon slope areas. ANOSIM also indicated there were significant differences among canyons and inter-canyon areas ($R = 0.54$, $p = 0.001$). The R-value was approximately the same as for the slope and shelf combined analysis, indicating strong differences among slope areas.

A division segregates the upper and lower sections of the Case C PCA plot with Pribilof Canyon below and Zhemchug Canyon above which are distinguished by grain size, sediment sorting, color, temperature and turbidity (Pribilof Canyon) and seafloor gradient and current (Zhemchug Canyon). Of the two focal canyons, Pribilof and Zhemchug, the related DFA indicated that group membership was highly predictable (for Pribilof Canyon stations (100% correct) compared to adjacent slope areas and highly predictable (91% and 71% correct) for adjacent slope areas and Zhemchug Canyon respectively. The results were very similar to the results from Case B although the addition of the physical variables collected in 2012 resulted in slightly worse discrimination of Zhemchug Canyon from the adjacent intercanyon areas. Sample sizes within each grouping in 2012 did not allow for quadratic DFA, so linear DFA was used instead. The distinguishing features of the linear discriminants for the 2012 slope data were sediment characteristics (grain size and sorting), ocean color and bottom temperature. ANOSIM also indicated there were significant differences among canyons and inter-canyon areas ($R = 0.36$, $p = 0.001$). The smaller R-value compared to $R = 0.56$ and $R = 0.54$ for all years data (above) likely occurred because sample sizes were reduced by including only 2012 data.

## Coral, sponge and sea whip distributions

The analysis of coral, sponge and sea whip presence-absence did not distinguish the canyons from the adjacent slope areas (Table 6). The DFA indicated that group membership was poorly predicted for Pribilof Canyon stations where 78% of stations were grouped with the adjacent

slope stations. No bottom trawl survey tows in Pribilof Canyon captured sea pens or whips, so this variable could not be used in the DFA. For Zhemchug Canyon, groupings were also inaccurate, as 84% of Zhemchug stations were grouped with stations from adjacent slope areas. Although the ANOSIM results were significant ($p = 0.001$), the R-value (0.052) indicated that there was very little dissimilarity among the different slope areas in coral, sponge and sea whip presence-absence.

The best-fitting GAMs of coral, sea whip and sponge explained 31-39% of deviance in presence-absence data (Table 7, S9-11). The significant explanatory variables were current (coral, sea whip, sponge), depth (sea whip, sponge), grain size (sponge), seafloor gradient (coral, sea whip, sponge), ocean color (sea whip, sponge) and location (coral, sea whip, sponge). Using threshold probabilities of 0.30 and 0.28, the models accurately predicted coral and sea pen presence-absence as they were correct 93% and 90% of the time (Table 8). Using a threshold probability of 0.53, sponge presence-absence was correctly predicted 77% of the time. The AUC and the Kappa statistics indicated an acceptable predictive ability for these models.

Coral (Figure 4a), sponge (Figure 4b) and sea whip (Figure 4c) are predicted to occur both inside and outside canyons. Predicted coral distribution is limited to sections of the slope, both within and between canyons. In contrast, predicted sea whip distribution includes sections of the outer shelf and is shallower than coral. Predicted sponge distribution occurred for sections of the slope, both within and between canyons, as well as outer shelf. Within Pribilof Canyon, there is some tendency for more coral presence inside or adjacent to the lateral wings of these two canyons. Sea whips are predicted to occur adjacent to Zhemchug but not Pribilof Canyon.

More coral habitat was predicted for slope areas (61%) than for the outer shelf (39%) (Table 9). Within slope areas, the highest amount of coral habitat was predicted to be in Pribilof Canyon (33%). Only 1% of coral habitat for slope areas was predicted for Zhemchug Canyon and the rest was primarily in the Pribilof-Zhemchug inter-canyon area (29%), in the Zhemchug-Pervenets inter-canyon area (18%) and in Navarin Canyon (13%).

One unique feature of the focal canyons is that one third (33%) of the coral habitat predicted for the eastern Bering Sea slope occurs in Pribilof Canyon, an area that comprises only about 10% of the total slope area. The area of predicted coral habitat in Pribilof Canyon extends into the Pribilof-Zhemchug intercanyon area (Figure 4a). In contrast, about two-thirds of sponge (64%) and most sea whip (91%) habitat was predicted to occur on the outer shelf, an area that

comprises about 82% of the total area of the slope and outer shelf. In the combined slope areas, Pribilof and Zhemchug canyons contained about 28% of the predicted total sponge habitat. For sea whip there is no predicted occurrence in Pribilof Canyon and only 14% of the total slope sea whip habitat occurs in Zhemchug Canyon.

Coral and sponge are less common on the Bering Sea slope compared to the Aleutian Islands. The average densities of coral were 0.28 colonies $m^{-2}$ (Pribilof Canyon) and 0.15 (Zhemchug Canyon), much less than the average density for the Aleutian Islands (1.23) (Stone 2006) (Figure 5a). The average densities of sponge were 0.10 (Pribilof Canyon) and 0.21 (Zhemchug Canyon), again much less than the average density for the Aleutian Islands (5.25) (Stone and Alcorn, in press). From trawl surveys, coral frequency of occurrence was highest for the Aleutian Islands (0.54) and about five times that for the Bering Sea slope and Gulf of Alaska (both ~0.1) (Figure 5b). Sponge frequency of occurrence was more similar among these three regions (0.57-0.95) but still highest for the Aleutian Islands (0.95). Common taxa from the visual surveys of Pribilof and Zhemchug canyons were the gorgonian coral *Plumarella aleutiana*, the sponges *Aphrocallistes vastus*, *Heterchone calyx*, *Acanthascus vastus* and *Acanthascus* spp. and the sea pen *Halipteris willemoesi*.

## Fish and crab distributions

Like the analysis of coral and sponge, the analysis of fish and crab did not reliably distinguish the canyons from the adjacent slope areas. The DFA indicated that group membership was not very predictable, as only 30% of stations in Pribilof Canyon were classified correctly (Table 6). For Zhemchug Canyon, only 51% of stations were classified correctly as being from Zhemchug Canyon. The ANOSIM indicated statistical differences among slope data ($p = 0.001$), but the dissimilarity among groups was not great, as indicated by the low R-value (0.127).

Generalized additive modeling explained 31-91% of deviance in fish and crab spatial distributions (Table 10, S12-28). Latitude, longitude and depth were significant explanatory variables for all species. All of the variables considered were significant in at least seven of the models. Sediment characteristics were important for all of the species. Predictions were reasonable; observations and predictions generally followed a 1:1 line. The predicted catches occurred in areas with observed catch to a large extent and the areas with little or no positive catches did not have predicted high abundance. Less variability was explained for Pacific

halibut, rougheye/blackspotted rockfish and shortraker rockfish. The two rockfish taxa were caught in only a small proportion of the bottom trawl hauls.

Habitat associations generally were reasonably predicted and stereotypical habitats were correctly assigned for a shelf species, arrowtooth flounder (Figure 6a), a shelf break species, Pacific ocean perch (Figure 6b) and a slope species, sablefish (Figure 6c). By modeling the entire data set without regards to year, interannual variability in catches or overall trends in abundance were not considered. Within one year of the survey, Pacific ocean perch often exhibit a patchy distribution in trawl survey catches, even though their depth distribution is well defined. By combining trawl survey years for analysis, predicted Pacific ocean perch abundance occurred as a band of high abundance within a well-defined depth range (Figure 6b), which over the years, matches the observations of positive catches reasonably well for the slope and less so for the outer shelf.

## Are the canyons homogeneous?

The canyons are not homogeneous. For example, coral habitat is predicted to be concentrated in the western wing of Pribilof Canyon (Figure 4a) and sponge habitat is predicted to be concentrated in central Zhemchug Canyon (Figure 4b). In addition, fish typically exhibit depth preferences and so are concentrated in a depth band within a canyon (e.g., sablefish, Figure 6c). However these patterns of patchiness and depth preference are not limited to canyons and occur for other sections of the slope as well.

## Overlap of fishing and vulnerable habitats

Average habitat vulnerability indices were higher for Pribilof Canyon than other areas but not markedly greater than averages for Pribilof-Zhemchug or Zhemchug Canyon. Higher vulnerability indices were found both within and between canyons and were not unique to Pribilof and Zhemchug canyons (Figure 7). Higher vulnerability indices also were found in sections of the outer shelf. The average vulnerability range was 2.5-6 (Figure 8). The highest index was for Pribilof Canyon (6), then Bering Canyon (5) which was closely followed by Pribilof-Zhemchug, Zhemchug Canyon, Pervenets Canyon and Navarin Canyon (all >4).

Bottom trawl (fishing) effort and pot effort were more concentrated spatially than pelagic trawl effort and longline effort (Figure 9). For the outer shelf and slope, bottom trawl effort was

599 concentrated in Bering Canyon and relatively low elsewhere; pot effort was concentrated in
600 sections of Bering and Pribilof canyons and the outer shelf between Pribilof and Zhemchug
601 canyons (Figure 9). In contrast pelagic trawl effort and longline effort extended the entire length
602 of the Bering slope and outer shelf. The highest concentrations of pelagic trawl effort occurred in
603 Bering and Pribilof canyons and the outer shelf. The highest concentrations of longline effort
604 occurred in Pribilof and Zhemchug canyons, the Pribilof-Zhemchug, Zhemchug-Pervenets and
605 Pervenets-Navarin intercanyon areas and the outer shelf.

606 Overlap indices were computed from the fishing effort information and the habitat
607 vulnerability indices (Figure 10). The maximum value was about 40 (about 1.6 on the log-scale
608 plots in Figure 10). For the slope including canyons, overlap indices were greater than ten (1.0
609 on log-scale) for the southeastern wing of Pribilof Canyon (pelagic trawl), northwestern wing of
610 Pribilof Canyon (pot) and the central section of Zhemchug Canyon and some of the slope habitat
611 between Zhemchug and Pribilof canyons (longline). The overlap indices were less than ten for
612 bottom trawl for all of the slope including canyons.

613 Average overlap indices were low for bottom trawl (Figure 11) because this fishery
614 largely concentrates in areas outside our study area (i.e., inner and middle shelf). The average
615 overlap indices for pot gear were still low but somewhat higher in Bering and Pribilof canyons
616 than other areas. In contrast, the overlap indices were higher for longline and pelagic trawl than
617 the other fishing gears. For longline, the overlap indices were higher for Pribilof and Zhemchug
618 canyons, Pribilof-Zhemchug and Zhemchug-Pervenets intercanyon areas. For pelagic trawl, the
619 overlap indices were higher for Bering and Pribilof canyons.

620 # Discussion

621 ## The five questions

622 In this paper, we address a request by the NPFMC in 2012 to determine whether Pribilof and
623 Zhemchug canyons provide unique coral and sponge habitats for managed fish species. Our
624 analyses address five questions from the NPFMC; our answers are summarized here:
625

1. Are the canyons unique habitats? Zhemchug and Pribilof canyons have distinct physical characteristics including sediment characteristics, ocean color and seafloor gradient that distinguish them from the rest of the Bering Sea slope. These physical differences are more tied to latitude than characteristics unique to these two canyons; for example, both ocean color and temperature decrease northward. These two canyons cannot be distinguished based on biological characteristics because coral and sponge presence and fish and crab densities are similar in canyons and the adjacent slope. One unique feature of the focal canyons is that about one third of the coral habitat predicted for the eastern Bering Sea slope occurs in Pribilof Canyon, an area that comprises only about 10% of the total slope area. Although concentrated there, the average density of coral for Pribilof Canyon (0.28 colonies $m^{-2}$) is much less than the density for the Aleutian Islands (1.23 colonies $m^{-2}$).

2. Are the canyons homogeneous habitats? The physical and biological characteristics of Zhemchug and Pribilof canyons are not spatially homogeneous. Turbidity and oxygen concentrations varied within these two canyons. Coral habitat was more common in some areas of Pribilof Canyon than others. Each fish species generally occupied a distinct depth zone.

3. What are the fish associations with habitat features? Coral, sponge, fish and crab distributions were associated with specific physical habitat characteristics. The presence of coral and sponge could be predicted based on location, depth, current speed and sediment characteristics. The abundance of fish and crab could be predicted based on location, depth and sediment characteristics.

4. What is the vulnerability of the canyons? Average habitat vulnerability indices were higher for Pribilof Canyon than other areas but not markedly greater than averages for Pribilof-Zhemchug or Zhemchug Canyon.

5. Are benthic habitats vulnerable? Concentrated fishing effort overlapped areas of Pribilof and Zhemchug canyons with higher vulnerability indices for two of the four fishing

gears. Longline fishing overlapped areas of the Bering slope with higher vulnerability indices including both Pribilof and Zhemchug canyons and adjacent slope. Pelagic trawling overlapped sections of Pribilof Canyon with higher vulnerability indices but not Zhemchug Canyon. Most bottom trawling and pot fishing occurred in less vulnerable areas except perhaps Bering and Pribilof canyons for pot fishing. These vulnerability and overlap indices provide relative values but are not absolute measures of fishing effects.

## Validation of results

Our estimates of coral and sponge densities based on visual survey information differed from Miller et al. (2012) in part because we used a different approach to estimate density; we followed the approach of Stone (2006). We estimated coral densities of 0.28 colonies $m^{-2}$ (Pribilof Canyon) and 0.15 (Zhemchug Canyon), compared to 0.97 and 0.18, respectively (Miller et al. 2012); we estimated sponge densities of 0.10 colonies $m^{-2}$ (Pribilof Canyon) and 0.21 (Zhemchug Canyon), compared to 0.41 and 0.02, respectively (Miller et al. 2012). In our approach, density was computed for each canyon by dividing total count by total area surveyed, whereas Miller et al. (2012): 1) computed density by video frame; 2) computed the mean density for each transect; 3) computed the mean density for each canyon. One way to think of this difference is that in our approach, density is weighted by sample effort (frame size and transect length) whereas Miller et al. 2012 treated each video frame and transect equally regardless of sample effort. One other difference is that Miller et al. (2012) analyzed only the 2007 data (all that was available at the time) whereas we also analyzed the new data collected in 2012.

We compared visual survey information to our predictions based on trawl survey information in order to understand the reliability of these predictions. The limited visual survey data generally supports our predictions of coral and sponge distributions but indicates some mismatch with our predictions of sea whip distributions. We predicted coral (Figure 4a) primarily for slope habitat of Pribilof and Zhemchug canyons, which matches Miller et al. (2012) who found most coral were present at depth 200-400 m (slope) and were absent at depth 150-200 m (outer shelf). We predicted sponge (Figure 4b) in both slope and outer shelf habitat of these two canyons; Miller et al. (2012) found most sponge at depth 200-400 m (slope) but absent from outer shelf habitat (150-200 m). However, Miller et al. (2012) may have missed sponges in outer shelf habitat because their sample size was only 77 video frames. We predicted sea whip habitat

primarily for outer shelf habitat adjacent to Zhemchug but not Pribilof Canyon (Figure 4c). Miller et al. (2012) found more sea whips in Pribilof (0.07 $m^{-2}$) than Zhemchug (0.001 $m^{-2}$) canyon at depth 254-488 m (slope).

Brodeur (2001) found sea whips in the western wing of Pribilof Canyon but we predicted none there (Figure 4a). In 5 of 7 ROV deployments there, Brodeur (2001) reported areas containing dense aggregations of 1-2 m high sea whips (*Halipteris willemoesi*) evenly spaced about 2 m apart over the depth interval of 185-240 m (i.e., outer shelf and slope habitat). The absence of sea whips in the prediction for the outer shelf likely occurred because trawl survey effort is minimal there. Slope survey effort covers the depth range of 200-1,200 m and shelf survey effort covers the depth range of 20-200 m, but is reduced below depth of 165 m because few standard 37 km x 37 km grid cells occur there. As a result, sampling effort by depth was 65.6% for depths <165 m and 33.9% (>205 m) but only 0.5% (165-205 m) (n = 2,696).

The frequency of occurrence of coral in trawl surveys but not sponge was similar to their frequency of occurrence in visual surveys. Miller et al. (2012) reported that corals are patchy in the canyons and separated by large areas of open silt/sand habitat, such that only 15% of frames contained coral for their 2007 data. For both 2007 and 2012 visual data, we found that 10% of frames contained coral, the same frequency as the 10% of tows that caught coral during slope surveys (Figure 5b). Miller et al. (2012) did not report the frequency of occurrence of sponge, but we found that for both 2007 and 2012 visual data, 13% of frames contained sponge, much less than the frequency of occurrence of sponge from 2002 to 2012 Bering slope trawl surveys of nearly 60%. Given that the area sampled by a trawl is much larger than that sampled in a video frame, this difference in occurrence implies that sponge are ubiquitous but sparse.

Most of our study area was available to the trawl survey gear and major areas of the slope missed by our analyses were few. Major areas that were untrawlable totaled about 5% of slope habitat and were found in Pribilof-Zhemchug (intercanyon area) (13% of this area was untrawlable), Zhemchug Canyon (17%), Zhemchug-Pervenets (1%) and Pervenets-Navarin (8%) (S29). In general, survey scientists characterized these untrawlable areas as “too steep and bumpy” to trawl. Of the two focal canyons, one area of Zhemchug Canyon was untrawlable and covered a linear length of about 25 km of the southeast wall of this canyon; no large area of Pribilof Canyon was considered untrawlable. A statistical analysis comparing habitat characteristics derived from a multibeam map of Pribilof Canyon to locations of successful trawl

718 tows also indicated that Pribilof Canyon within the surveyed depths (< 1,200 m) is available to
719 the trawl survey gear.

720 ## Overlap of fishing and vulnerable habitats

721 The potential for fishing effects on benthic habitat depends on the benthic community
722 composition, gear type and the spatial overlap of fishing and vulnerable habitats. Stable
723 communities of low-mobility, long-lived species are more vulnerable to acute and chronic
724 physical disturbance than are short-lived species in dynamic environments (NRC 2002).
725 Structurally complex habitats (e.g., biogenic reefs) and those that are relatively undisturbed by
726 natural perturbations (e.g., deep-water mud substrata) are more adversely affected by fishing
727 than unconsolidated sediment habitats that occur in shallow coastal waters (Kaiser et al. 2002).
728 In the context of the Bering Sea, these findings imply that the inner shelf that is frequently
729 impacted by winter storms is less vulnerable than the deeper and more stable outer shelf and
730 slope. Nevertheless, trawling effects on benthic invertebrates have been documented for the inner
731 shelf, including both positive and negative changes in biomass of individual taxa, as well as
732 reduced species diversity, niche breadth, and mean body sizes (McConnaughey et al. 2000,
733 Brown et al. 2005, McConnaughey et al. 2005). In some cases, these effects were small relative
734 to natural variability in the surrounding area (McConnaughey et al. 2005).

735 Pelagic trawls used in the pollock fishery are not designed to be fished on the seafloor,
736 however some contact occurs when larger, more valuable pollock aggregate near the seafloor. A
737 measure of this occurrence is the catch of crabs which are strictly benthic. Crab bycatch in the
738 pollock fishery averaged 15,955 crabs during 2007-2011 (Ianelli et al. 2012). The overlap index
739 identifies areas where fishing effects on coral and sponge habitat may occur. For the pelagic
740 trawl fishery, the actual effect will depend on how often and in what areas bottom contact
741 commonly occurs.

742 Within the classification of bottom trawls, rock-hopper otter trawls disturb the seabed
743 most intensively, whereas for lighter gears such as smaller otter trawls, disturbance is largely
744 restricted to the trawl boards except when erect benthic invertebrates such as sponge are present
745 and the warps and footrope of either otter trawl can detach individuals from the seafloor (Kaiser
746 et al. 2002). Trawl effects studies in Alaska have found that large epifaunal invertebrates were
747 removed or damaged by a single trawl pass (Freese et al. 1999), sponges were slow to recover

from trawling effects (Freese 2001), and chronic bottom trawling affected the abundance and diversity of epibenthos (Stone et al. 2005). Trawl effects can be reduced by gear modifications that reduce seafloor contact (Rose et al. 2010).

Fishing effort tends to be patchy and the same grounds are fished year after year (Kaiser et al. 2002). For most habitats that are vulnerable to fishing, a consistently patchy distribution of a given level of trawling effort from year to year is likely to have lower environmental impacts than if the same trawling effort were distributed evenly because the initial effect usually is greater than recurrent effects (Kaiser et al. 2002). For this reason, tabulation of fishing effort should account for overlap in assessing effects of fishing which can be challenging (Rose and Jorgensen 2005). It is also important to consider the consequences of redistributed effort if new closures are implemented (Fujioka 2006).

The computation of the vulnerability index implies that an area is highly vulnerable where, for example, upright corals or sponges are common. The computation of the overlap index implies that there is higher potential for a fishing effect if fishing effort is intense there. However the vulnerability and overlap indices are relative values and are not absolute measures of fishing effects. While an index value of 3 implies more effect than a value of 1, the effect is not 3 times greater for the former than the latter. Further a relatively high value does not explain whether effects were light, medium or high (i.e., not scaled to actual damage), just that effects likely were greater compared to other areas. An alternate approach to defining vulnerability is to define an organism as vulnerable if it is rare. We did not follow this population-based approach and instead focused on identifying areas where higher coral and sponge densities overlapped higher fishing effort.

## Other ecological considerations related to coral and sponge

Coral and sponge densities were much less in the Bering Canyons compared to the Aleutian Islands. Compared to Aleutian Islands average coral density of 1.23 colonies $m^{-2}$ (Stone 2006), using the same computational method we found that Pribilof Canyon average coral density (0.28) was 23% of the Aleutians value and that Zhemchug Canyon average coral density (0.15) was 12% of the Aleutian value. The frequency of occurrence of coral from trawl surveys was about 10% for the eastern Bering Sea slope and like the numeric densities, much less than the frequency of occurrence for the Aleutian Islands (~50%). Compared to Aleutian Islands average

778 sponge density of 5.25 colonies $m^{-2}$ (Stone and Alcorn in press), we found that Pribilof Canyon
779 average sponge density (0.10) was 2% of the Aleutians value and that Zhemchug Canyon
780 average coral density (0.21) was 4% of the Aleutian value. The frequency of occurrence of
781 sponge from trawl surveys was nearly 60% for the eastern Bering Sea slope and unlike the
782 numeric densities, only somewhat less than the frequency of occurrence for the Aleutian Islands
783 (nearly 100%).

784 No coral taxa, with one possible exception, are known to be endemic to the eastern
785 Bering Sea (Stone et al. in preparation). Reviews of the biogeographical distribution of corals in
786 Alaskan waters indicate that there are 19 taxa found throughout the eastern Bering Sea (Stone et
787 al. in preparation). A single recently described demosponge *Aaptos kanuxx* (Lehnert et al. 2008)
788 is known only from Pribilof Canyon so may be endemic to that region. Reviews of the
789 biogeographical distribution of sponges in Alaskan waters indicate that there are 67 taxa found
790 throughout the Bering Sea (Stone et al. 2011).

791 Our analysis of the 2002-2012 trawl surveys of the eastern Bering Sea slope found 17
792 coral, 25 sponge and 10 sea whip and sea pen taxa. Whenever two or more specimens of a taxon
793 were caught, at least one specimen was found in both canyon and non-canyon slope areas.
794 Sometimes only one specimen was caught. However this commonly happened in both canyons
795 and non-canyon slope, indicating that this occurred due to chance rather than endemism in
796 canyons. Of taxa only caught once, 13% occurred in canyons and 27% occurred in non-canyons.
797 Comparing 2002-2012 trawl survey data for eastern Bering Sea slope to other regions of Alaska,
798 we found only three taxa that occurred only on the eastern Bering Sea slope. These three taxa
799 were *Calcigorgia beringi*, Isididae unidentified (an unidentified bamboo coral) and *Antipatheria*
800 unidentified (an unidentified black coral). However *Calcigorgia beringi* ranges from the eastern
801 Bering Sea south to Washington State (Stone et al. in preparation). Additionally, at least one
802 species of bamboo coral (*Keratoisis* sp. A) and one species of black coral (*Lillipathes wingi*) are
803 known from the eastern Bering Sea and broadly distributed throughout Alaskan waters (Stone et
804 al. in preparation).

805 Recovery rates from disturbance of cold-water corals and sponges depend on several
806 factors including growth rate, recruitment rate, and reproductive ecology. Alaskan corals,
807 including *Keratoisis* sp. A (Andrews et al. 2009) and *Primnoa pacifica* (Andrews et al. 2002),
808 are slow-growing and consequently long-lived given the maximum sizes observed for these taxa.

The stylasterid corals in the Aleutian Islands (Brooke and Stone, 2007) and *Primnoa pacifica* in the Gulf of Alaska (Waller et al. in preparation) are gonochoristic brooders with limited potential to provide sources of recruits to disjunct disturbed habitats. Limited biological information for sponges indicates that they too are very susceptible to physical disturbance with long recovery periods from disturbance (Stone et al. 2011).

## Other ecological considerations related to fish, seabirds and marine mammals

There are consistent seasonal patterns of pollock spawning locations in the eastern Bering Sea, but these patterns are not uniquely associated with any eastern Bering Sea canyon; seasonally, Bacheler et al. (2012) showed that peak spawning occurs early in the year (March) in the Bogoslof and Islands of Four Mountains regions and progresses toward the slope area and around the Pribilof Islands by May. The latter concentration is found around and slightly east of the Pribilof Islands (Bacheler et al. 2010) and not limited to Pribilof Canyon.

Skates (Rajidae) deposit their large leathery egg cases in specific areas often found in eastern Bering Sea canyons. To date 14 skate nursery sites have been identified in the eastern Bering Sea. Ten of the 14 sites are at the heads of large canyons (Navarin 1, Pervenets 3, Zhemchug 2, Pribilof 2, Bering 2) with the additional 4 sites at the heads of smaller deeper canyons. Nursery sites occur on relatively flat sandy to muddy bottom with little relief or bottom structure (Hoff 2010), which is the most common eastern Bering Sea bottom type. The reason for the strong association with undersea canyons is believed to be correlated with oceanographic conditions such as bottom currents, oxygen content and productivity, but a clear understanding of site location is still being investigated (G. Hoff, pers. comm.). Recent action by the NPFMC recognized six skate nursery sites in the eastern Bering Sea as Habitat Areas of Particular Concern (HAPC) and recommended additional research into habitat and oceanographic conditions driving site selection and into impacts of disturbances on these important skate nursery areas.

Some marine mammal and seabird species commonly are found along the outer shelf and slope, sometimes associated with Bering Sea canyons. In marine mammal surveys during 1999-2004 (Friday et al. 2012), only fin whales and Dall's porpoise consistently occupied the outer and middle shelf; there was no concentration of fin whales related to Zhemchug or Pribilof canyons, whereas Dall's porpoise was concentrated in Pribilof Canyon in one of three survey

years. Both female (Call et al. 2008) and juvenile male (Sterling and Ream 2004) fur seal forage widely away from the Pribilof Islands and while sometimes located in Pribilof Canyon, show no concentration there. In seabird surveys during the 1960s, seabirds often were concentrated along the continental slope and outer shelf but not limited to canyons (Shuntov 1993). Foraging seabirds tied to a colony often forage nearby but even black-legged kittiwakes on St. George Island near Pribilof Canyon may forage farther away and not at the nearby canyon (Paredes et al. 2012). Some seabird species near the Pribilof Islands showed spatial preferences (e.g. thick-billed murres south and west of the islands) and others did not (e.g. short-tailed shearwaters showed no preference relative to the islands); no species concentrated over Pribilof Canyon (Jahncke et al. 2008). In contrast, short-tailed albatross were more common along the slope northwest of the Pribilof Islands and may concentrate in Zhemchug and Pervenets canyons (Piatt et al. 2006).

# Acknowledgments

We thank Al Hermann, NOAA's Pacific Marine Environmental Laboratory, for providing the model-based estimates of ocean currents; Carla J. Moore, NOAA's National Geophysical Data Center, for providing the sediment data; and John Hocevar, Greenpeace, for providing visual survey data of Pribilof and Zhemchug canyons. We thank Gary Greene, Moss Landing Marine Laboratory, and Dave Scholl, US Geological Survey, for advice on canyon definitions. We also thank Jon Heifetz, Carol Ladd, Bob Lauth, Ivan Mateo and Paul Spencer for their reviews and useful comments.

## References

Andrews AH, Cordes EE, Mahoney MM, Munk K, Coale KH, Cailliet GM, Heifetz J. 2002. Age, growth and radiometric age validation of a deep-sea, habitat-forming gorgonian (*Primnoa resedaeformis*) from the Gulf of Alaska. Hydrobiologia 471: 101-110.

Andrews AH, Stone RP, Lundstrom CC, DeVogelaere AP. 2009. Growth rate and age determination of bamboo corals from the northeastern Pacific Ocean using refined $^{210}$Pb dating. Marine Ecology Progress Series 397: 173–185.

Bacheler NM, Ciannelli L, Bailey KM, Duffy-Anderson JT. 2010. Spatial and temporal patterns of walleye pollock (*Theragra chalcogramma*) spawning in the eastern Bering Sea inferred from egg and larval distributions. Fisheries Oceanography 19: 107-120.

Bacheler NM, Ciannelli L, Bailey KM, Bartolino V. 2012. Do walleye pollock exhibit flexibility in where or when they spawn based on variability in water temperature? Deep-Sea Research Part II: Topical Studies in Oceanography.

Baker ET, Hickey BM. 1986. Contemporary sedimentation processes in and around an active west coast submarine canyon. Marine Geology 71: 15-34.

Behrenfeld MJ, Falkowski PG. 1997. Photosynthetic rates derived from satellite-based chlorophyll concentration. Limnology and Oceanography 42: 1-20.

Brooke S, Stone R. 2007. Reproduction of deep-water hydrocorals (family Stylasteridae) from the Aleutian Islands, Alaska. Bulletin of Marine Science 81: 519-532.

Brodeur RD. 2001. Habitat-specific distribution of Pacific ocean perch (*Sebastes alutus*) in Pribilof Canyon, Bering Sea. Continental Shelf Research 21: 207-224.

Brown EJ, Finney B, Hills S, Dommisse M. 2005. Effects of commercial otter trawling on benthic communities in the southeastern Bering Sea. In Barnes PW, Thomas JP (editors). Benthic habitats and the effects of fishing. American Fisheries Society Symposium 41, Bethesda, Maryland.

Brown ZW, van Dijken GL, Arrigo KR. 2011. A reassessment of primary production and environmental change in the Bering Sea. Journal of Geophysical Research 16, C08014, doi:10.1029/2010JC006766.

Busby MS, Mier KL, Brodeur RD. 2005. Habitat associations of demersal fishes and crabs in the Pribilof Islands regions of the Bering Sea. Fisheries Research 75: 15-28.

Call KA, Ream RR, Johnson D, Sterling JT, Towell RG. 2008. Foraging route tactics and site fidelity of adult female northern fur seal (*Callorhinus ursinus*) around the Pribilof Islands. Deep-Sea Research Part II: Topical Studies in Oceanography 55: 1883-1896.

Clement Kinney J, Maslowski W, Okkonen S. 2009. On the processes controlling shelf–basin exchange and outer shelf dynamics in the Bering Sea. Deep-Sea Research Part II: Topical Studies in Oceanography 56: 1351-1362.

Coachman LK. 1986. Circulation, water masses and fluxes on the southeastern Bering Sea shelf. Continental Shelf. Research 5: 23-108.

Danielson S, Curchitser E, Hedstrom K, Weingartner T, Stabeno P. 2011. On ocean and sea ice modes of variability in the Bering Sea, Journal of Geophysical Research 116, C12034, doi:10.1029/2011JC007389.

Danielson S, Hedstrom K, Aagaard K, Weingartner T, Curchitser E. 2012. Wind-induced reorganization of the Bering shelf circulation. Geophysical Research Letters 39, doi:10.1029/2012GL051231

De Leo FC, Smith CR, Rowden AA, Bowden DA, Clark MR. 2010. Submarine canyons: hotspots of benthic biomass and productivity in the deep sea. Proceedings Royal Society B 277: 2783–2792.

Efron B, Tibshirani R. 1993. An introduction to the bootstrap. Chapman & Hall/CRC. 437 p.

ESRI 2009. ArcGIS Desktop: Release 9. Redlands, CA: Environmental Systems Research Institute.

927 Fielding AH, Bell JF. 1997. A review of methods for the assessment of prediction errors in
928 conservation presence/absence models. Environmental Conservation 24: 38-49.
929
930 Freese L, Auster PJ, Heifetz J, Wing BL. 1999. Effects of trawling on seafloor habitat and
931 associated invertebrate taxa in the Gulf of Alaska. Marine Ecology Progress Series 182: 119-126.
932
933 Freese JL. 2001. Trawl-induced damage to sponges observed from a research submersible.
934 Marine Fisheries Review 63(3): 7-13.
935
936 Friday NA, Waite JM, Zerbini AN, Moore SE. 2012. Cetacean distribution and abundance in
937 relation to oceanographic domains on the eastern Bering Sea shelf: 1999–2004. Deep-Sea
938 Research Part II: Topical Studies in Oceanography.
939
940 Fujioka JT. 2006. A model for evaluating fishing impacts on habitat and comparing fishing
941 closure strategies. Canadian Journal of Fisheries and Aquatic Sciences, 63: 2330-2342.
942
943 Harris PT, Whiteway T. 2011. Global distribution of large submarine canyons: Geomorphic
944 differences between active and passive continental margins. Marine Geology 285: 69-86.
945
946 Hastie T, Tibshirani R. 1990. Generalized additive models. Chapman & Hall/CRC. 335 p.
947
948 Hickey BM. 1995. Coastal submarine canyons. Topographic effects in the ocean. SOEST Special
949 publications, 95-110.
950
951 Hickey BM. 1997. The response of a steep-sided, narrow canyon to time-variable wind forcing.
952 Journal of Physical Oceanography 27: 697-726.
953
954 Hoff GR. 2010. Identification of skate nursery habitat in the eastern Bering Sea. Marine Ecology
955 Progress Series 403: 243-254.
956

957 Hoff GR, Britt LL. 2011. Results of the 2010 eastern Bering Sea upper continental slope survey
958 of groundfish and invertebrate resources. U.S. Department Commerce, NOAA Technical
959 Memorandum NMFS-AFSC-224, 300 p.
960
961 Hosmer DW, Lemeshow S. 2005. Multiple logistic regression. Applied Logistic Regression,
962 Second Edition, 31-46.
963
964 Ianelli JN, Honkalehto T, BarbeauS, Kotwicki S, Aydin K, Williamson N. 2012. Assessment of
965 the walleye pollock stock in the Eastern Bering Sea. In Stock assessment and fishery evaluation
966 report for the groundfish resources of the Bering Sea/Aleutian Islands regions. North Pacific
967 Fishery Management Council, Anchorage, Alaska.
968
969 Jahncke J, Vlietstra LS, Decker MB, Hunt GL. 2008. Marine bird abundance around the Pribilof
970 Islands: a multi-year comparison. Deep-Sea Research Part II: Topical Studies in Oceanography,
971 55: 1809-1826.
972
973 Kaiser MJ, Collie JS, Hall SJ, Jennings S, Poiner IR. 2002. Modification of marine habitats by
974 trawling activities: prognosis and solutions. Fish and Fisheries 3(2), 114-136.
975
976 Karl HA, Carlson PR, Gardner JV. 1996. Aleutian Basin of the Bering Sea: Styles of
977 sedimentation and canyon development. In Gardner JF, Field ME, Twichell DC. Geology of the
978 United States seafloor: the view from GLORIA. Press Syndicate of the University of Chicago.
979
980 Kim YJ, Gu C. 2004. Smoothing spline Gaussian regression: more scalable computation via
981 efficient approximation. Journal of the Royal Statistical Society: Series B (Statistical
982 Methodology) 66: 337-356.
983
984 Kowalik Z, Stabeno P. 1999. Trapped motion around the Pribilof Islands in the Bering
985 Sea. Journal Geophysical Research, 104(C11), 25667–25684, doi:10.1029/1999JC900209.
986

Ladd C, Stabeno PJ, O'Hern JE. 2012. Observations of a Pribilof eddy. Deep-Sea Research Part I: Oceanographic Research Papers 66: 67-76.

Lauth RR. 2011. Results of the 2010 eastern and northern Bering Sea continental shelf bottom trawl survey of groundfish and invertebrate fauna. U.S. Dep. Commerce, NOAA Technical Memorandum NMFS-AFSC-227, 256 p.

Lehnert H, Hocevar J, Stone RP. 2008. A new species of *Aaptos* (Porifera, Hadromerida, Suberitidae) from Pribilof Canyon, Bering Sea, Alaska. Zootaxa 1939: 65–68.

McConnaughey RA, Smith KR. 2000. Associations between flatfish abundance and surficial sediments in the eastern Bering Sea. Canadian Journal of Fisheries and Aquatic Science 56: 2410-2419.

McConnaughey, R. A., Mier, K., and Dew, C. B. 2000. An examination of chronic trawling effects on soft-bottom benthos of the eastern Bering Sea. ICES Journal of Marine Science 57: 1377-1388.

McConnaughey R, Syrjala SE, Dew CB. 2005. Effects of chronic bottom trawling on the size structure of soft-bottom benthic invertebrates. In Barnes PW, Thomas JP (editors). Benthic habitats and the effects of fishing. American Fisheries Society Symposium 41, Bethesda, Maryland. Pages 425-437.

McConnaughey RA, Amend M, Berger J, Busby M, Campbell G, Hoff J, Ito D, Lang G, Lunsford C, Nichol D, Rodgveller C, Rose C, Shotwell K, Smith K, Stone R. 2006. A review of scientific information related to Bering Sea canyons and skate nursery areas. Available North Pacific Fisheries Management Council, 605 West 4th, Suite 306, Anchorage, Alaska 99501-2252.

McConnaughey RA, Syrjala SE. 2009. Statistical relationships between the distributions of groundfish and crabs in the eastern Bering Sea and processed returns from a single-beam echosounder. ICES Journal of Marine Science 66:1425-1432.

Miller RJ, Hocevar J, Stone RP, Fedorov DV. 2012. Structure-forming corals and sponges and their use as fish habitat in Bering Sea submarine canyons. PLoS ONE 7(3): e33885.doi:10.1371/journal.pone.0033885.

NRC (National Research Council). 2002. Effects of trawling and dredging on seafloor habitat. National Academy Press, Washington, D.C.

Normarck WR, Carlson PR. 2003. Giant submarine canyons: Is size any clue to their importance in the rock record? Geological Society America, Special Paper 370.

Paredes R, Harding A, Irons DB, Roby DD, Suryan RM, Orben RA, Renner H, Young R, Kitaysky A. 2012. Proximity to multiple foraging habitats enhances seabirds' resilience to local food shortages. Marine Ecology Progress Series 471: 253-269.

Piatt JF, Wetzel J, Bell K, DeGange AR, Balogh GR, Drew GS, Geernaert T, Ladd C, Byrd GV. 2006. Predictable hotspots and foraging habitat of the endangered short-tailed albatross (*Phoebastria albatrus*) in the North Pacific: Implications for conservation. Deep-Sea Research Part II: Topical Studies in Oceanography 53: 387-398.

Rho T, Whitledge TE. 2007. Characteristics of seasonal and spatial variations of primary production over the southeastern Bering Sea shelf. Continental Shelf Research 27: 2556-2569.

Rooper CN, Hoff GR, De Robertis A. 2010. Assessing habitat utilization and rockfish (*Sebastes* sp.) biomass in an isolated rocky ridge using acoustics and stereo image analysis. Can. J. Fish. Aquat. Sci. 67: 1658-1670.

Rose CS, Jorgensen EM. 2005. Spatial and temporal distributions of bottom trawling off Alaska: consideration of overlapping effort when evaluating the effects of fishing on habitat. In Barnes PW, Thomas JP (editors). Benthic habitats and the effects of fishing. American Fisheries Society Symposium 41, Bethesda, Maryland.

Rose CS, Gauvin JR, Hammond CF. 2010. Effective herding of flatfish by cables with minimal seafloor contact. Fishery Bulletin, U.S. 108: 136-144.

Ross RE, Howell KL. 2013. Use of predictive habitat modelling to assess the distribution and extent of the current protection of 'listed'deep-sea habitats. Diversity and Distributions 19: 433-445.

Schumacher JD, Reed RK. 1992. Characteristics of currents over the continental slope of the eastern Bering Sea. Journal of Geophysical Research 97(C6), 9423-9433.

Schumacher JD. Stabeno PJ. 1994. Ubiquitous eddies of the eastern Bering Sea and their coincidence with concentrations of larval pollock. Fisheries Oceanography 3: 182-190.

Shuntov VP. 1993. Biological and physical determinantsof marine bird distribution in the Bering Sea. In: The status, ecology, and conservation of marine birds of the North Pacific, Editors Vermeer K, Briggs KT, Morgan KH, Siegel-Causey D.

Smith KR, McConnaughey RA. 1999. Surficial sediments of the eastern Bering Sea continental shelf: EBSSED database documentation. U.S. Department Commerce, NOAA Tech. Memo. NMFS-AFSC-104, 41 p.

Springer AM, McRoy CP, Flint MV. 1996. The Bering Sea Green Belt: shelf-edge processes and ecosystem production. Fisheries Oceanography, 5: 205–223. doi: 0.1111/j.1365-2419.1996.tb00118.x

Stabeno PJ, Schumacher JD, Ohtani K. 1999. The physical oceanography of the Bering Sea. In: Loughlin, T.R., Ohtani, K. (Eds.), Dynamics of the Bering Sea: A Summary of Physical, Chemical, and Biological Characteristics, and a Synopsis of Research on the Bering Sea, North Pacific Marine Science Organization (PICES), University of Alaska Sea Grant, AK-SG-99-03, Fairbanks, Alaska, USA, pp. 1–28.

Stabeno PJ, Kachel N, Mordy C, Righi D, Salo S. 2008. An examination of the physical variability around the Pribilof Islands in 2004. Deep-Sea Res. II 55: 1701-1716.

Sterling JT, Ream RR. 2004. At-sea behavior of juvenile male northern fur seals (*Callorhinus ursinus*). Canadian Journal of Zoology, 82: 1621-1637.

Stone RP, Masuda MM, Malecha PW. 2005. Effects of bottom trawling on soft-sediment epibenthic communities in the Gulf of Alaska. In American Fisheries Society Symposium (Vol. 41, p. 461). American Fisheries Society.

Stone RP. 2006. Coral habitat in the Aleutian Islands of Alaska: depth distribution, fine-scale species associations, and fisheries interactions. Coral Reefs 25: 229-238.

Stone RP, Alcorn D. In press. The ecology of deep-sea coral and sponge habitats of the central Aleutian Islands of Alaska.

Stone RP, Lehnert H, Reiswig H. 2011. A guide to the deep-water sponges of the Aleutian Island Archipelago. U.S. Department of Commerce, NOAA Professional Paper NMFS 12, 187 p.

Stone R, Guinotte J, Cohen A, Cairns SD. In preparation. Calcium carbonate mineralogy of Alaskan corals. NOAA Technical Memorandum.

Venables WN, Ripley BD. 2002. Modern Applied Statistics With S. Springer New York, 2002. 495 p.

Vetter EW, Dayton PK. 1999. Organic enrichment by macrophyte detritus, and abundance patterns of megafaunal populations in submarine canyons. Marine Ecology Progress Series 186, 137–148.

Waller RG, Stone R, Johnstone J, Mondragon J. In preparation. Sexual reproduction and seasonality of the Alaskan red tree coral *Primnoa pacifica*.

Wood SN. 2006. Generalized additive models: an introduction with R (Vol. 66). Chapman & Hall.

Woodby D, Carlile D, Hulbert L. 2009. Predictive modeling of coral distribution in the Central Aleutian Islands, USA. Marine Ecology Progress Series 397: 227-240.

Table 1. Data groupings for multivariate analyses of habitat data. Case A: all years when both surveys occurred (2002, 2004, 2008, 2010 and 2012) using data from both surveys; Case B: data from the same 5 years, slope survey only; Case C: 2012 slope survey data only (when additional types of oceanographic measurements were collected).

| | **Case A** | **Case B** | **Case C** |
|---|---|---|---|
| **Variable** | all years, shelf and slope | all years, slope | 2012 |
| depth | X | X | X |
| slope | X | X | X |
| grain size | X | X | X |
| ocean color | X | X | X |
| sediment sorting | X | X | X |
| current | X | X | X |
| temperature | X | X | X |
| salinity | | | X |
| oxygen | | | X |
| turbidity | | | X |
| pH | | | X |

1127 Table 2. Top 10 fish and crab species by survey (longline, shelf trawl, slope trawl) during 2002-
1128 2012.
1129

| Common name | longline | shelf trawl | slope trawl |
|---|---|---|---|
| Alaska skate | | X | |
| Aleutian skate | X | | X |
| arrowtooth flounder | X | X | X |
| Kamchatka flounder | | | X |
| Greenland turbot | X | | X |
| Pacific halibut | X | X | |
| flathead sole | | X | X |
| yellowfin sole | | X | |
| northern rock sole | | X | |
| Alaska plaice | | X | |
| sablefish | X | | |
| giant grenadier | X | | X |
| Pacific grenadier | | | X |
| Pacific cod | X | X | |
| walleye pollock | X | X | X |
| shortspine thornyhead | X | | X |
| shortraker rockfish | X | | |
| rougheye or blackspotted rockfish | X | | |
| Pacific ocean perch | | | X |
| snow crab | | X | |

Table 3. Data groupings for coral, sponge and sea whip/sea pen data. For each taxa, the number and weight caught and their higher-level groupings (e.g. hard corals) used in the statistical analyses are shown. In addition, scores for susceptibility to physical damage by taxa are shown.

| High-level grouping | Mid-level grouping | Taxon | Number caught | Weight (kg) caught | Susceptibility score |
|---|---|---|---|---|---|
| Corals | Paragorgiidae | *Paragorgia* sp. | 7 | 1.68 | 3 |
| Corals | Paragorgiidae | *Paragorgia arborea* | 30 | 55.41 | 3 |
| Corals | Primnoidae | *Amphilaphis* sp. (*Plumarella* spp.) | 23 | 3.78 | 2 |
| Corals | Primnoidae | *Primnoa willeyi* | 3 | 0.70 | 3 |
| Corals | Primnoidae | *Plumarella* sp. | 7 | 0.36 | 2 |
| Corals | Primnoidae | *Primnoa* sp. | 4 | 2.10 | 3 |
| Corals | Primnoidae | *Plumarella* sp. 1 (Bayer) | 1 | 0.02 | 2 |
| Corals | Antipatharia | Antipatharia | 5 | 0.24 | 3 |
| Corals | Antipatharia | *Lillipathes* sp. B | 2 | 0.20 | 3 |
| Corals | Antipatharia | *Crysopathes speciosa* | 1 | 0.20 | 3 |
| Corals | Plexauridae | *Swiftia* sp. | 13 | 0.74 | 1 |
| Corals | Plexauridae | *Swiftia pacifica* | 1 | 0.00 | 1 |
| Corals | Plexauridae | *Swiftia* cf. *beringi* | 4 | 0.07 | 1 |
| Corals | Plexauridae | Muriceides cf. cylindrical (*Calcigorgia beringi*) | 1 | 0.02 | 1 |
| Corals | Isididae | *Isidella* sp. | 26 | 11.73 | 3 |
| Corals | Isididae | *Keratoisis* sp. | 3 | 1.41 | 3 |
| Corals | Isididae | Isididae (unidentified) | 1 | 4.57 | 3 |
| Sea whips | Pennatulacea | Pennatulacea | 41 | 31.59 | 3 |
| Sea whips | Pennatulacea | *Virgularia* sp. (*Halipteris* sp. A) | 16 | 32.46 | 3 |
| Sea whips | Pennatulacea | Virgulariidae (*Halipteris* sp. A) | 63 | 119.95 | 3 |
| Sea whips | Pennatulacea | *Stylatula* sp. | 11 | 0.22 | 2 |
| Sea whips | Pennatulacea | *Halipteris* sp. | 11 | 0.65 | 3 |
| Sea whips | Pennatulacea | *Halipteris willemoesi* | 20 | 1.34 | 3 |
| Sea whips | Pennatulacea | *Halipteris californica* | 1 | 0.00 | 3 |
| Sea whips | Pennatulacea | *Ombellula* sp. | 1 | 0.00 | 1 |
| Sea whips | Pennatulacea | *Anthoptilum murrayi* (*Halipteris* sp. B) | 5 | 13.45 | 2 |
| Sponges | Hexactinellid | *Aphrocallistes vastus* | 119 | 120.26 | 3 |
| Sponges | Porifera | Sponge unidentified | 405 | 789.83 | 2 |
| Sponges | Porifera | Vase sponge | 11 | 32.52 | 3 |
| Sponges | Demosponge | *Suberites* sp. | 6 | 24.84 | 1 |
| Sponges | Demosponge | *Suberites ficus* | 6 | 0.02 | 1 |

| | | | | | |
|---|---|---|---|---|---|
| Sponges | Demosponge | *Mycale* sp. | 2 | 0.75 | 2 |
| Sponges | Demosponge | *Mycale loveni* | 18 | 6.59 | 3 |
| Sponges | Demosponge | *Halichondria* sp. | 1 | 0.32 | 2 |
| Sponges | Demosponge | *Halichondria panicea* | 2 | 11.33 | 2 |
| Sponges | Demosponge | *Stelodoryx oxeata* (scapula) | 4 | 0.60 | 2 |
| Sponges | Demosponge | cf. *Myxilla lacunosa* | 1 | 0.10 | 2 |
| Sponges | Demosponge | *Isodictya quatsinoensis* | 2 | 0.03 | 2 |
| Sponges | Demosponge | *Axinella blanca* | 4 | 0.33 | 3 |
| Sponges | Demosponge | *Polymastia* sp. | 3 | 0.86 | 1 |
| Sponges | Demosponge | *Halichondria* cf. *sitiens* | 1 | 0.01 | 2 |
| Sponges | Demosponge | *Stelletta* sp. | 1 | 0.15 | 2 |
| Sponges | Hexactinellid | *Rhabdocalyptus* sp. | 9 | 8.44 | 2 |
| Sponges | Hexactinellid | *Staurocalyptus* sp. | 2 | 23.67 | 2 |

1134
1135

Table 4. Results of quadratic discriminant function analysis, where the model predicts group membership for the shelf and slope survey data from 2002, 2004, 2008, 2010, and 2012. Discrimination was performed using physical habitat variables.

| | | Predicted classification | | | | |
|---|---|---|---|---|---|---|
| Observed classification | Total stations | EBS Inner Shelf | EBS Middle Shelf | EBS Outer Shelf | Inter-canyon Slope | Canyon |
| EBS Inner Shelf | 444 | **0.97** | 0.03 | | | |
| EBS Middle Shelf | 871 | 0.06 | **0.90** | 0.04 | | |
| EBS Outer Shelf | 616 | | 0.12 | **0.80** | 0.04 | 0.04 |
| Inter-canyon Slope | 439 | | | 0.04 | **0.78** | 0.18 |
| Canyon | 326 | | | 0.11 | 0.10 | **0.79** |

Table 5. Results of quadratic discriminant function analysis, where the model predicts group membership for the eastern Bering Sea slope data as either a canyon or not a canyon from 2002, 2004, 2008, 2010, and 2012. Discrimination was performed using physical habitat variables.

| Observed classification | Total stations | Predicted classification Inter-canyon Slope | Canyon |
|---|---|---|---|
| Inter-canyon Slope | 326 | **0.89** | 0.11 |
| Canyon | 439 | 0.19 | **0.81** |

Results of quadratic discriminant function analysis, where the model predicts group membership for Pribilof canyon and its surrounding slope areas from 2002, 2004, 2008, 2010, and 2012. Discrimination was performed using the physical habitat variables.

| | | Predicted classification | |
|---|---|---|---|
| | Total stations | NOT | PC |
| NOT | 300 | **1.00** | 0.00 |
| PC | 60 | 0.02 | **0.98** |

Results of quadratic discriminant function analysis, where the model predicts group membership for Zhemchug canyon and its surrounding slope areas from 2002, 2004, 2008, 2010, and 2012. Discrimination was performed using the physical habitat variables.

| | | Predicted classification | |
|---|---|---|---|
| | Total stations | NOT | ZC |
| NOT | 236 | **0.98** | 0.02 |
| ZC | 76 | 0.01 | **0.99** |

Table 6. Results of quadratic discriminant function analysis, where the model predicts group membership for Pribilof canyon and its surrounding slope areas from 2002, 2004, 2008, 2010, and 2012. Discrimination was performed using the log-transformed CPUE of invertebrate species groups.

| | | Predicted classification | |
|---|---|---|---|
| | Total stations | NOT | PC |
| NOT | 300 | **0.95** | 0.05 |
| PC | 60 | 0.78 | **0.22** |

Results of quadratic discriminant function analysis, where the model predicts group membership for Zhemchug canyon and its surrounding slope areas from 2002, 2004, 2008, 2010, and 2012. Discrimination was performed using the log-transformed CPUE of invertebrate species groups.

| | | Predicted classification | |
|---|---|---|---|
| | Total stations | NOT | ZC |
| NOT | 236 | **0.89** | 0.11 |
| ZC | 76 | 0.84 | **0.16** |

Results of quadratic discriminant function analysis, where the model predicts group membership for Pribilof canyon and its surrounding slope areas from 2002, 2004, 2008, 2010, and 2012. Discrimination was performed using the CPUE of the top 20 fish species.

| | | Predicted classification | |
|---|---|---|---|
| | Total stations | NOT | PC |
| NOT | 300 | **0.97** | 0.03 |
| PC | 60 | 0.70 | **0.30** |

Results of quadratic discriminant function analysis, where the model predicts group membership for Zhemchug canyon and its surrounding slope areas from 2002, 2004, 2008, 2010, and 2012. Discrimination was performed using the CPUE of the top 20 fish species.

| | | Predicted classification | |
|---|---|---|---|
| | Total stations | NOT | ZC |
| NOT | 236 | **0.92** | 0.08 |
| ZC | 76 | 0.49 | **0.51** |

Table 7. Generalized additive model results for coral, sponge and sea whip data (n = 1,361) for Bering slope and outer shelf habitats and statistically significant variables, unbiased risk estimator (UBRE) score and deviance explained.

| Taxon | Significant variables ($p < 0.05$) | UBRE score | Deviance explained |
|---|---|---|---|
| Coral | Long*Lat, Seafloor gradient, Current speed | -0.638 | 0.393 |
| Sea whip | Long*Lat, Depth, Seafloor gradient, Bottom temperature, Current speed, Ocean color | -0.472 | 0.362 |
| Sponge | Long*Lat, Depth, Seafloor gradient, Bottom temperature, Current speed, Ocean color, Grain size, Sediment sorting | 0.0550 | 0.312 |

Table 8. Generalized additive model results for classification of coral, sponge and sea whip data for Bering slope and outer shelf habitats. The abbreviations are Cohen's Kappa (Fielding and Bell 1997) and area under the curve (AUC).

| | | | Predicted | | | | |
|---|---|---|---|---|---|---|---|
| Taxon | Threshold | Observed | Absent | Present | Percent correct | Kappa (sd) | AUC (sd) |
| Coral | 0.30 | Absent | 1251 | 44 | 93% | 0.44 (0.05) | 0.92 (0.01) |
| | | Present | 46 | 40 | | | |
| Sea whip | 0.28 | Absent | 1145 | 67 | 90% | 0.51 (0.04) | 0.90 (0.01) |
| | | Present | 65 | 84 | | | |
| Sponge | 0.53 | Absent | 548 | 158 | 77% | 0.54 (0.02) | 0.85 (0.01) |
| | | Present | 157 | 498 | | | |

Table 9. The predicted presence of each taxon expressed as the percentage of total area within a habitat, as a percentage of the total area of the slope and as a percentage of the total area within the slope and outer shelf habitats combined.

| Taxa | Area | Absent ($km^2$) | Present ($km^2$) | Within area (%) | Within slope (%) | Within slope and outer shelf (%) |
|---|---|---|---|---|---|---|
| Coral | Bering Canyon | 3294 | 17 | 1% | 1% | 0% |
| | Bering-Pribilof | 5330 | 38 | 1% | 1% | 1% |
| | Pribilof Canyon | 1888 | 982 | 34% | 33% | 20% |
| | Pribilof-Zhemchug | 4493 | 850 | 16% | 29% | 17% |
| | Zhemchug Canyon | 2976 | 28 | 1% | 1% | 1% |
| | Zhemchug-Pervenets | 3222 | 523 | 14% | 18% | 11% |
| | Pervenets Canyon | 1317 | 153 | 10% | 5% | 3% |
| | Pervenets-Navarin | 1188 | 0 | 0% | 0% | 0% |
| | Navarin Canyon | 1530 | 387 | 20% | 13% | 8% |
| | Outer shelf | 133163 | 1888 | 1% | na | 39% |
| Sea whip | Bering Canyon | 3174 | 137 | 4% | 5% | 0% |
| | Bering-Pribilof | 5003 | 365 | 7% | 14% | 1% |
| | Pribilof Canyon | 2870 | 0 | 0% | 0% | 0% |
| | Pribilof-Zhemchug | 4309 | 1034 | 19% | 38% | 4% |
| | Zhemchug Canyon | 2619 | 385 | 13% | 14% | 1% |
| | Zhemchug-Pervenets | 3354 | 391 | 10% | 15% | 1% |
| | Pervenets Canyon | 1430 | 40 | 3% | 1% | 0% |
| | Pervenets-Navarin | 1026 | 162 | 14% | 6% | 1% |
| | Navarin Canyon | 1744 | 173 | 9% | 6% | 1% |
| | Outer shelf | 108827 | 26224 | 19% | na | 91% |
| Sponge | Bering Canyon | 471 | 2840 | 86% | 17% | 6% |
| | Bering-Pribilof | 2706 | 2662 | 50% | 16% | 6% |
| | Pribilof Canyon | 210 | 2660 | 93% | 16% | 6% |
| | Pribilof-Zhemchug | 2240 | 3103 | 58% | 18% | 7% |
| | Zhemchug Canyon | 1032 | 1972 | 66% | 12% | 4% |
| | Zhemchug-Pervenets | 2418 | 1327 | 35% | 8% | 3% |
| | Pervenets Canyon | 500 | 970 | 66% | 6% | 2% |
| | Pervenets-Navarin | 984 | 204 | 17% | 1% | 0% |
| | Navarin Canyon | 814 | 1103 | 58% | 7% | 2% |
| | Outer shelf | 105164 | 29887 | 22% | na | 64% |

Table 10. General additive model results for fish and crab data (n = 1,361) for outer shelf and slope data and statistically significant variables, generalized cross-validation (GCV) score and deviance explained. Alaska plaice and yellowfin sole were dropped from this analysis because they are only found in the inner and middle shelf.

| Common name | Significant variables ($p < 0.05$) | GCV score | Deviance explained |
|---|---|---|---|
| Alaska skate | Long*Lat, Depth, Bottom temperature, Ocean color | 4.235 | 0.682 |
| Aleutian skate | Long*Lat, Depth, Current speed, Ocean color, Grain size, Sediment sorting | 5.322 | 0.578 |
| Arrowtooth flounder | Long*Lat, Depth, Bottom temperature, Current speed, Ocean color, Grain size | 1.619 | 0.826 |
| Flathead sole | Long*Lat, Depth, Bottom temperature, Current speed, Ocean color, Grain size, Sediment sorting | 2.475 | 0.796 |
| Giant grenadier | Long*Lat, Depth, Bottom temperature, Current speed, Ocean color, Grain size, Sediment sorting | 1.038 | 0.905 |
| Greenland turbot | Long*Lat, Depth, Seafloor gradient, Bottom temperature, Ocean color, Grain size | 5.965 | 0.652 |
| Kamchatka flounder | Long*Lat, Depth, Bottom temperature, Current speed, Grain size | 2.865 | 0.536 |
| Northern rock sole | Long*Lat, Depth, Bottom temperature, Ocean color, Grain size, Sediment sorting | 1.844 | 0.681 |
| Pacific cod | Long*Lat, Depth, Bottom temperature, Current speed, Ocean color, Grain size, Sediment sorting | 1.308 | 0.838 |
| Pacific grenadier | Long*Lat, Depth, Seafloor gradient, Current speed, Ocean color, Grain size, Sediment sorting | 1.519 | 0.792 |
| Pacific halibut | Long*Lat, Depth, Grain size, Sediment | 3.508 | 0.313 |

| | | | |
|---|---|---|---|
| | sorting | | |
| Pacific ocean perch | Long*Lat, Depth, Current speed, Ocean color, Grain size | 4.486 | 0.742 |
| Pollock | Long*Lat, Depth, Bottom temperature, Current speed, Grain size, Sediment sorting | 7.902 | 0.704 |
| Rougheye/black spotted rockfish | Long*Lat, Depth, Seafloor gradient, Bottom temperature, Ocean color, Grain size, Sediment sorting | 2.877 | 0.446 |
| Sablefish | Long*Lat, Depth, Seafloor gradient, Current speed, Ocean color, Sediment sorting | 0.983 | 0.719 |
| Shortraker rockfish | Long*Lat, Depth, Seafloor gradient, Current speed, Ocean color, Sediment sorting | 1.971 | 0.484 |
| Shortspine thornyhead | Long*Lat, Depth, Seafloor gradient, Bottom temperature, Current speed, Ocean color, Grain size, Sediment sorting | 4.694 | 0.833 |
| Snow crab | Long*Lat, Depth, Seafloor gradient, Bottom temperature, Grain size, Sediment sorting | 4.907 | 0.752 |

1196
1197

1198 Figure 1. Some of the largest submarine canyons in the world incise the eastern Bering Sea shelf
1199 break including Bering, Pribilof, Zhemchug, Pervenets and Navarin canyons.

1200

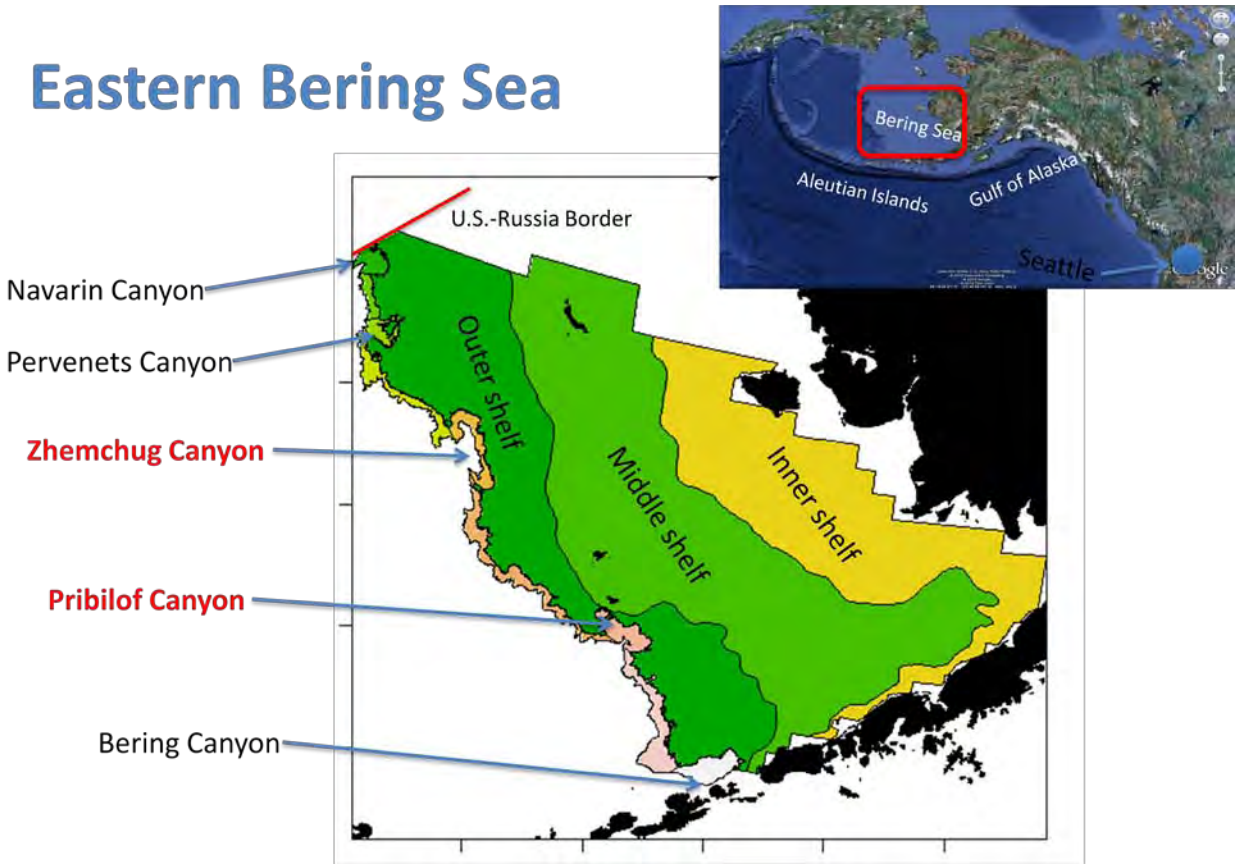


1201

1202

Figure 2. Biplot of principal components 1 and 2 of all years and areas of eastern Bering Sea survey data showing individual bottom trawl hauls labeled by their area classification (5 canyons, 5 intercanyon areas and outer shelf stations). The physical habitat variables are from data collected with the bottom trawl survey tow (depth), data interpolated from survey data (long term average temperature) and inferred from other sources (slope, color, speed, and phi). Survey tow locations from 2002, 2004, 2008, 2010 and 2012 are used (Case A). The continuous line oval indicates slope stations and the dashed line oval indicates shelf stations; for the latter, inner shelf stations are leftward, outer shelf stations are rightward and middle shelf stations are in between.

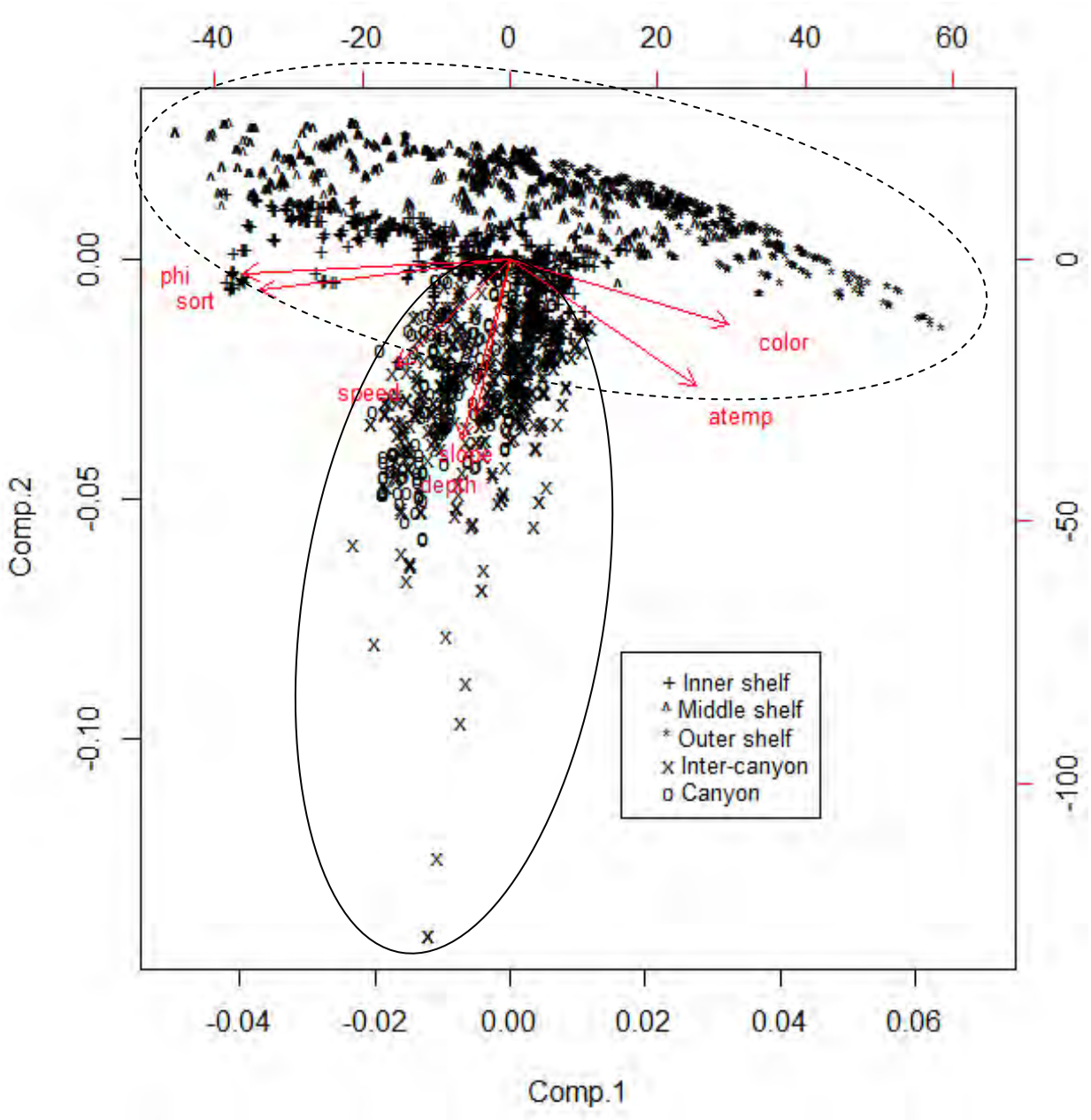

Figure 3. Biplots of principal components 1 to 3 of all years and areas of slope data showing individual bottom trawl hauls labeled by their area classification. The physical habitat variables are from data collected with the bottom trawl survey tow (depth), data interpolated from survey data (long-term average temperature) and inferred from other sources (slope, color, speed, and phi). Survey tow locations from 2002, 2004, 2008, 2010 and 2012 are used (Case B). The oval in the upper biplot (Figure 3a) indicates stations in Zhemchug Canyon. The oval in the lower biplot (Figure 3b) indicates stations in Pribilof Canyon.

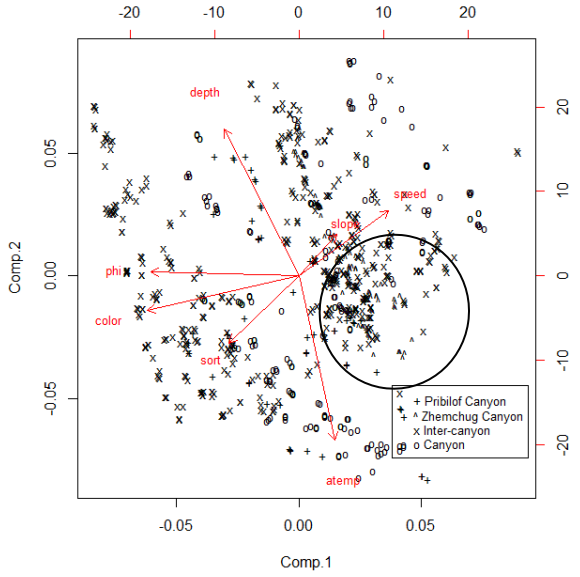


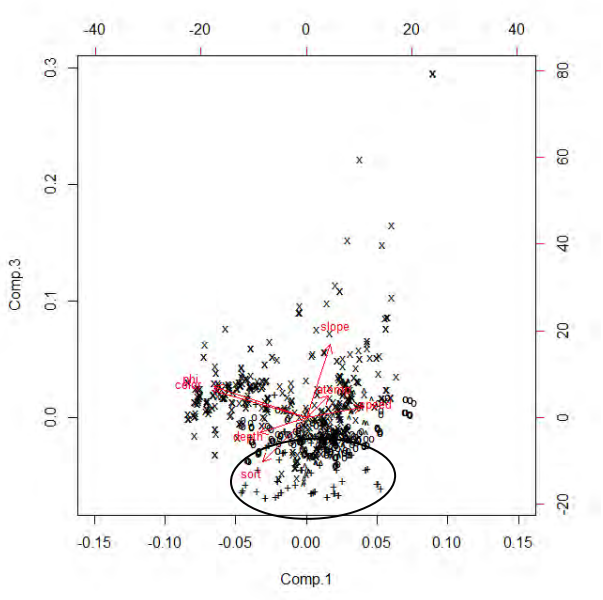

Figure 4a. Probability that coral is present by 1 x 1 km grid cell for the eastern Bering Sea shelf and outer slope based on generalized additive modeling. The x-axis label is easting and the y-axis label is northing and the unit is meters (Alaska Albers Equal Area Conic projection with center latitude = 50° N and center longitude = 154° W).

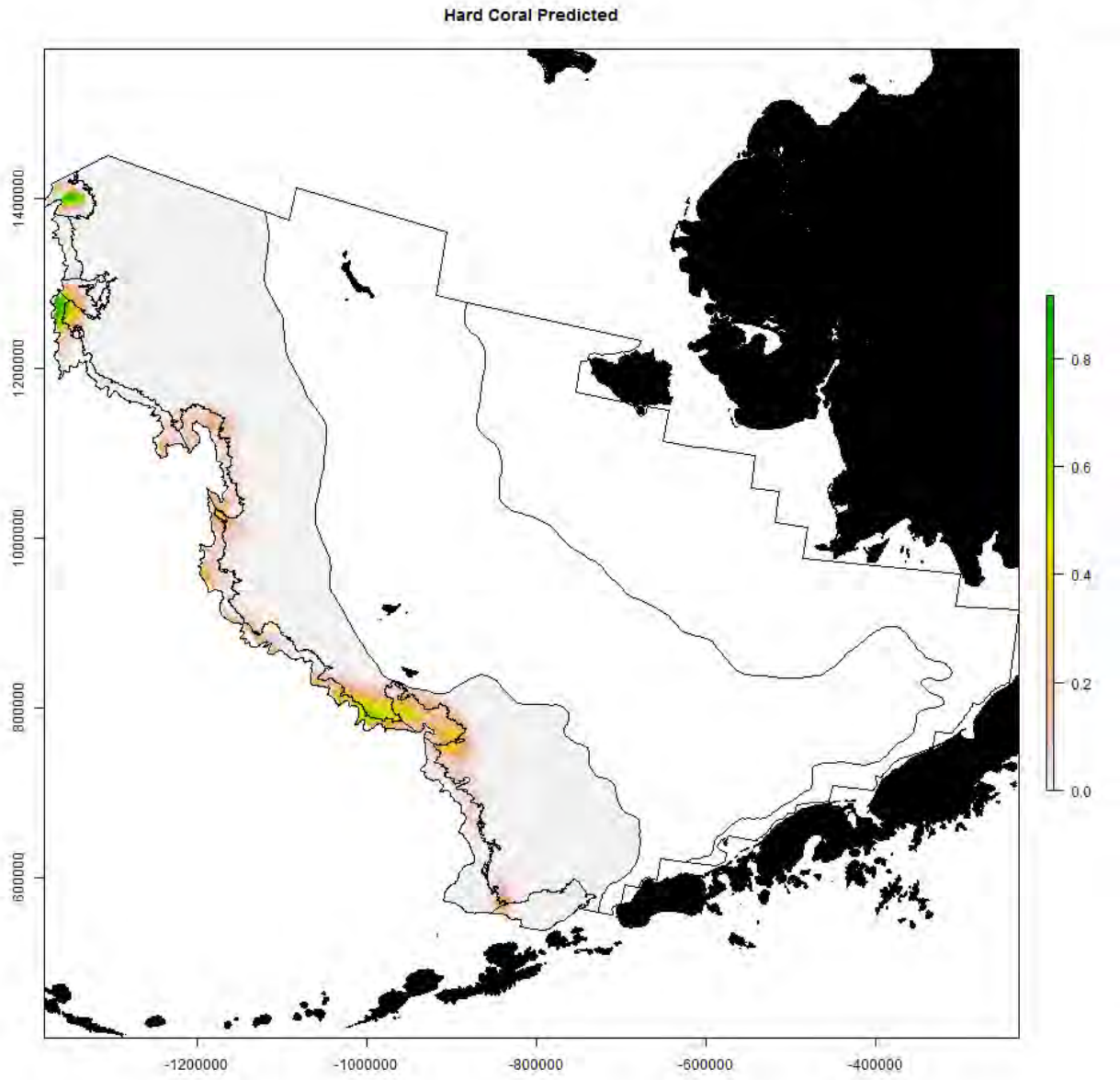

Figure 4b. Probability that sponge is present by 1 x 1 km grid cell for the eastern Bering Sea shelf and outer slope based on generalized additive modeling. The x-axis label is easting and the y-axis label is northing and the unit is meters (Alaska Albers Equal Area Conic projection with center latitude = 50° N and center longitude = 154° W).

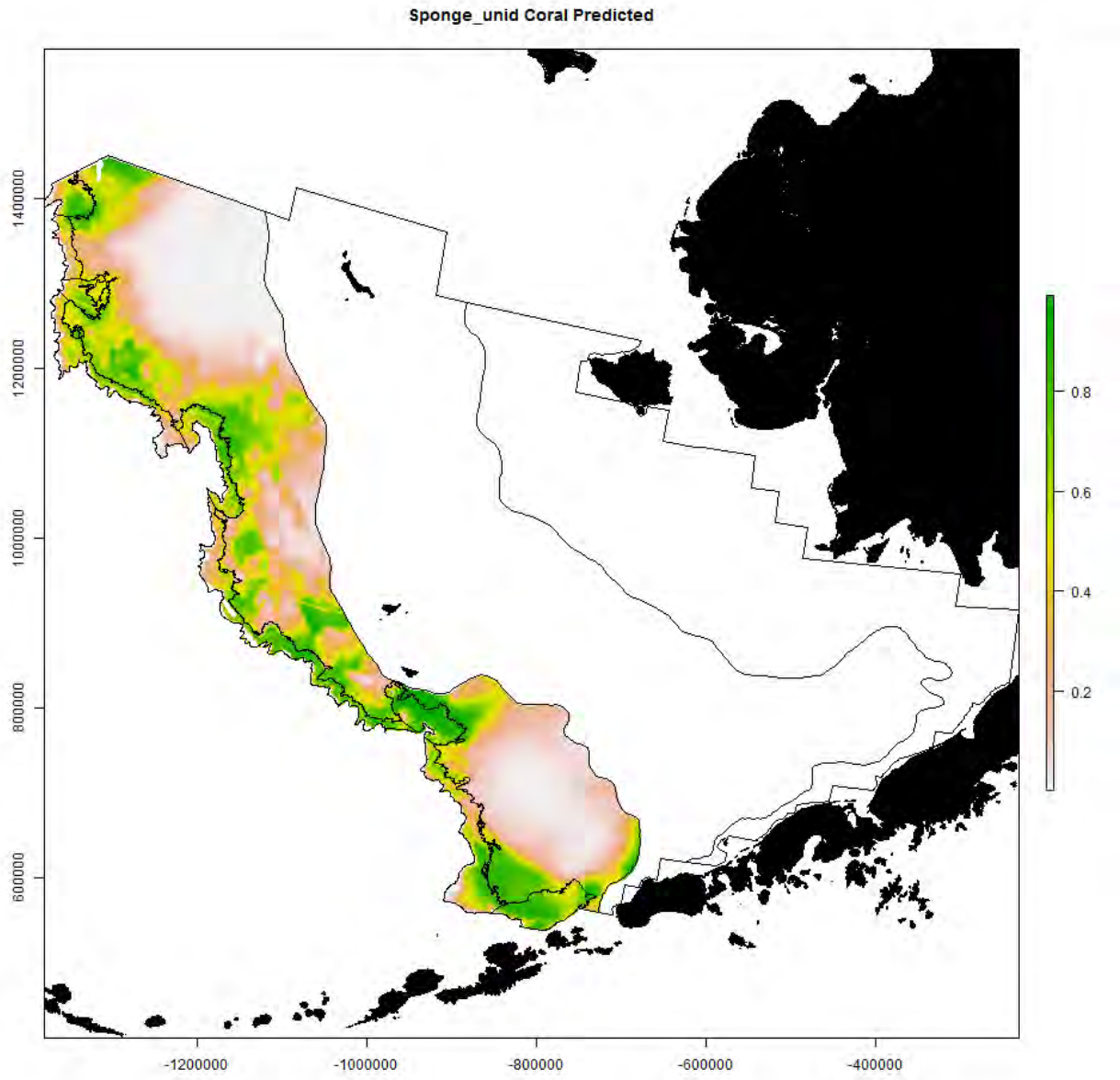

Figure 4c. Probability that sea whip is present by 1 x 1 km grid cell for the eastern Bering Sea shelf and outer slope based on generalized additive modeling. The x-axis label is easting and the y-axis label is northing and the unit is meters (Alaska Albers Equal Area Conic projection with center latitude = 50° N and center longitude = 154° W).

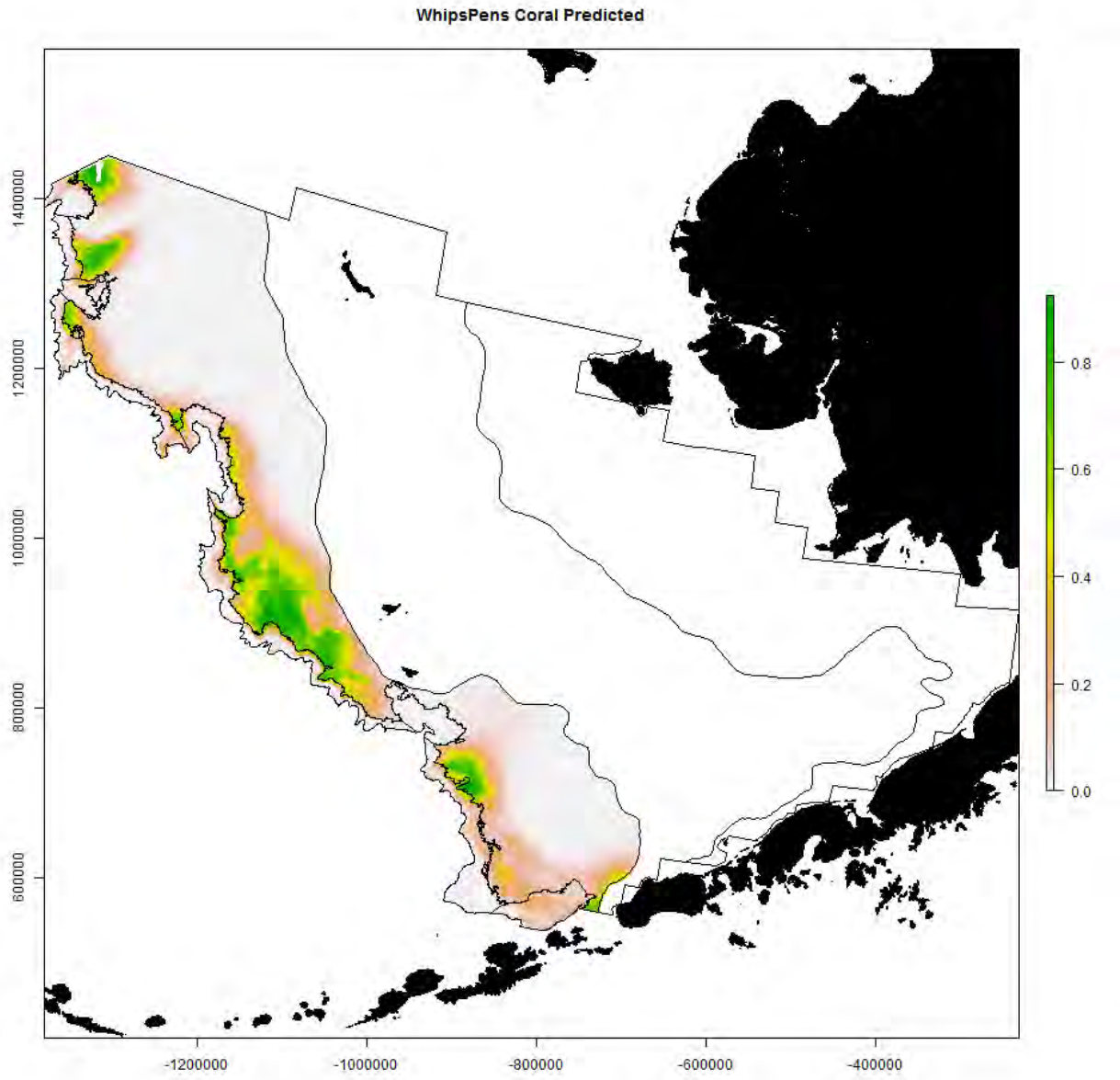

Figure 5a. Numerical densities (colonies $m^{-2}$) of coral and sponge from visual surveys. Pribilof and Zhemchug canyons data courtesy of John Hocevar, Greenpeace (do not cite without permission of J. Hocevar). Aleutian data from Stone (2006).

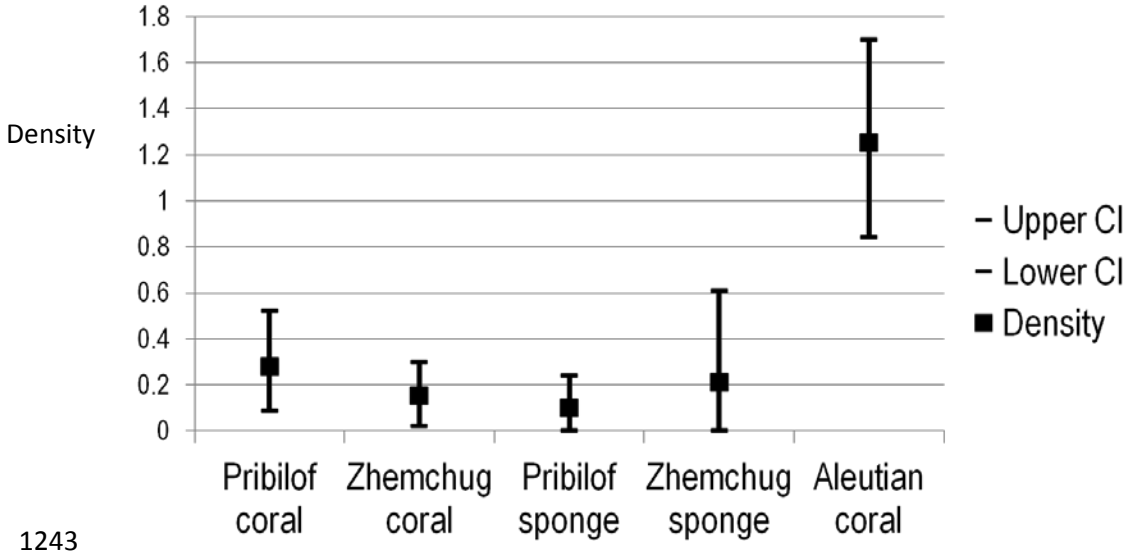


Figure 5b. Frequency of occurrence of coral, sponge and sea whip during trawl surveys in Alaska.

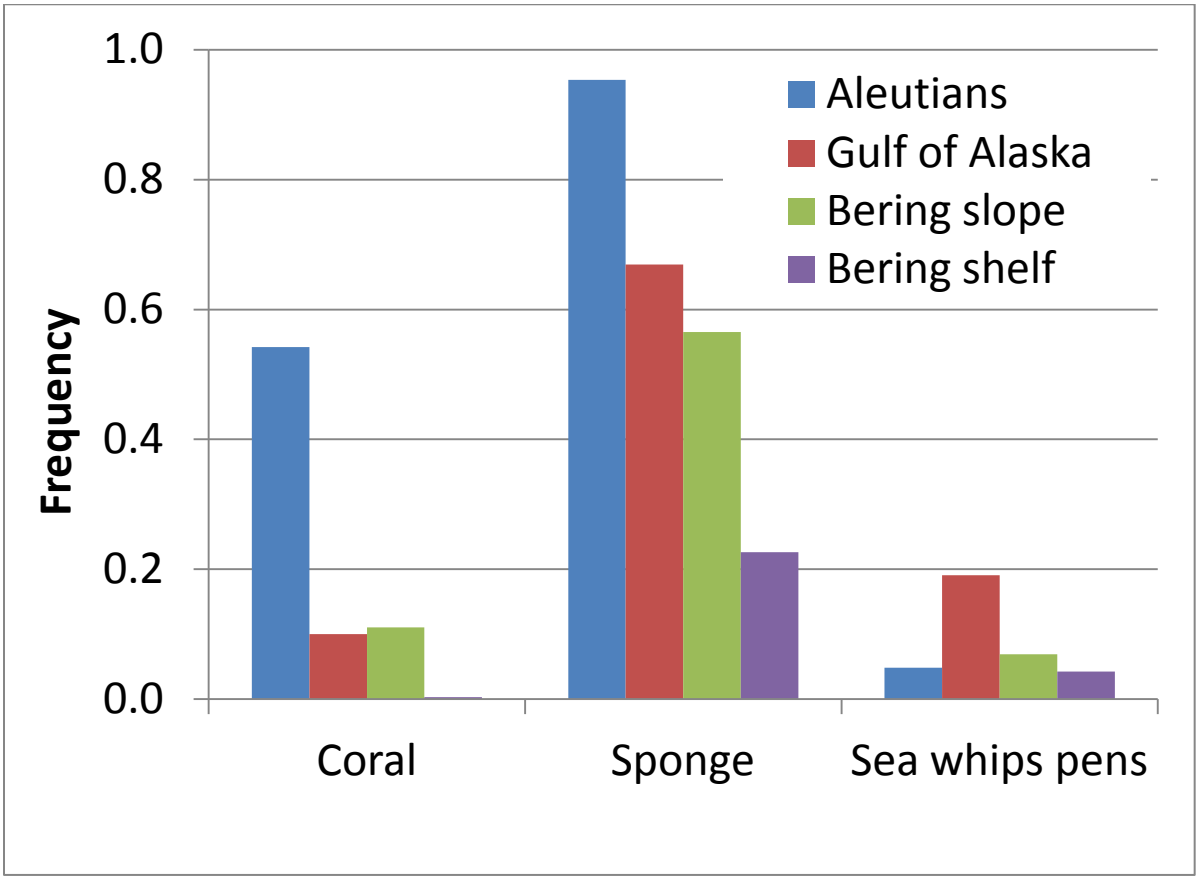

Figure 6a. Predicted LCPUE of arrowtooth flounder, a shelf species, by 1 x 1 km grid cell for the eastern Bering Sea shelf and outer slope based on generalized additive modeling. Red crosses indicate survey tow locations from 2002, 2004, 2008, 2010 and 2012 where arrowtooth flounder was observed. The x-axis label is easting and the y-axis label is northing and the unit is meters (Alaska Albers Equal Area Conic projection with center latitude = 50° N and center longitude = 154° W).

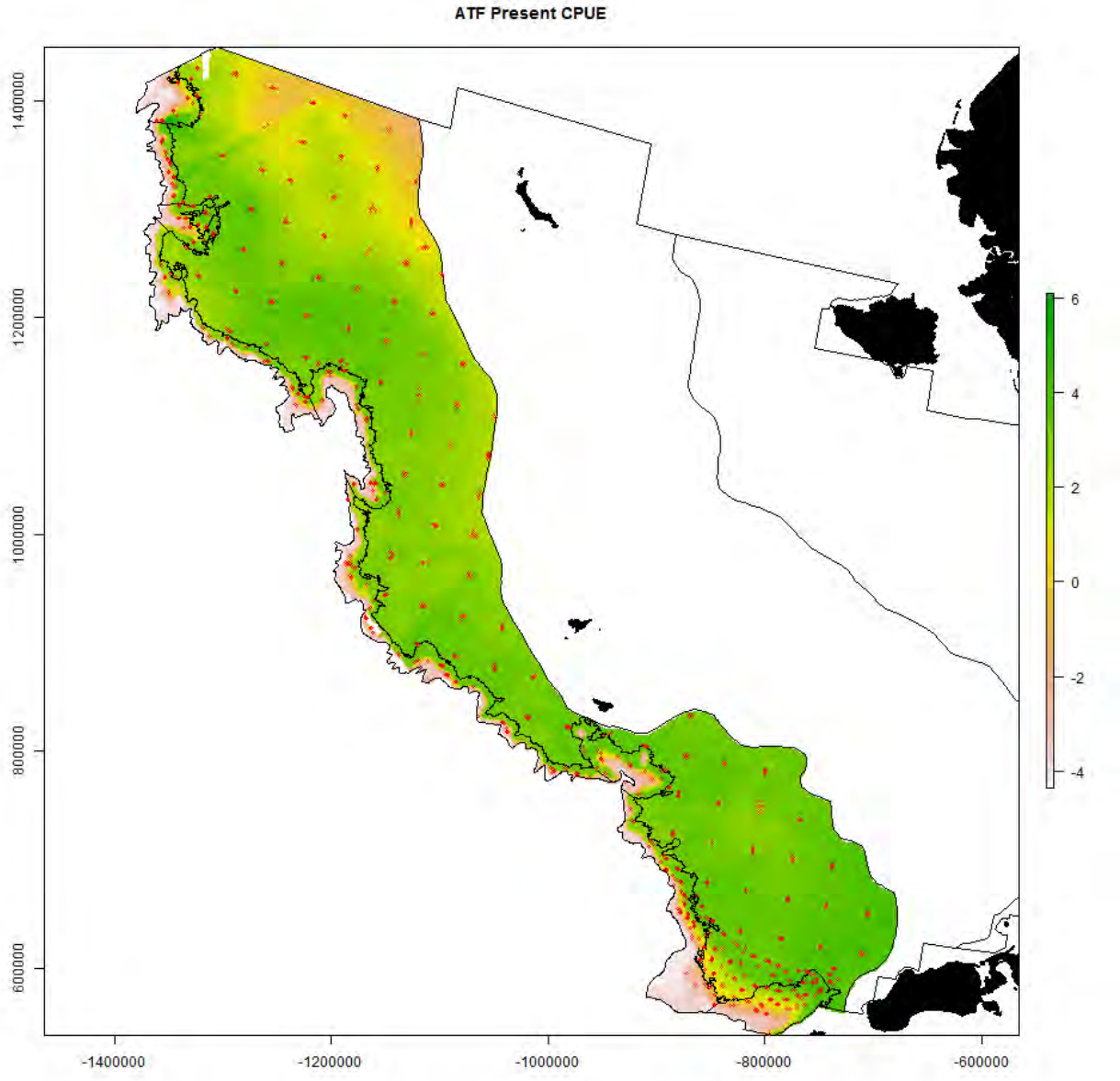

Figure 6b. Predicted LCPUE of Pacific ocean perch, a shelf break species, by 1 x 1 km grid cell for the eastern Bering Sea shelf and outer slope based on generalized additive modeling. Red crosses indicate survey tow locations from 2002, 2004, 2008, 2010 and 2012 where Pacific ocean perch was observed. The x-axis label is easting and the y-axis label is northing and the unit is meters (Alaska Albers Equal Area Conic projection with center latitude = 50° N and center longitude = 154° W).

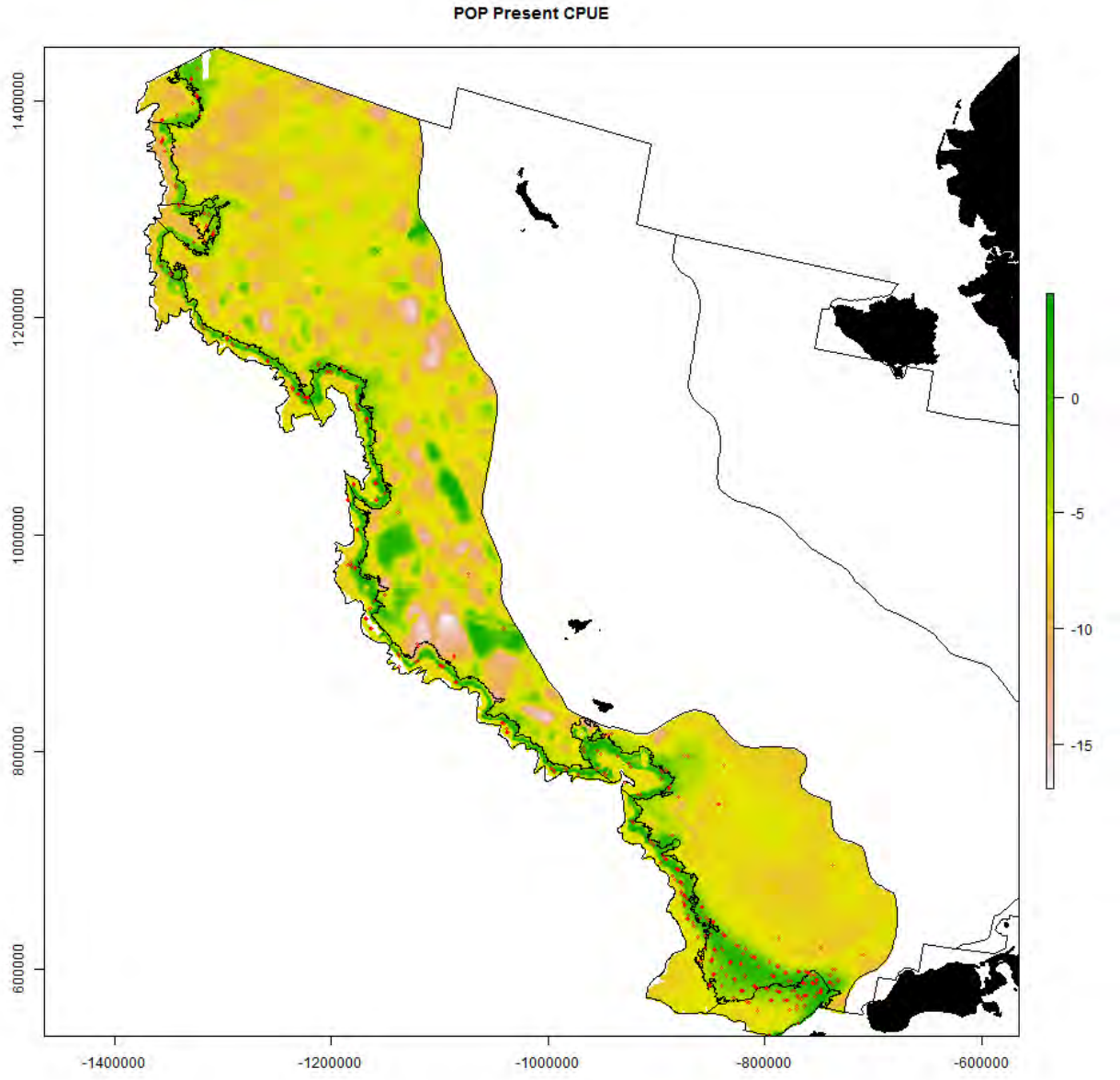

Figure 6c. Predicted LCPUE of sablefish, a slope species, by 1 x 1 km grid cell for the eastern Bering Sea shelf and outer slope based on generalized additive modeling. Red crosses indicate survey tow locations from 2002, 2004, 2008, 2010 and 2012 where sablefish was observed. The x-axis label is easting and the y-axis label is northing and the unit is meters (Alaska Albers Equal Area Conic projection with center latitude = 50° N and center longitude = 154° W).

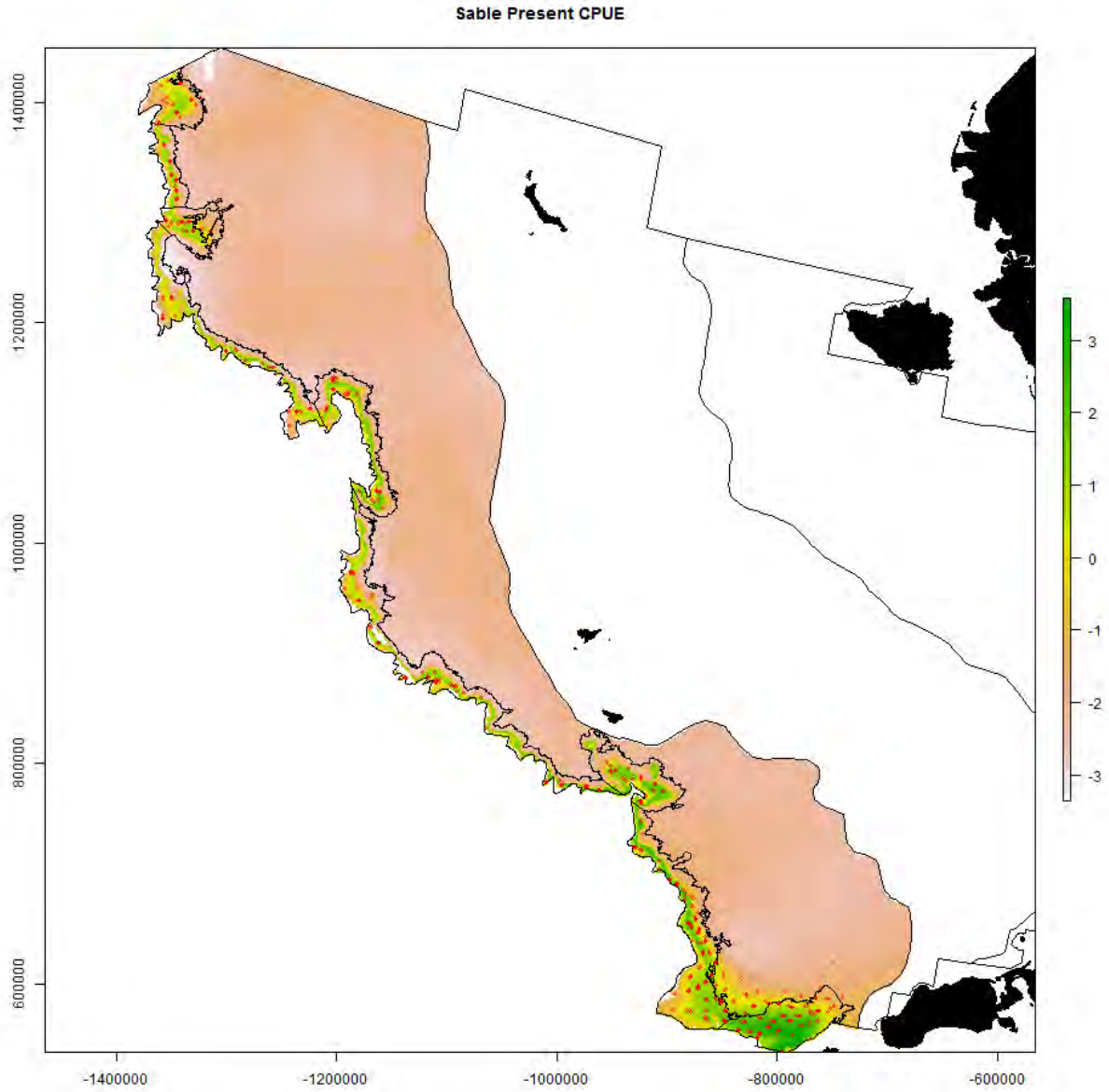

Figure 7. Habitat vulnerability indices by 1 x 1 km grid cell for the eastern Bering Sea shelf and outer slope based on generalized additive modeling. The x-axis label is easting and the y-axis label is northing and the unit is meters (Alaska Albers Equal Area Conic projection with center latitude = 50° N and center longitude = 154° W).

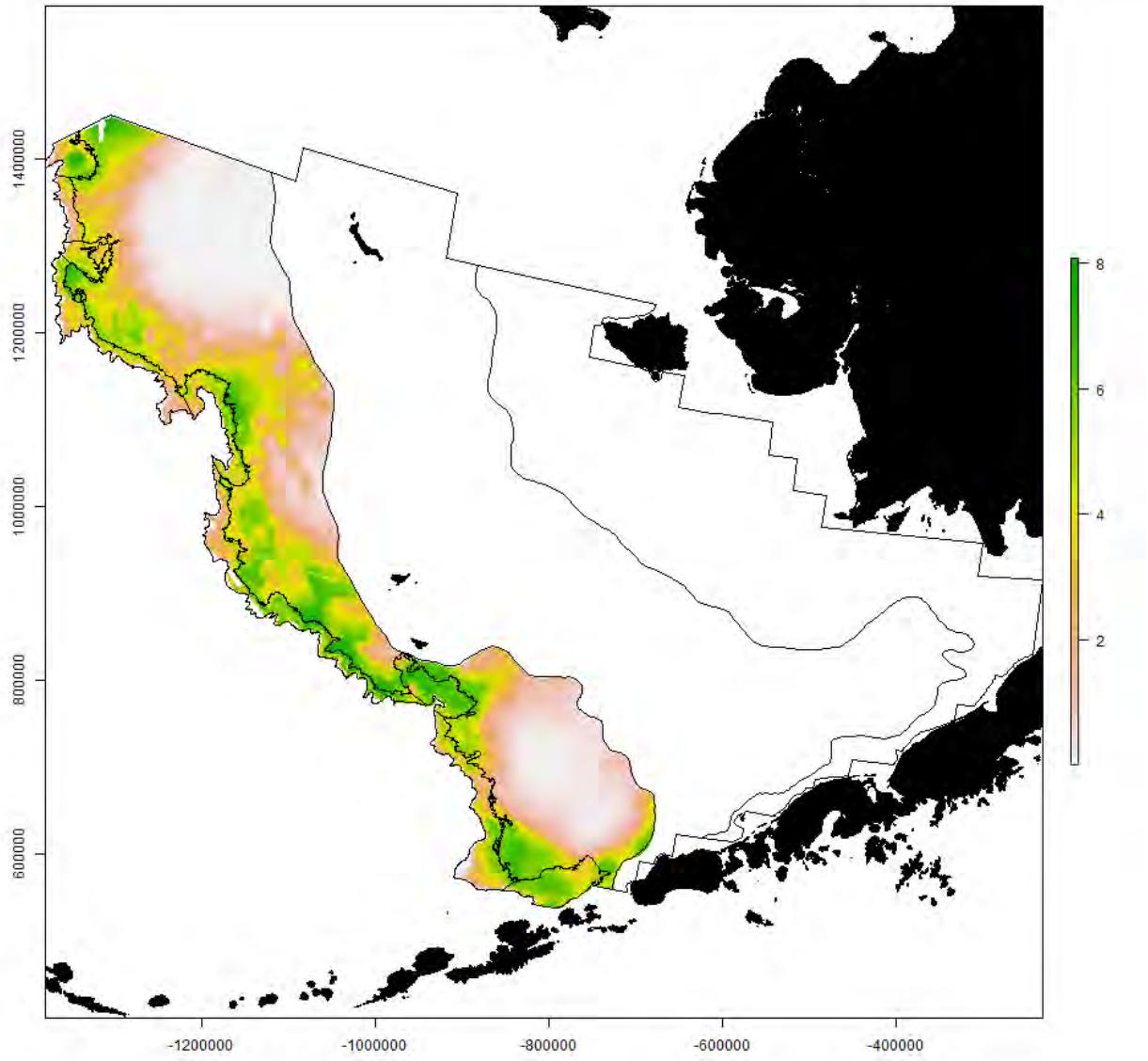

1277 Figure 8. Average vulnerability indices by area for the eastern Bering Sea slope and outer shelf.

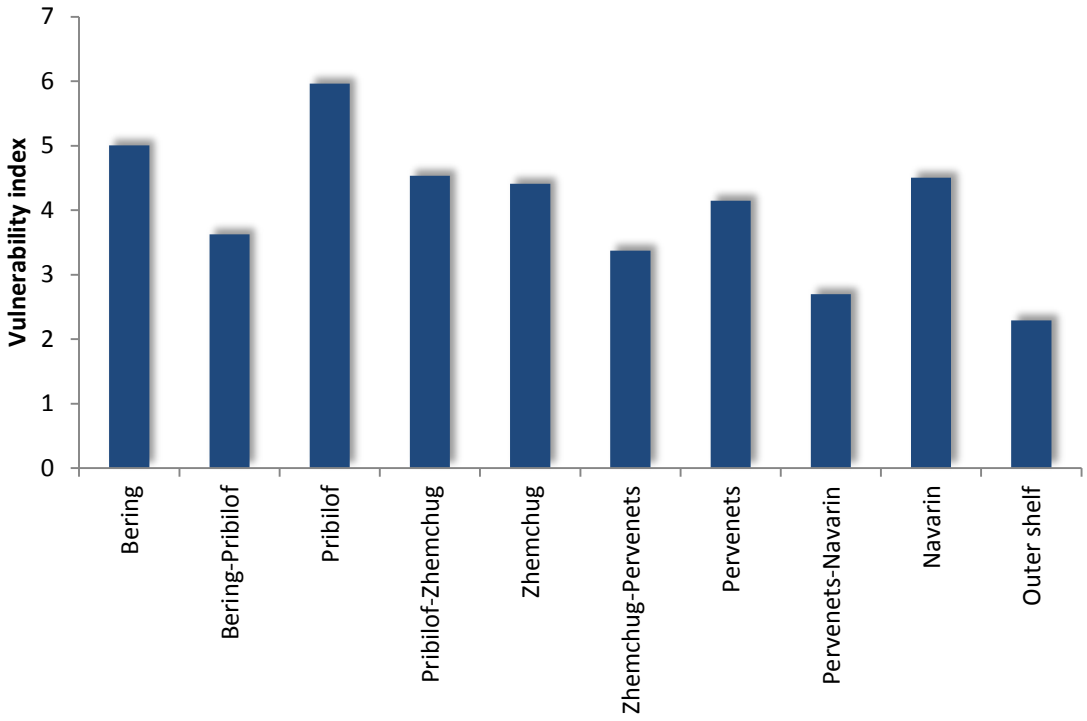


1278

Figure 9. Fishing effort by gear type including bottom trawl, pelagic trawl, pot and longline for the eastern Bering Sea slope and outer shelf. Fishing effort is expressed as the number of sets per 1 x 1 km grid cell during 2002-2011 and then log-transformed in the maps for display. The x-axis label is easting and the y-axis label is northing and the unit is meters (Alaska Albers Equal Area Conic projection with center latitude = 50° N and center longitude = 154° W).

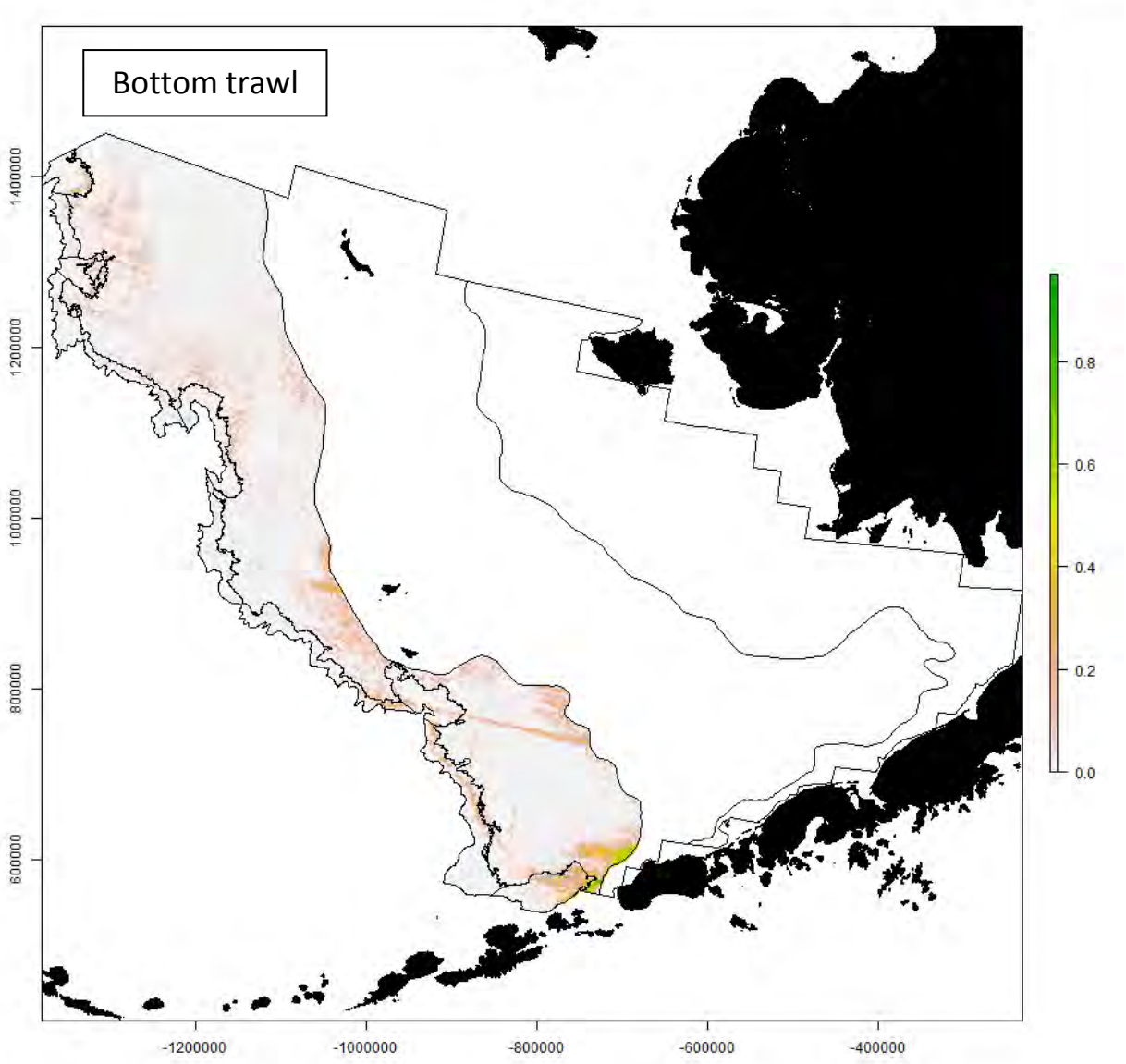

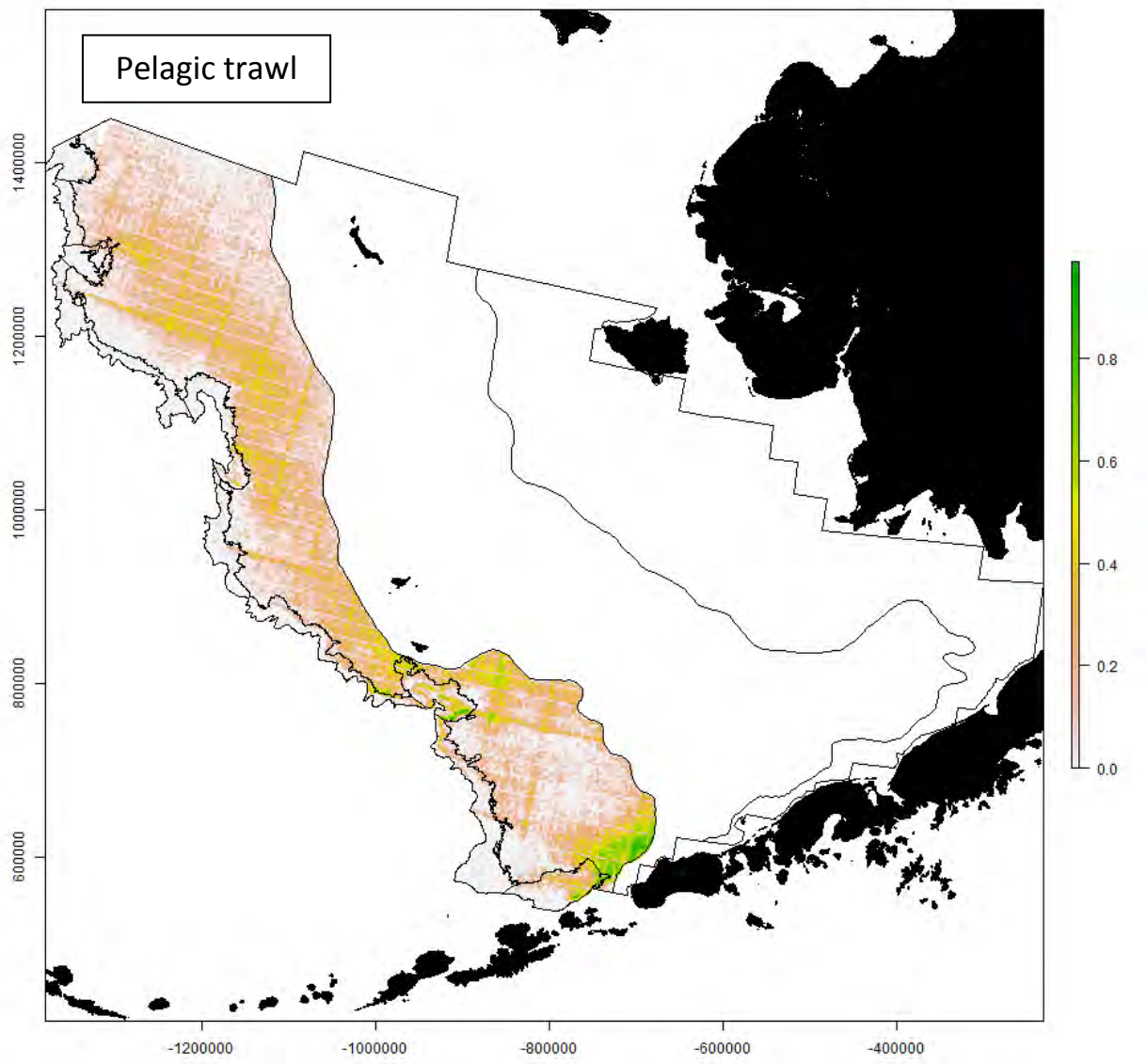
Pelagic trawl
1400000
1200000
1000000
800000
600000
-1200000
-1000000
-800000
-600000
-400000
0.8
0.6
0.4
0.2
0.0

1286

1287

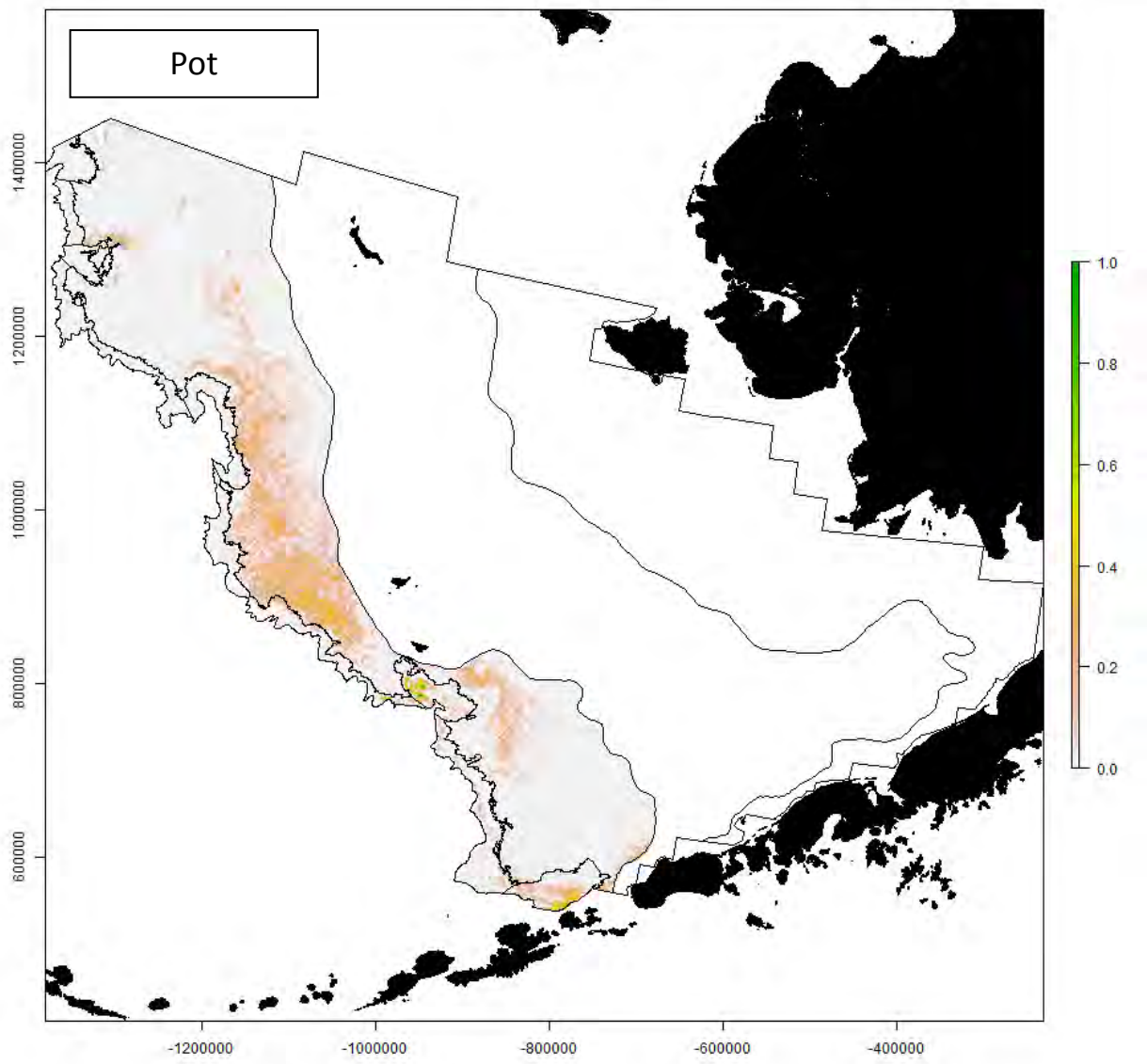
Pot
1400000
1200000
1000000
800000
600000
-1200000
-1000000
-800000
-600000
-400000
1.0
0.8
0.6
0.4
0.2
0.0

1288

1289

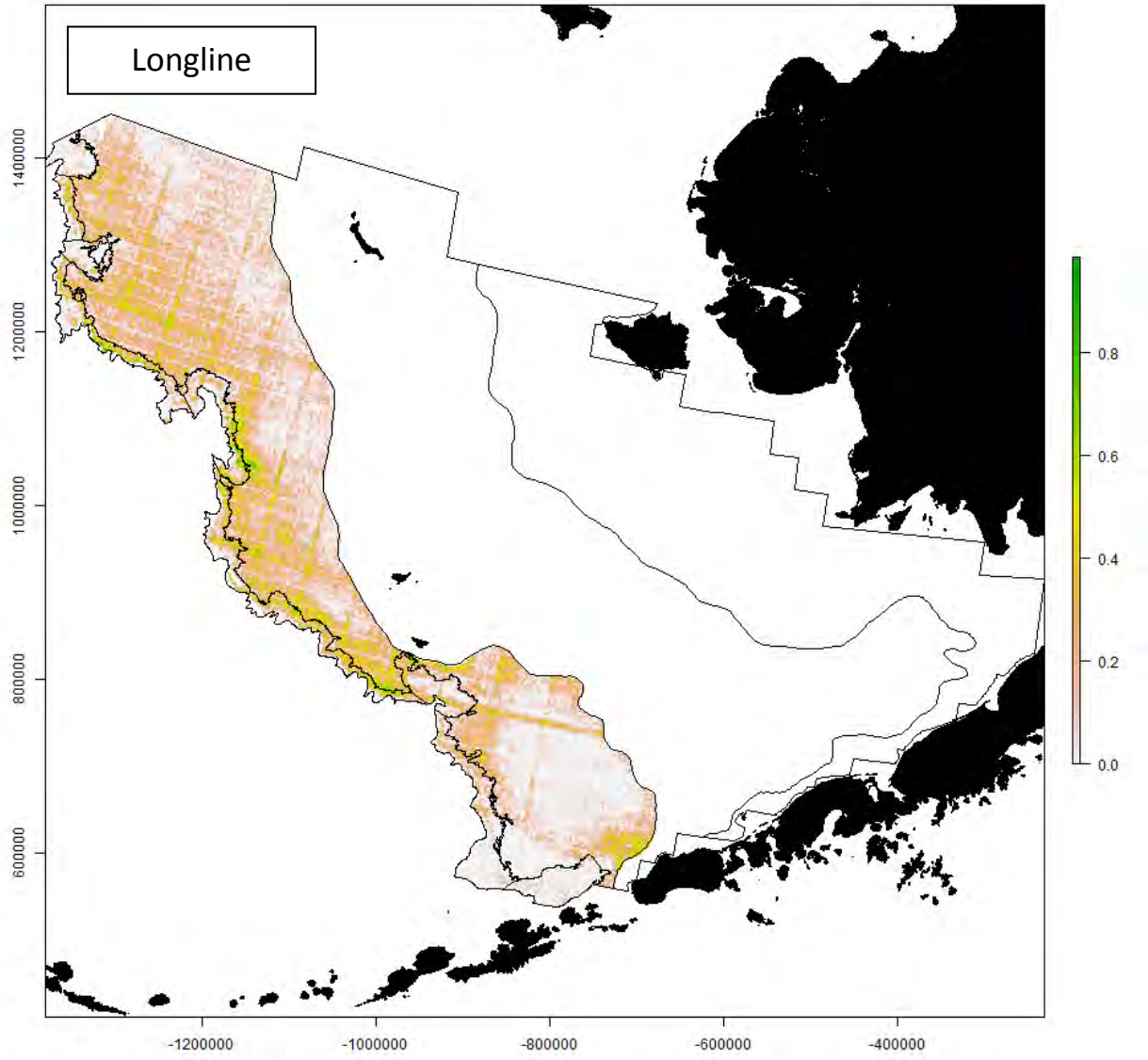
Longline
1400000
1200000
1000000
800000
600000
-1200000
-1000000
-800000
-600000
-400000
0.8
0.6
0.4
0.2
0.0

1290

1291

Figure 10. Overlap indices of fishing and vulnerable habitats by 1 x 1 km grid cell and by gear type including bottom trawl, pelagic trawl, pot and longline for the eastern Bering Sea slope and outer shelf. The overlap indices are log-transformed in the maps for display. The x-axis label is easting and the y-axis label is northing and the unit is meters (Alaska Albers Equal Area Conic projection with center latitude = 50° N and center longitude = 154° W).

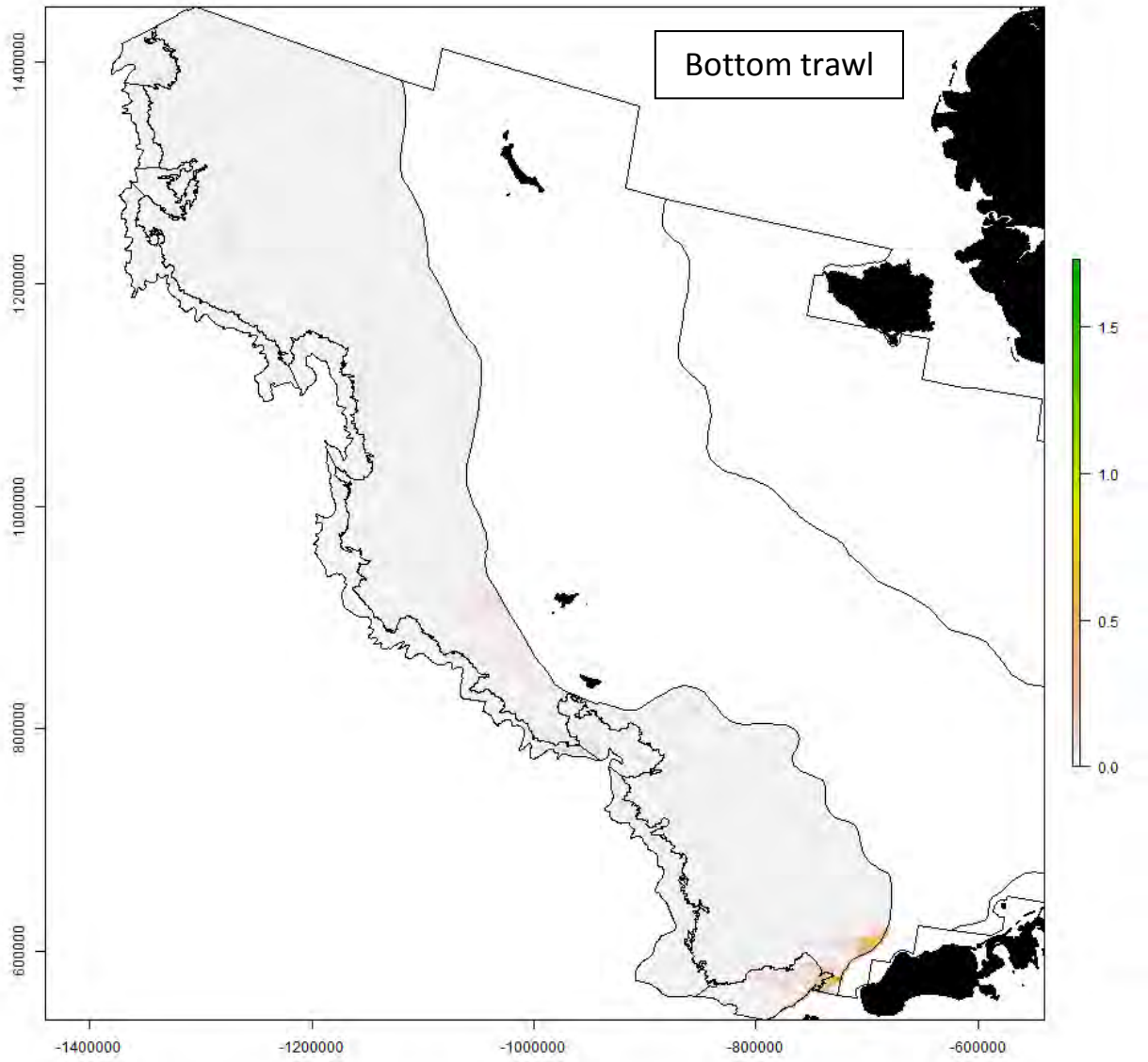

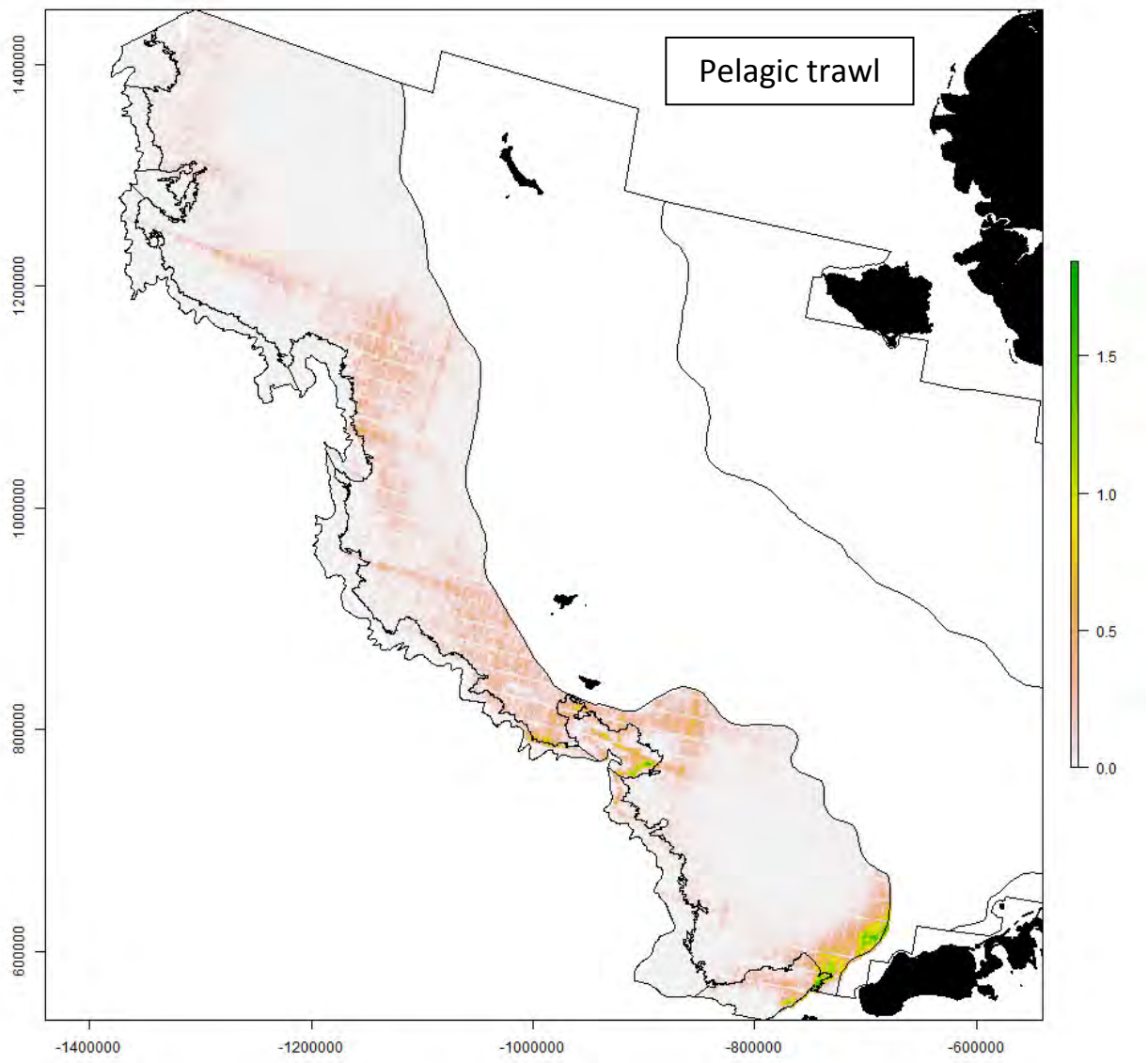
Pelagic trawl
1400000
1200000
1000000
800000
600000
-1400000
-1200000
-1000000
-800000
-600000
1.5
1.0
0.5
0.0

1299

1300

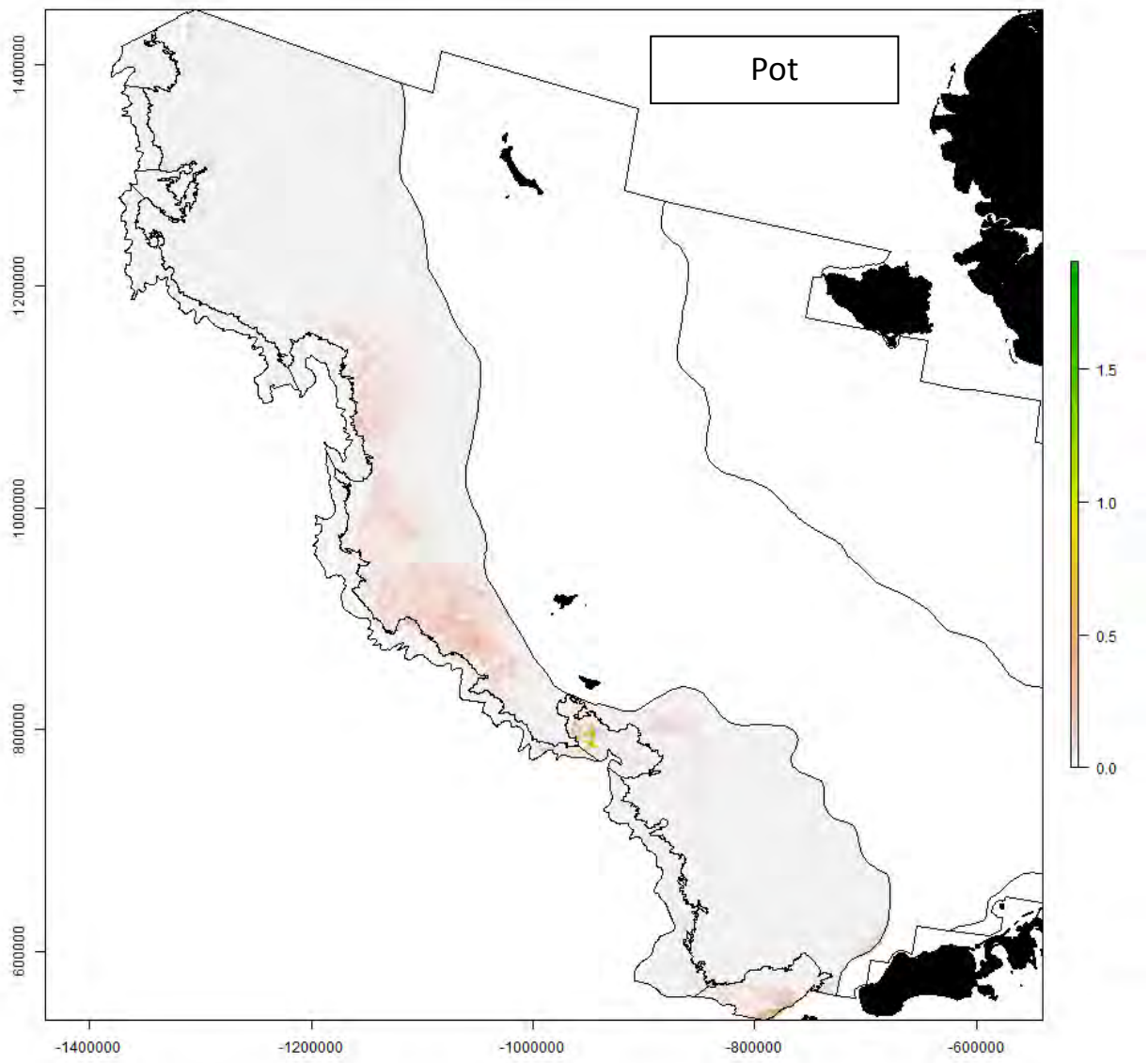
Pot
1400000
1200000
1000000
800000
600000
-1400000
-1200000
-1000000
-800000
-600000
1.5
1.0
0.5
0.0

1301

1302

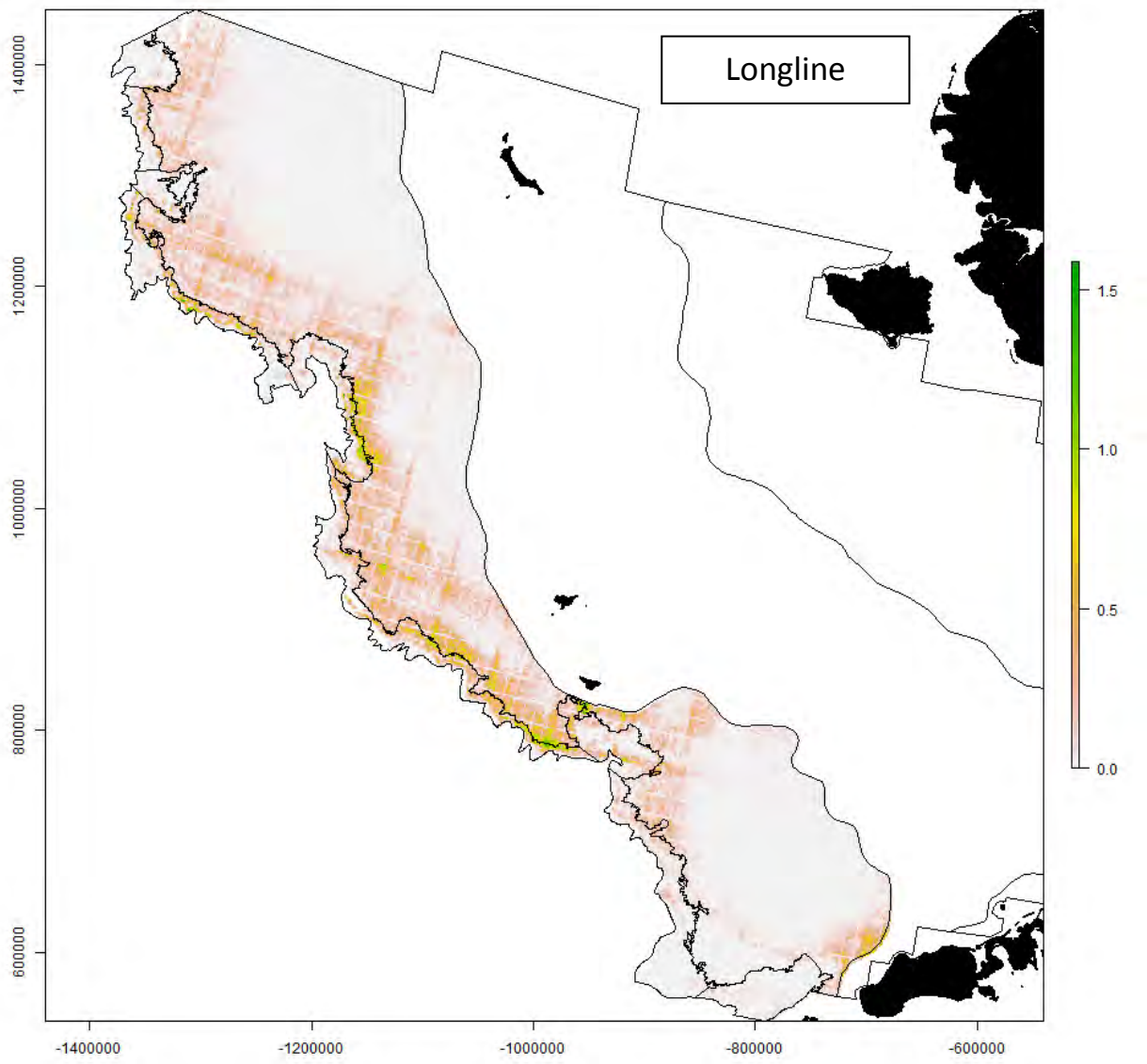
Longline
1400000
1200000
1000000
800000
600000
-1400000
-1200000
-1000000
-800000
-600000
1.5
1.0
0.5
0.0

1303
1304

Figure 11. Average overlap indices by area and gear type (bottom trawl, pelagic trawl, pot, longline) for the eastern Bering Sea slope and outer shelf.

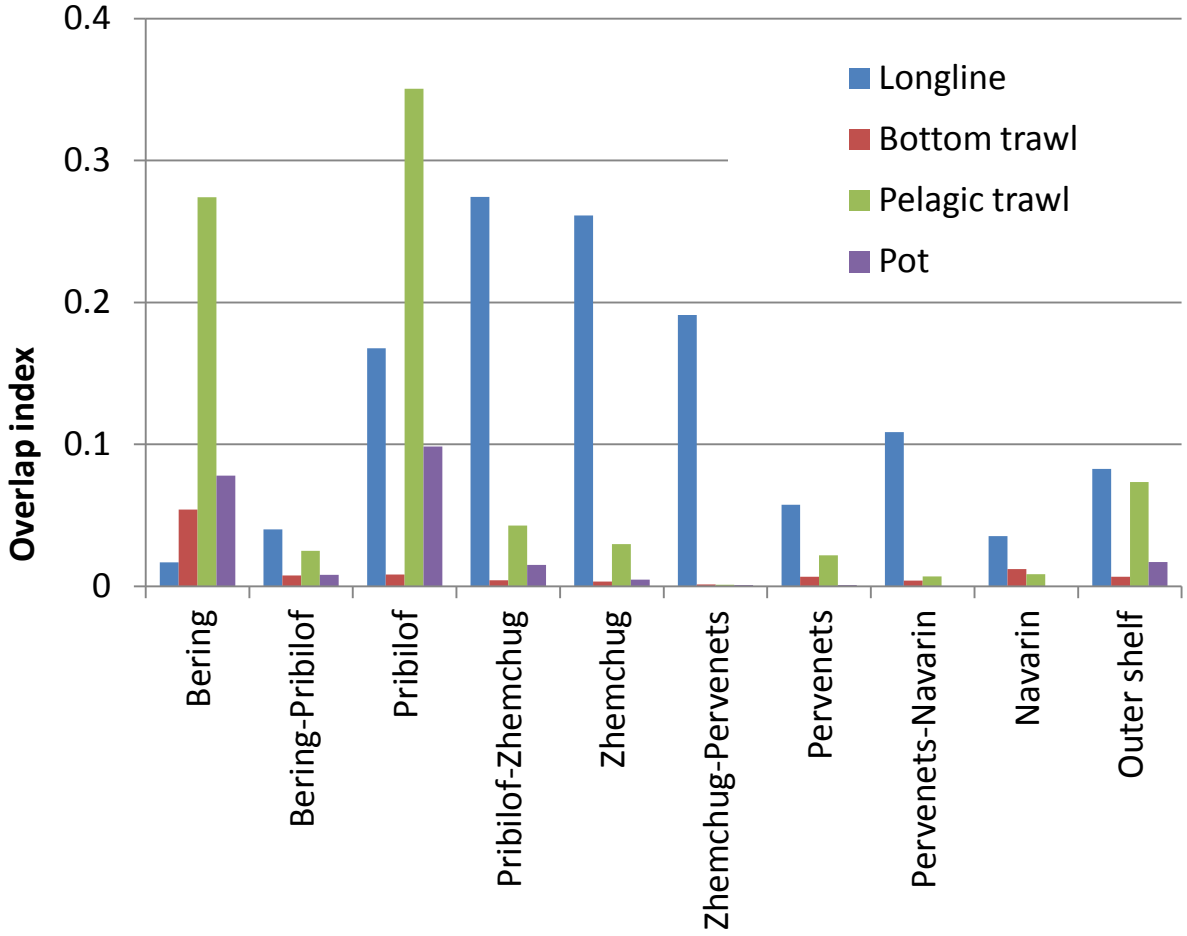

S1. Long-term average of summer bottom temperature in the eastern Bering Sea. The upper right panel shows sample locations (black dots). Source: NOAA Alaska Fisheries Science Center bottom trawl surveys, 1996-2012, n = 7,177.

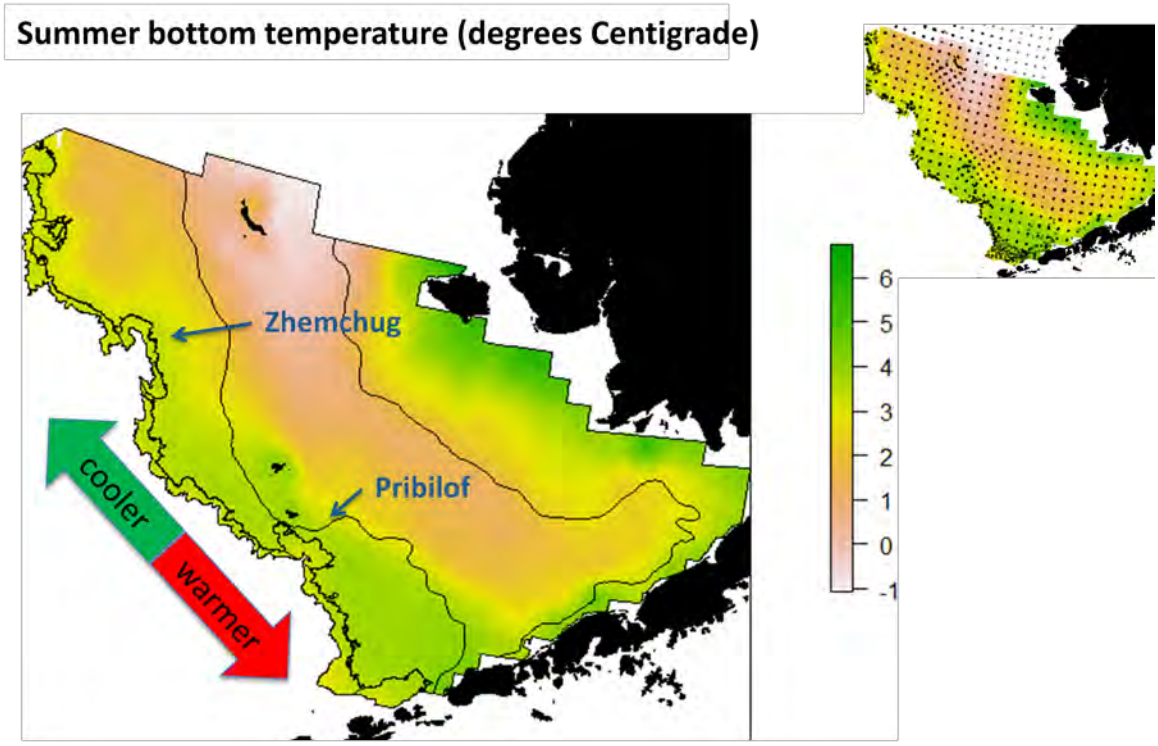

S2. Long-term average of summer ocean color in the eastern Bering Sea. The upper right panel shows sample locations (black dots). Source: Oregon State University's Ocean Productivity website (Behrenfeld and Falkowski 1997), n = 58,070, May-September 2003-2011.

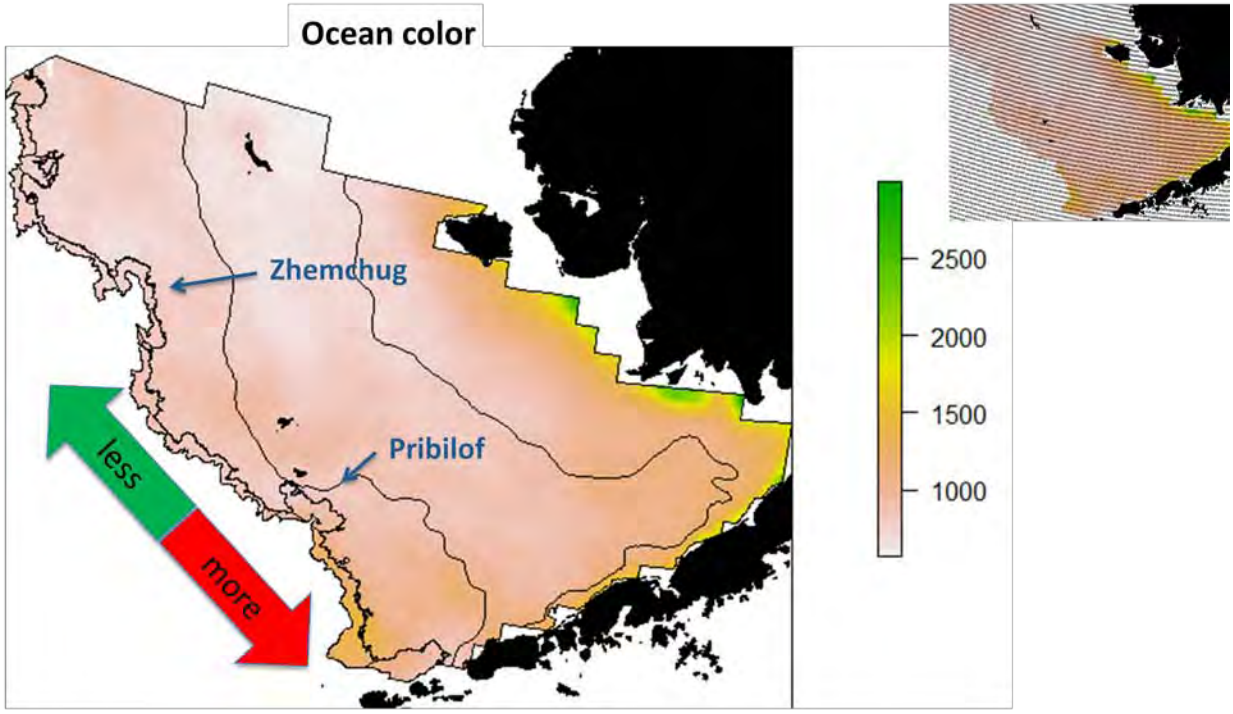

S3. Long-term average of ocean current in the eastern Bering Sea. The upper right panel shows model grid (black dots). Source: ROMS model output (A. Hermann, NOAA's Pacific Marine Environmental Laboratory, pers. comm., October 2012), n = 109,194, gridded average from 1975-2010.

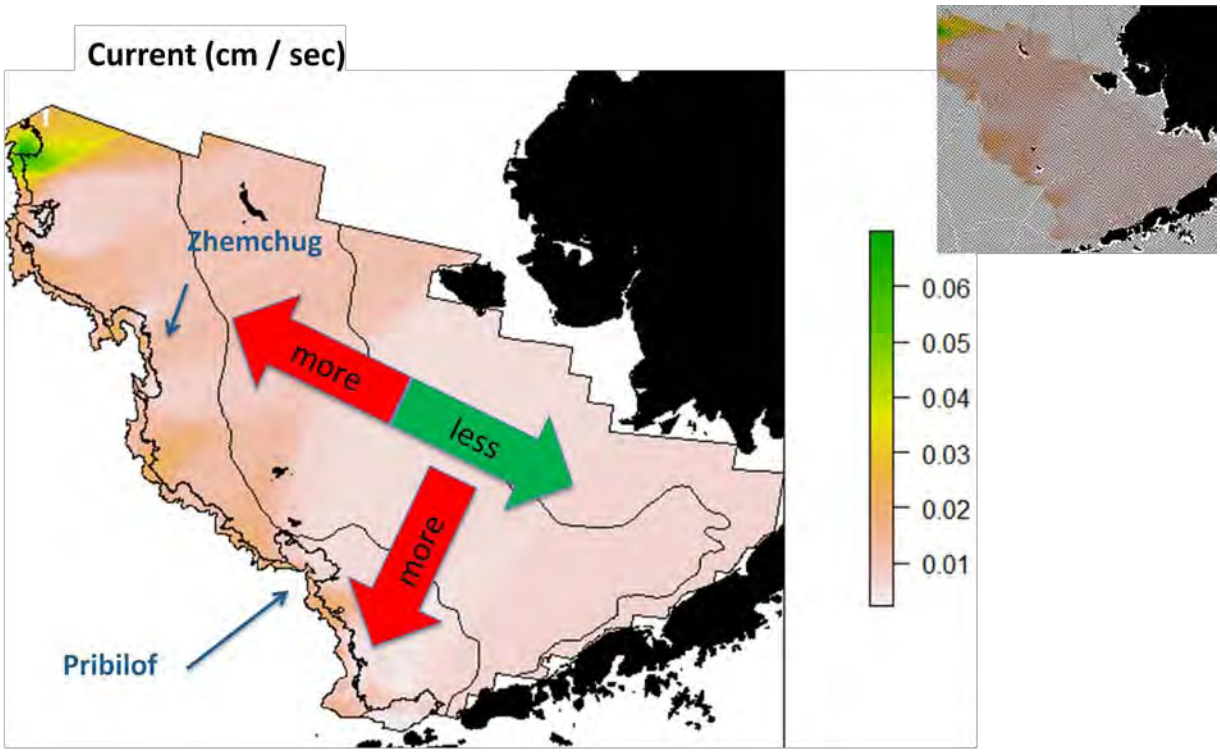

S4. Predicted sediment grain size in the eastern Bering Sea. The upper right panel shows sample locations (black dots). Source: Eastern Bering Sea Sediment (EBSSed) database (Smith and McConnaughey 1999), n = 1,201.

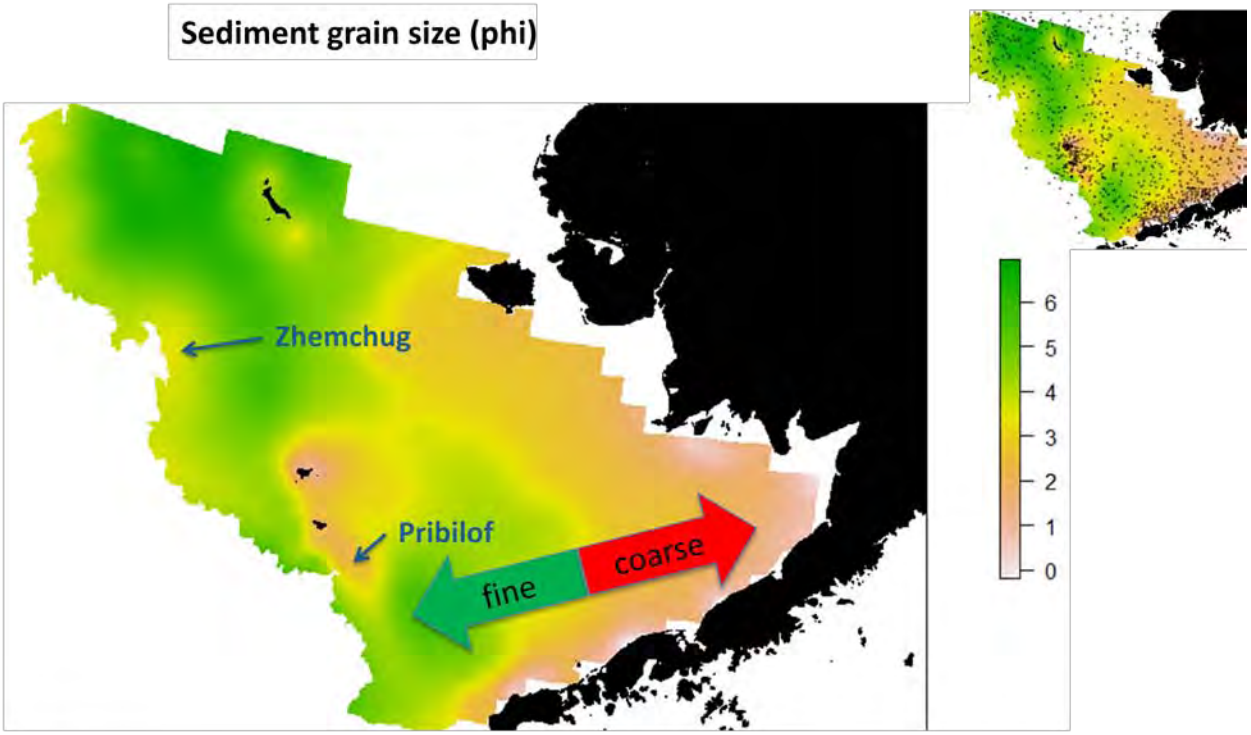

S5. Predicted sediment sorting in the eastern Bering Sea. The upper right panel shows sample locations (black dots). Source: Eastern Bering Sea Sediment (EBSSed) database (Smith and McConnaughey 1999), n = 1,201.

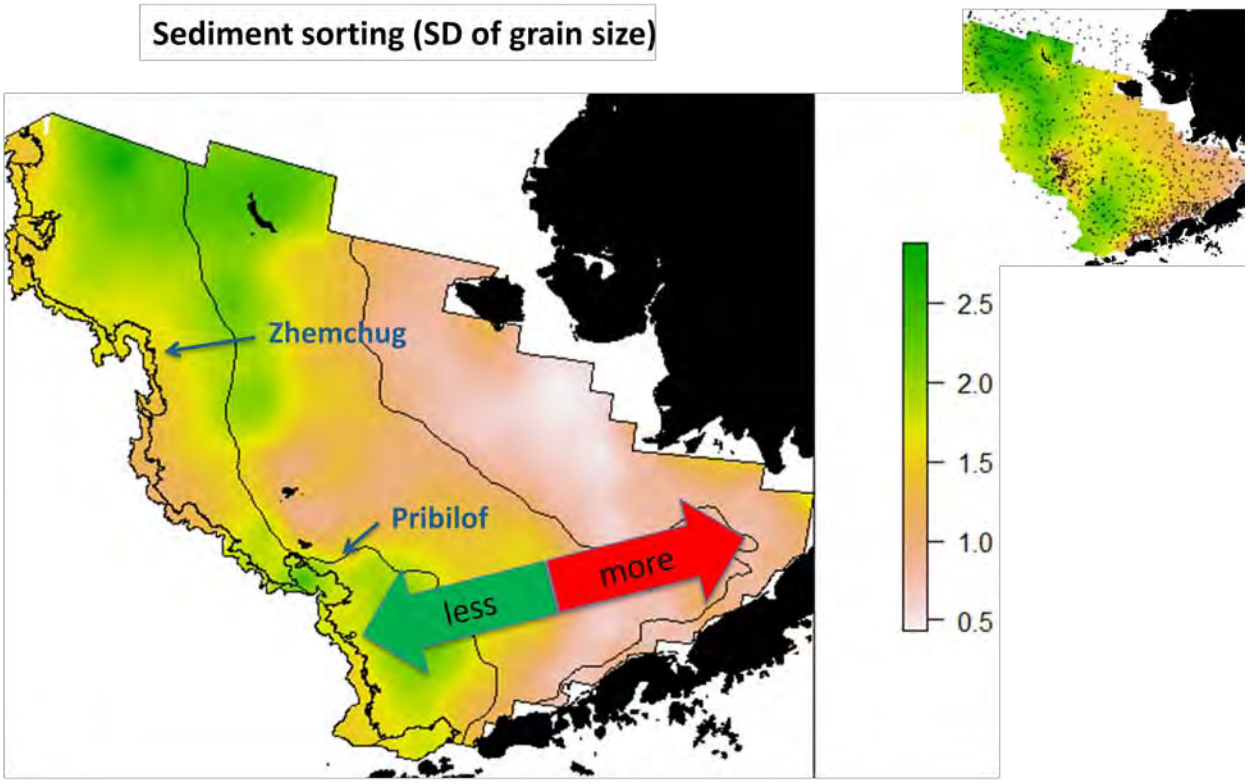

S6. Summer 2012 bottom oxygen and pH in the eastern Bering Sea. The lower right panel shows sample locations (black dots). The values were extrapolated onto the outer shelf even though samples were collected only on the slope (sample locations are the open circles shown in the lower right map). Source: Eastern Bering Sea slope survey, n = 188.

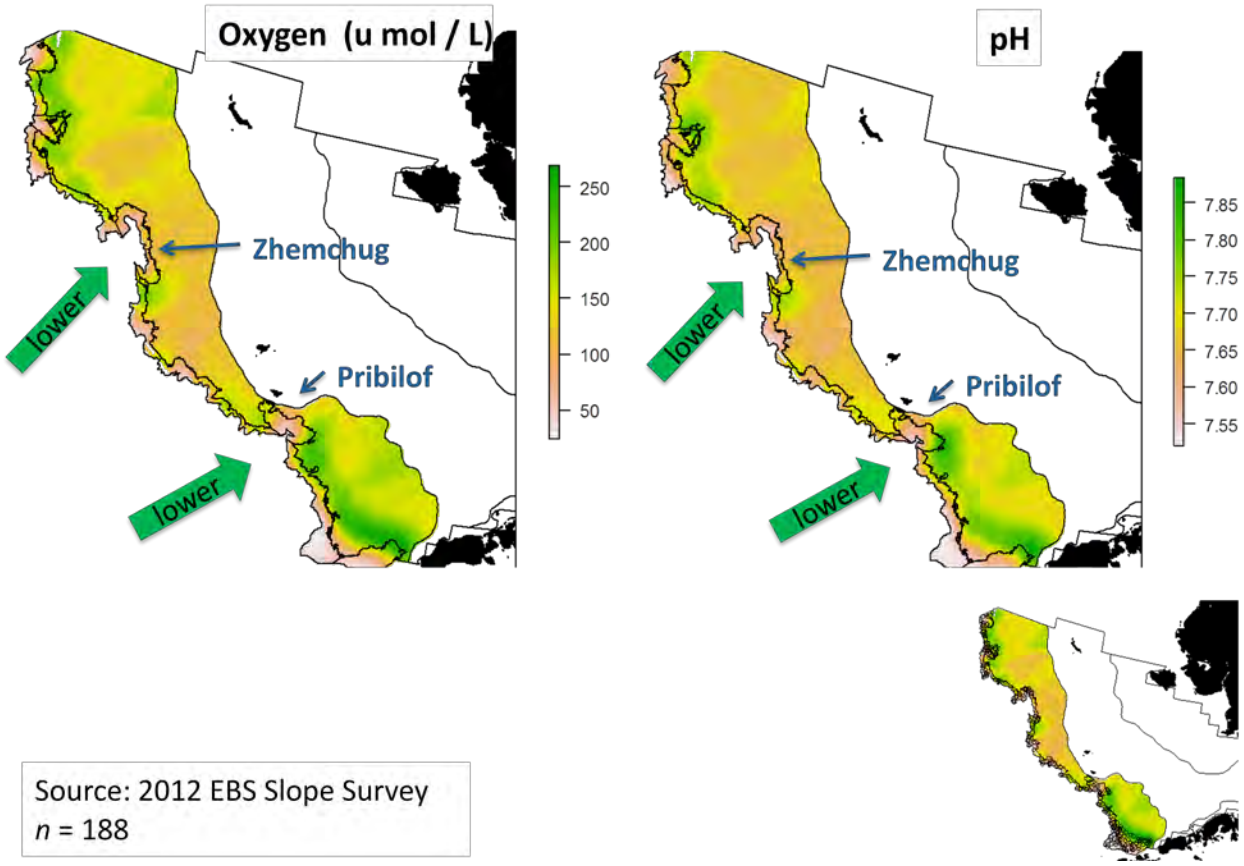

S7. Summer 2012 turbidity in the eastern Bering Sea. The upper right panel shows sample locations (black dots). The values were extrapolated onto the outer shelf even though samples were collected only on the slope (sample locations are the open circles shown in the righthand map). Source: Eastern Bering Sea slope survey, n = 188.

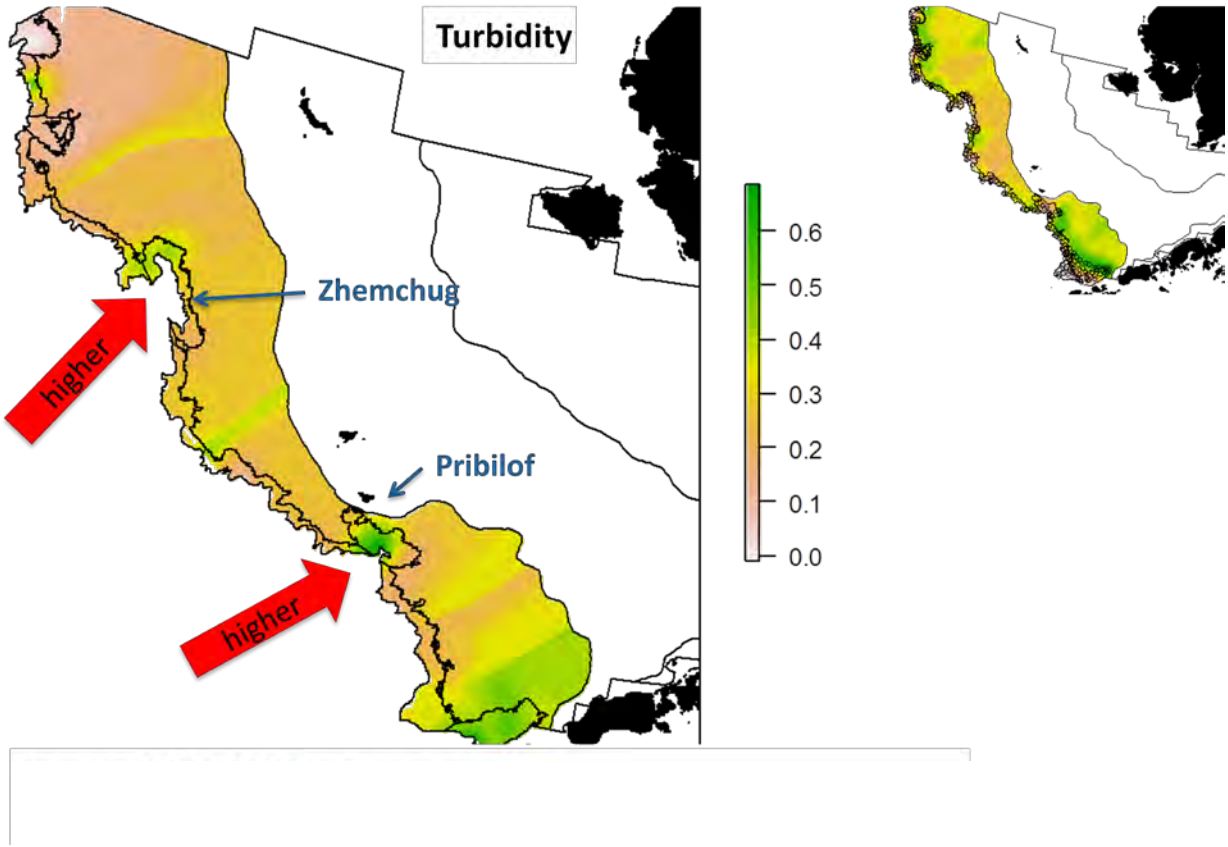

1343 S8. Summer 2012 salinity in the eastern Bering Sea. The upper right panel shows sample
1344 locations (black dots). Source: Eastern Bering Sea shelf and slope surveys, n = 512.

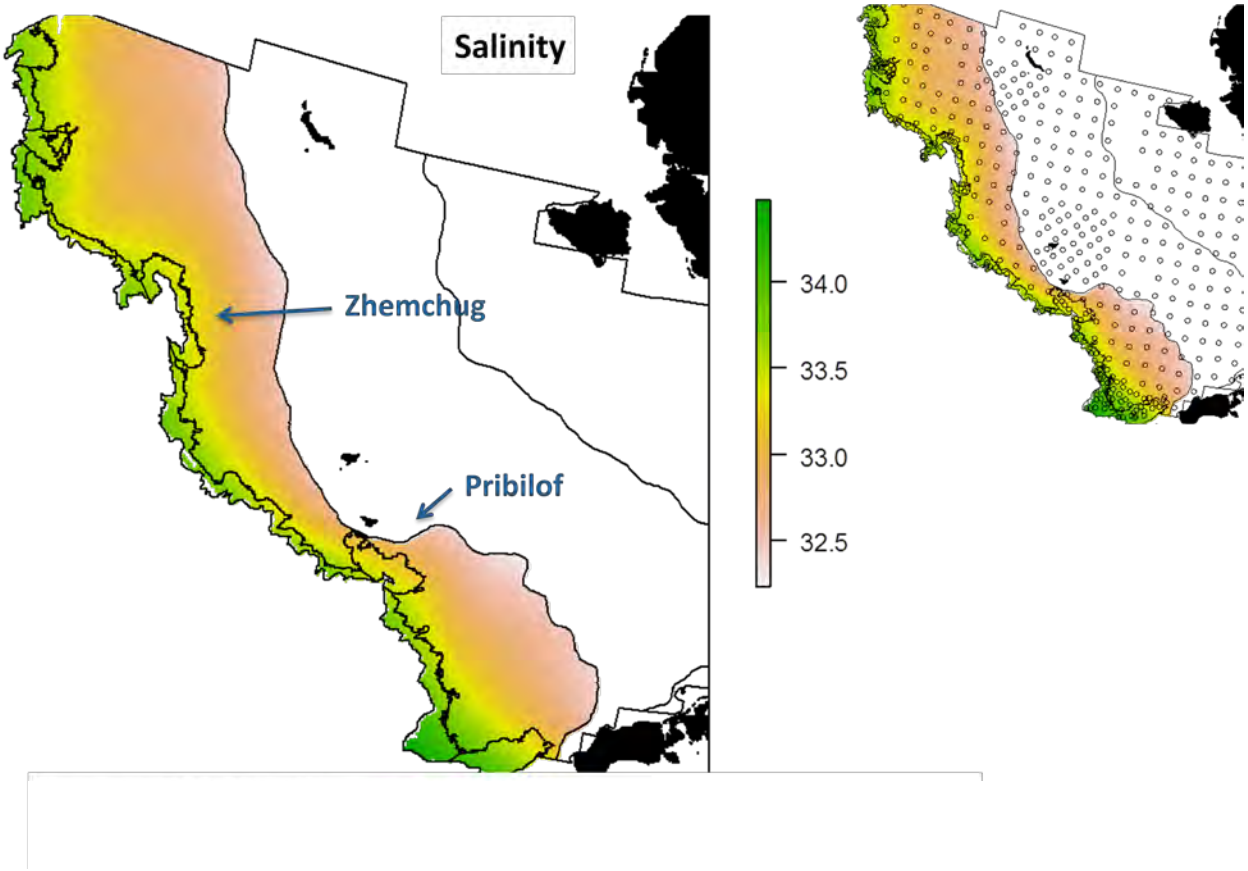


1345
1346

S9. Generalized additive modeling results for coral. In the spatial plots, the x-axis label is easting and the y-axis label is northing and the unit is meters (Alaska Albers Equal Area Conic projection with center latitude = 50° N and center longitude = 154° W).

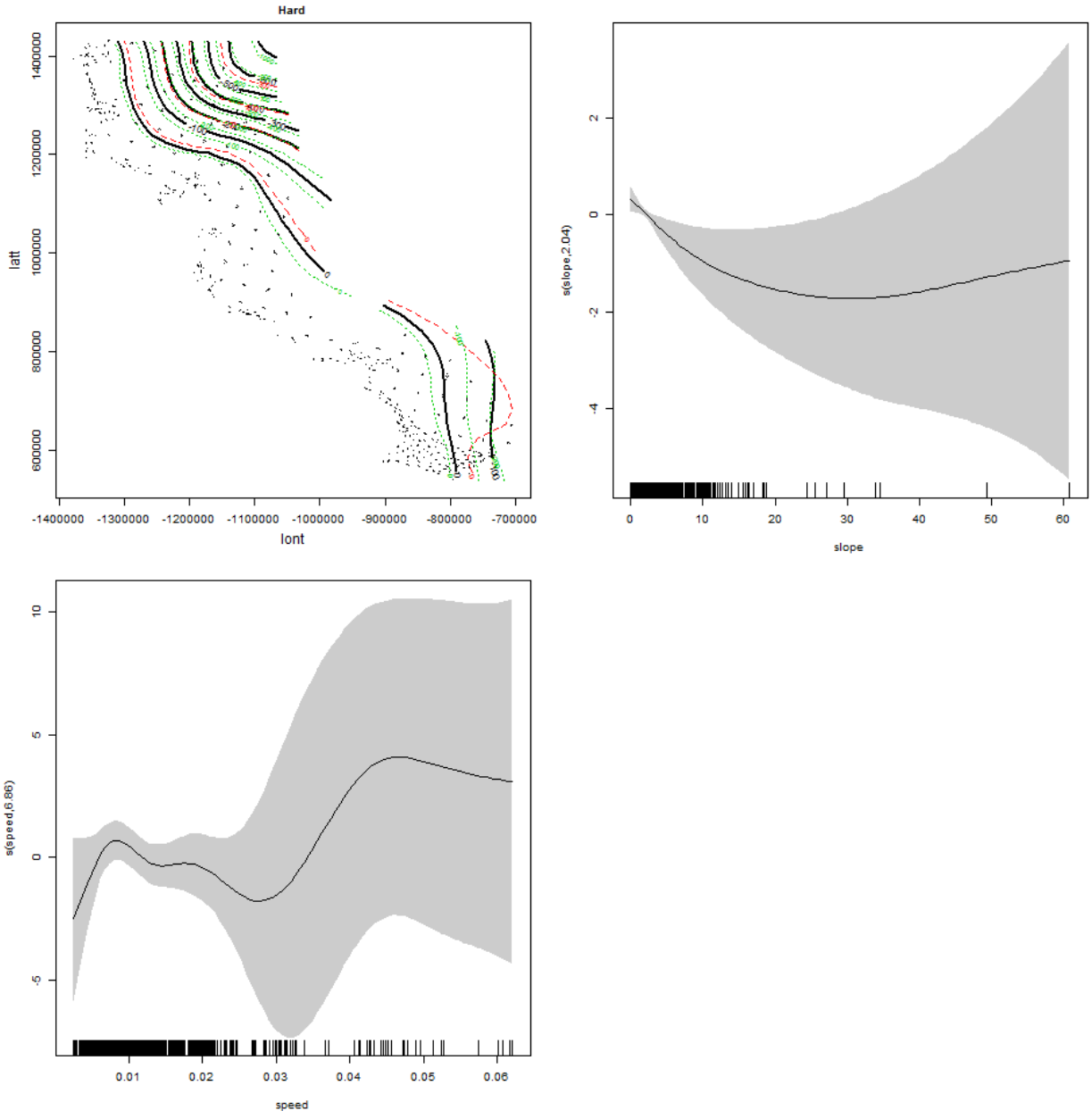

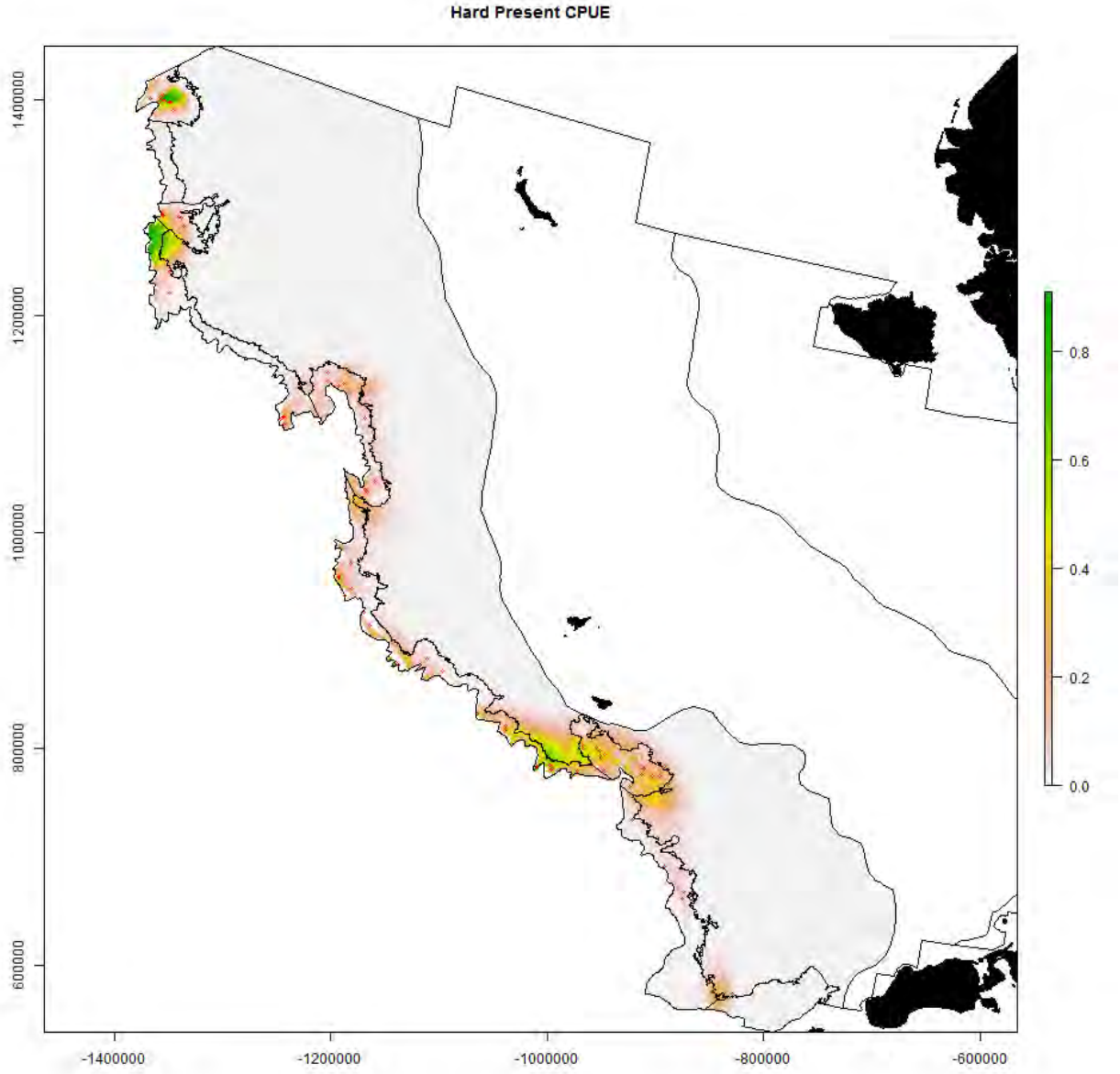
Hard Present CPUE
1400000
1200000
1000000
800000
600000
-1400000
-1200000
-1000000
-800000
-600000
0.8
0.6
0.4
0.2
0.0

1352

1353

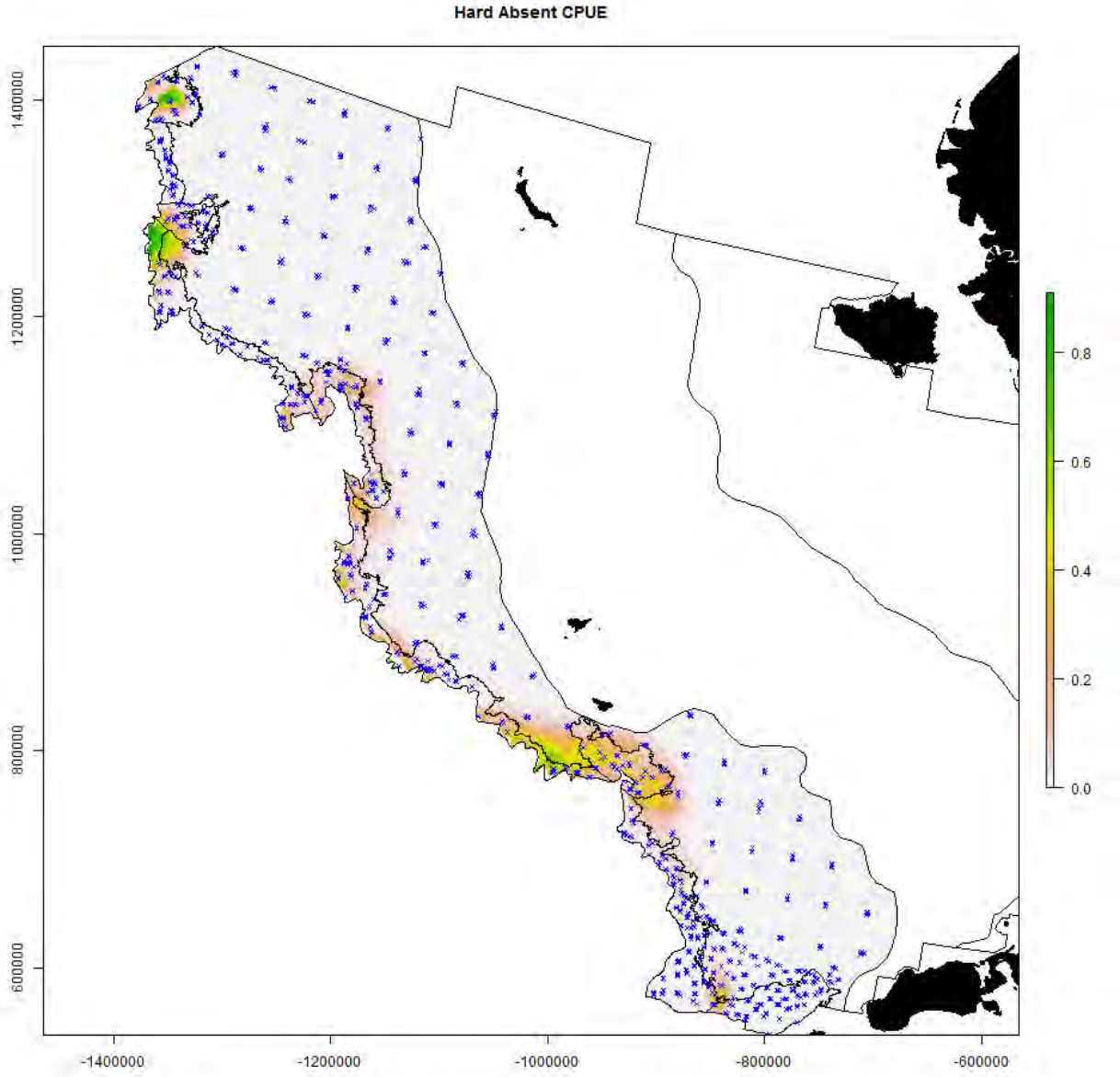
Hard Absent CPUE
1400000
1200000
1000000
800000
600000
-1400000
-1200000
-1000000
-800000
-600000
0.8
0.6
0.4
0.2
0.0

1354
1355

S10. Generalized additive modeling results for sponge. In the spatial plots, the x-axis label is easting and the y-axis label is northing and the unit is meters (Alaska Albers Equal Area Conic projection with center latitude = 50° N and center longitude = 154° W).

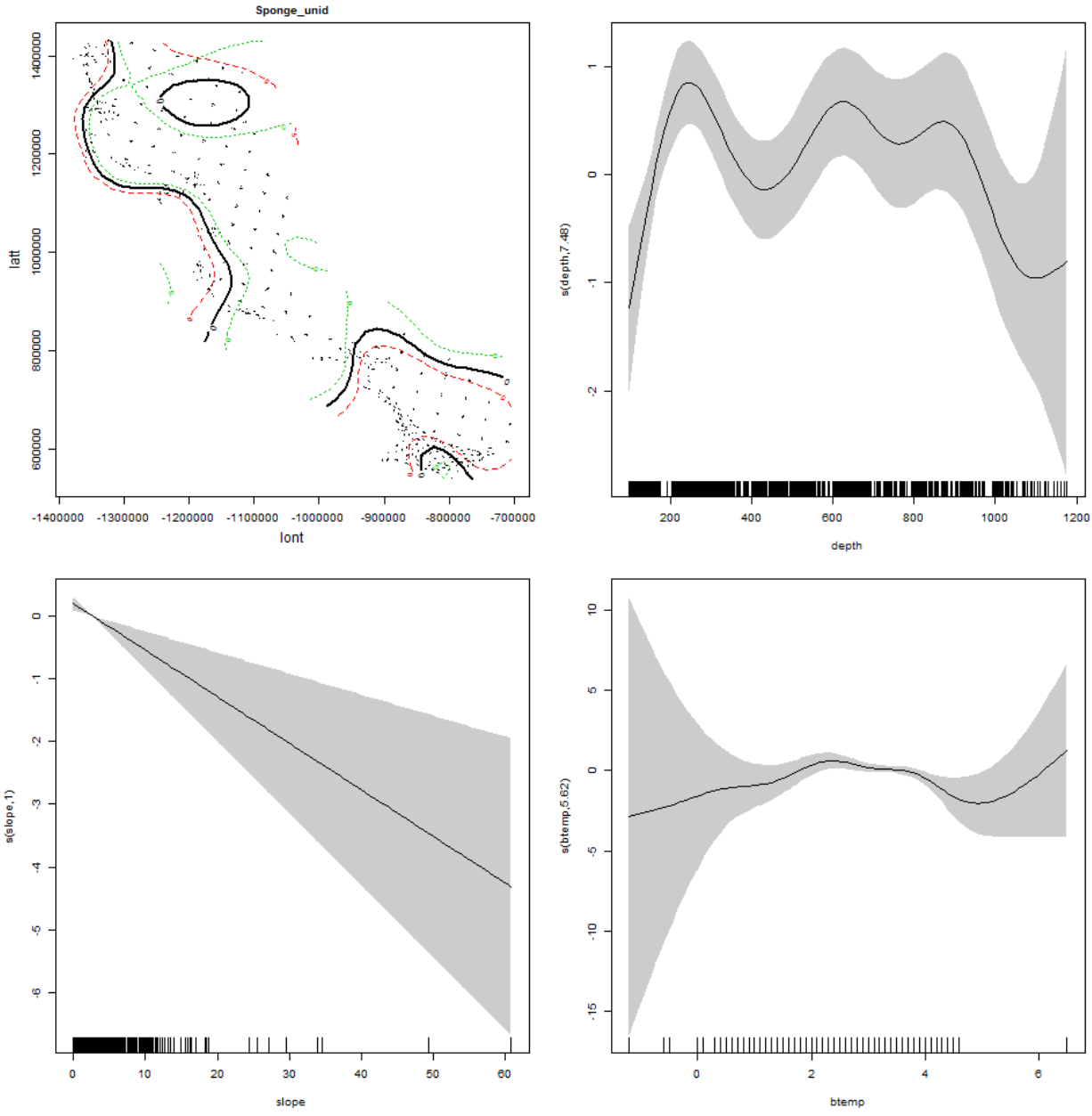

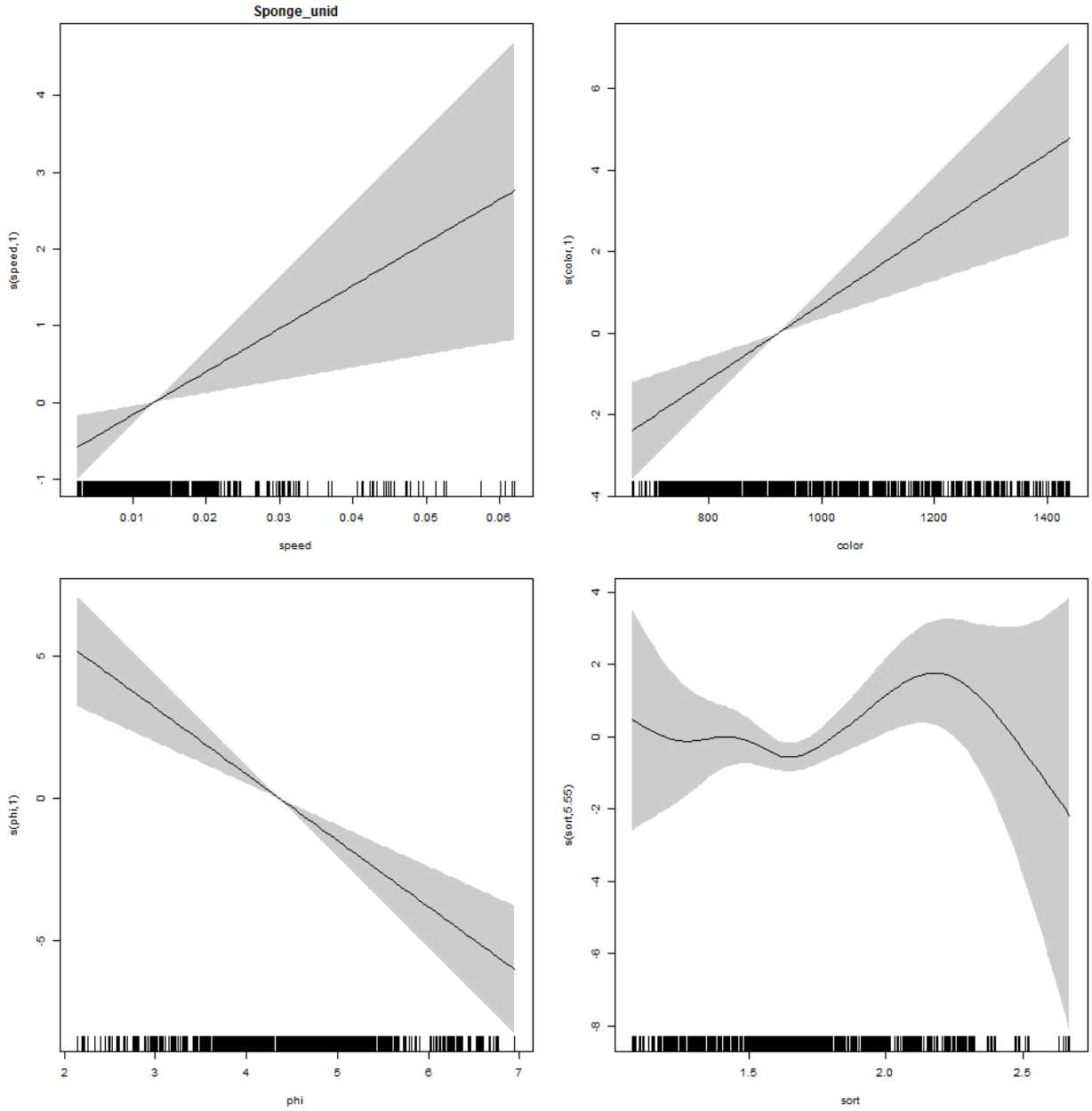
Sponge_unid
s(speed,1)
speed
s(color,1)
color
s(phi,1)
phi
s(sort,5.55)
sort

1361

1362

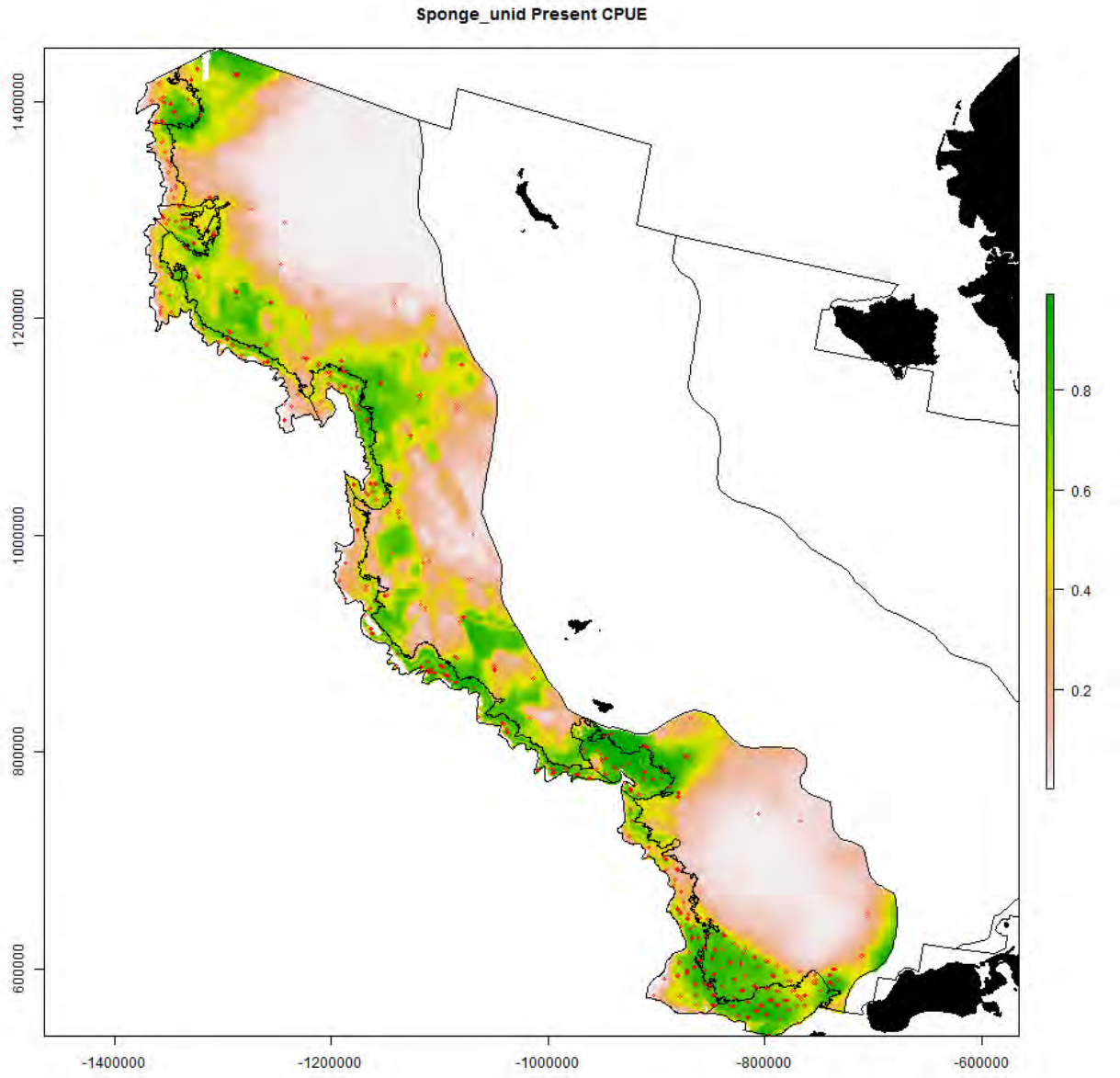
Sponge_unid Present CPUE
1400000
1200000
1000000
800000
600000
-1400000
-1200000
-1000000
-800000
-600000
0.8
0.6
0.4
0.2

1363

1364

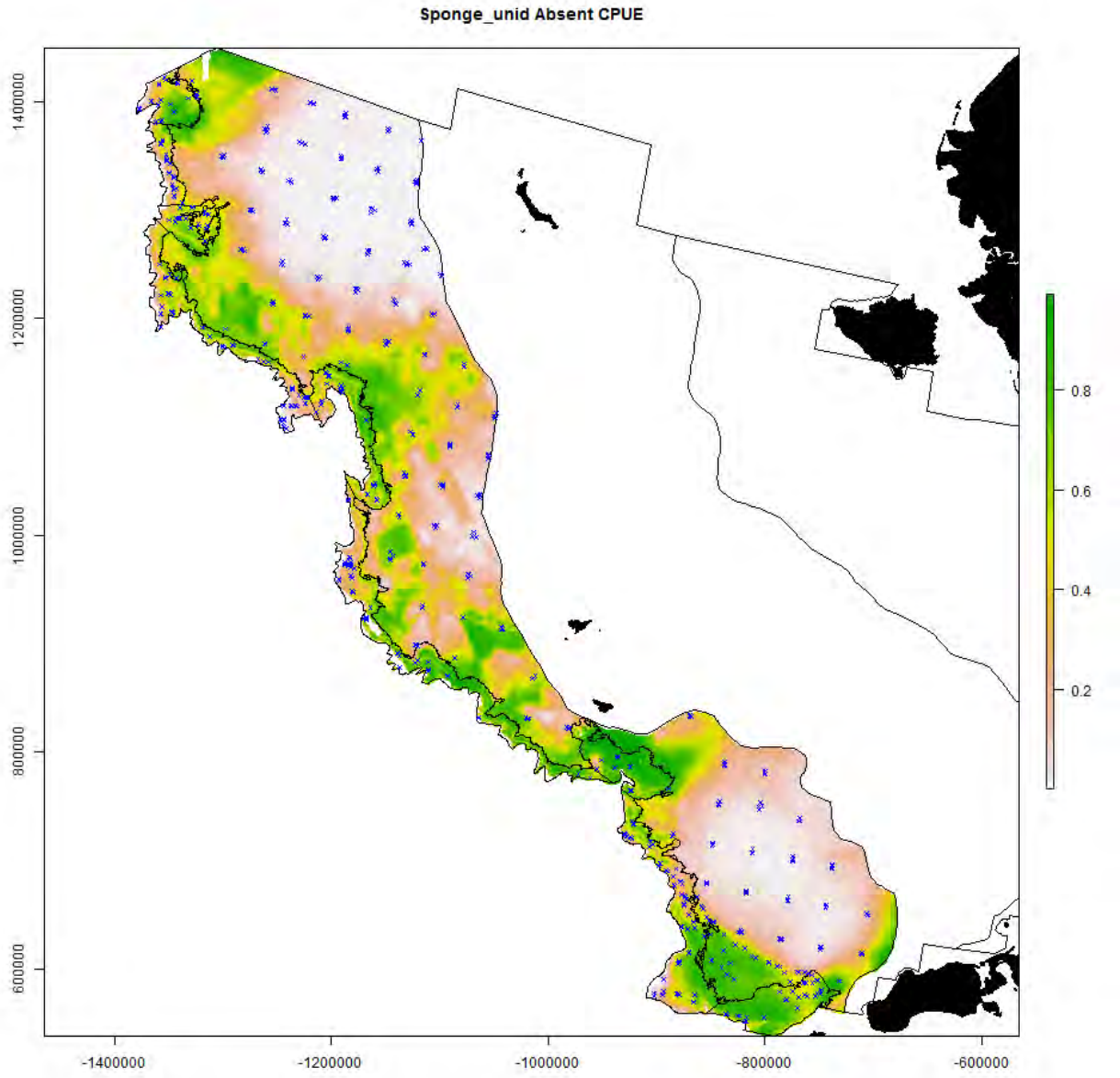
Sponge_unid Absent CPUE
1400000
1200000
1000000
800000
600000
-1400000
-1200000
-1000000
-800000
-600000
0.8
0.6
0.4
0.2

1365

1366

S11. Generalized additive modeling results for sea whip. In the spatial plots, the x-axis label is easting and the y-axis label is northing and the unit is meters (Alaska Albers Equal Area Conic projection with center latitude = 50° N and center longitude = 154° W).

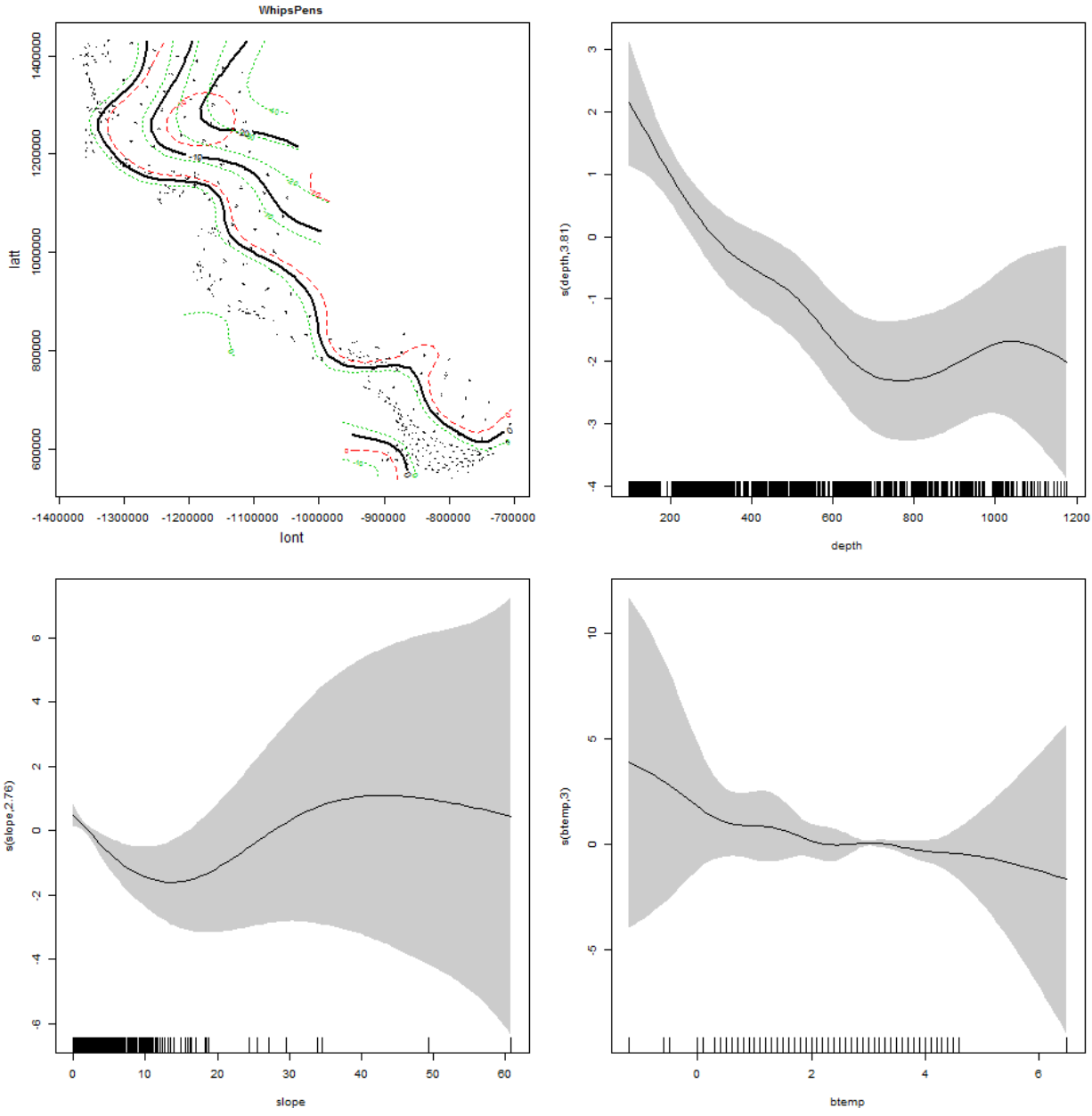

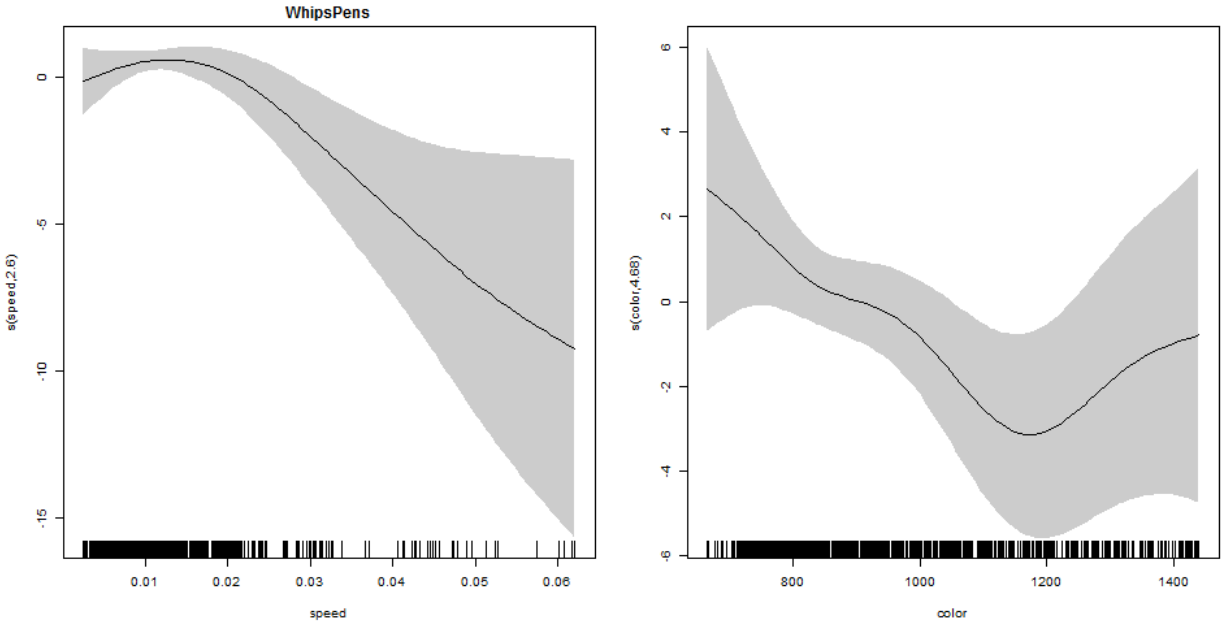
WhipsPens
s(speed,2.6)
0
-5
-10
-15
0.01
0.02
0.03
0.04
0.05
0.06
speed
s(color,4.68)
6
4
2
0
-2
-4
-6
800
1000
1200
1400
color

1372

1373

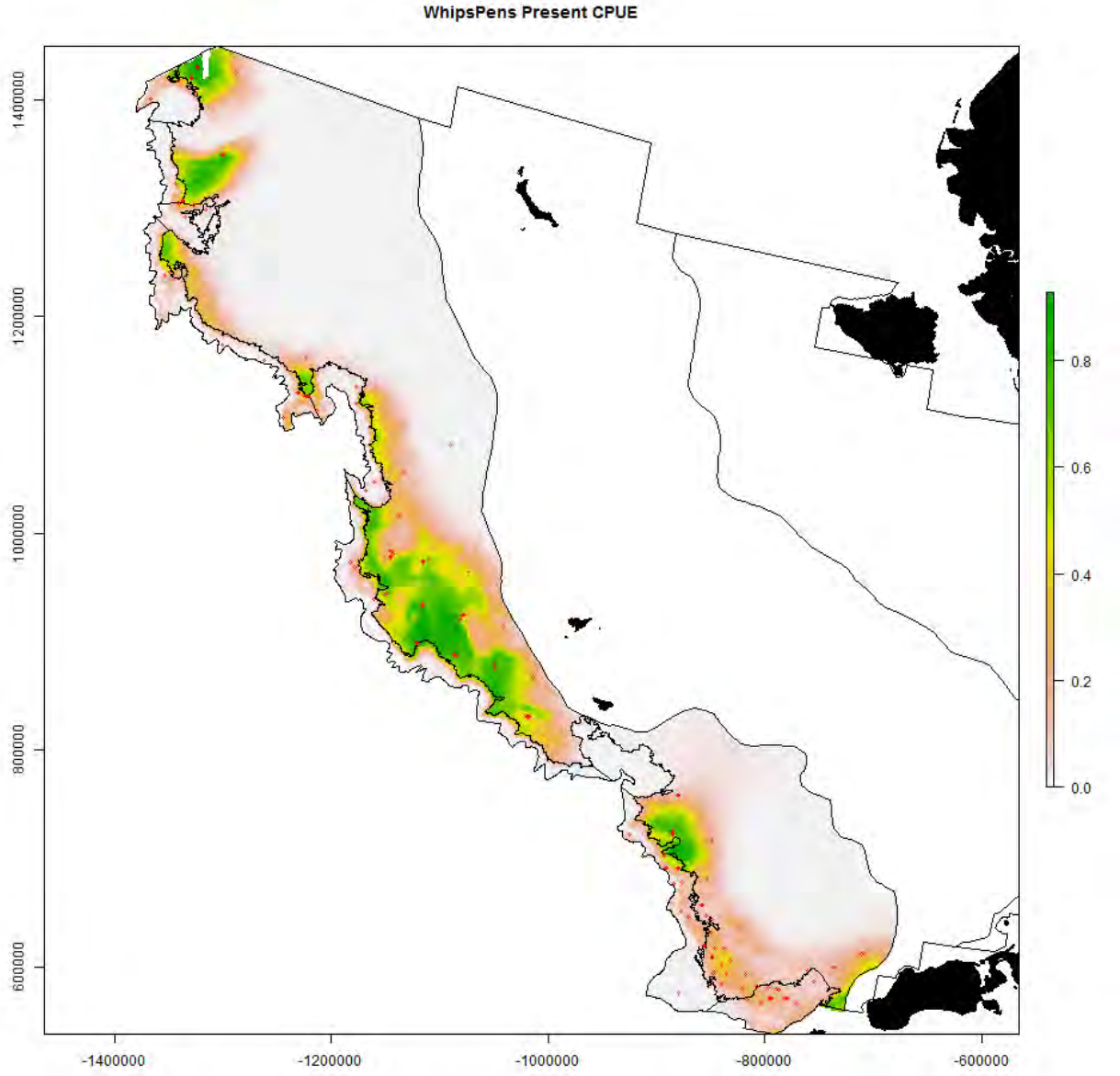
WhipsPens Present CPUE
1400000
1200000
1000000
800000
600000
-1400000
-1200000
-1000000
-800000
-600000
0.8
0.6
0.4
0.2
0.0

1374

1375

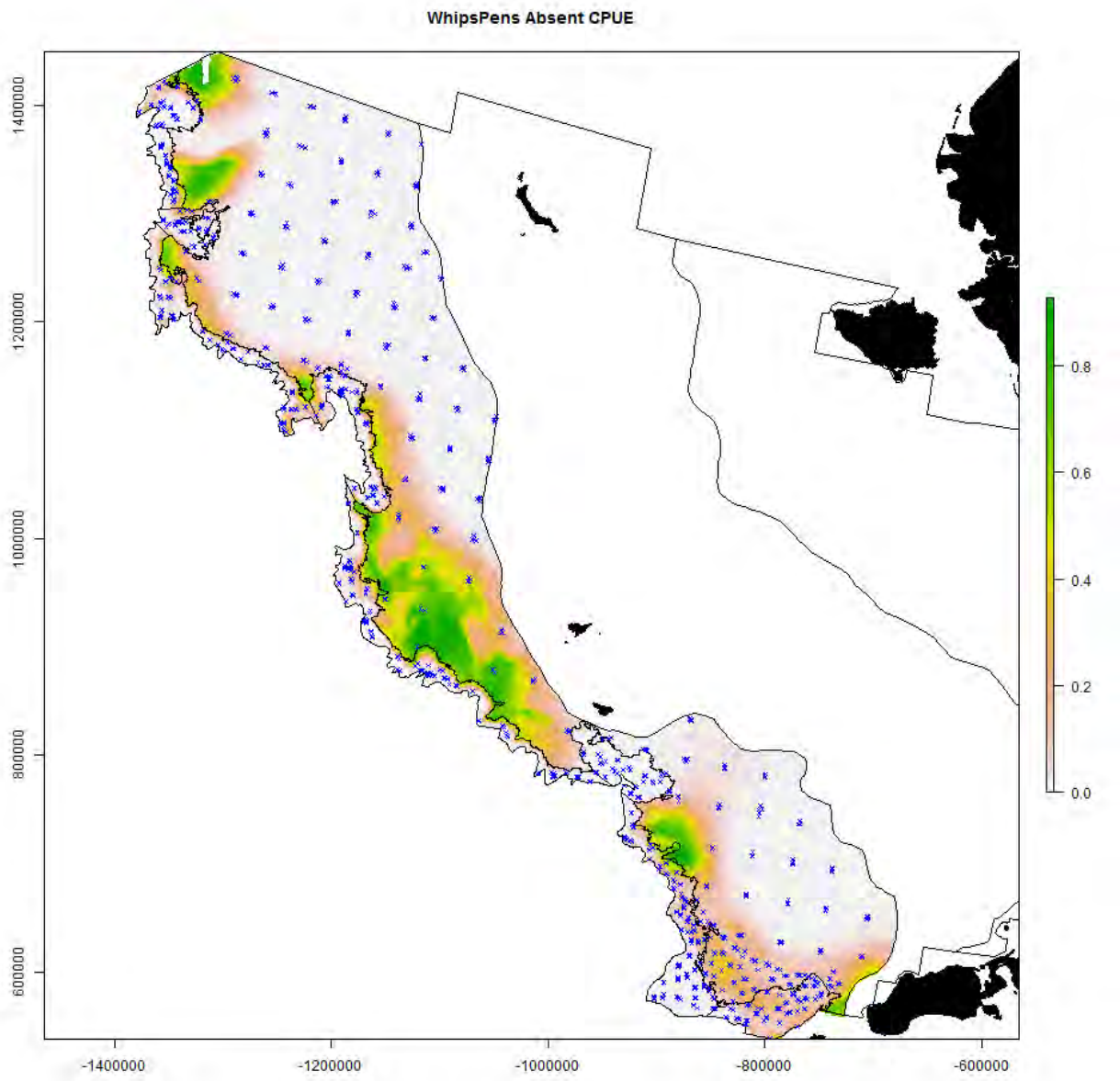
WhipsPens Absent CPUE
1400000
1200000
1000000
800000
600000
-1400000
-1200000
-1000000
-800000
-600000
0.8
0.6
0.4
0.2
0.0

1376

1377

S12. Generalized additive modeling results for Alaska skate. In the spatial plots, the x-axis label is easting and the y-axis label is northing and the unit is meters (Alaska Albers Equal Area Conic projection with center latitude = 50° N and center longitude = 154° W).

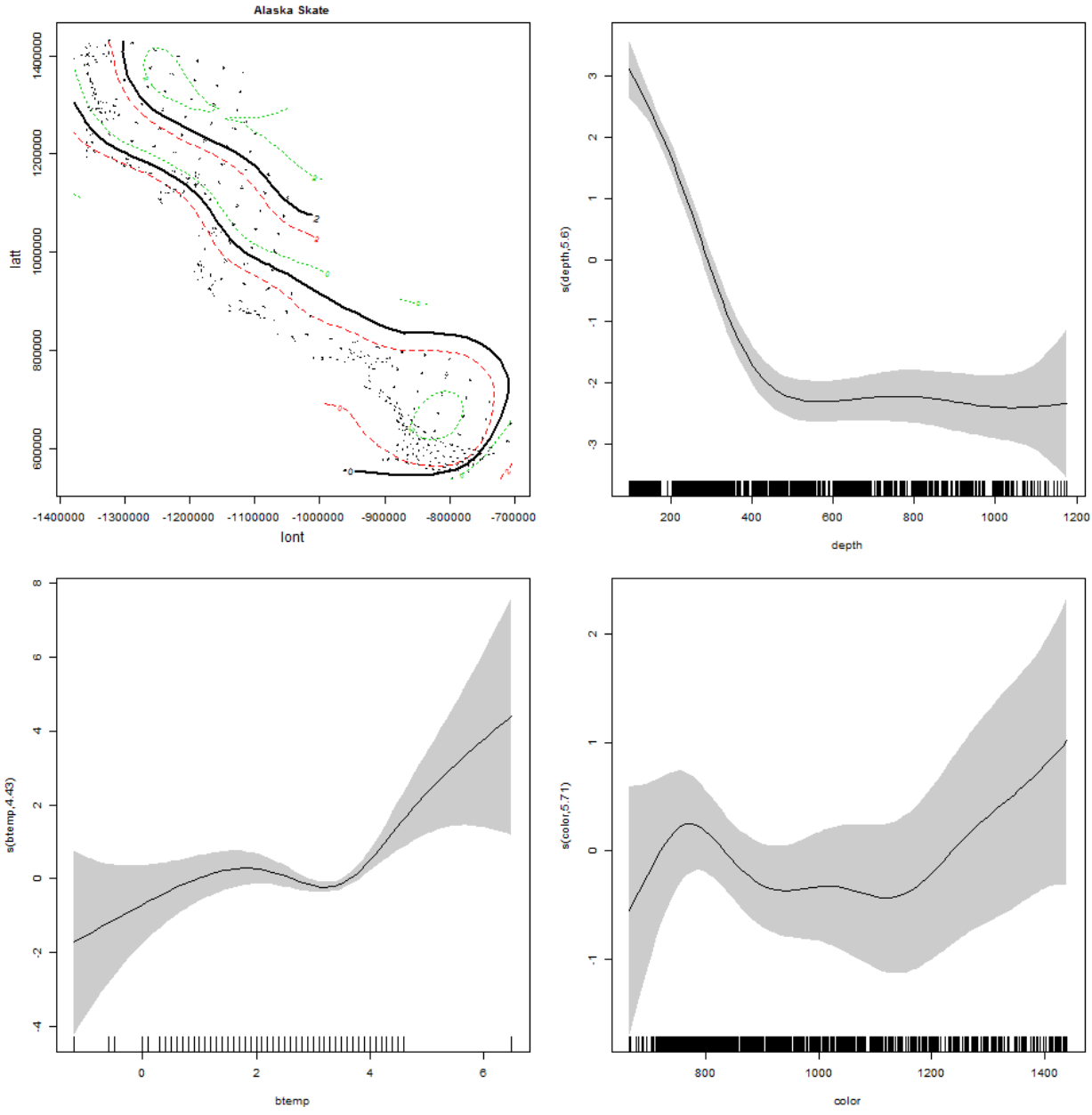

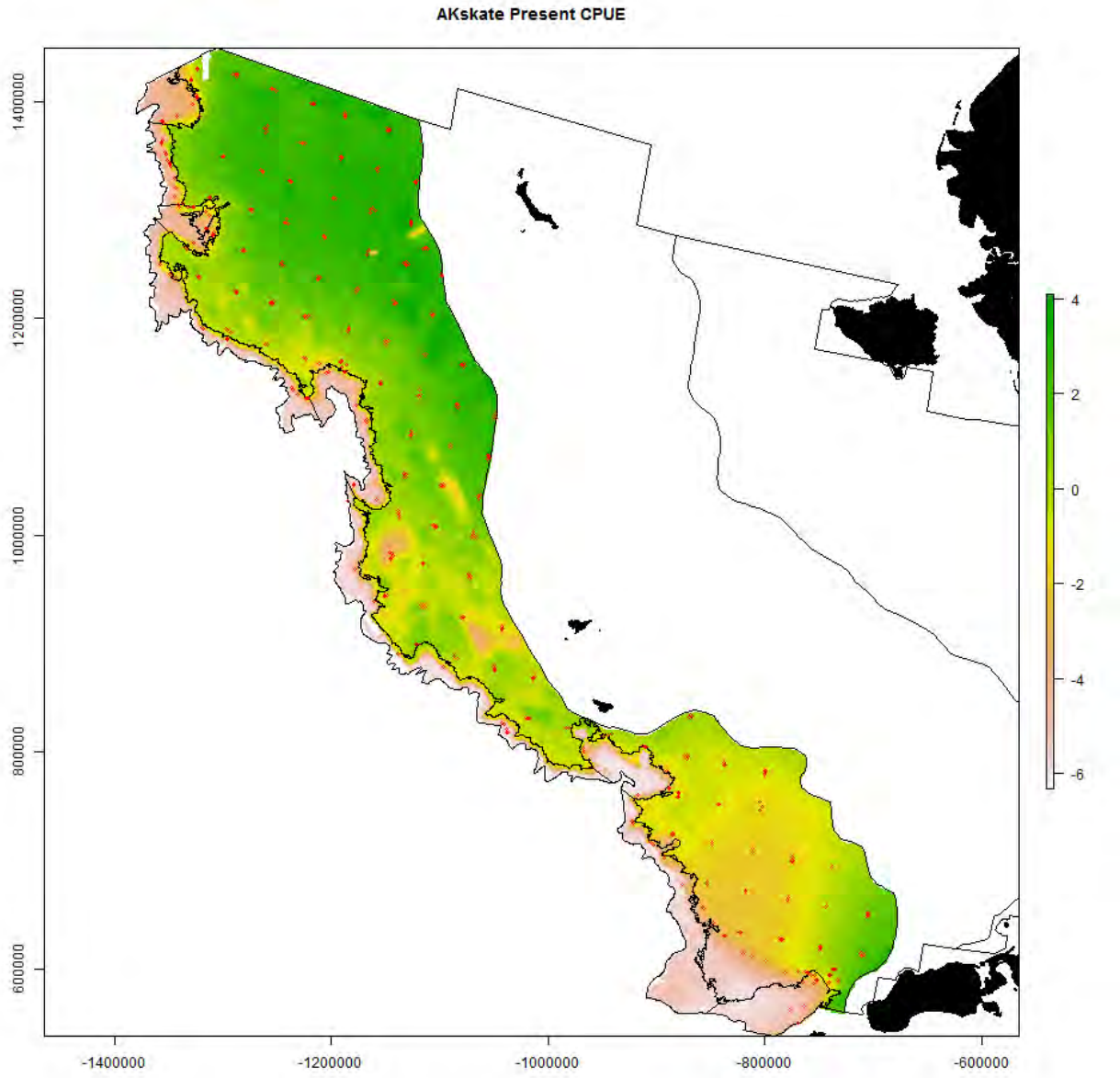
AKskate Present CPUE
1400000
1200000
1000000
800000
600000
-1400000
-1200000
-1000000
-800000
-600000
4
2
0
-2
-4
-6

1383

1384

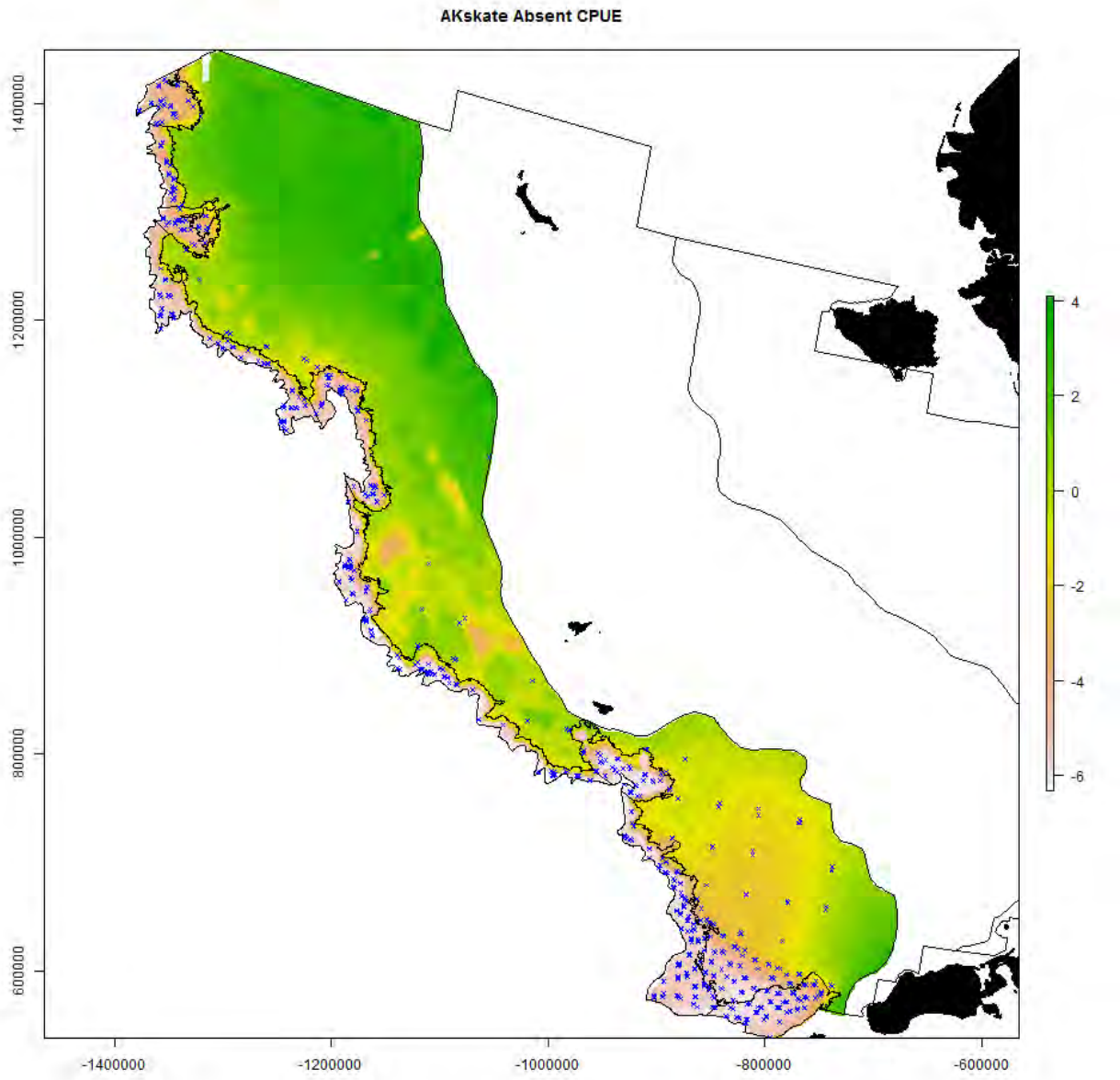
AKskate Absent CPUE
1400000
1200000
1000000
800000
600000
-1400000
-1200000
-1000000
-800000
-600000
4
2
0
-2
-4
-6

1385

1386

S13. Generalized additive modeling results for Aleutian skate. In the spatial plots, the x-axis label is easting and the y-axis label is northing and the unit is meters (Alaska Albers Equal Area Conic projection with center latitude = 50° N and center longitude = 154° W).

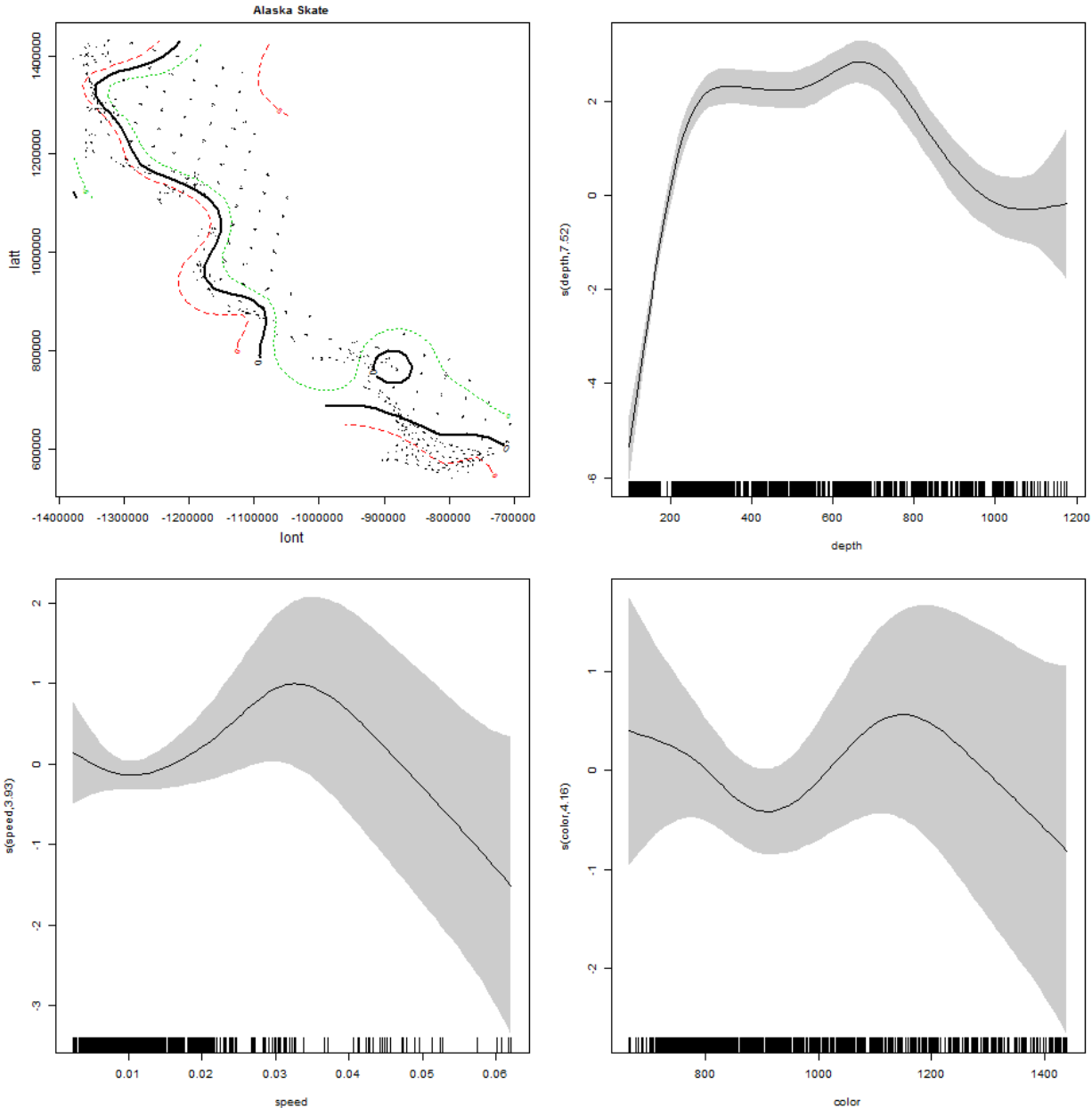

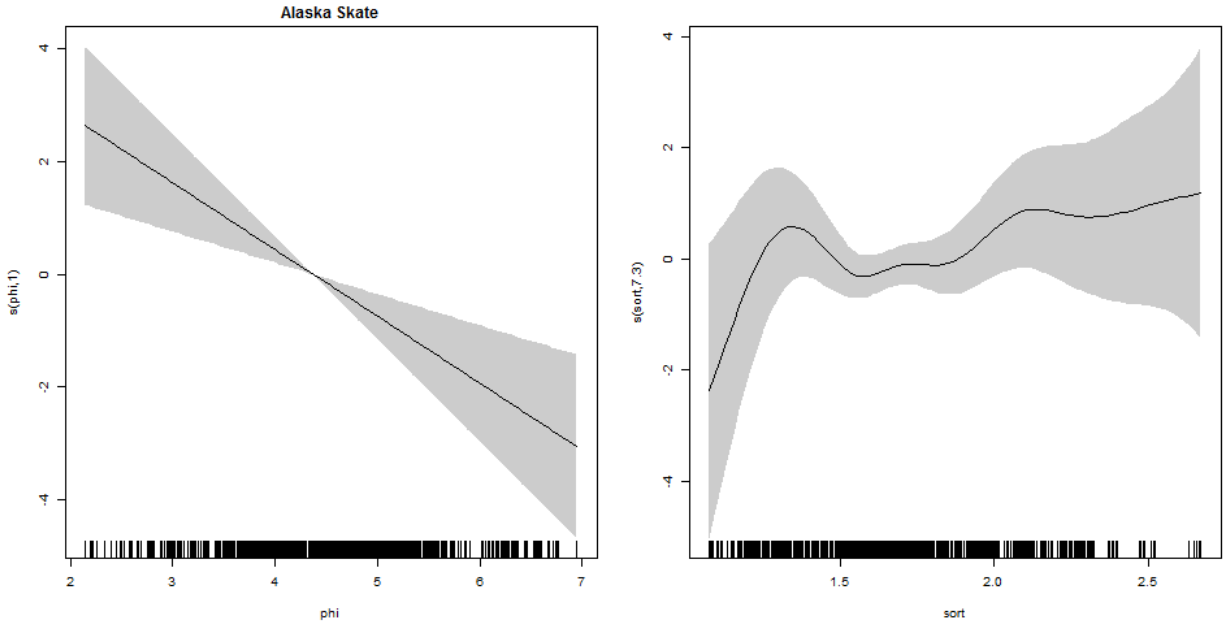


1391

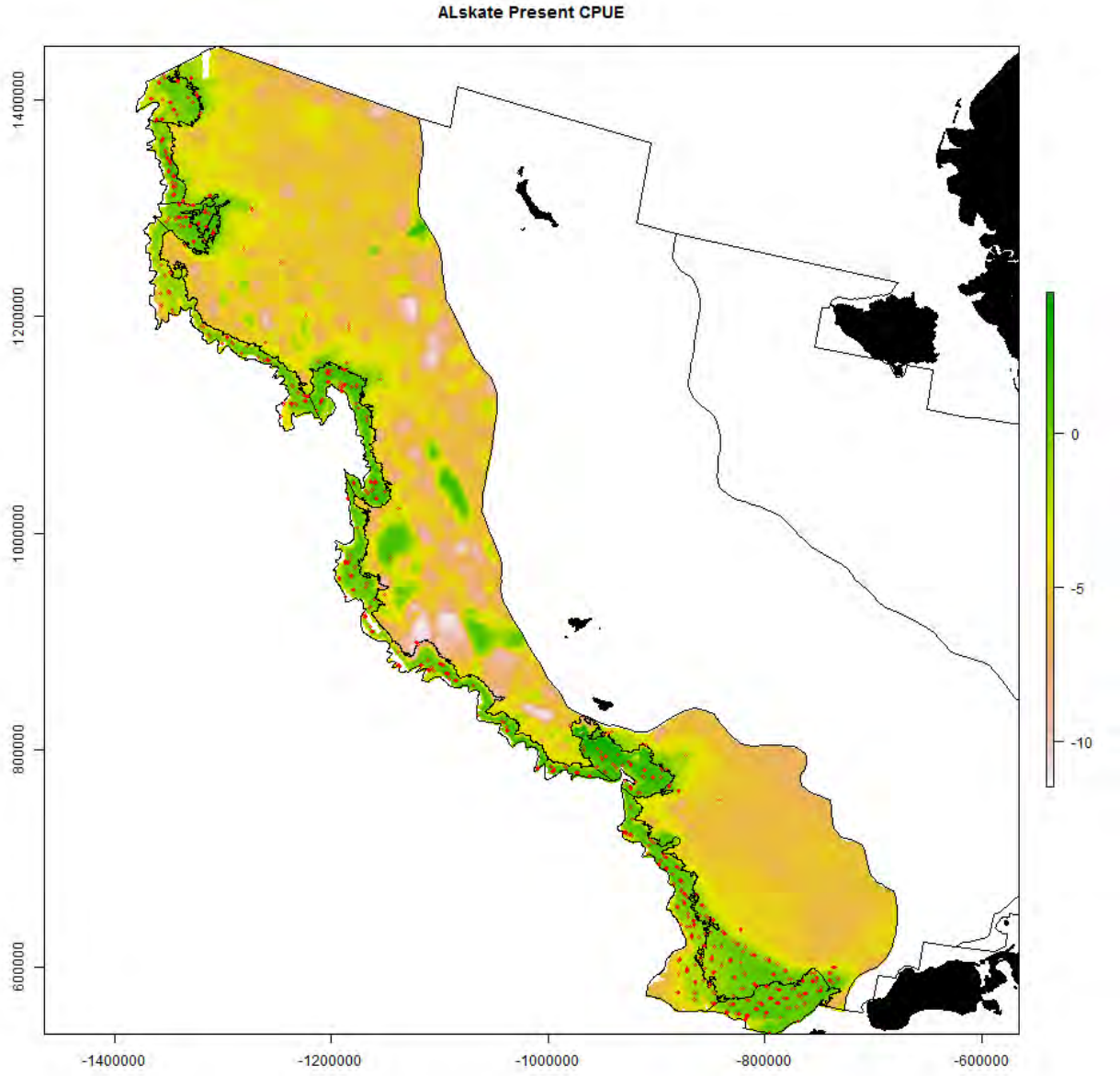
ALskate Present CPUE
1400000
1200000
1000000
800000
600000
-1400000
-1200000
-1000000
-800000
-600000
0
-5
-10

1392

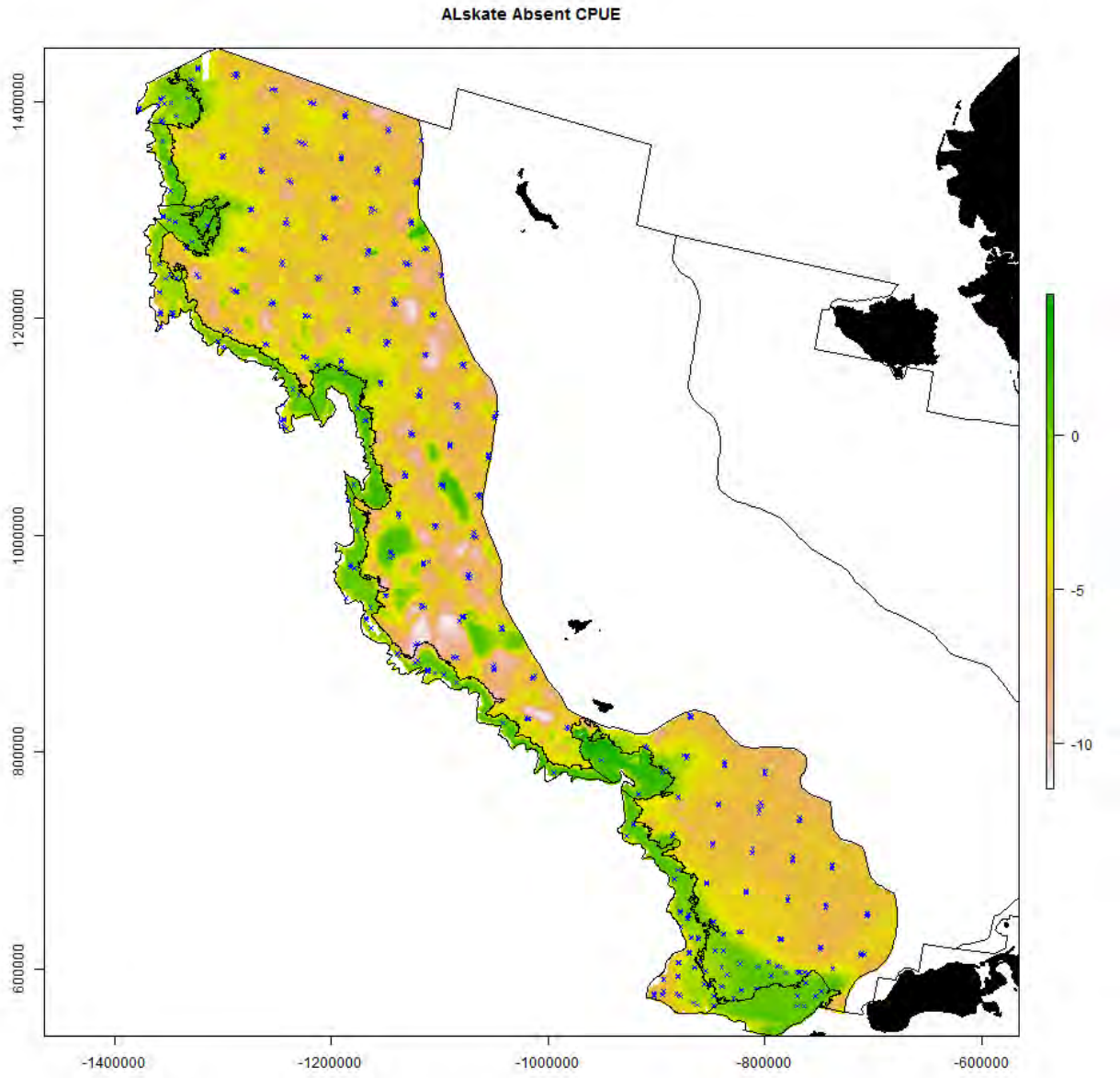
ALskate Absent CPUE
1400000
1200000
1000000
800000
600000
-1400000
-1200000
-1000000
-800000
-600000
0
-5
-10

1393

1394

S14. Generalized additive modeling results for flathead sole. In the spatial plots, the x-axis label is easting and the y-axis label is northing and the unit is meters (Alaska Albers Equal Area Conic projection with center latitude = 50° N and center longitude = 154° W).

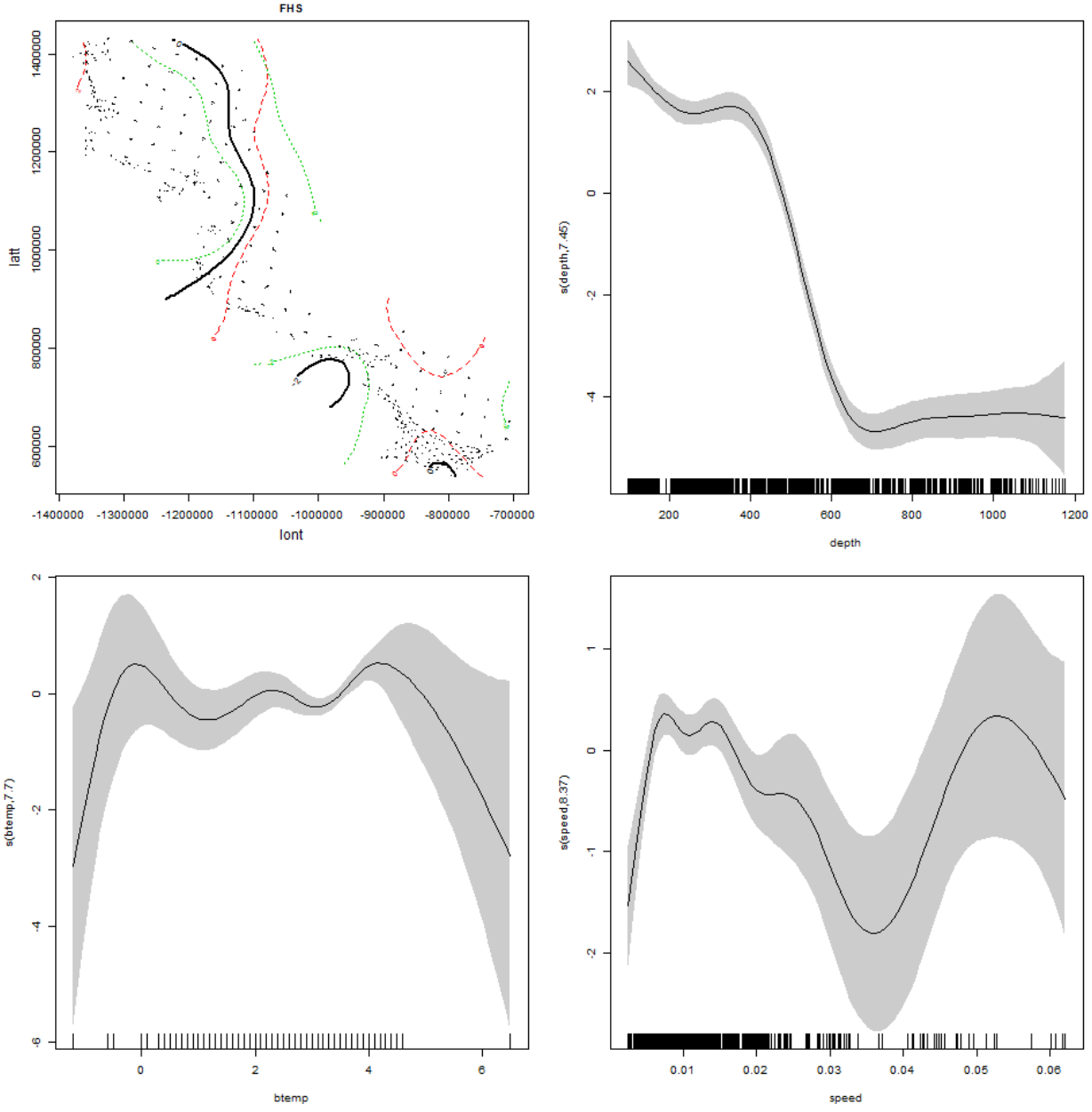

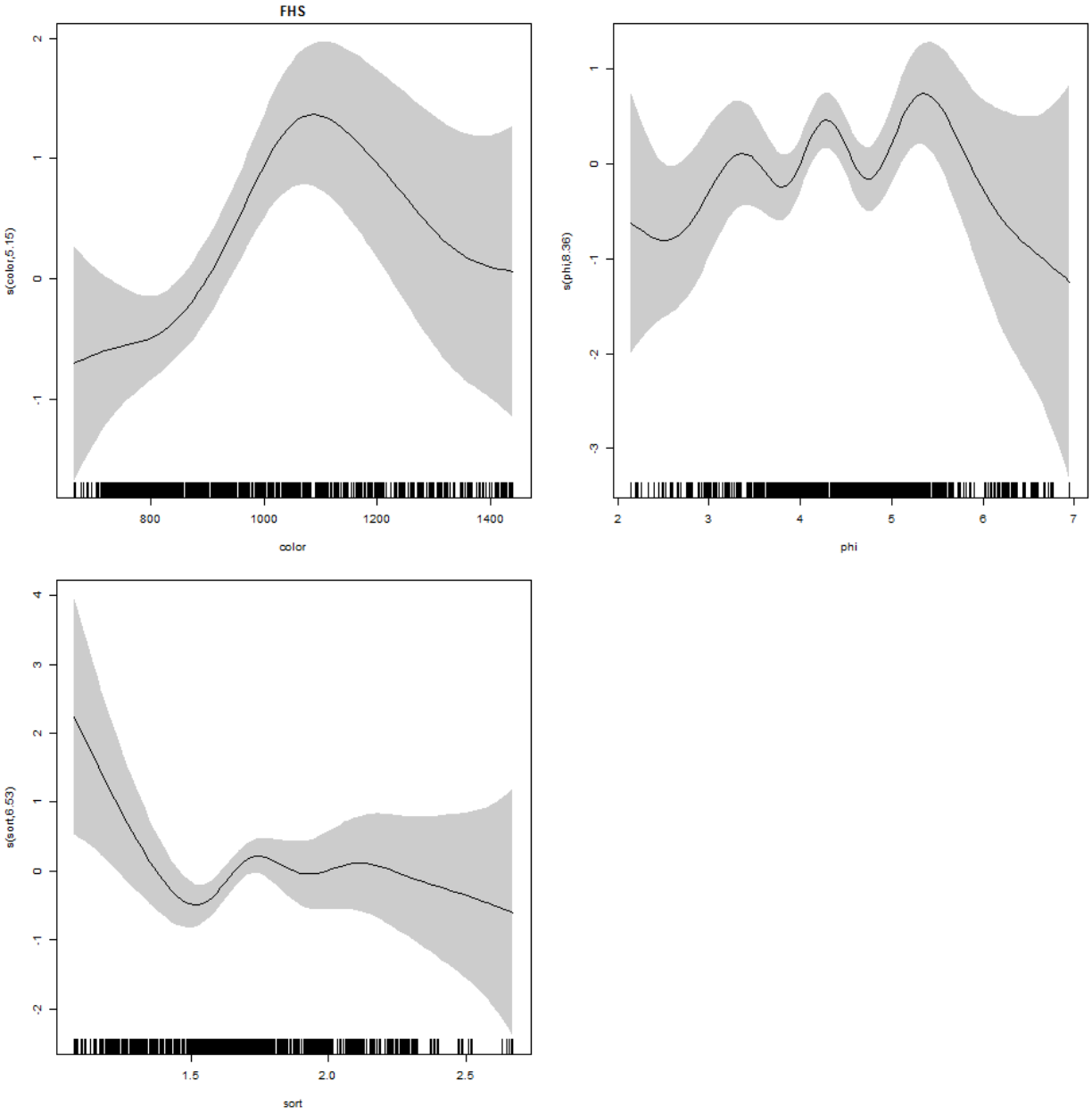


1399

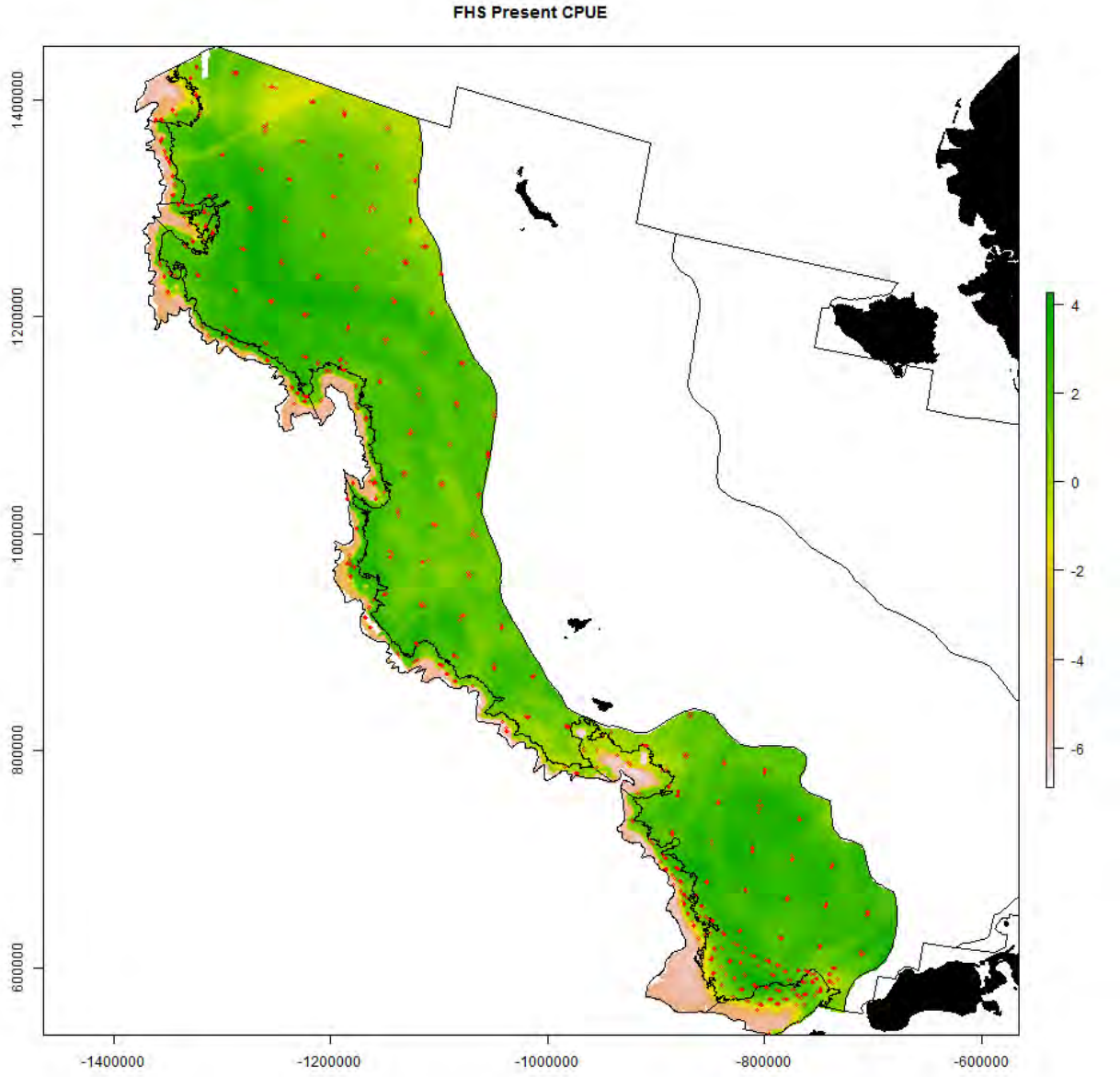
FHS Present CPUE
1400000
1200000
1000000
800000
600000
-1400000
-1200000
-1000000
-800000
-600000
4
2
0
-2
-4
-6

1400

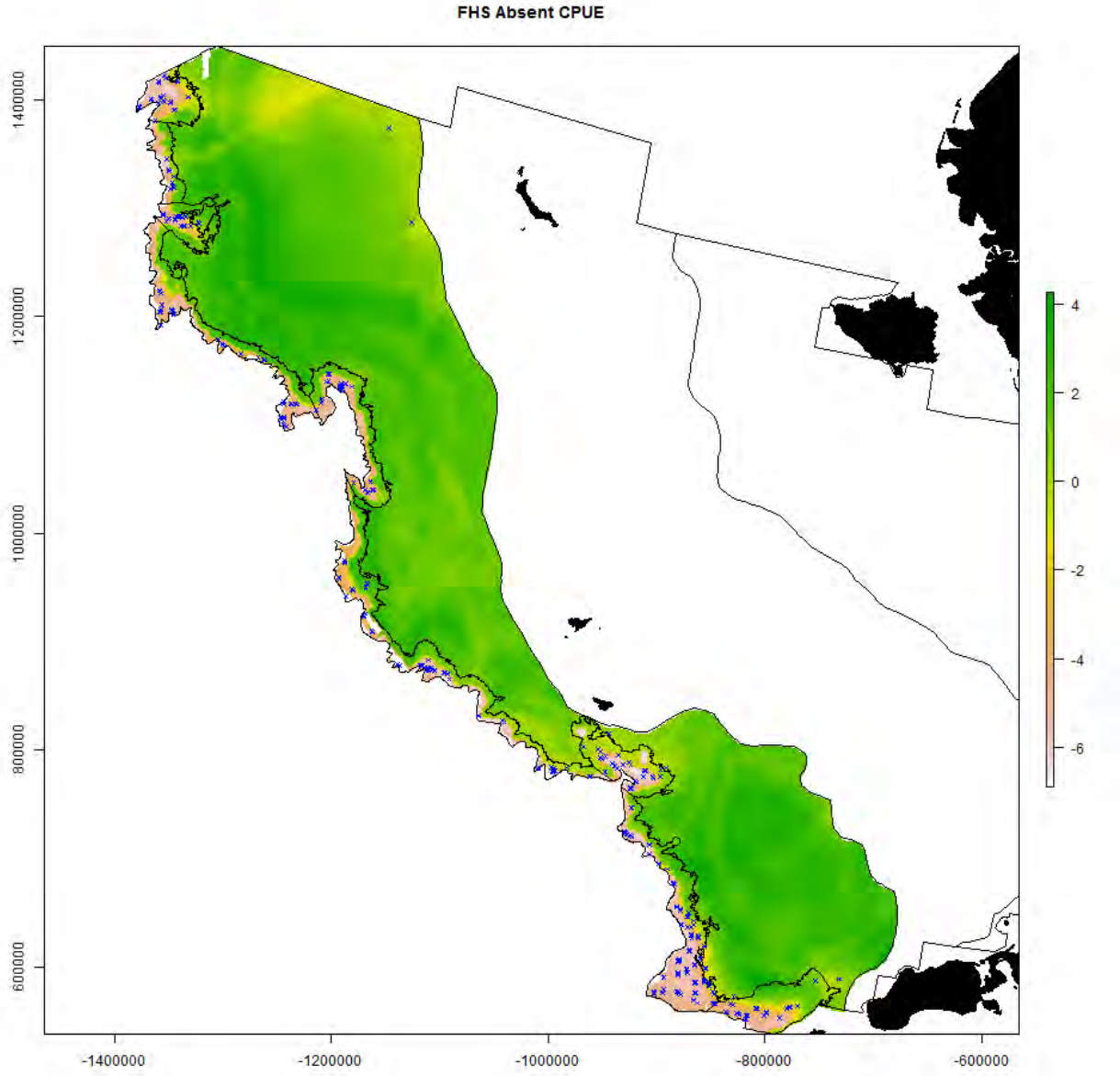
FHS Absent CPUE
1400000
1200000
1000000
800000
600000
-1400000
-1200000
-1000000
-800000
-600000
4
2
0
-2
-4
-6

1401

1402

S15. Generalized additive modeling results for giant grenadier. In the spatial plots, the x-axis label is easting and the y-axis label is northing and the unit is meters (Alaska Albers Equal Area Conic projection with center latitude = 50° N and center longitude = 154° W).

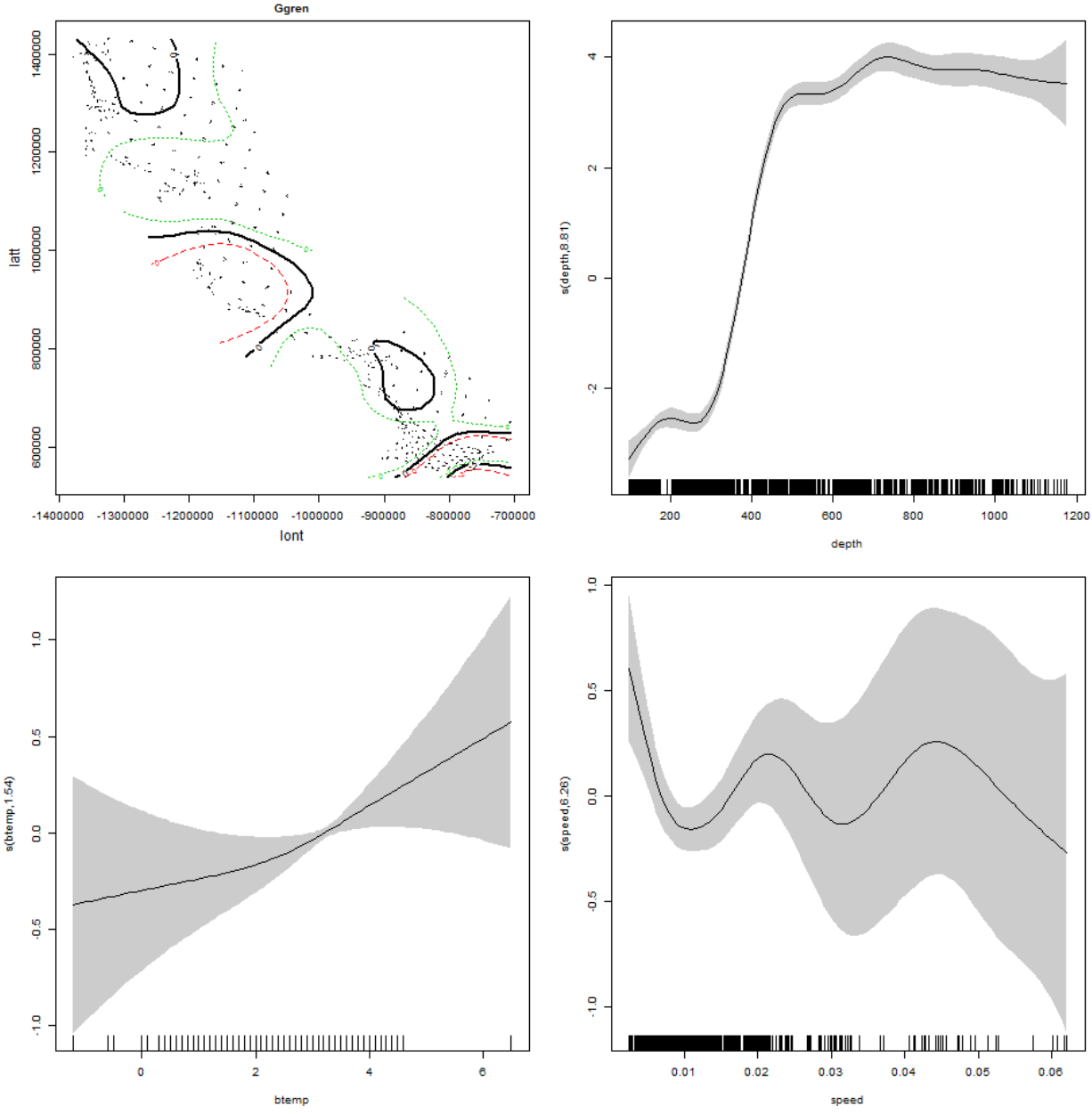

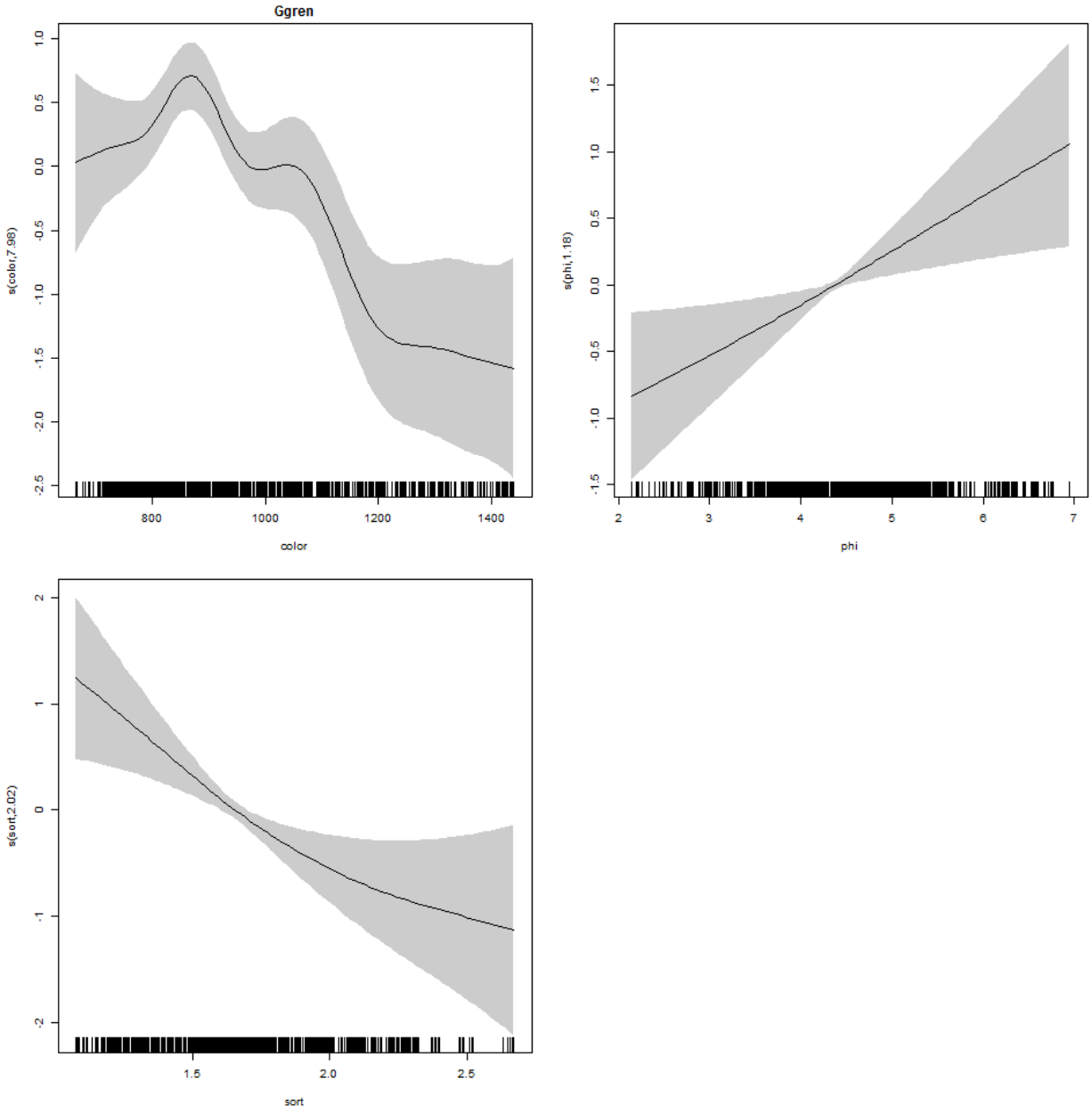


1407

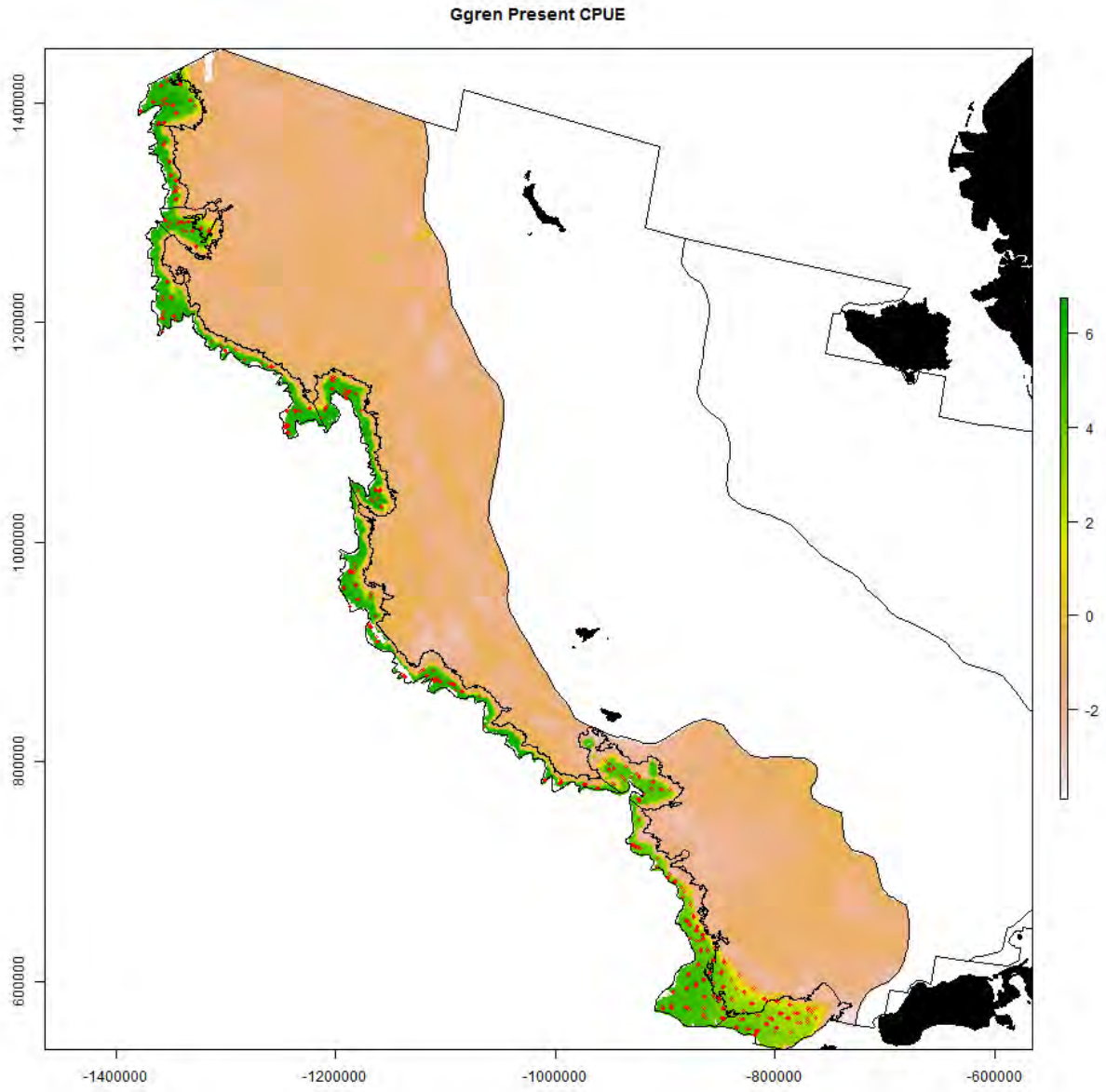
Ggren Present CPUE
1400000
1200000
1000000
800000
600000
-1400000
-1200000
-1000000
-800000
-600000
6
4
2
0
-2

1408

1409

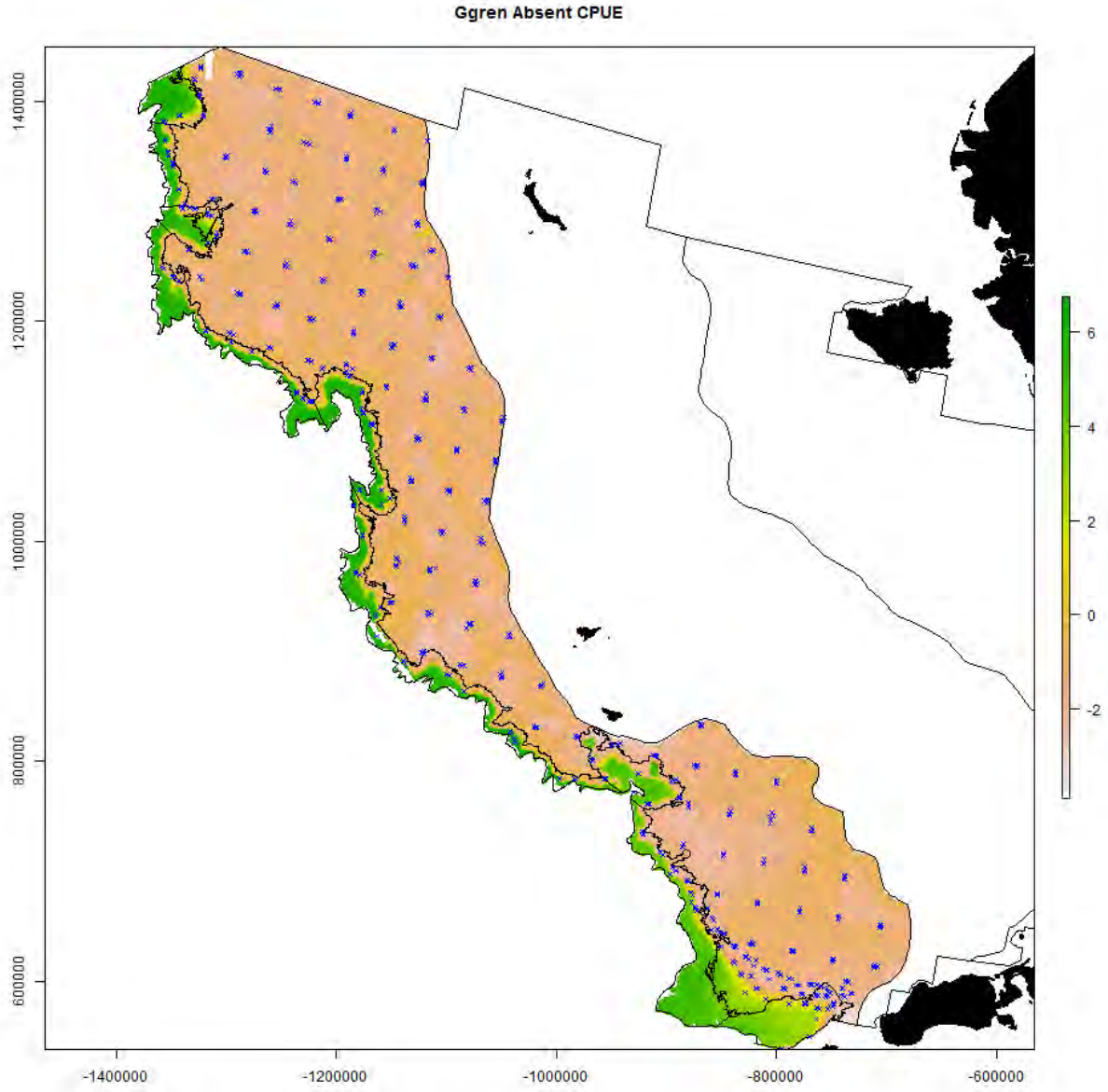
Ggren Absent CPUE
1400000
1200000
1000000
800000
600000
-1400000
-1200000
-1000000
-800000
-600000
6
4
2
0
-2

1410
1411

1412 S16. Generalized additive modeling results for Greenland turbot. In the spatial plots, the x-axis
1413 label is easting and the y-axis label is northing and the unit is meters (Alaska Albers Equal Area
1414 Conic projection with center latitude = 50° N and center longitude = 154° W).

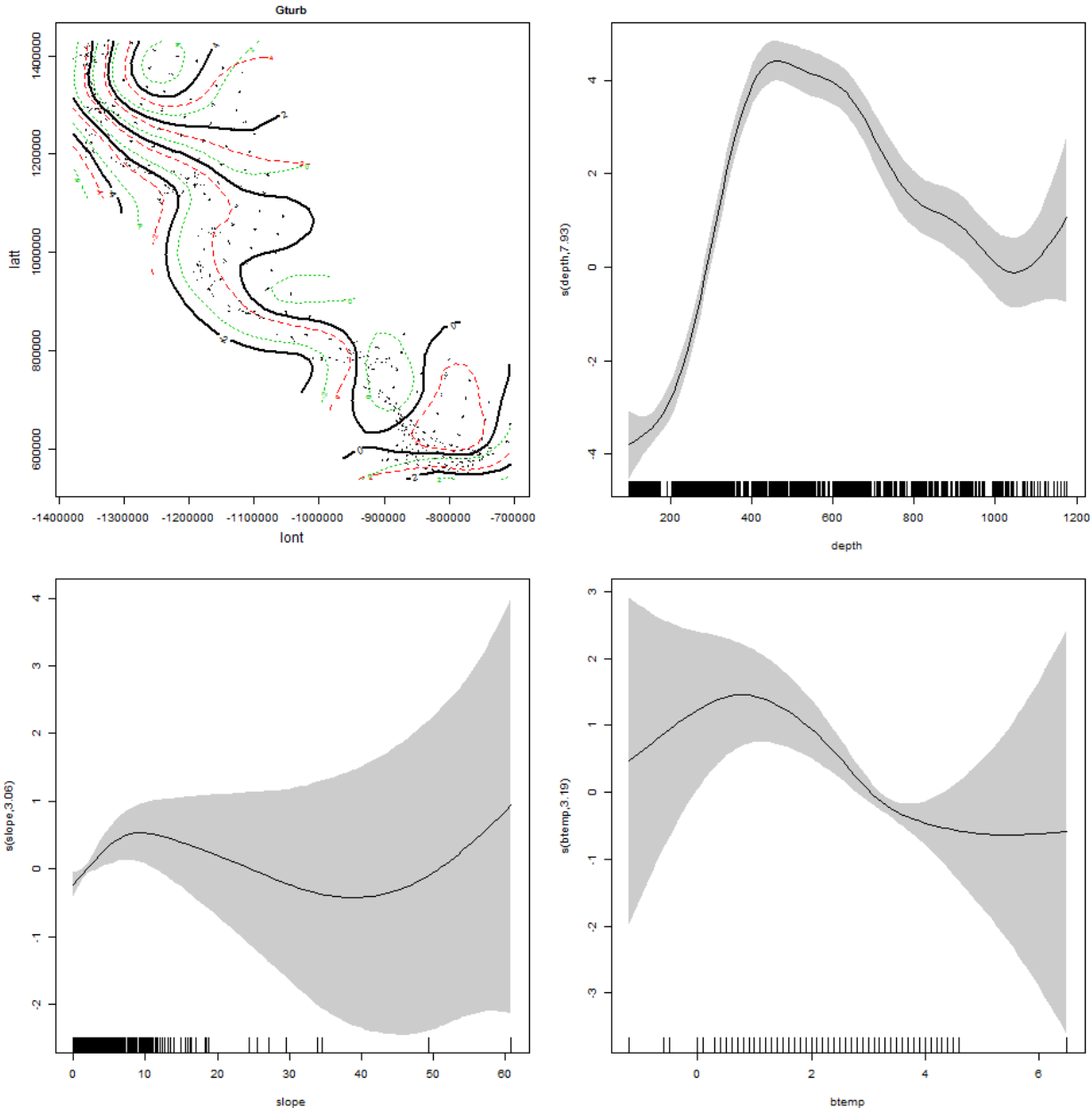


1415

1416

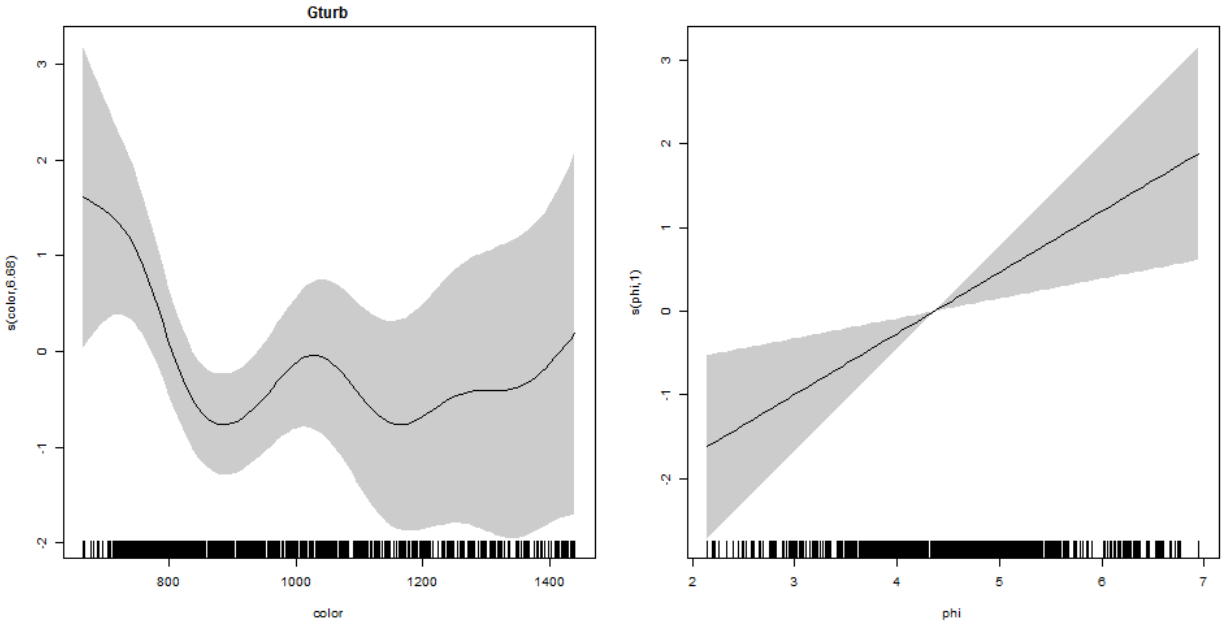


1417

1418

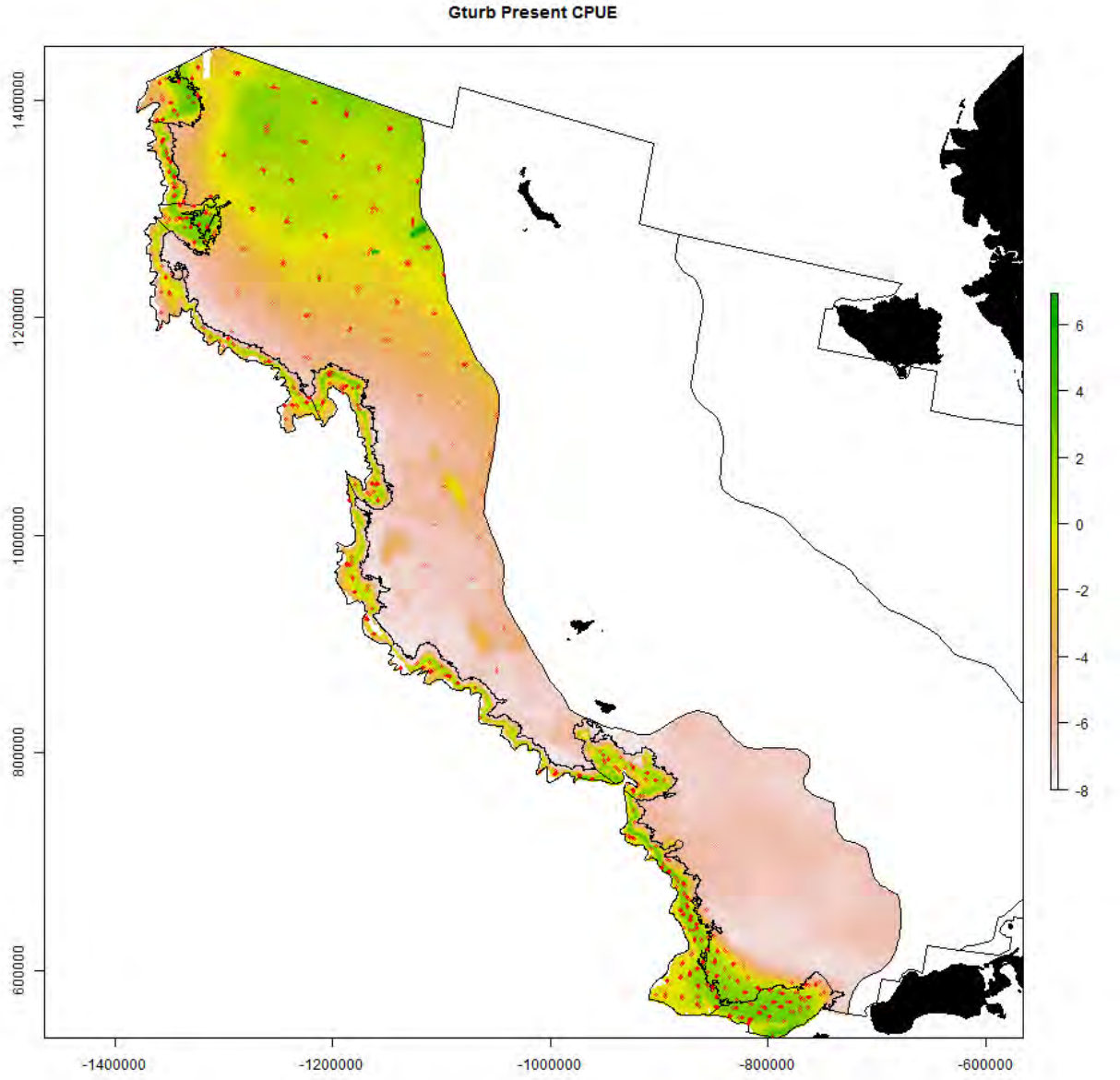
Gturb Present CPUE
1400000
1200000
1000000
800000
600000
-1400000
-1200000
-1000000
-800000
-600000
6
4
2
0
-2
-4
-6
-8

1419

1420

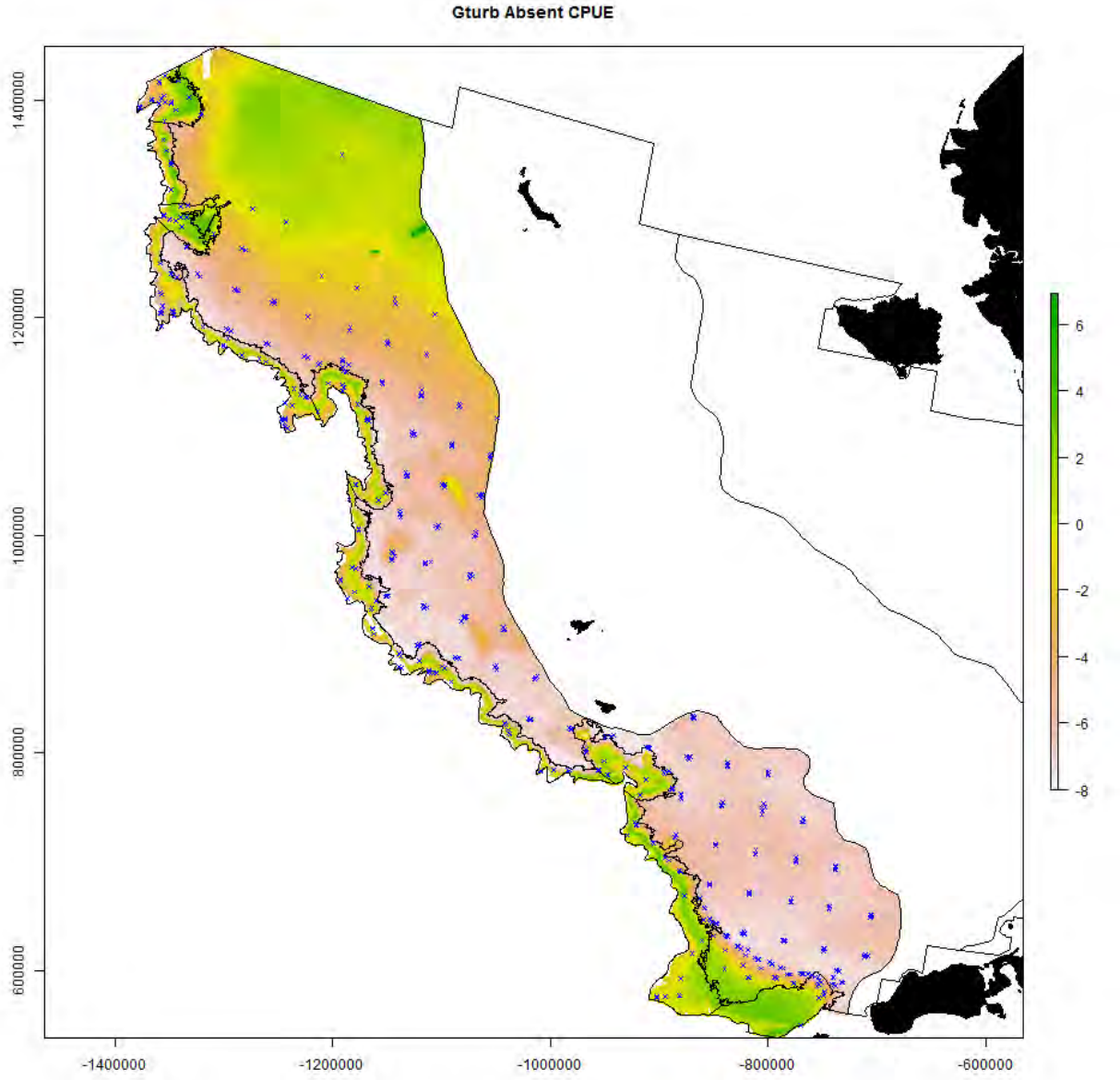
Gturb Absent CPUE
1400000
1200000
1000000
800000
600000
-1400000
-1200000
-1000000
-800000
-600000
6
4
2
0
-2
-4
-6
-8

1421
1422

1423 S17. Generalized additive modeling results for Kamchatka flounder. In the spatial plots, the x-
1424 axis label is easting and the y-axis label is northing and the unit is meters (Alaska Albers Equal
1425 Area Conic projection with center latitude = 50° N and center longitude = 154° W).

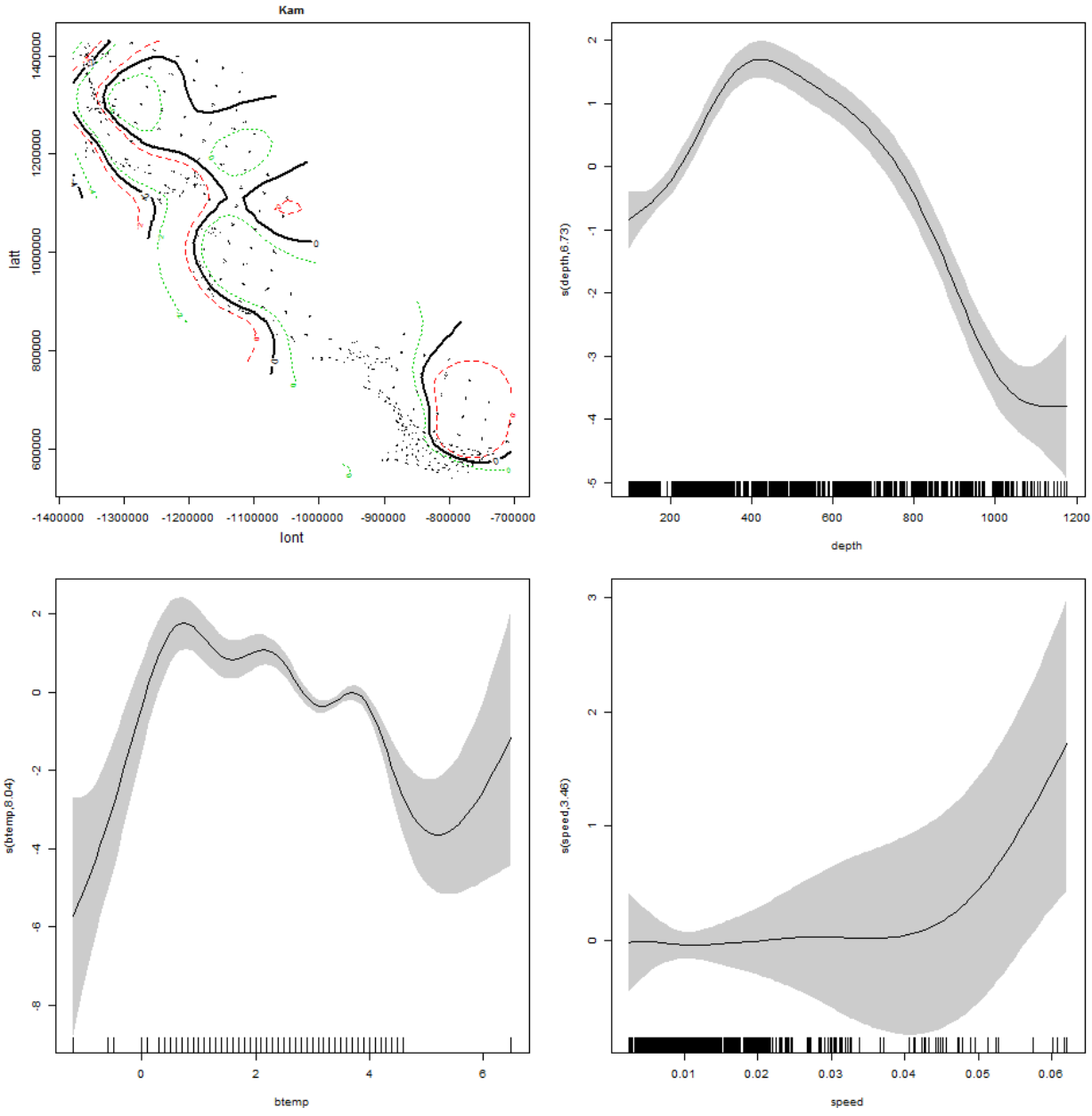


1426

1427

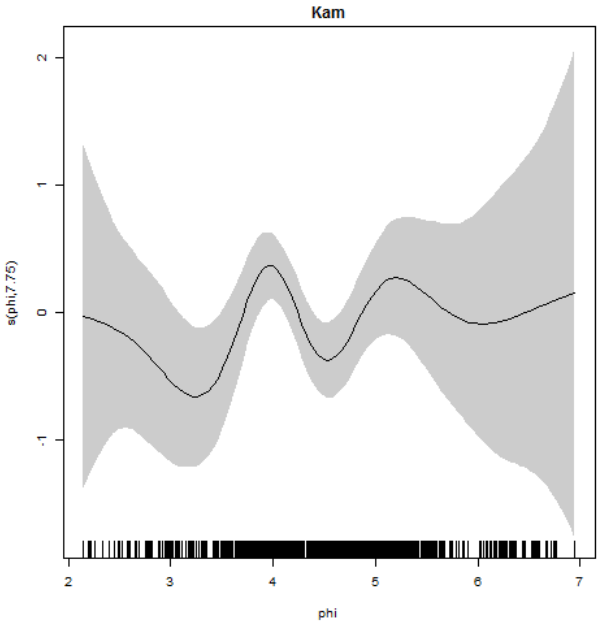


1428

1429

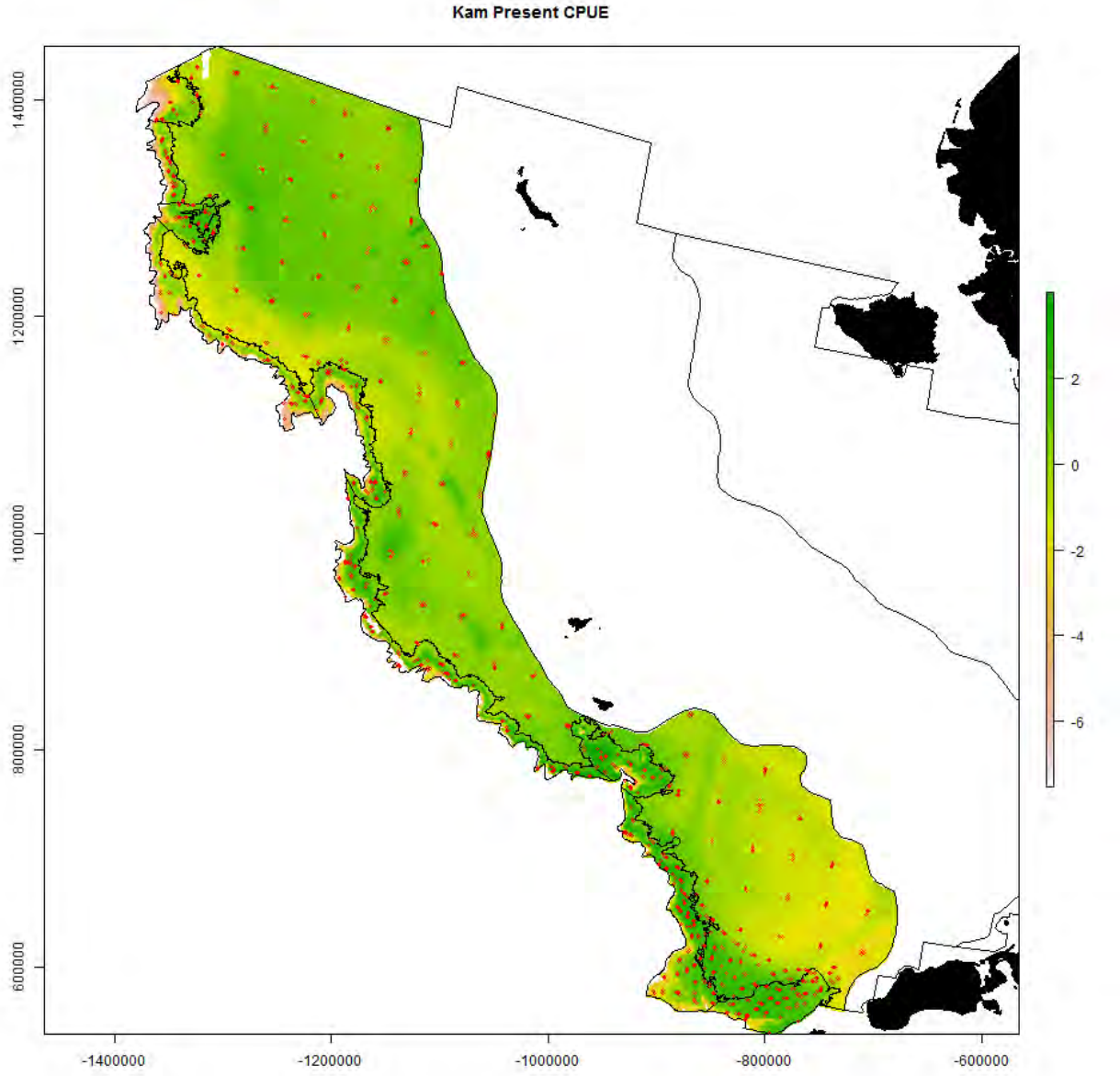
Kam Present CPUE
1400000
1200000
1000000
800000
600000
-1400000
-1200000
-1000000
-800000
-600000
2
0
-2
-4
-6

1430

1431

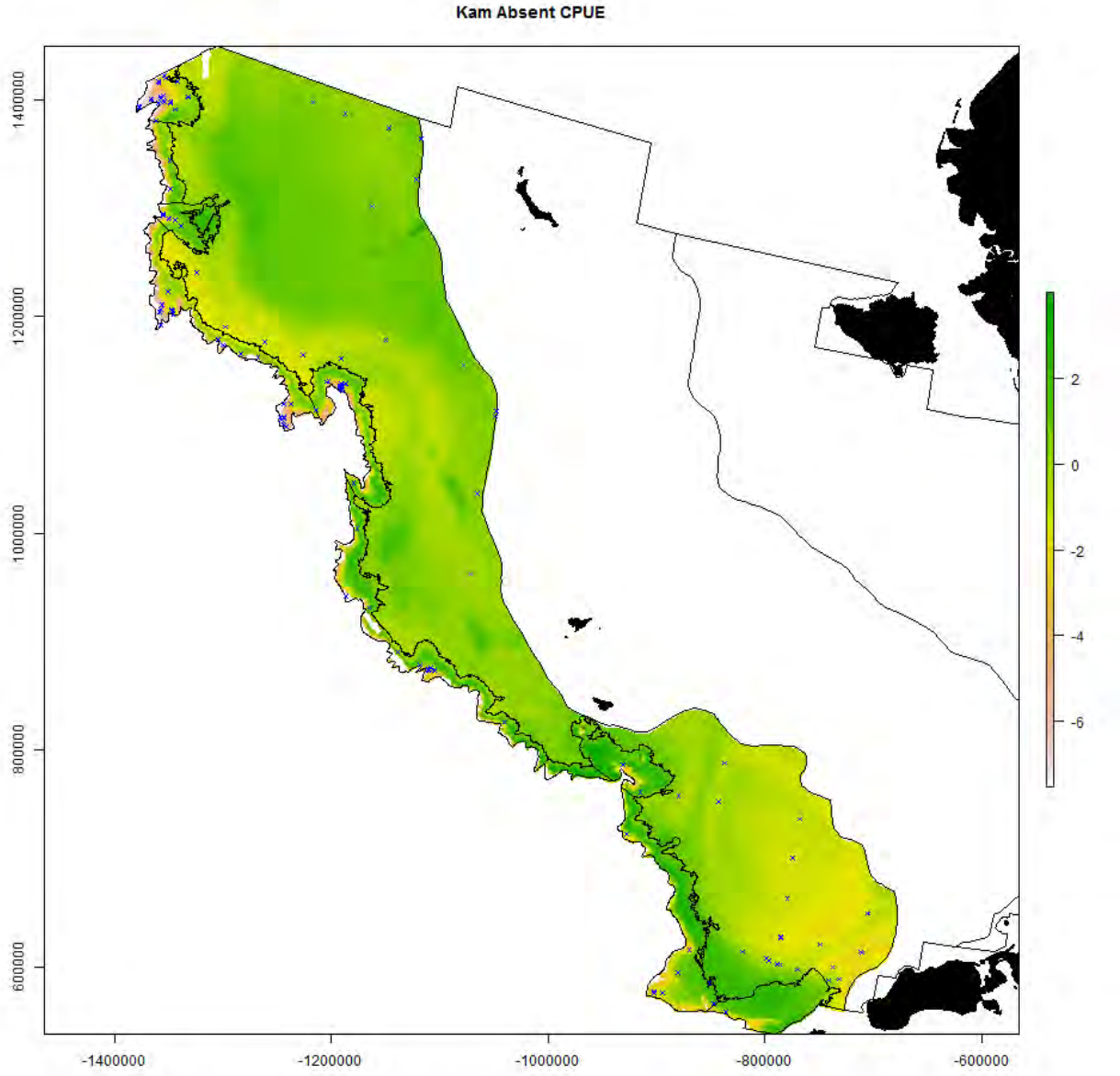
Kam Absent CPUE
1400000
1200000
1000000
800000
600000
-1400000
-1200000
-1000000
-800000
-600000
2
0
-2
-4
-6

1432
1433

S18. Generalized additive modeling results for northern rock sole. In the spatial plots, the x-axis label is easting and the y-axis label is northing and the unit is meters (Alaska Albers Equal Area Conic projection with center latitude = 50° N and center longitude = 154° W).

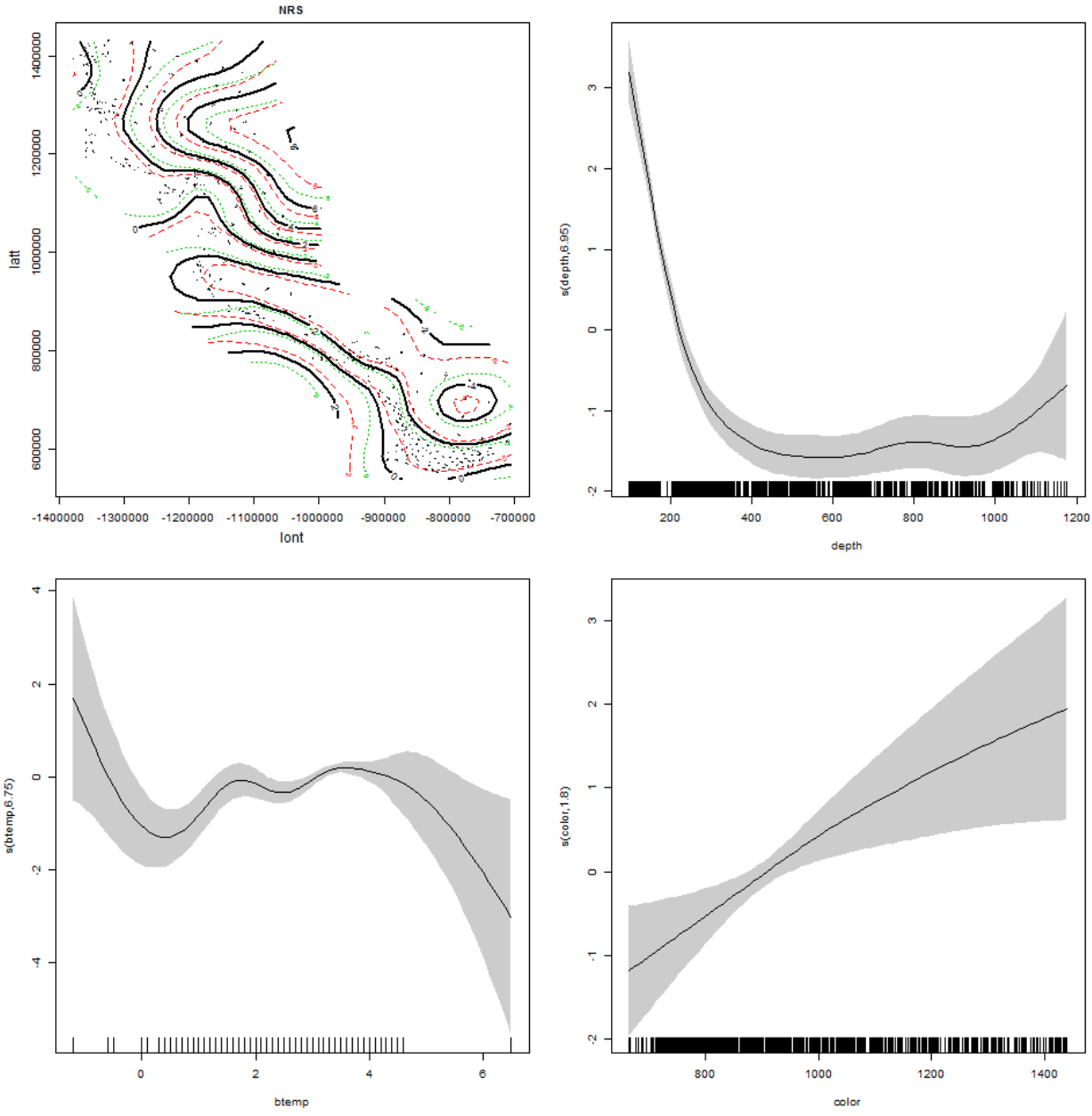

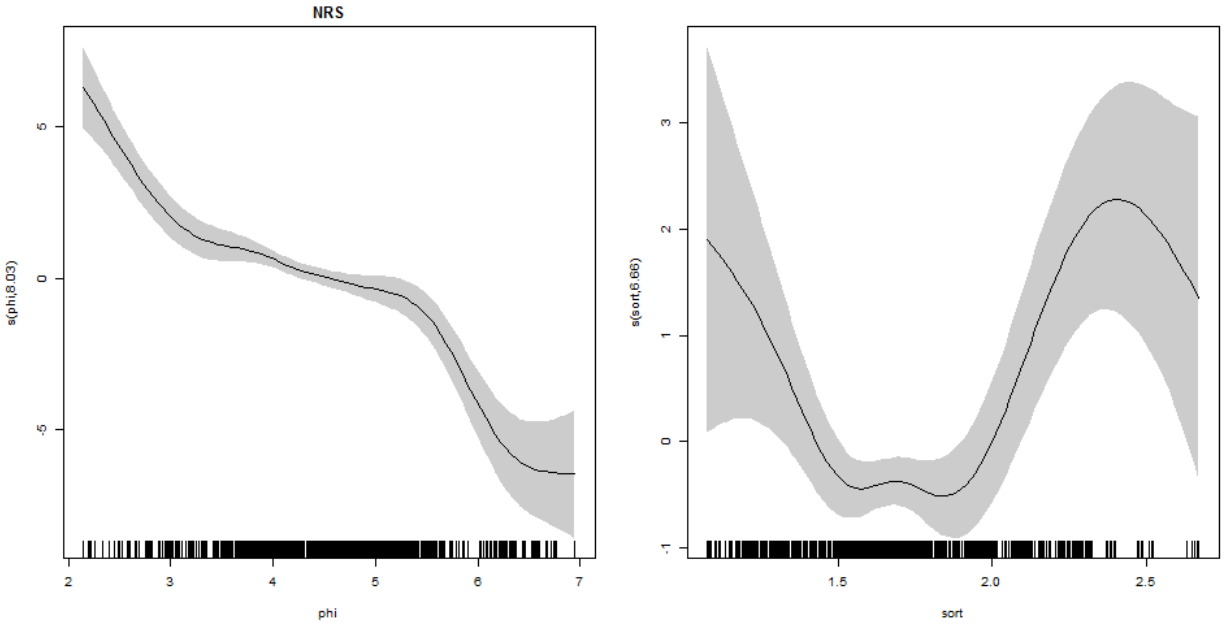


1439

1440

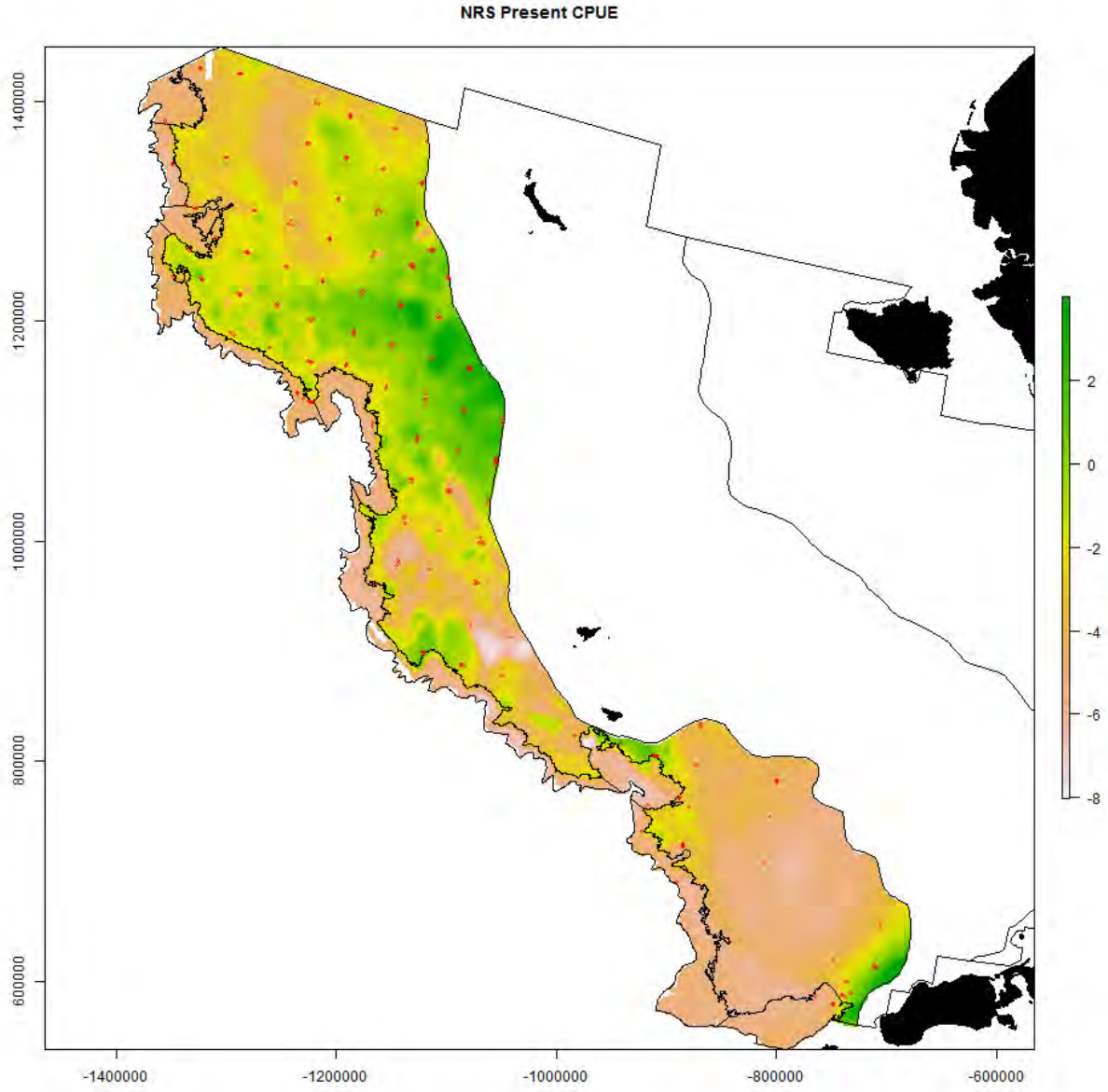
NRS Present CPUE
1400000
1200000
1000000
800000
600000
-1400000
-1200000
-1000000
-800000
-600000
2
0
-2
-4
-6
-8

1441

1442

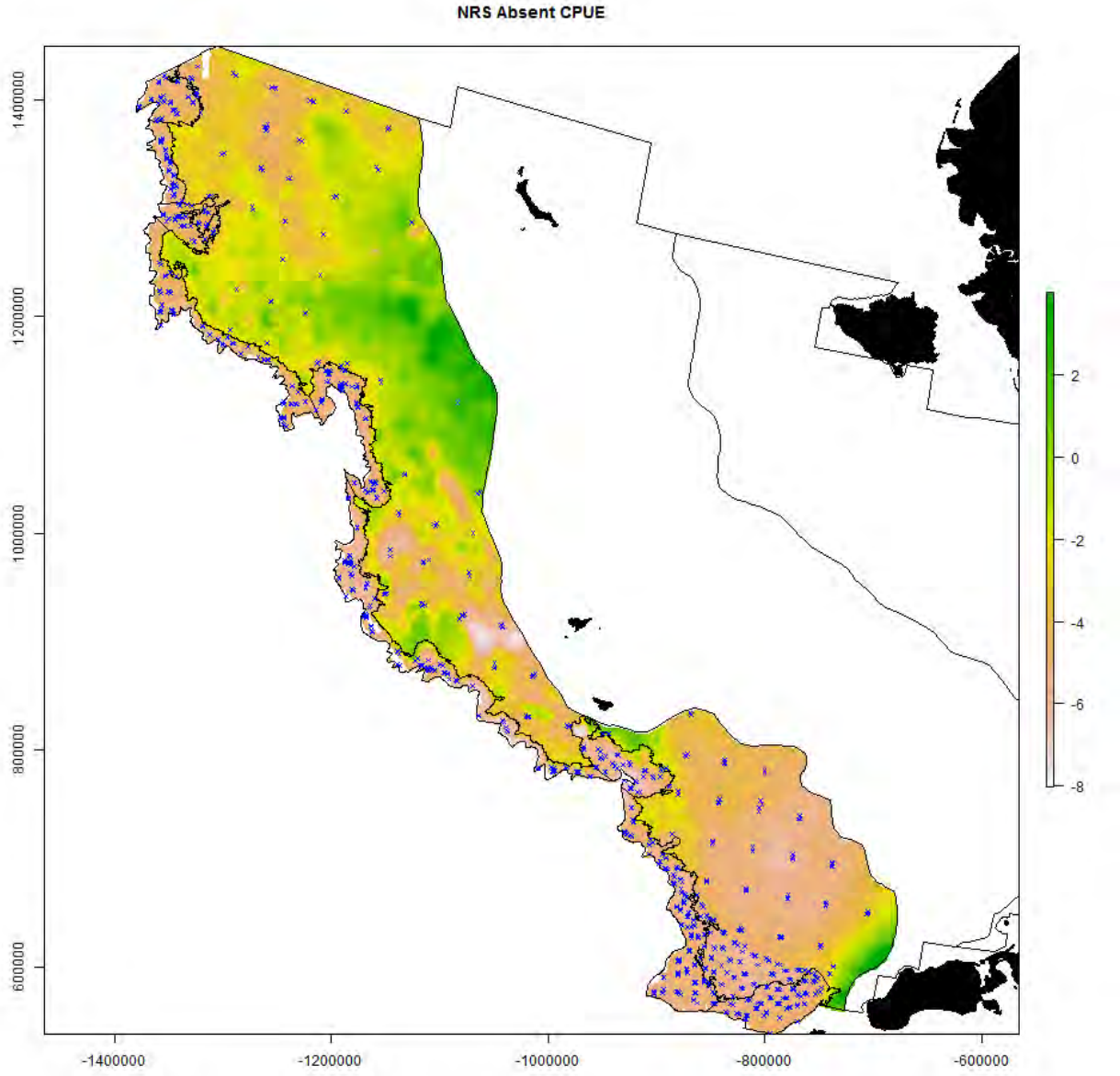
NRS Absent CPUE
1400000
1200000
1000000
800000
600000
-1400000
-1200000
-1000000
-800000
-600000
2
0
-2
-4
-6
-8

1443
1444

S19. Generalized additive modeling results for Pacific cod. In the spatial plots, the x-axis label is easting and the y-axis label is northing and the unit is meters (Alaska Albers Equal Area Conic projection with center latitude = 50° N and center longitude = 154° W).

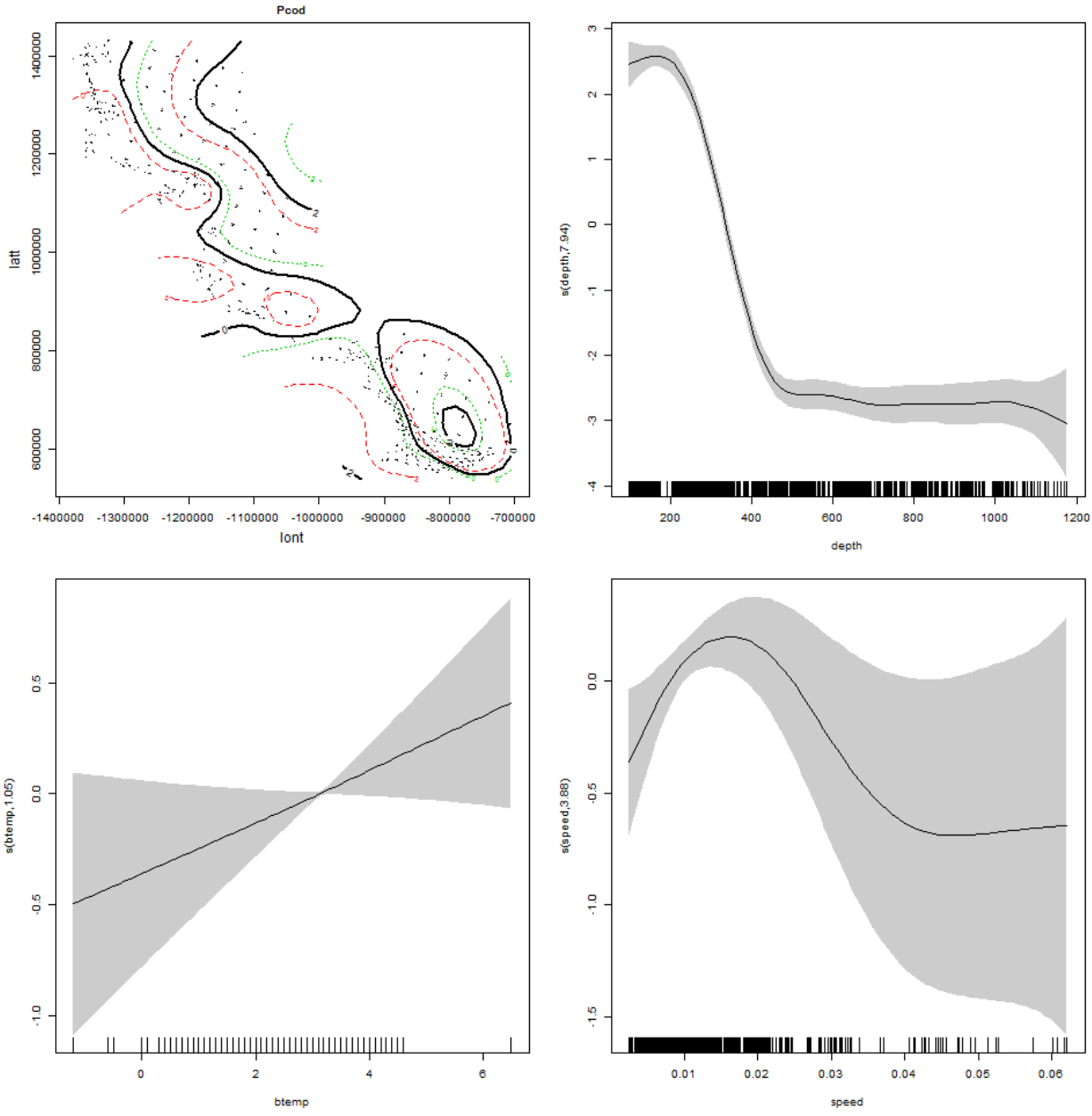

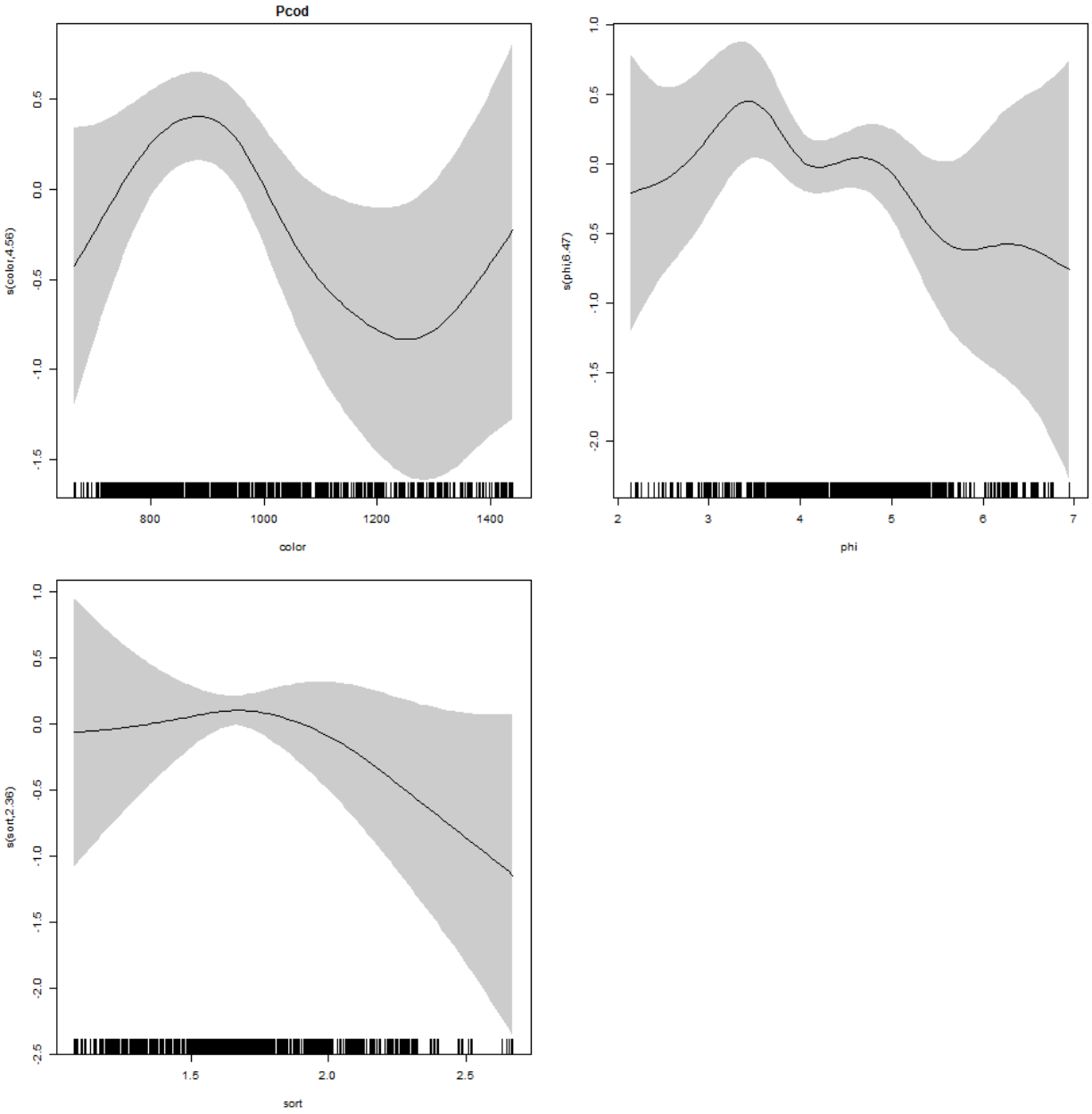


1450

1451

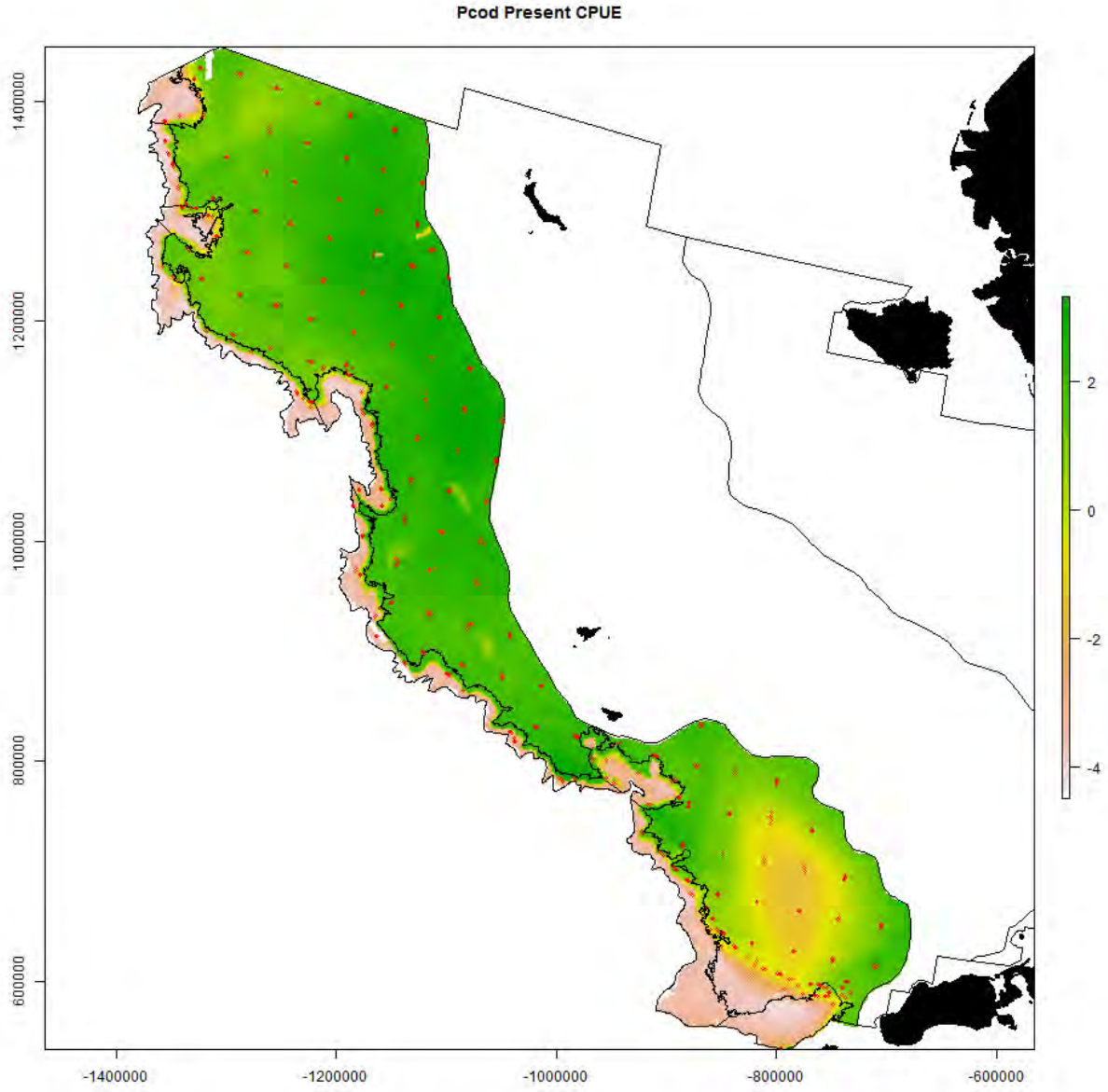
Pcod Present CPUE
1400000
1200000
1000000
800000
600000
-1400000
-1200000
-1000000
-800000
-600000
2
0
-2
-4

1452

1453

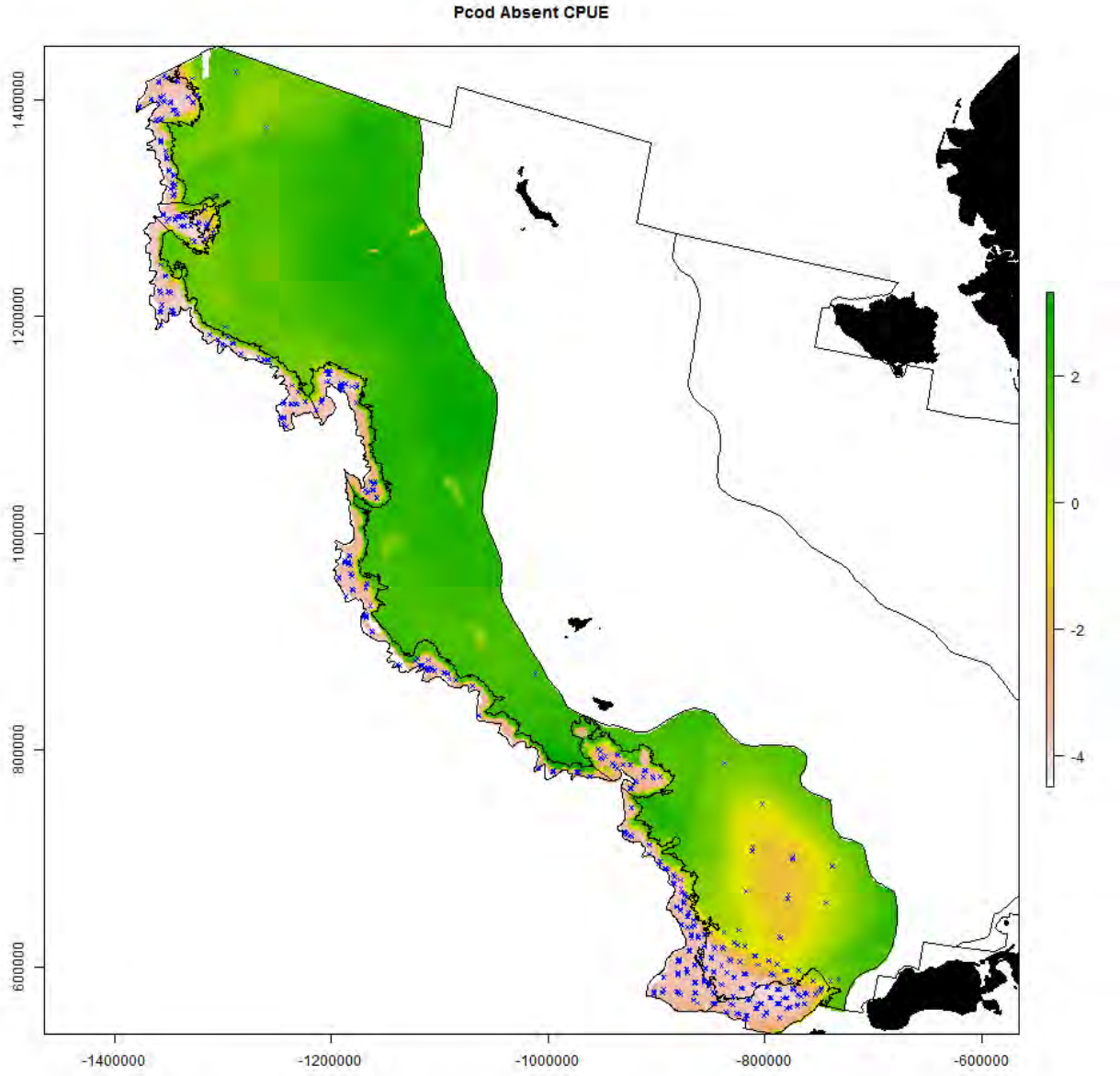
Pcod Absent CPUE
1400000
1200000
1000000
800000
600000
-1400000
-1200000
-1000000
-800000
-600000
2
0
-2
-4

1454
1455

S20. Generalized additive modeling results for Pacific grenadier. In the spatial plots, the x-axis label is easting and the y-axis label is northing and the unit is meters (Alaska Albers Equal Area Conic projection with center latitude = 50° N and center longitude = 154° W).

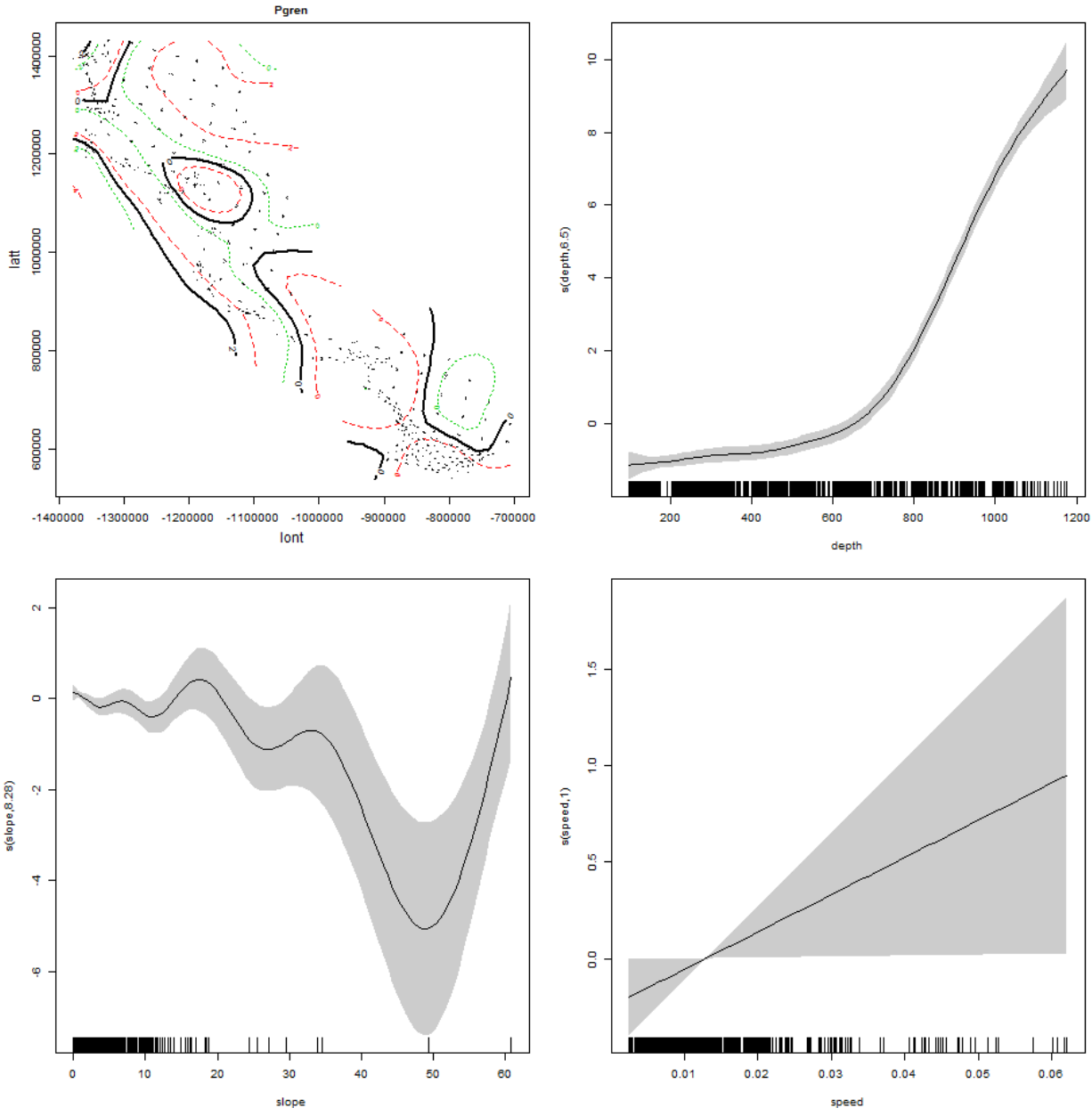

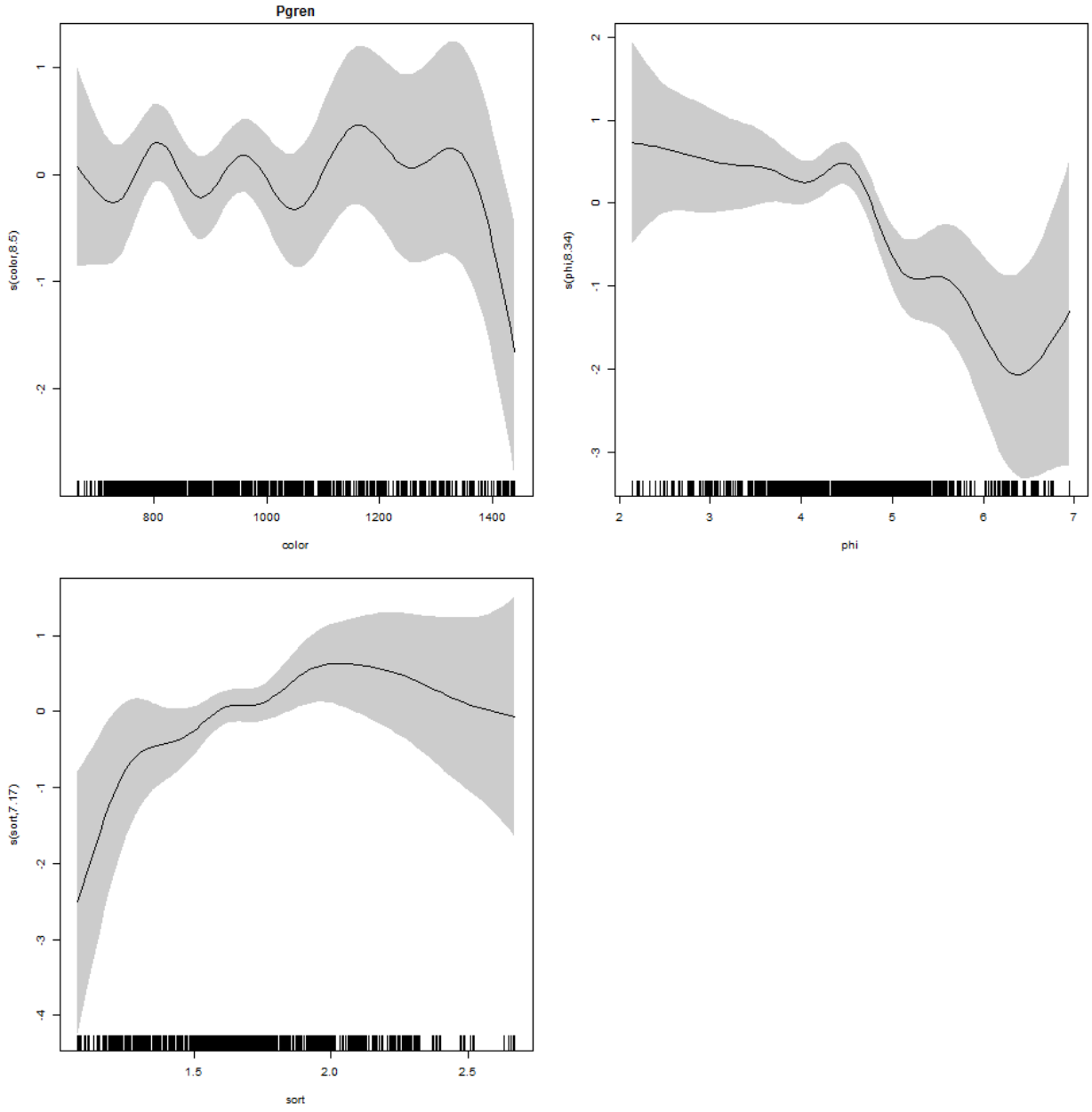


1461

1462

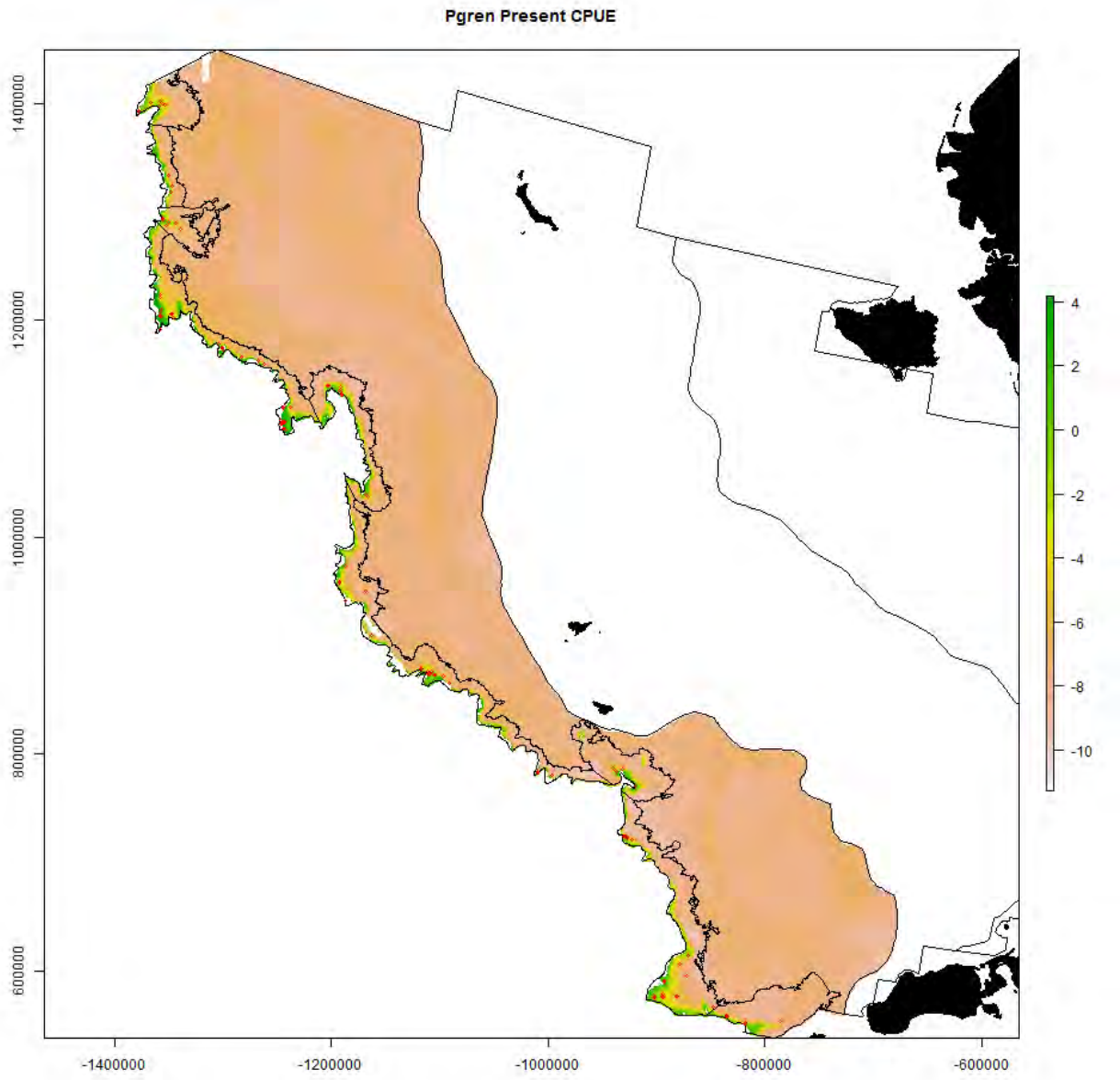
Pgren Present CPUE
1400000
1200000
1000000
800000
600000
-1400000
-1200000
-1000000
-800000
-600000
4
2
0
-2
-4
-6
-8
-10

1463

1464

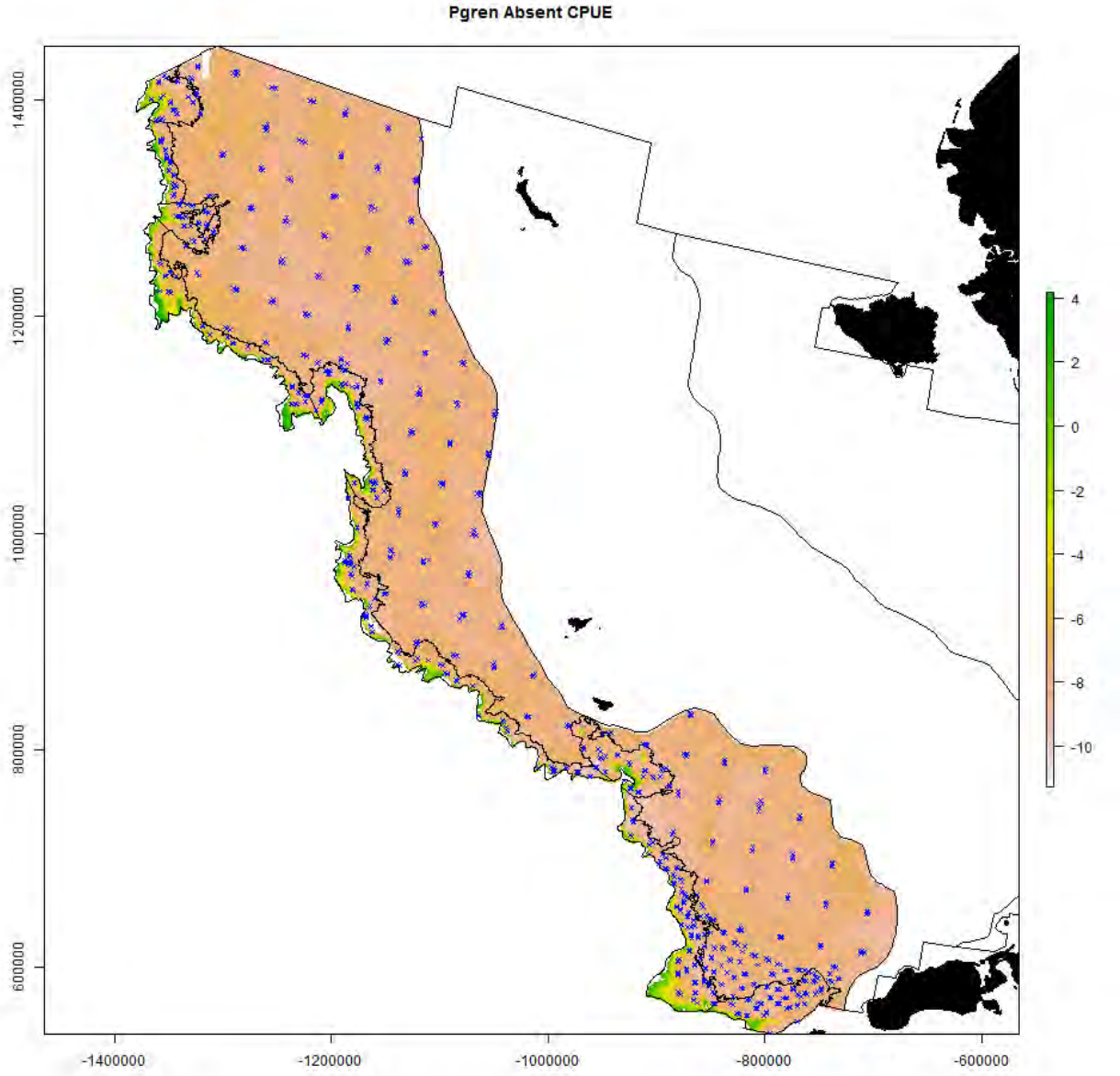
Pgren Absent CPUE
1400000
1200000
1000000
800000
600000
-1400000
-1200000
-1000000
-800000
-600000
4
2
0
-2
-4
-6
-8
-10

1465
1466

S21. Generalized additive modeling results for Pacific halibut. In the spatial plots, the x-axis label is easting and the y-axis label is northing and the unit is meters (Alaska Albers Equal Area Conic projection with center latitude = 50° N and center longitude = 154° W).

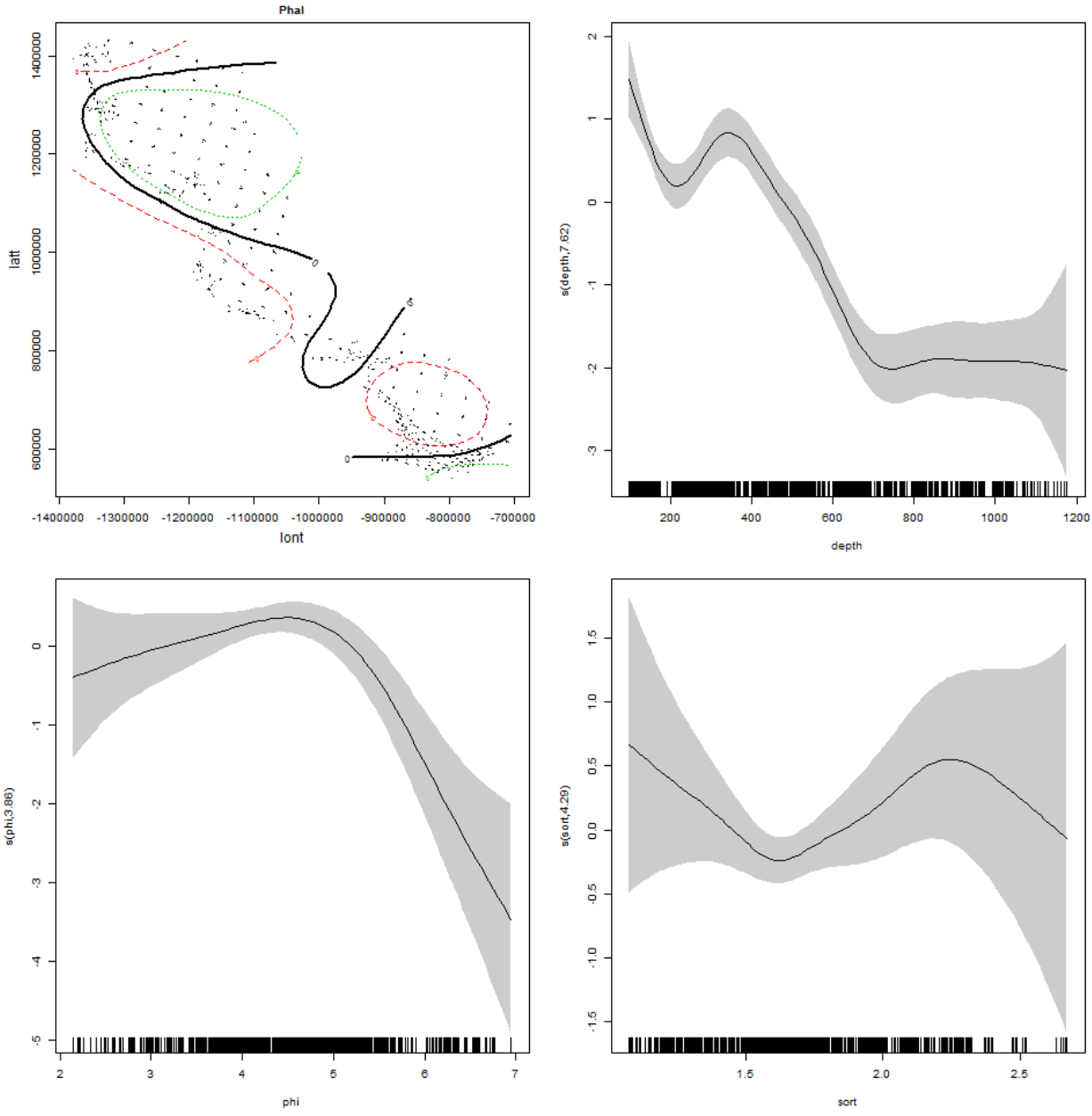

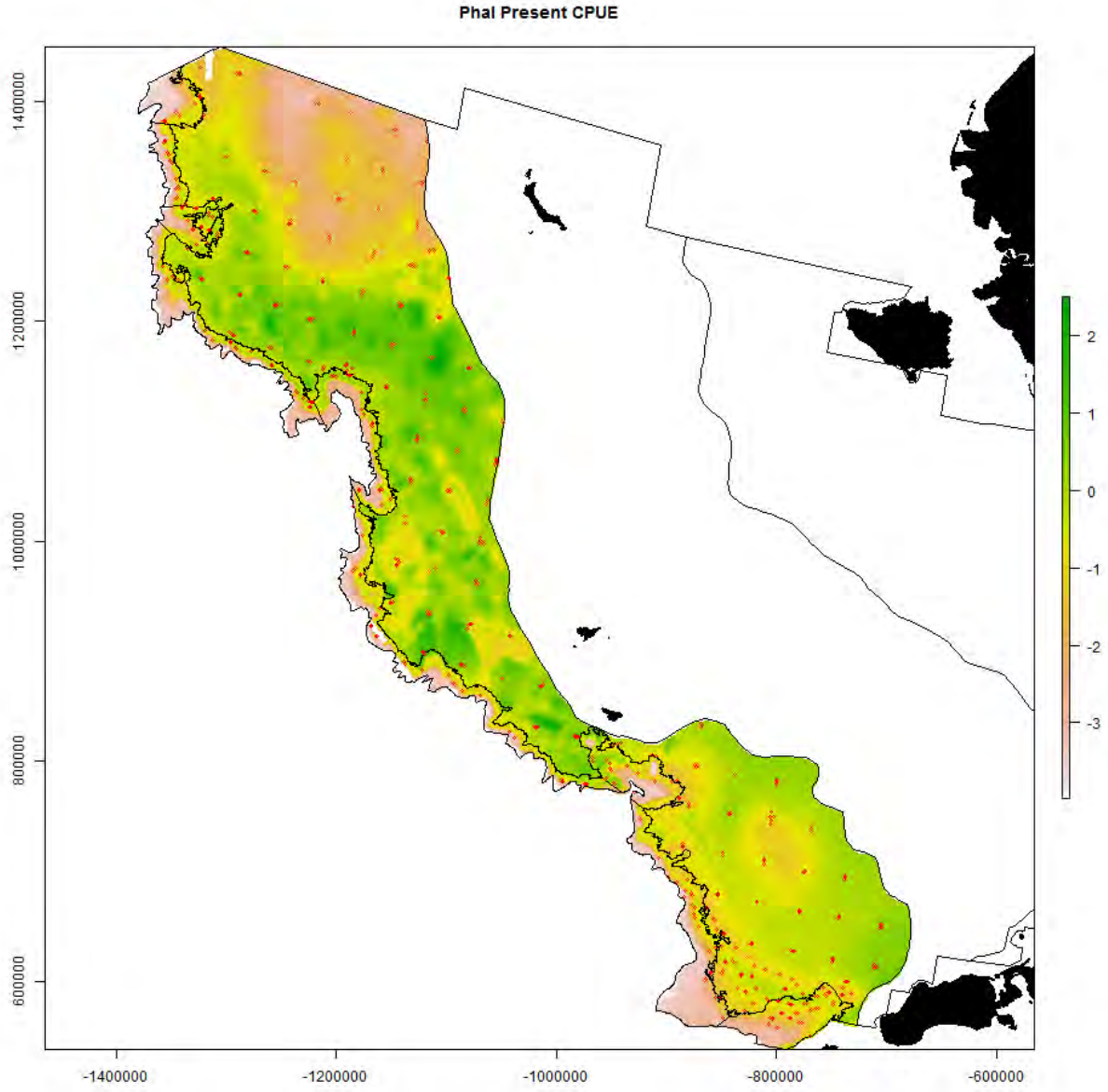
Phal Present CPUE
1400000
1200000
1000000
800000
600000
-1400000
-1200000
-1000000
-800000
-600000
2
1
0
-1
-2
-3

1472

1473

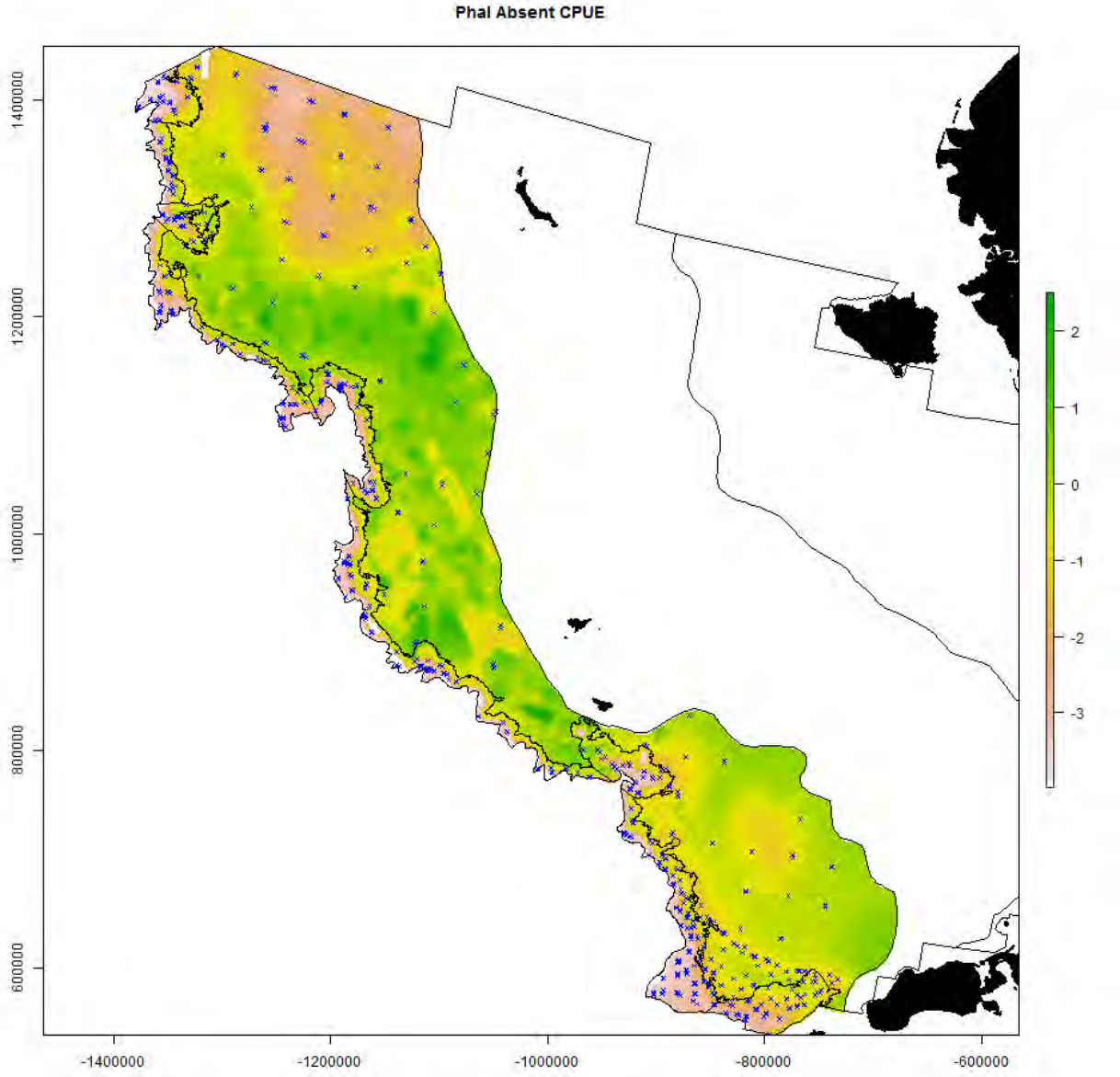
Phal Absent CPUE
1400000
1200000
1000000
800000
600000
-1400000
-1200000
-1000000
-800000
-600000
2
1
0
-1
-2
-3

1474

1475

S22. Generalized additive modeling results for Pacific Ocean perch. In the spatial plots, the x-axis label is easting and the y-axis label is northing and the unit is meters (Alaska Albers Equal Area Conic projection with center latitude = 50° N and center longitude = 154° W).

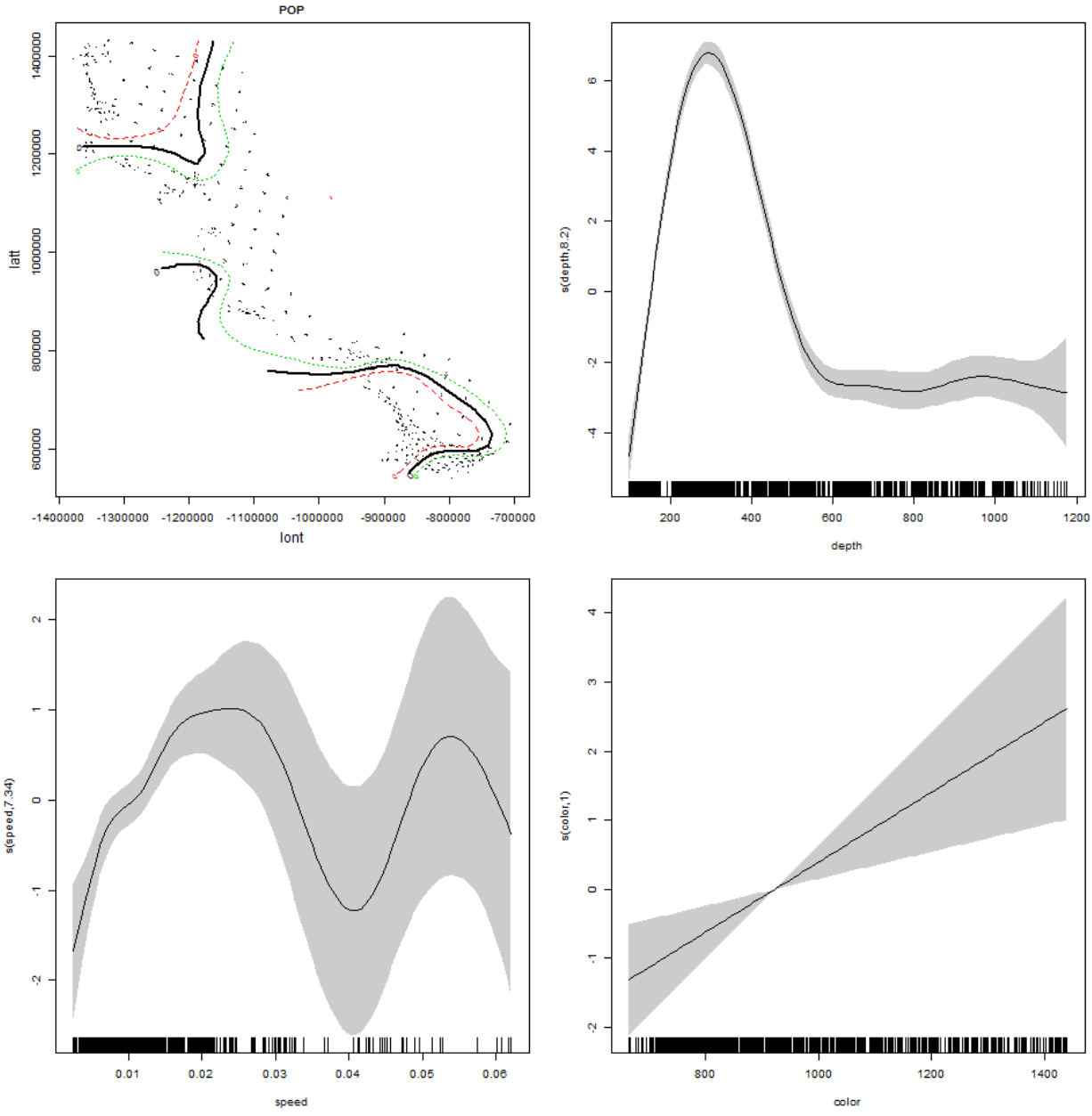

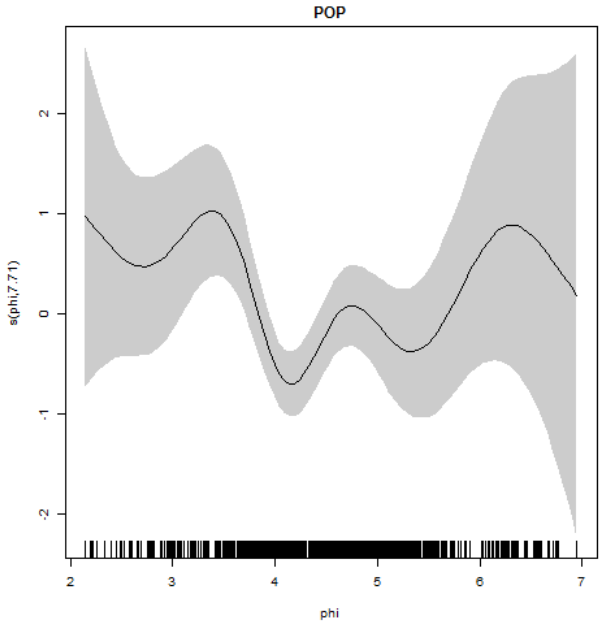


1481

1482

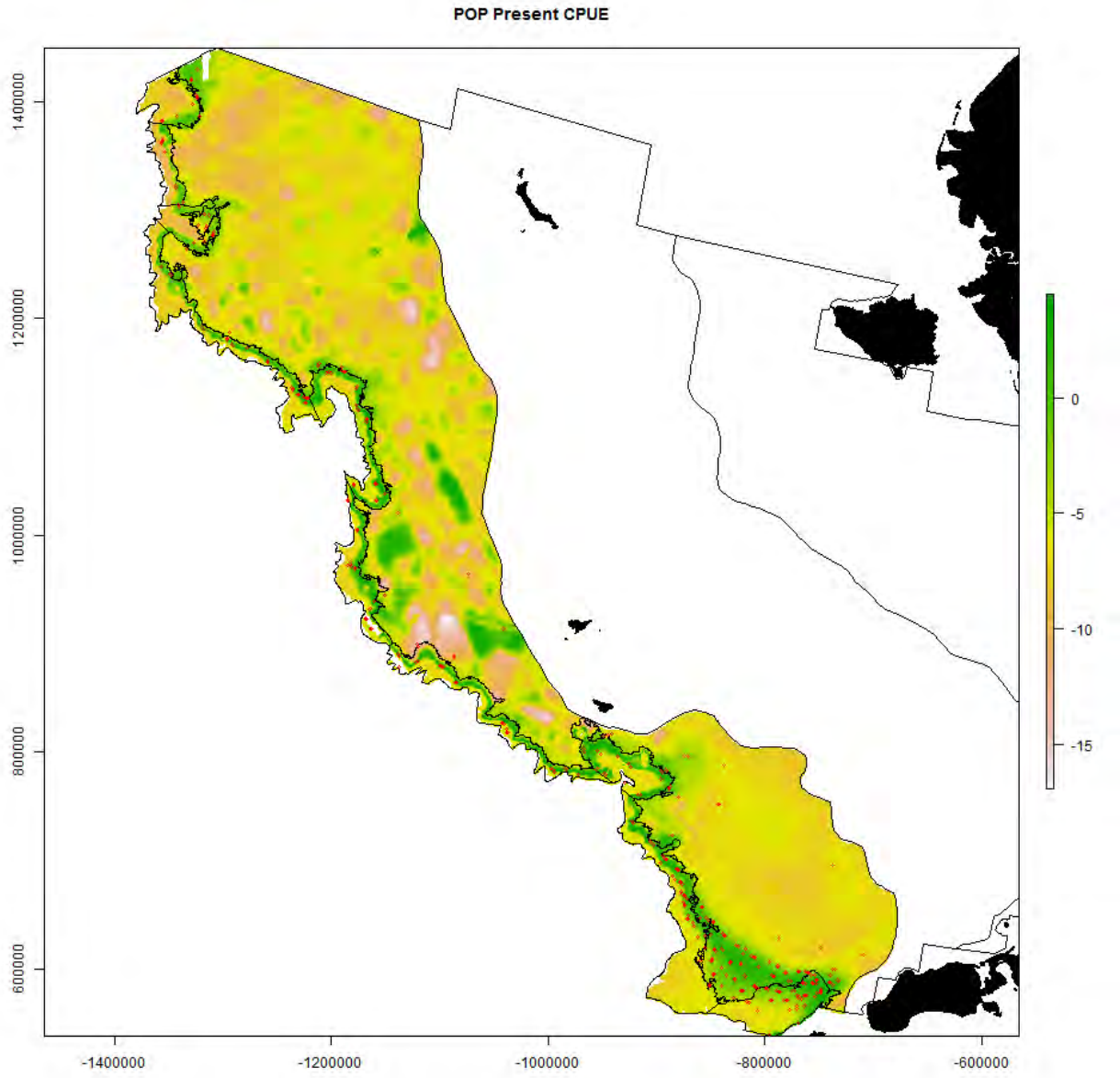
POP Present CPUE
1400000
1200000
1000000
800000
600000
-1400000
-1200000
-1000000
-800000
-600000
0
-5
-10
-15

1483

1484

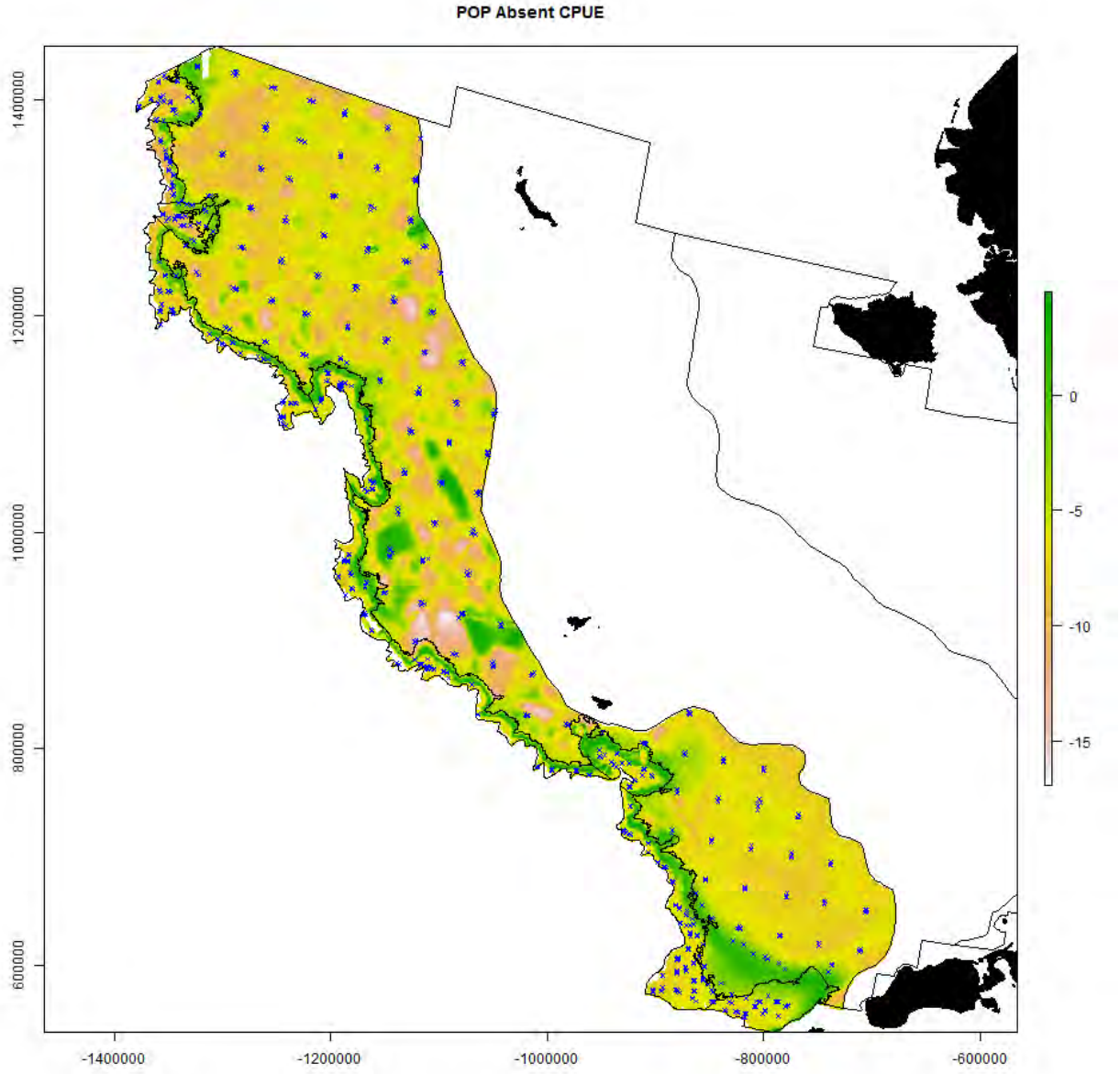
POP Absent CPUE
1400000
1200000
1000000
800000
600000
-1400000
-1200000
-1000000
-800000
-600000
0
-5
-10
-15

1485
1486

S23. Generalized additive modeling results for walleye pollock. In the spatial plots, the x-axis label is easting and the y-axis label is northing and the unit is meters (Alaska Albers Equal Area Conic projection with center latitude = 50° N and center longitude = 154° W).

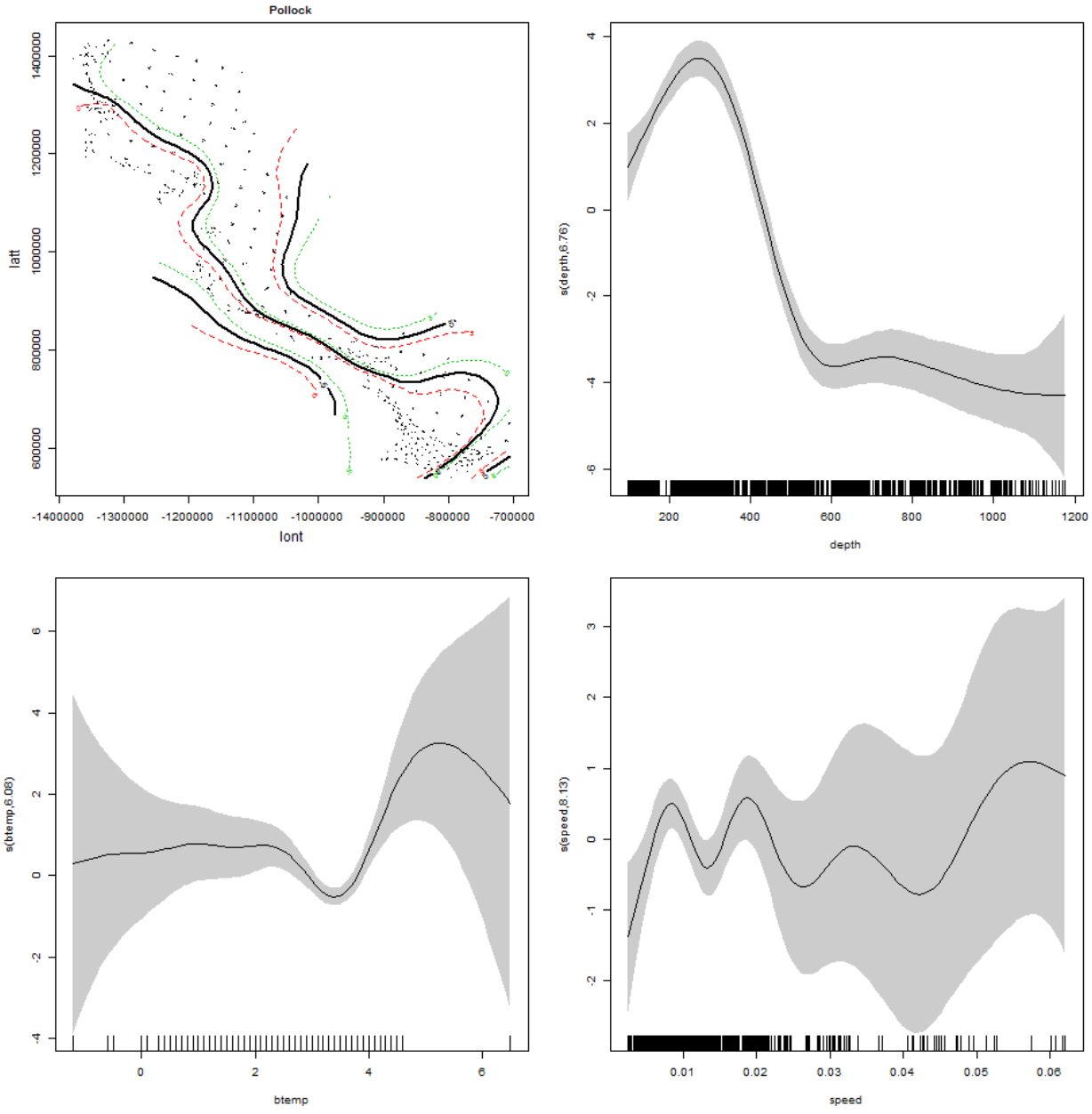

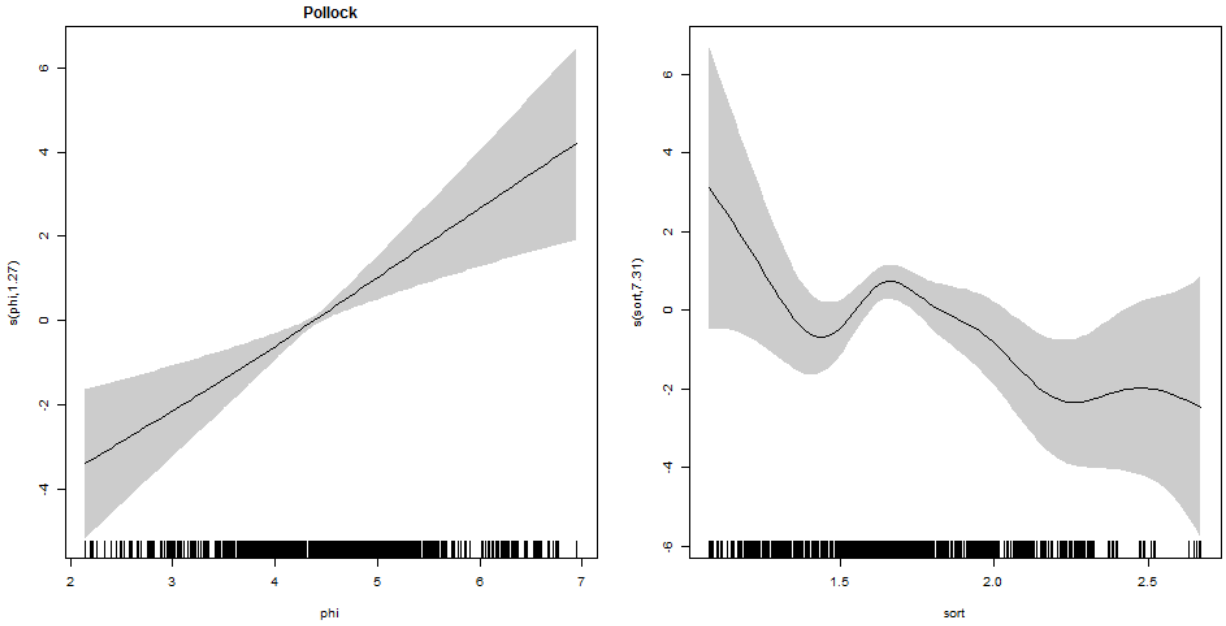


1492

1493

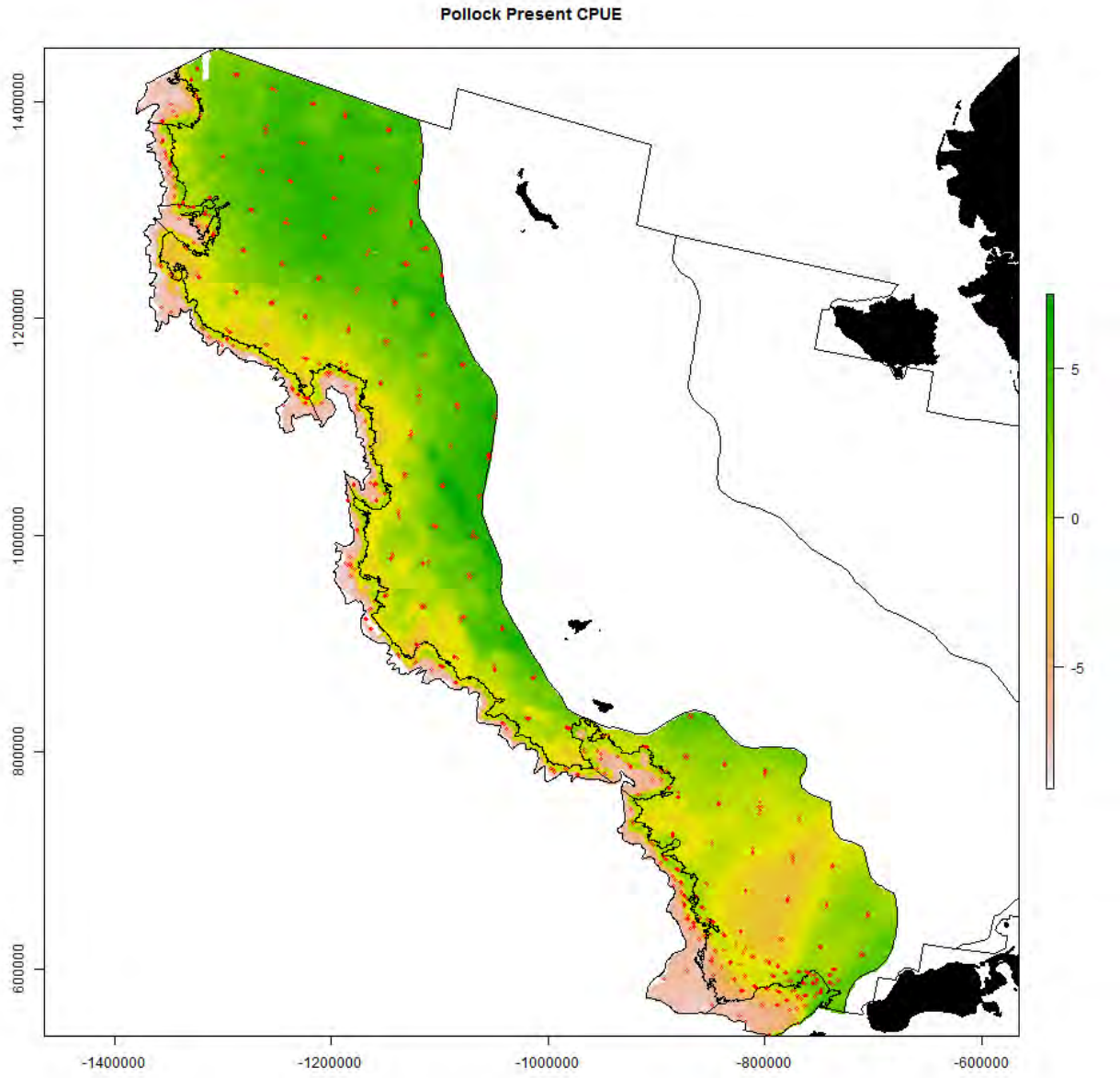
Pollock Present CPUE
1400000
1200000
1000000
800000
600000
-1400000
-1200000
-1000000
-800000
-600000
5
0
-5

1494

1495

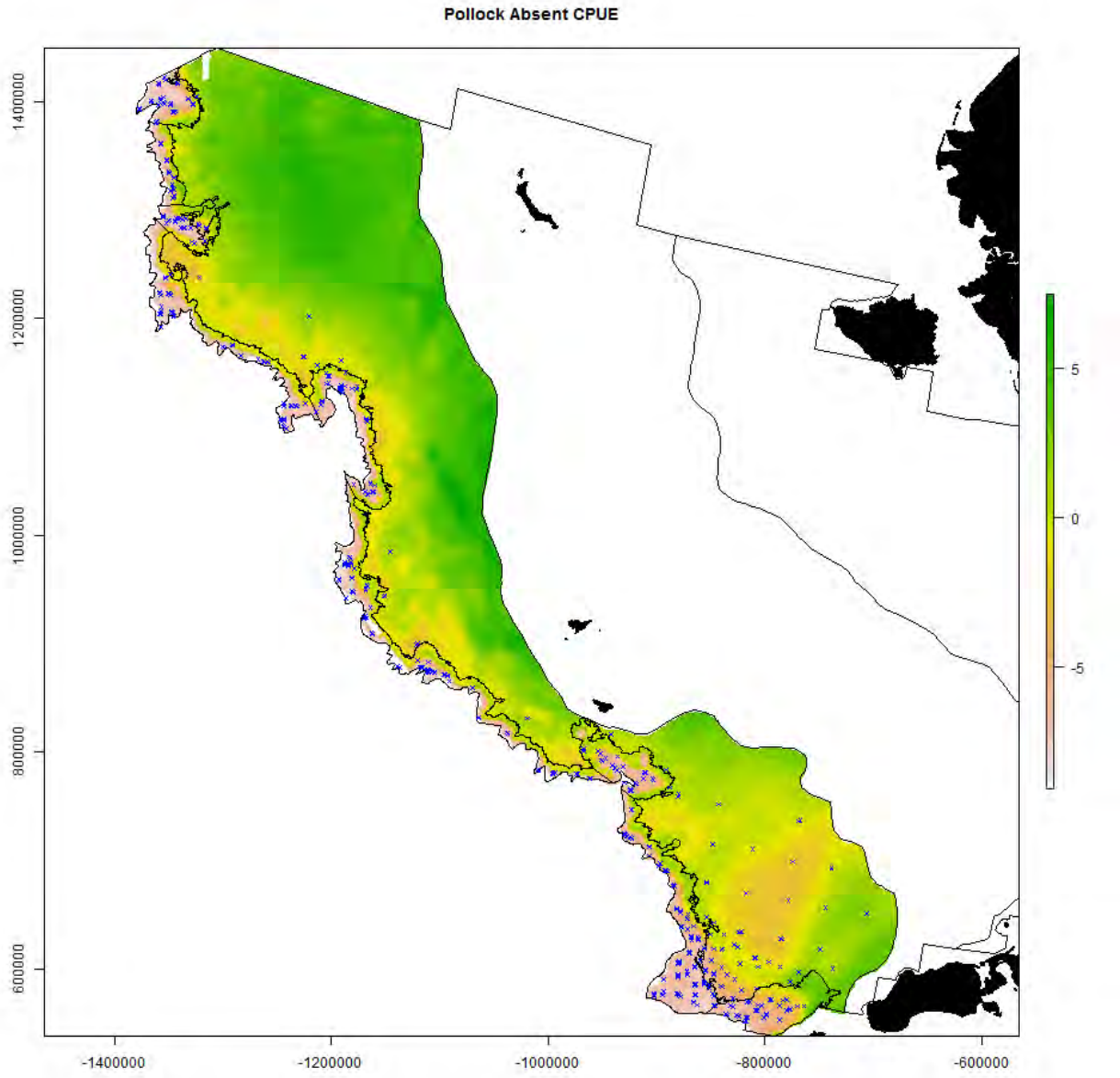
Pollock Absent CPUE
1400000
1200000
1000000
800000
600000
-1400000
-1200000
-1000000
-800000
-600000
5
0
-5

1496
1497

S24. Generalized additive modeling results for rougheye/blackspotted rockfish. In the spatial plots, the x-axis label is easting and the y-axis label is northing and the unit is meters (Alaska Albers Equal Area Conic projection with center latitude = 50° N and center longitude = 154° W).

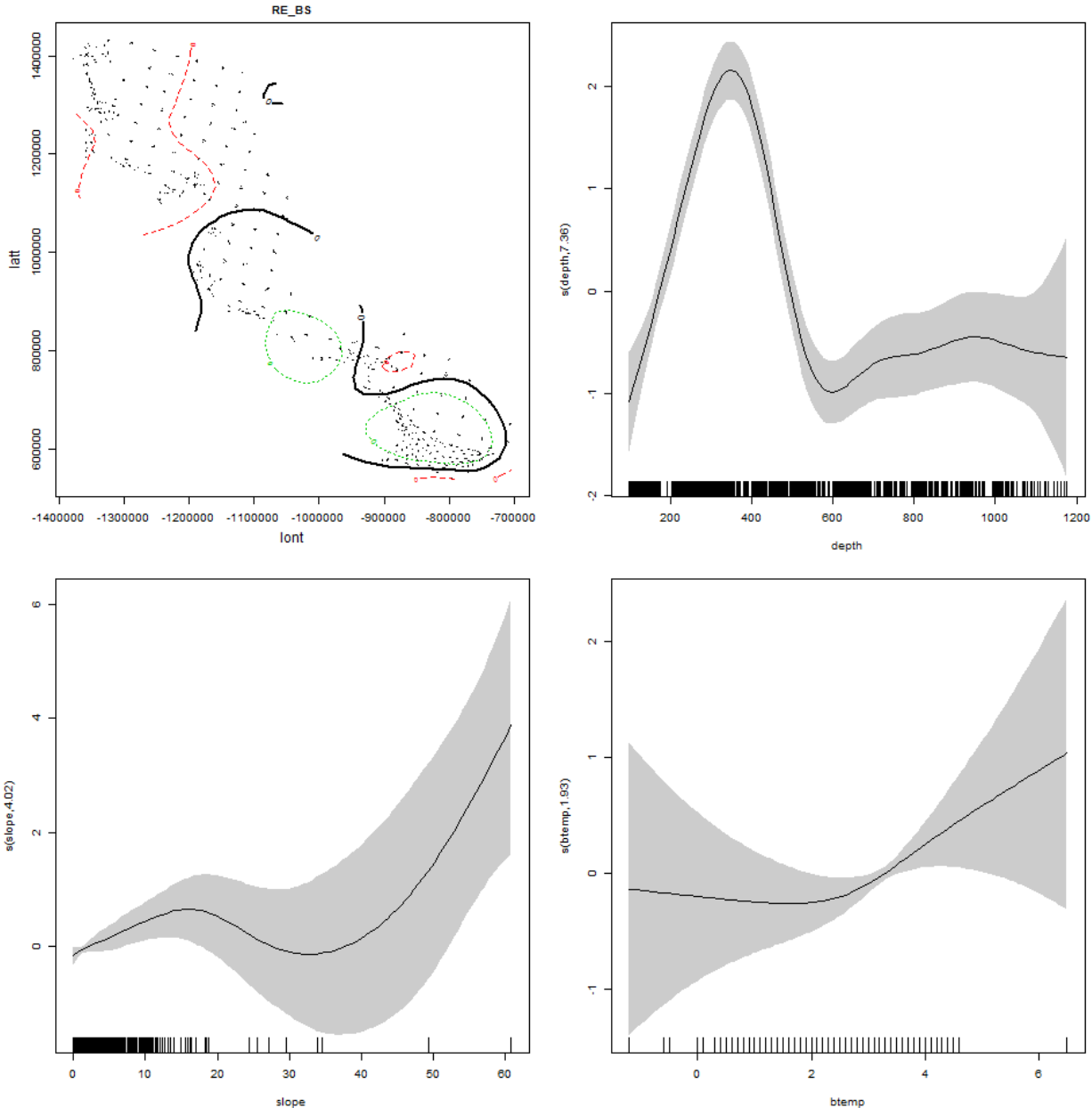

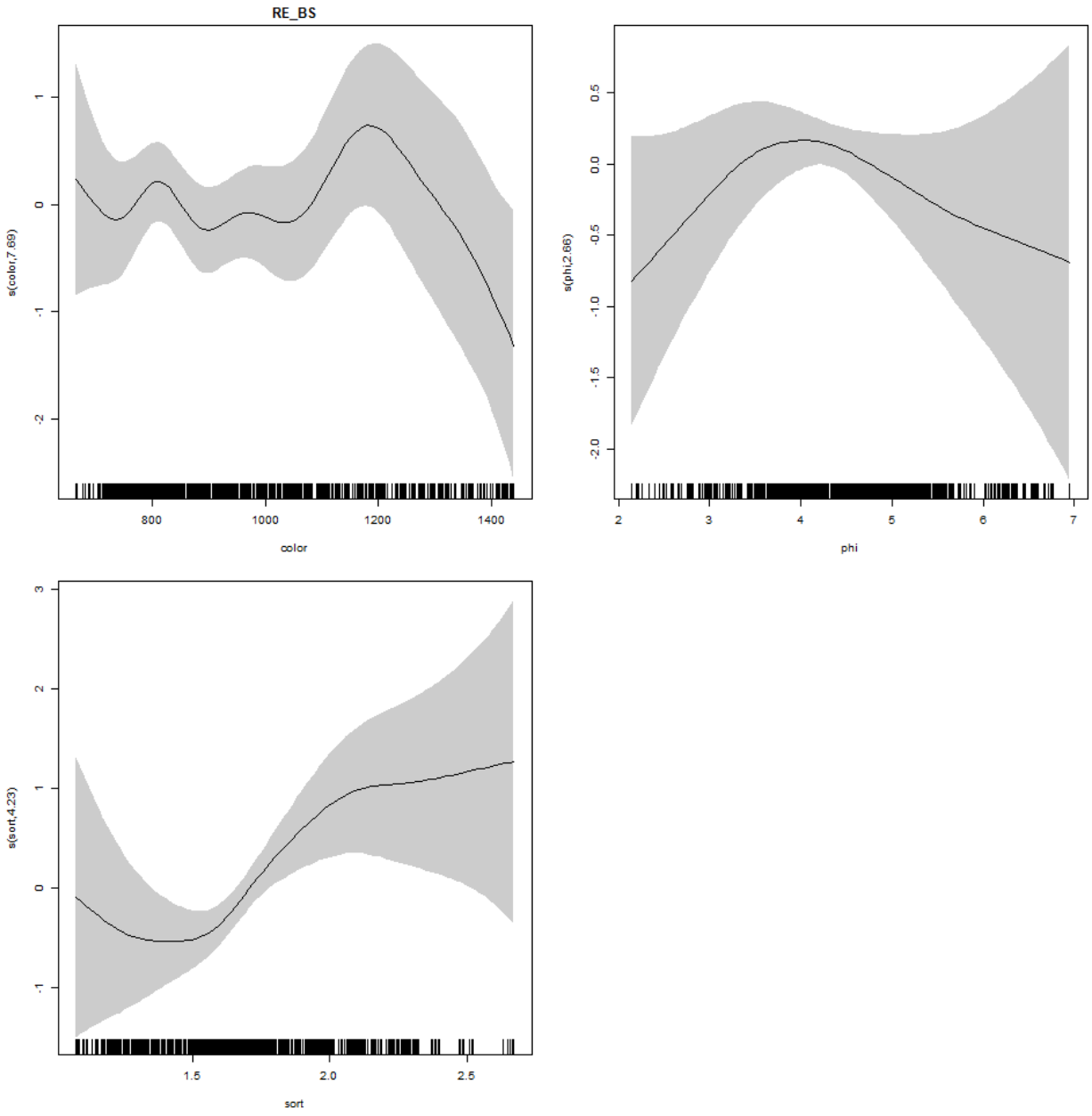


1503

1504

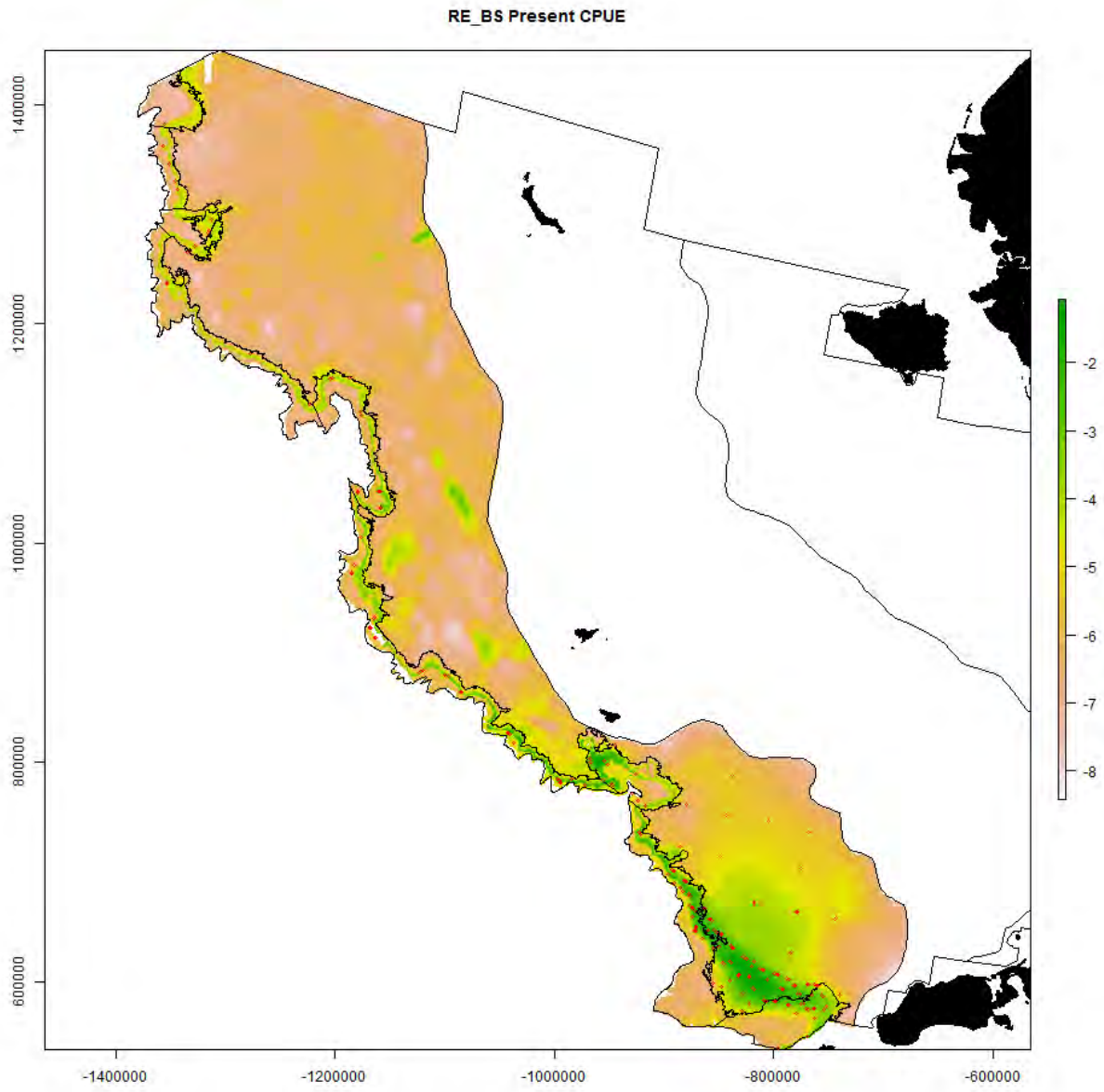
RE_BS Present CPUE
1400000
1200000
1000000
800000
600000
-1400000
-1200000
-1000000
-800000
-600000
-2
-3
-4
-5
-6
-7
-8

1505

1506

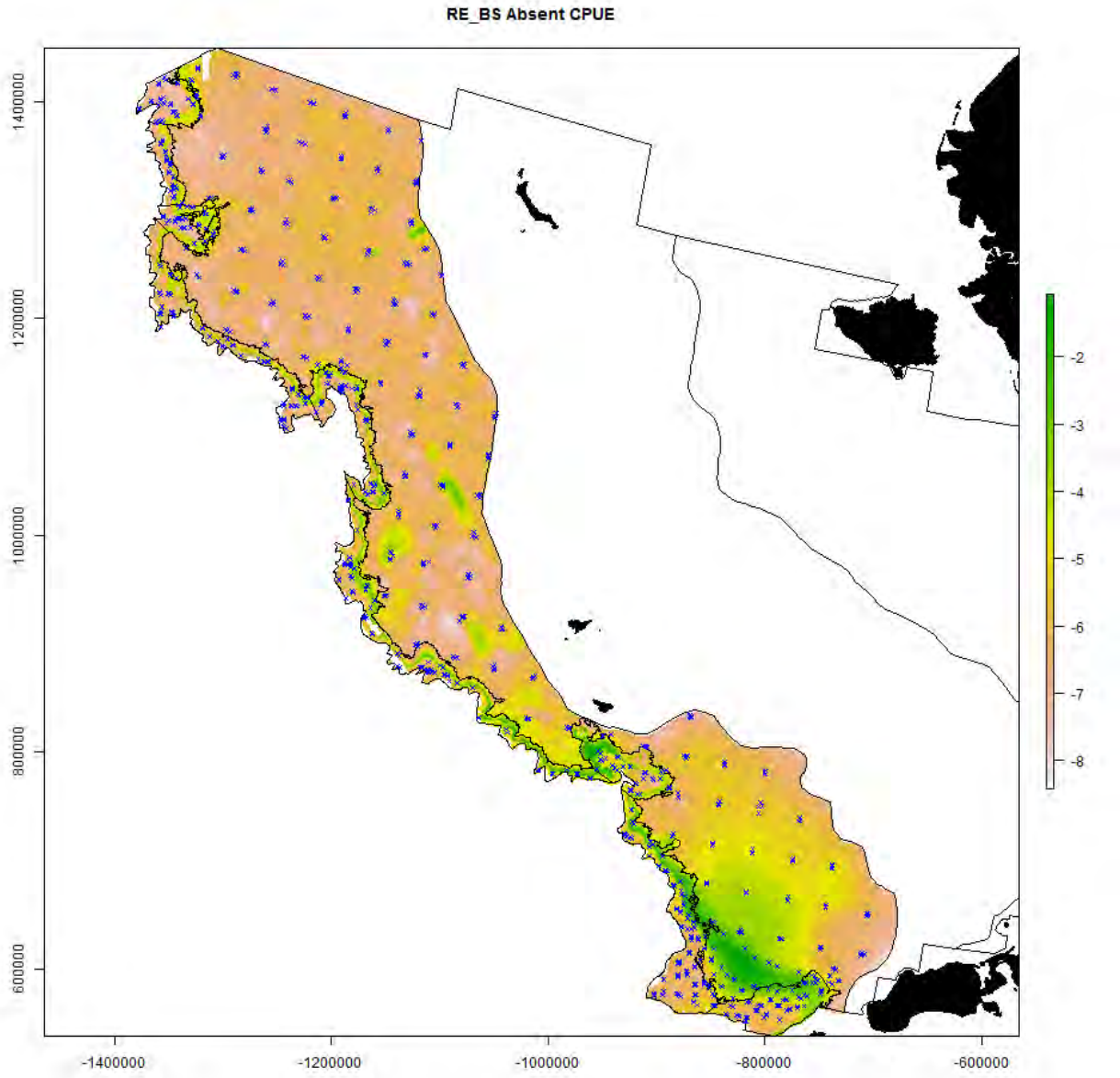
RE_BS Absent CPUE
1400000
1200000
1000000
800000
600000
-1400000
-1200000
-1000000
-800000
-600000
-2
-3
-4
-5
-6
-7
-8

1507
1508

S25. Generalized additive modeling results for sablefish. In the spatial plots, the x-axis label is easting and the y-axis label is northing and the unit is meters (Alaska Albers Equal Area Conic projection with center latitude = 50° N and center longitude = 154° W).

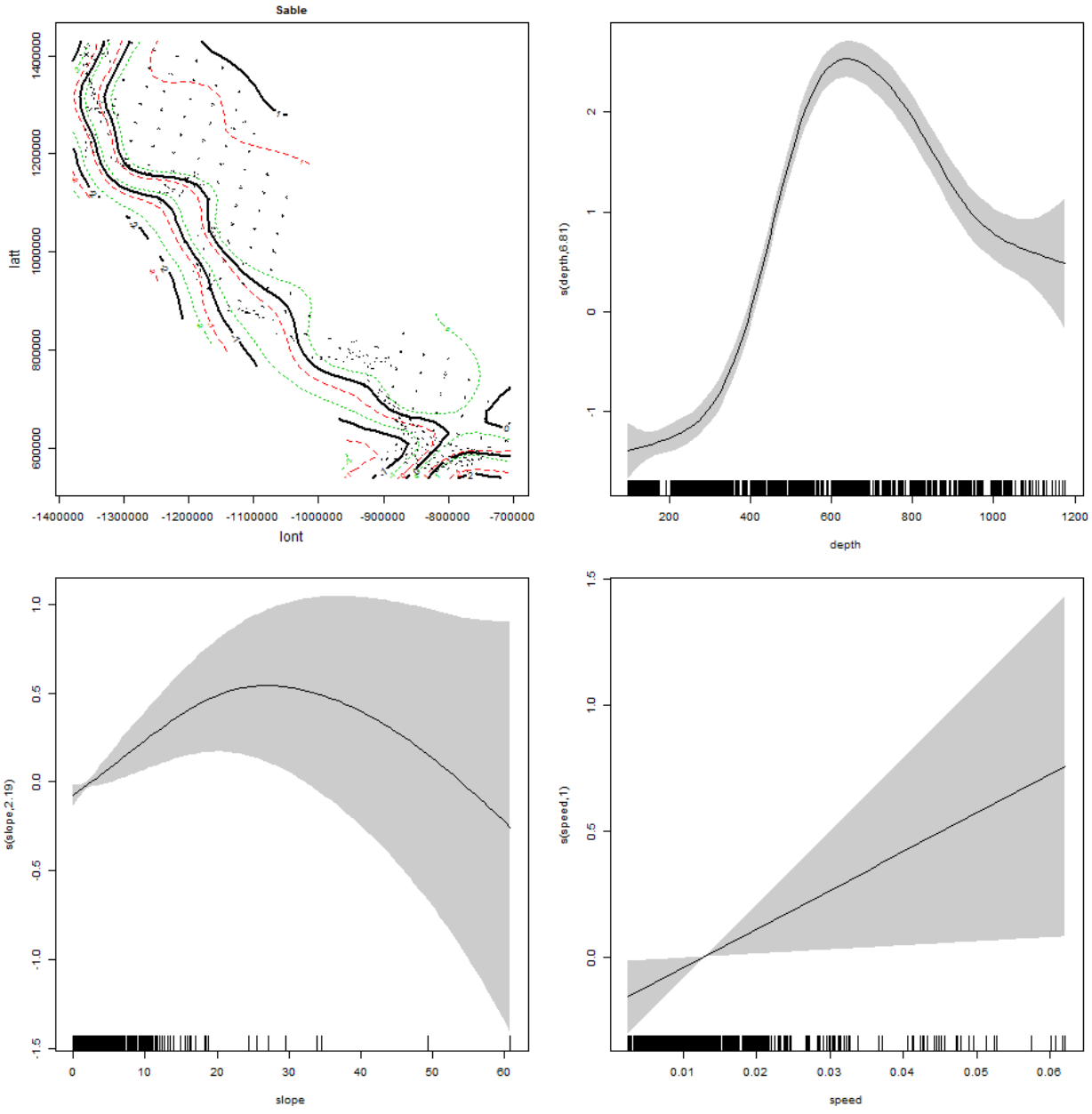

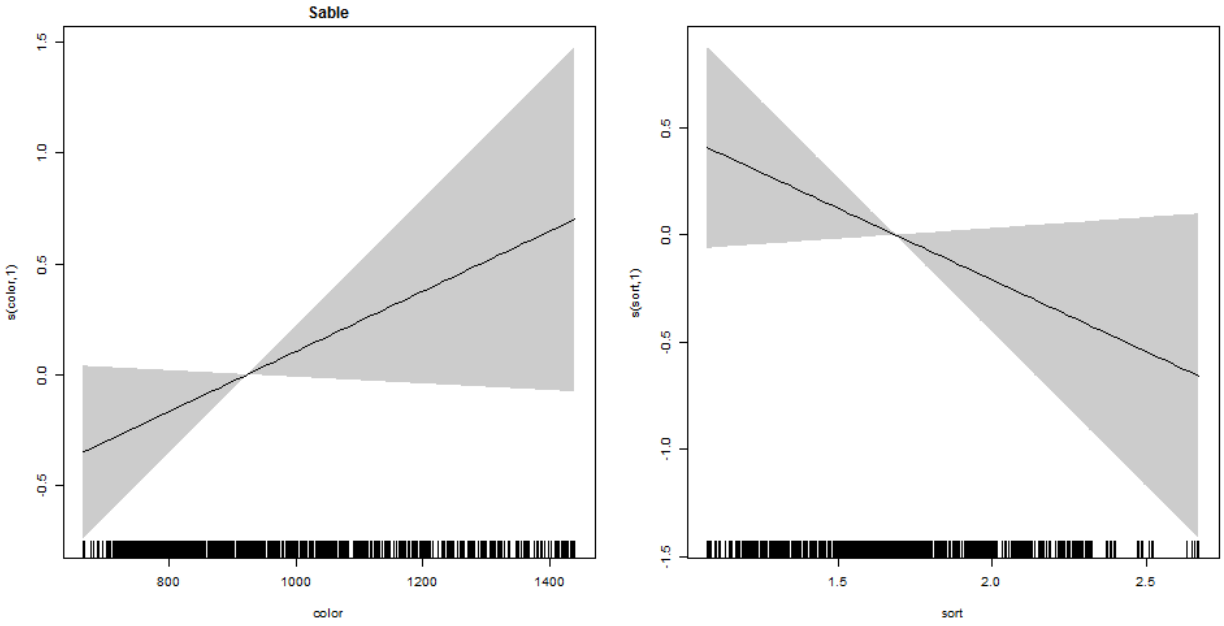
Sable
s(color,1)
color
800
1000
1200
1400
-0.5
0.0
0.5
1.0
1.5
s(sort,1)
sort
1.5
2.0
2.5
-1.5
-1.0
-0.5
0.0
0.5

1514

1515

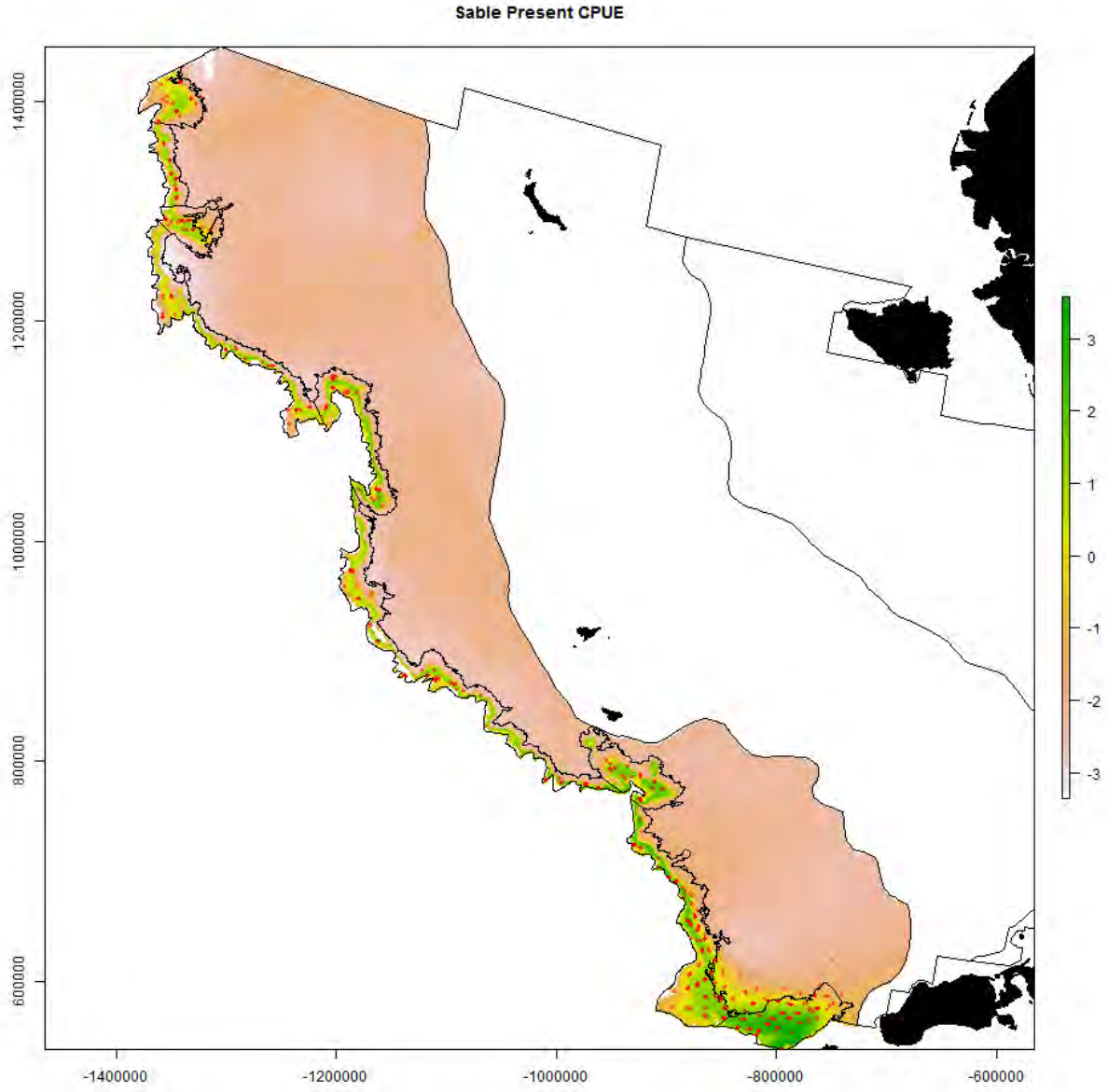
Sable Present CPUE
1400000
1200000
1000000
800000
600000
-1400000
-1200000
-1000000
-800000
-600000
3
2
1
0
-1
-2
-3

1516

1517

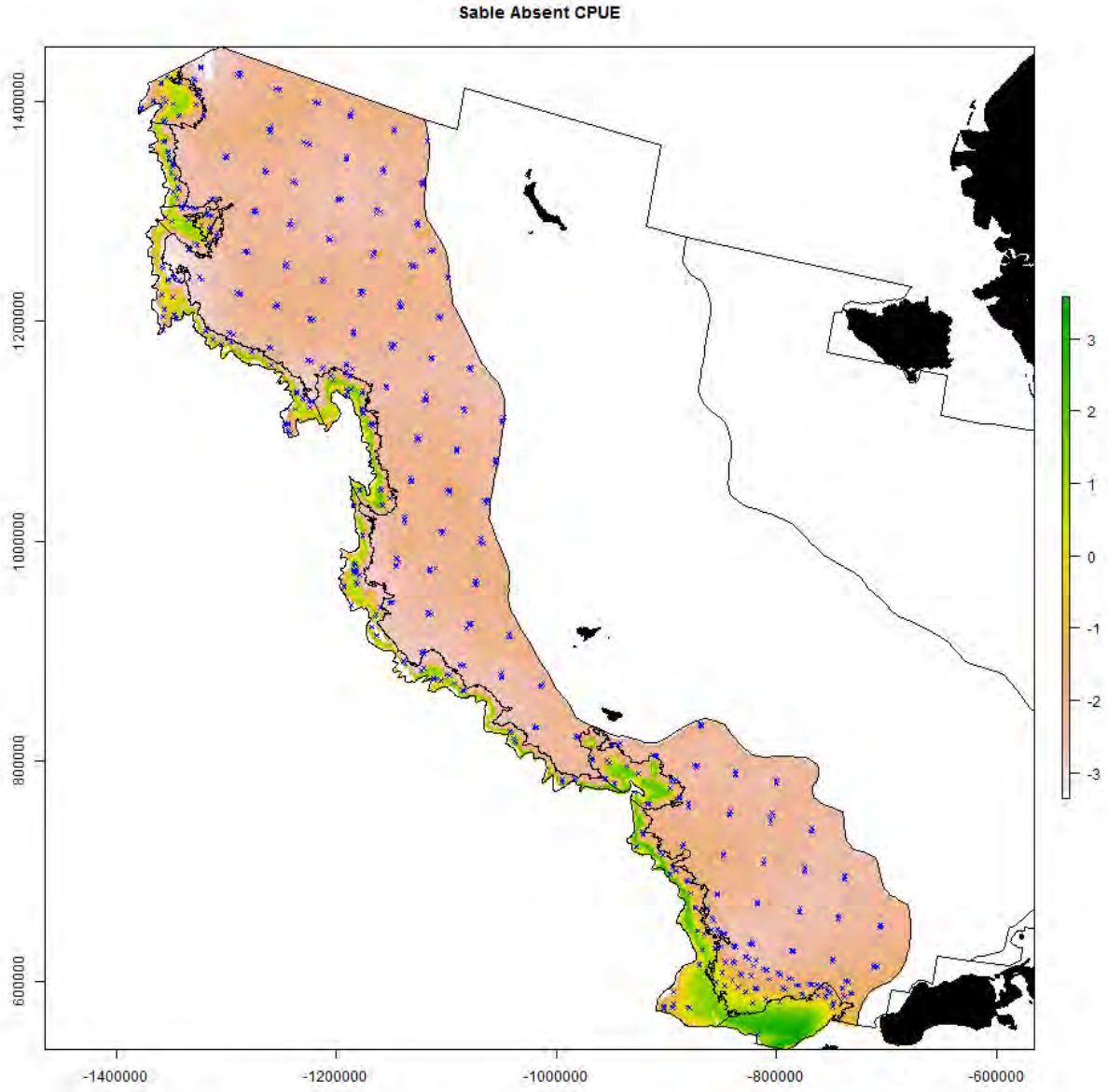
Sable Absent CPUE
1400000
1200000
1000000
800000
600000
-1400000
-1200000
-1000000
-800000
-600000
3
2
1
0
-1
-2
-3

1518
1519

1520 S26. Generalized additive modeling results for shortraker rockfish. In the spatial plots, the x-axis
1521 label is easting and the y-axis label is northing and the unit is meters (Alaska Albers Equal Area
1522 Conic projection with center latitude = 50° N and center longitude = 154° W).

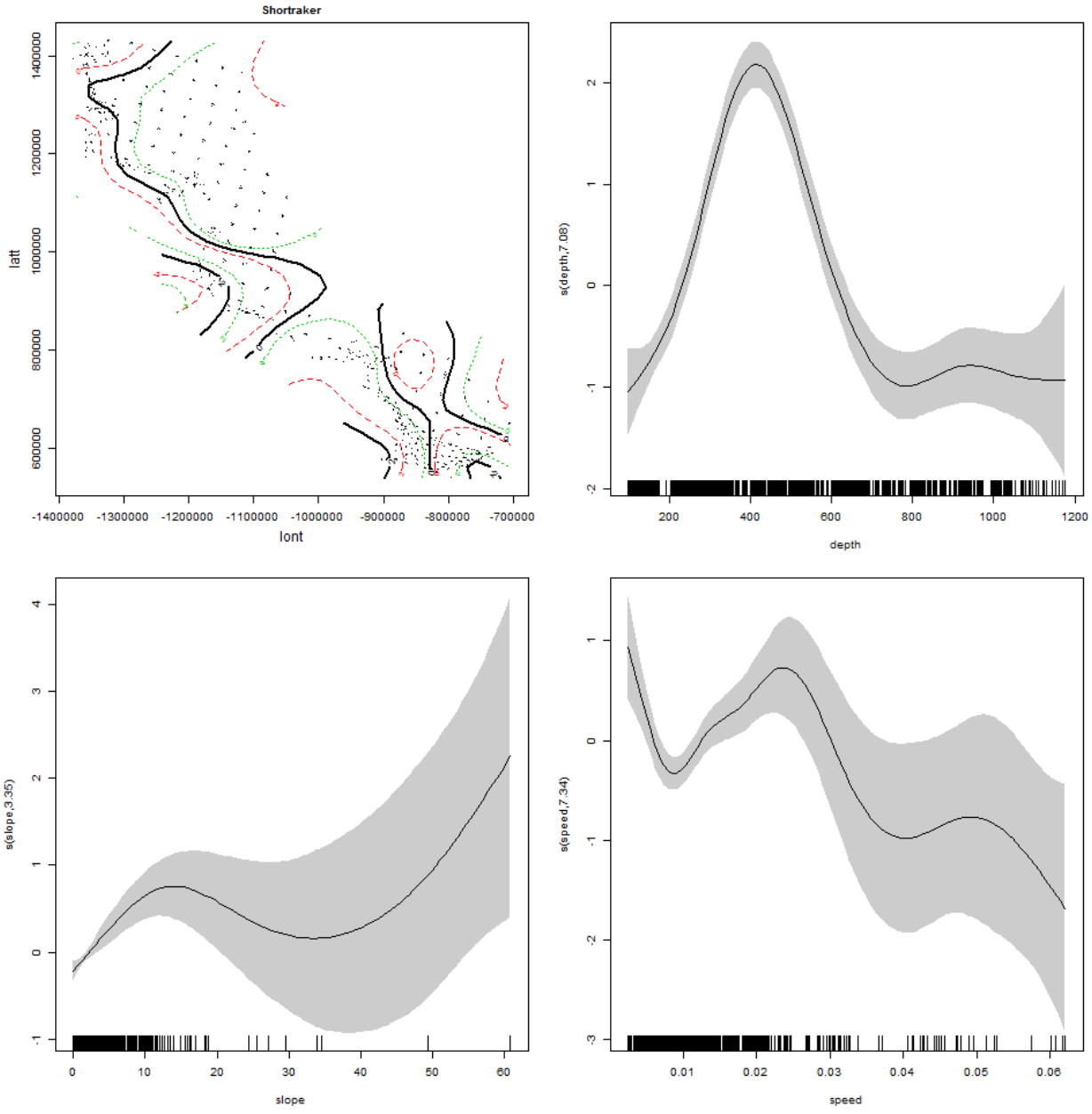


1523

1524

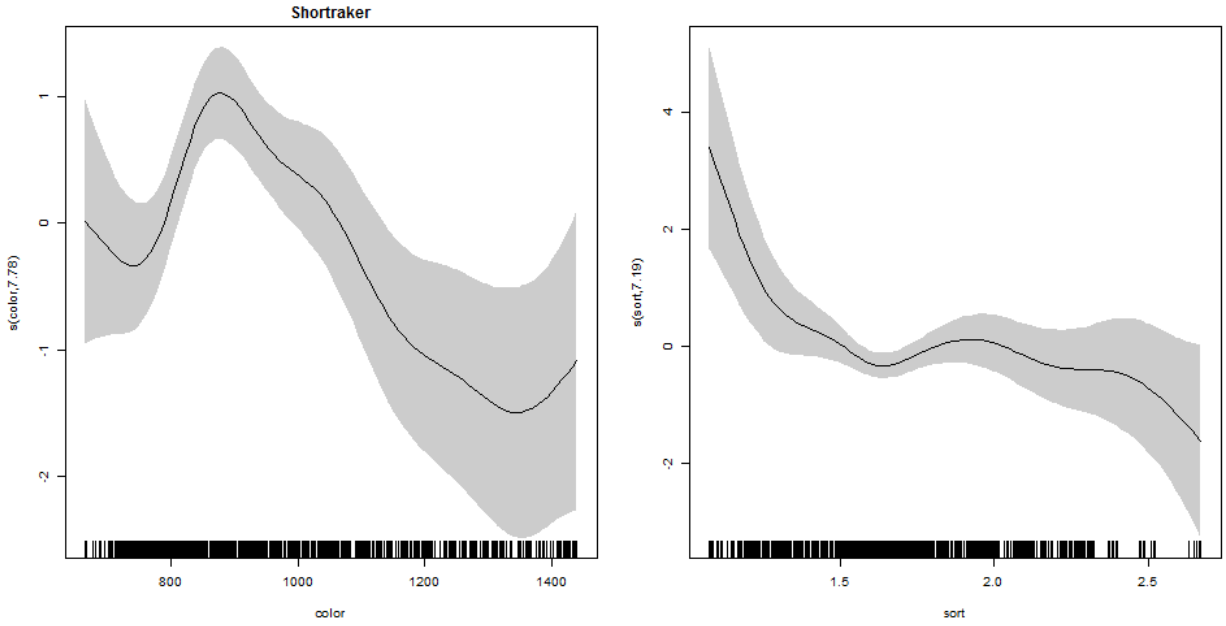
Shortraker
s(color,7.78)
color
800
1000
1200
1400
1
0
-1
-2
s(sort,7.19)
sort
1.5
2.0
2.5
4
2
0
-2

1525

1526

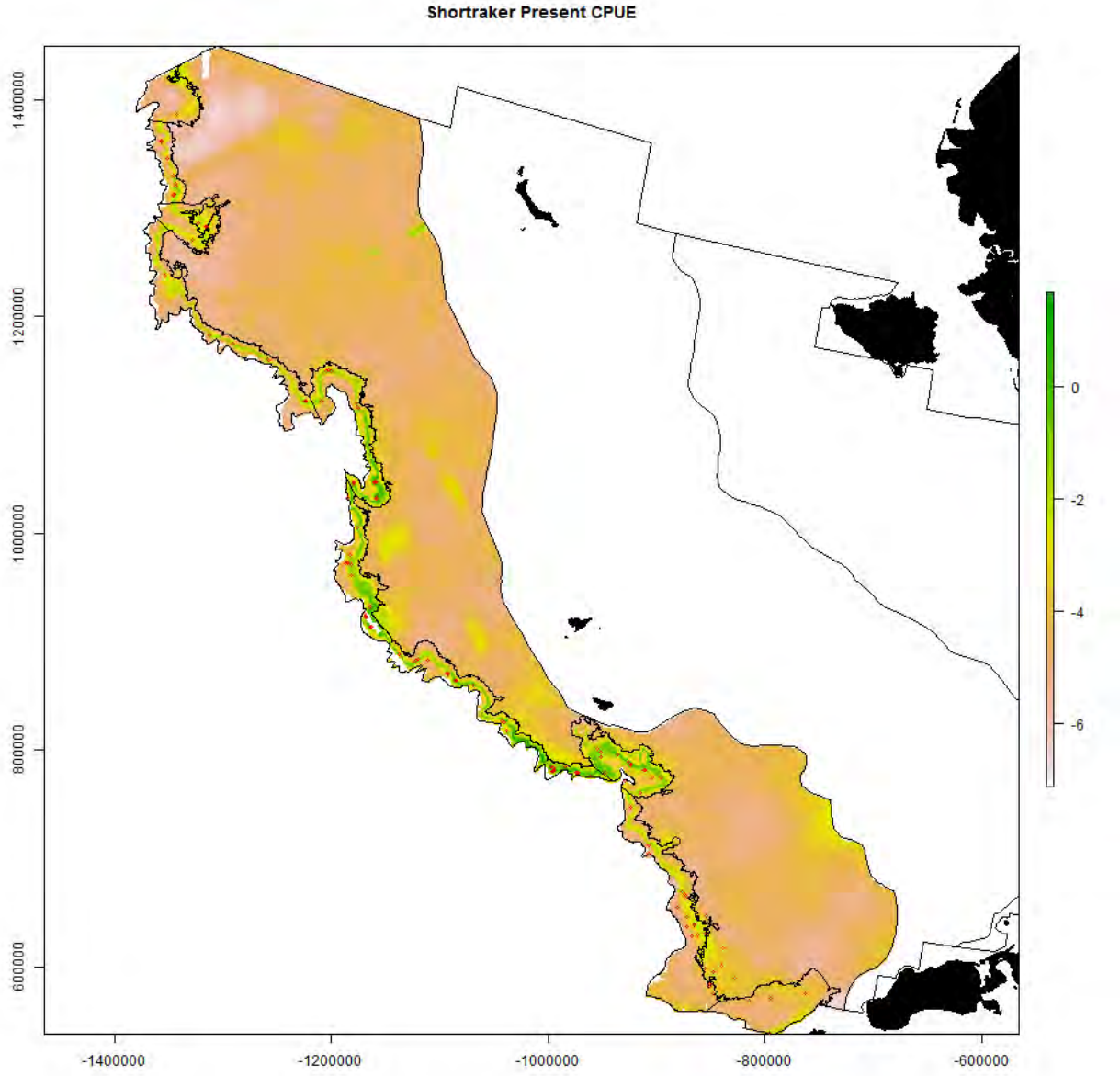
Shortraker Present CPUE
1400000
1200000
1000000
800000
600000
-1400000
-1200000
-1000000
-800000
-600000
0
-2
-4
-6

1527

1528

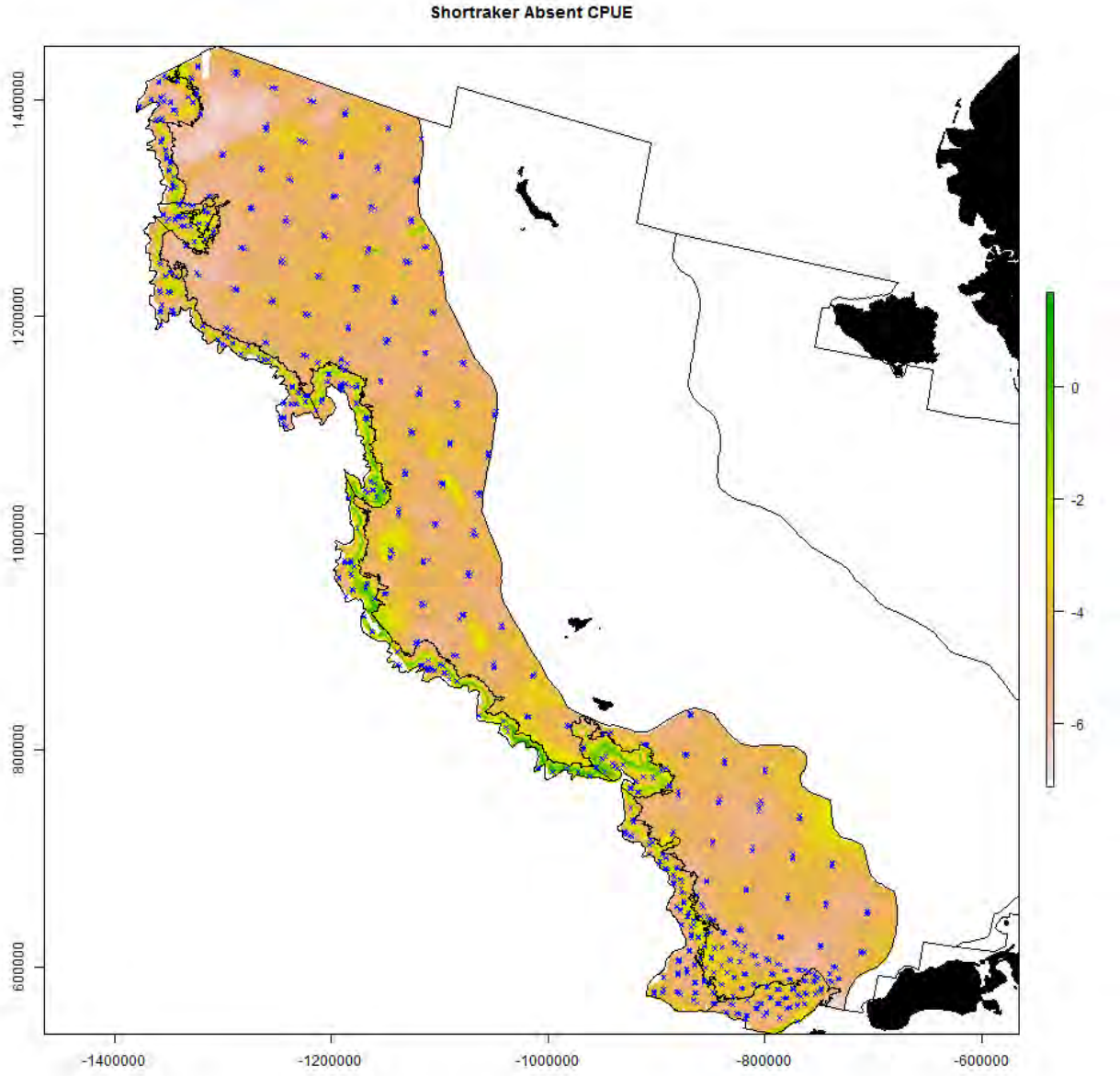
Shortraker Absent CPUE
1400000
1200000
1000000
800000
600000
-1400000
-1200000
-1000000
-800000
-600000
0
-2
-4
-6

1529
1530

S27. Generalized additive modeling results for shortspine thornyhead. In the spatial plots, the x-axis label is easting and the y-axis label is northing and the unit is meters (Alaska Albers Equal Area Conic projection with center latitude = 50° N and center longitude = 154° W).

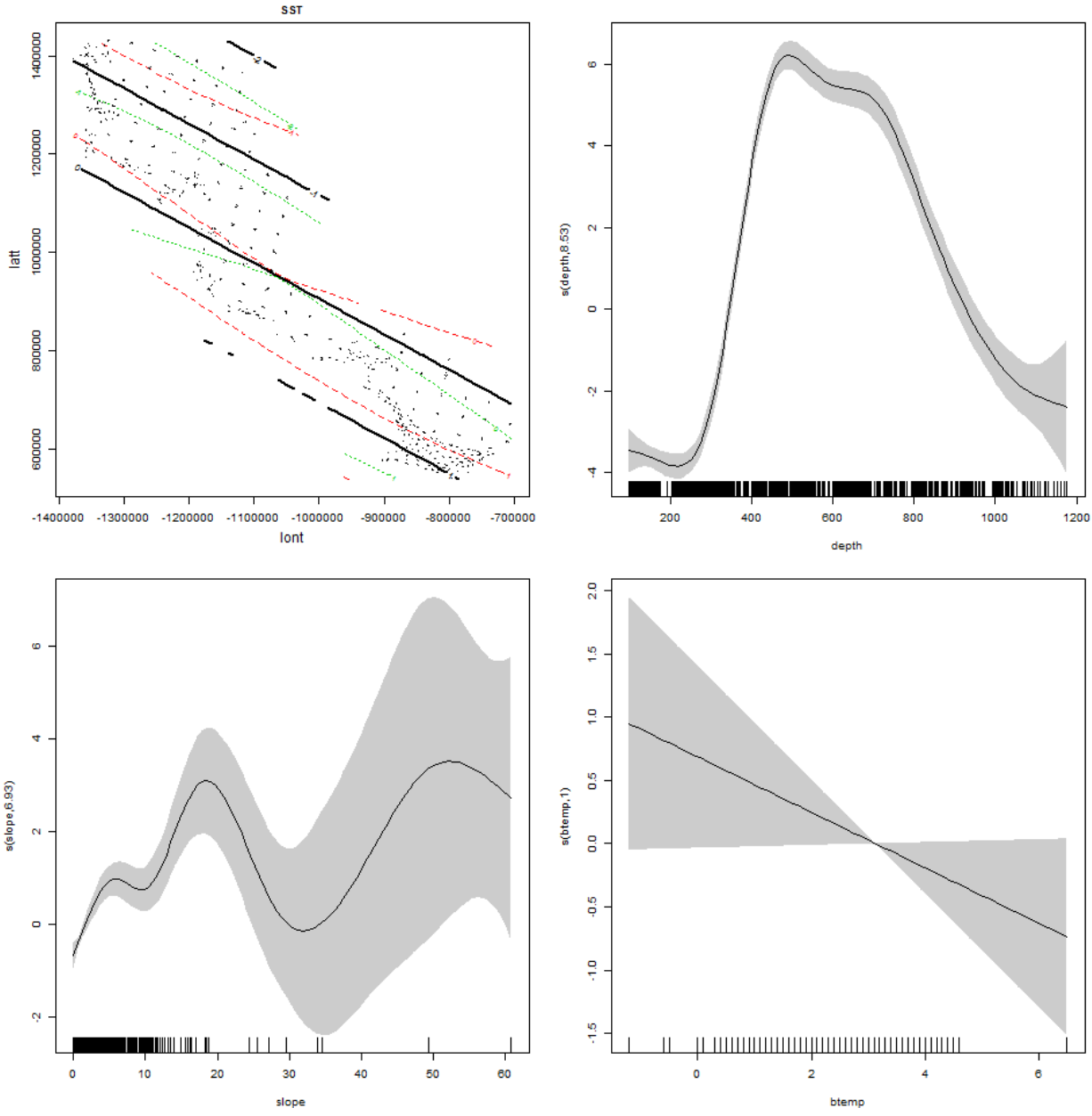

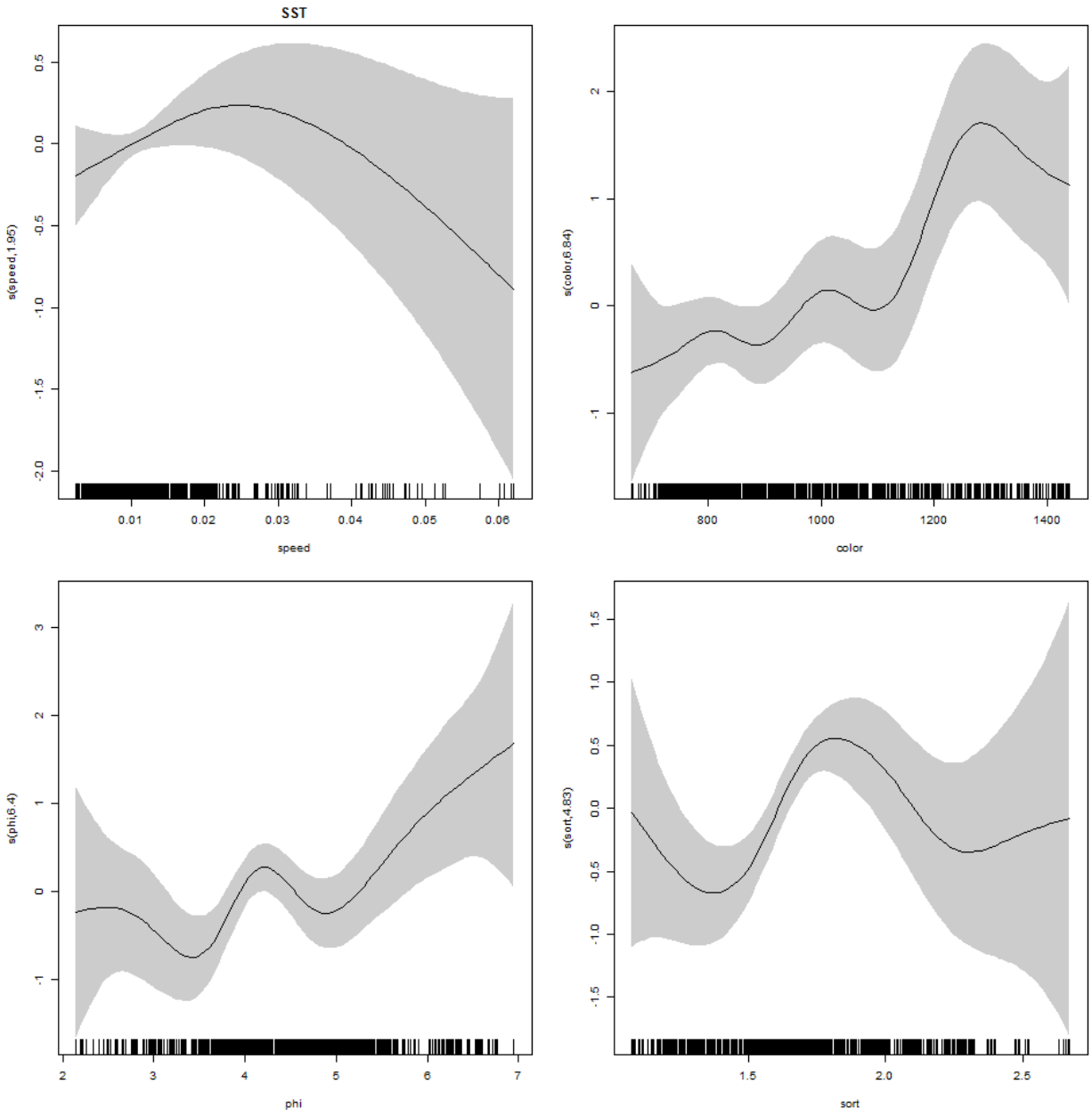
SST
s(speed,1.95)
speed
s(color,6.84)
color
s(phi,6.4)
phi
s(sort,4.83)
sort

1536

1537

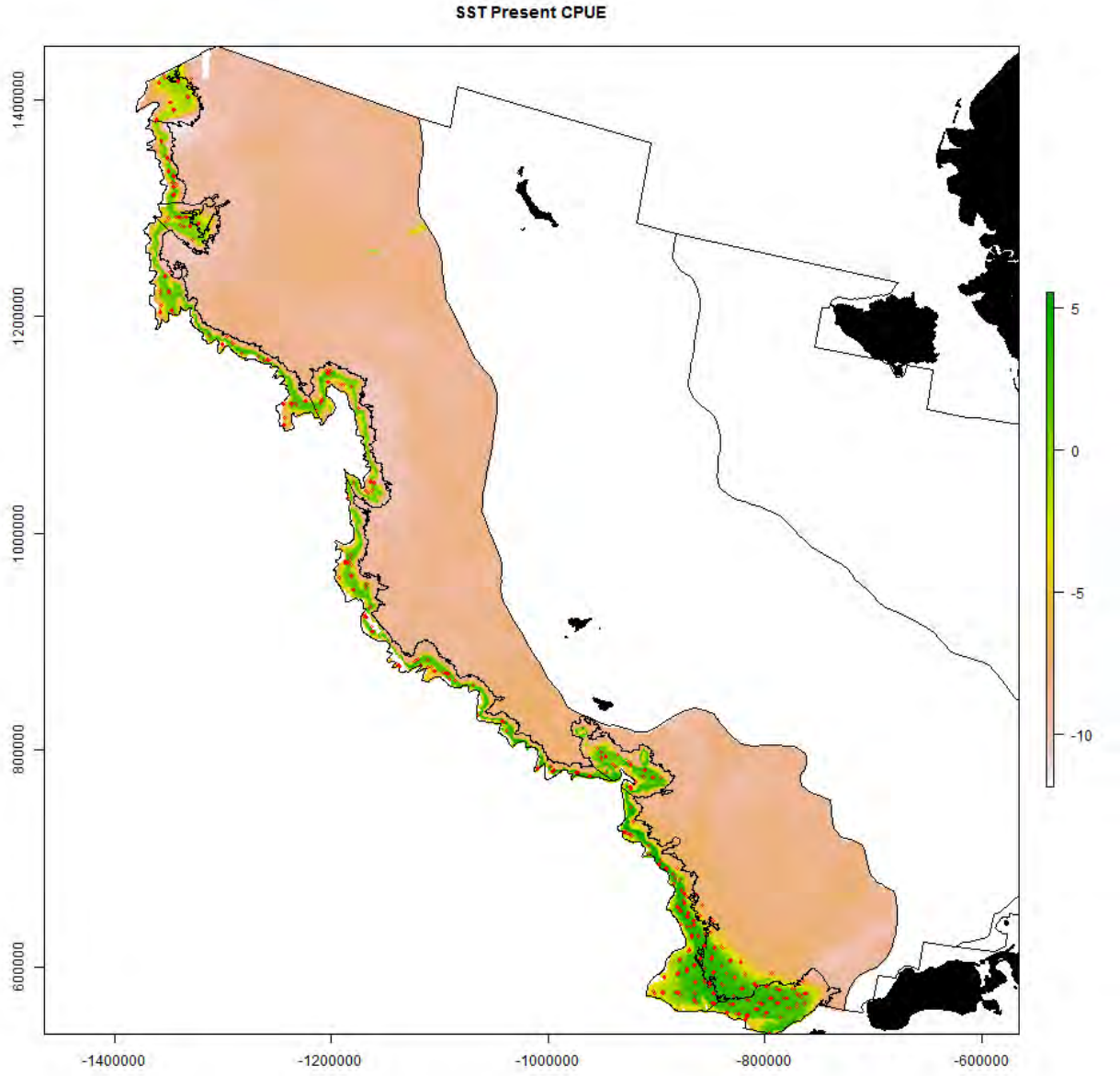
SST Present CPUE
1400000
1200000
1000000
800000
600000
-1400000
-1200000
-1000000
-800000
-600000
5
0
-5
-10

1538

1539

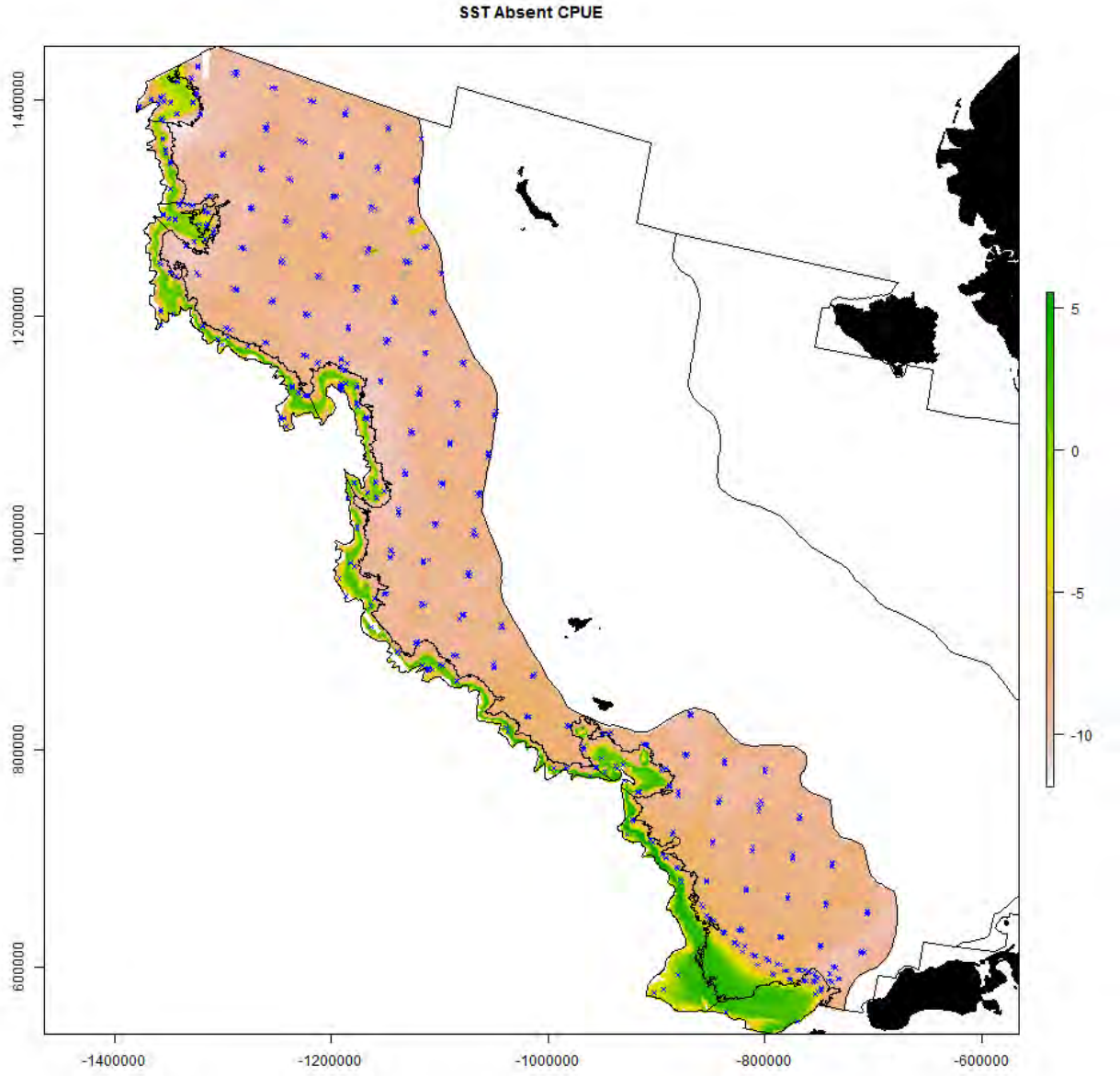
SST Absent CPUE
1400000
1200000
1000000
800000
600000
-1400000
-1200000
-1000000
-800000
-600000
5
0
-5
-10

1540

1541

1542 S28. Generalized additive modeling results for snow crab. In the spatial plots, the x-axis label is
1543 easting and the y-axis label is northing and the unit is meters (Alaska Albers Equal Area Conic
1544 projection with center latitude = 50° N and center longitude = 154° W).

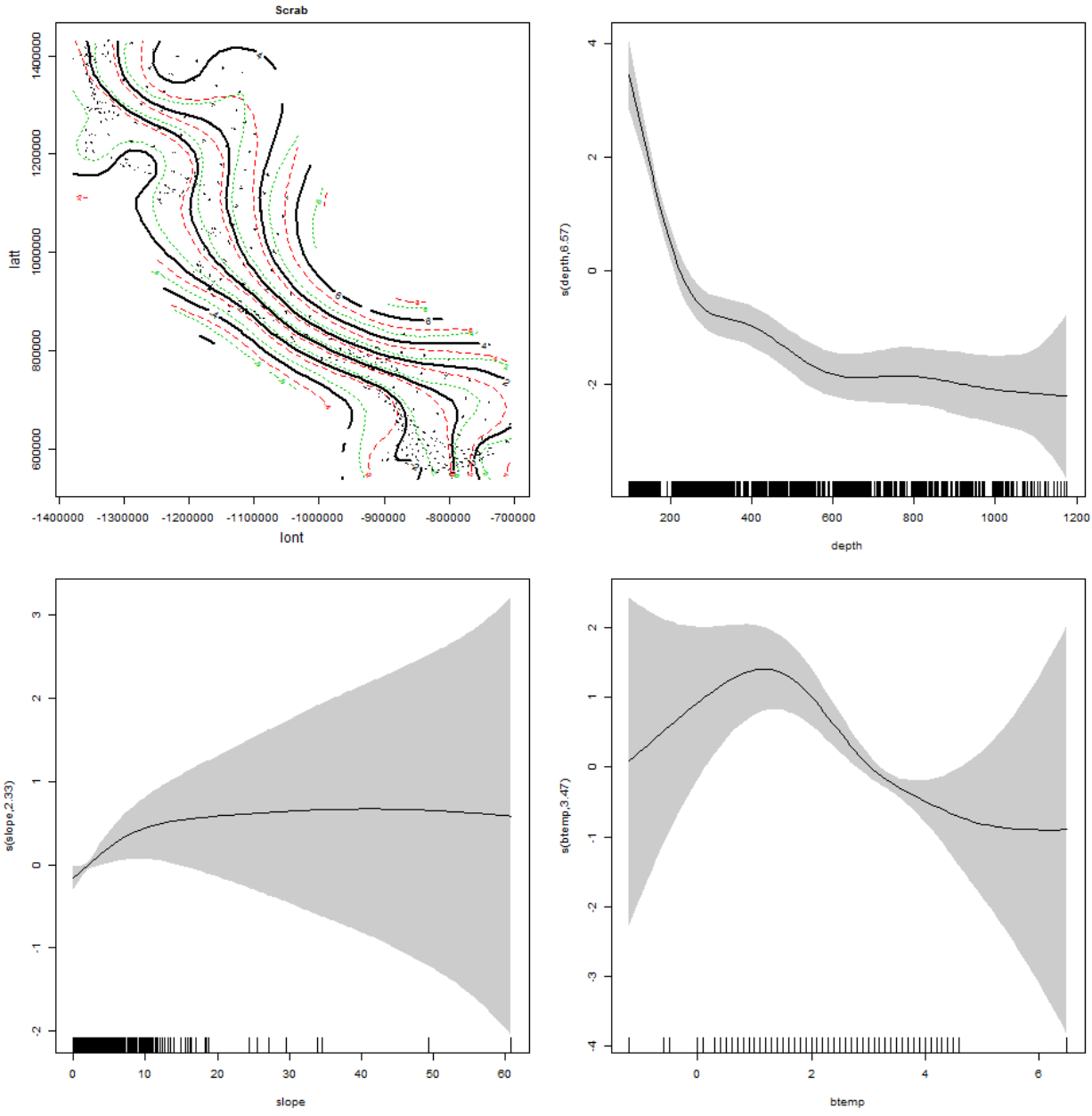


1545

1546

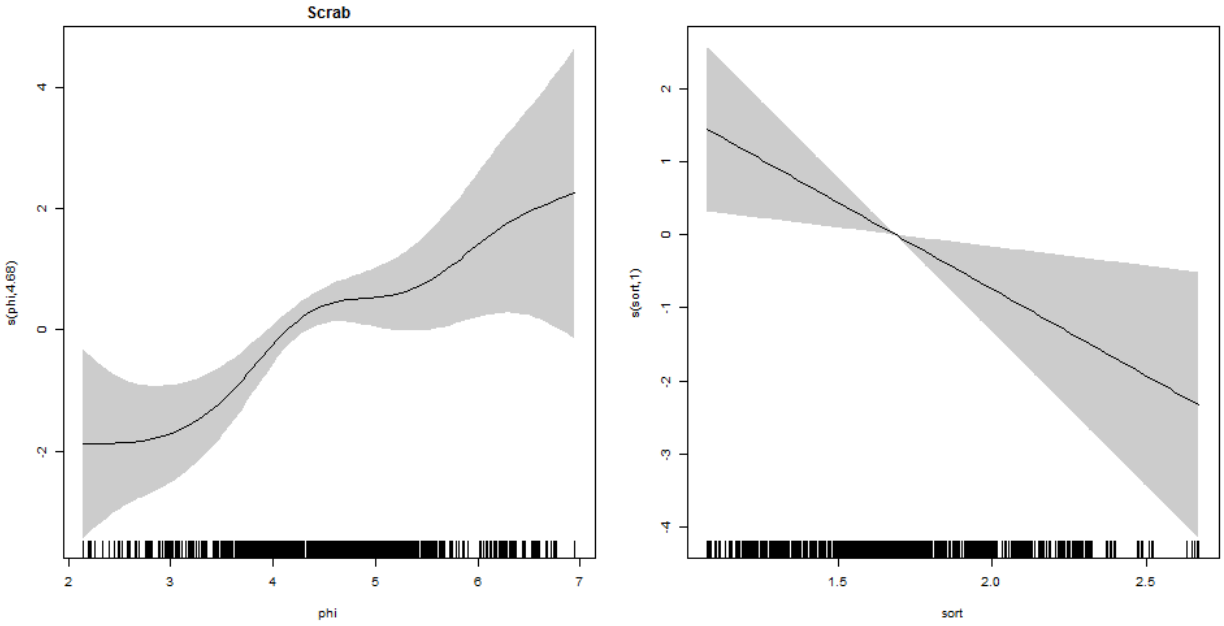


1547

1548

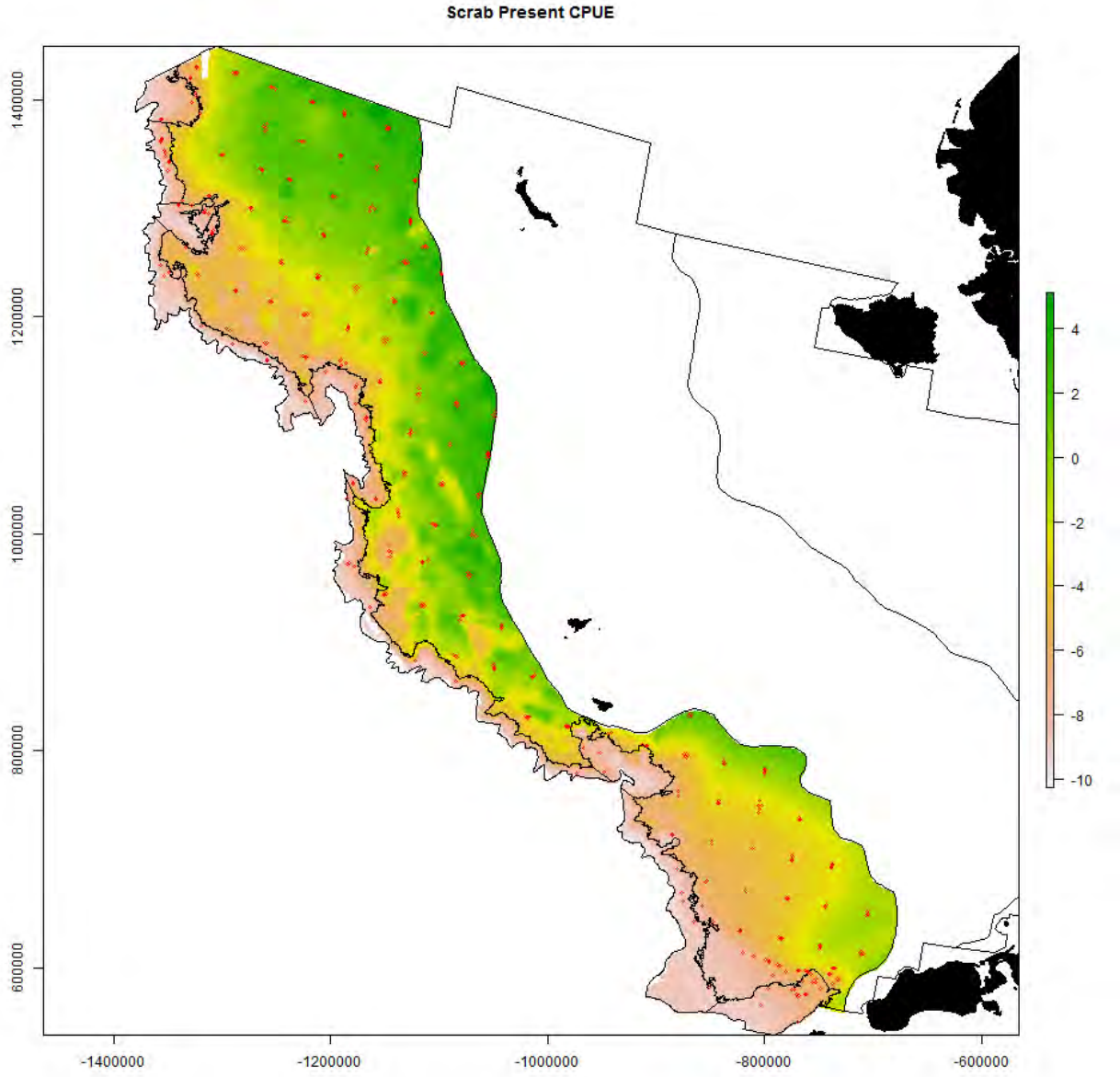
Scrab Present CPUE
1400000
1200000
1000000
800000
600000
-1400000
-1200000
-1000000
-800000
-600000
4
2
0
-2
-4
-6
-8
-10

1549

1550

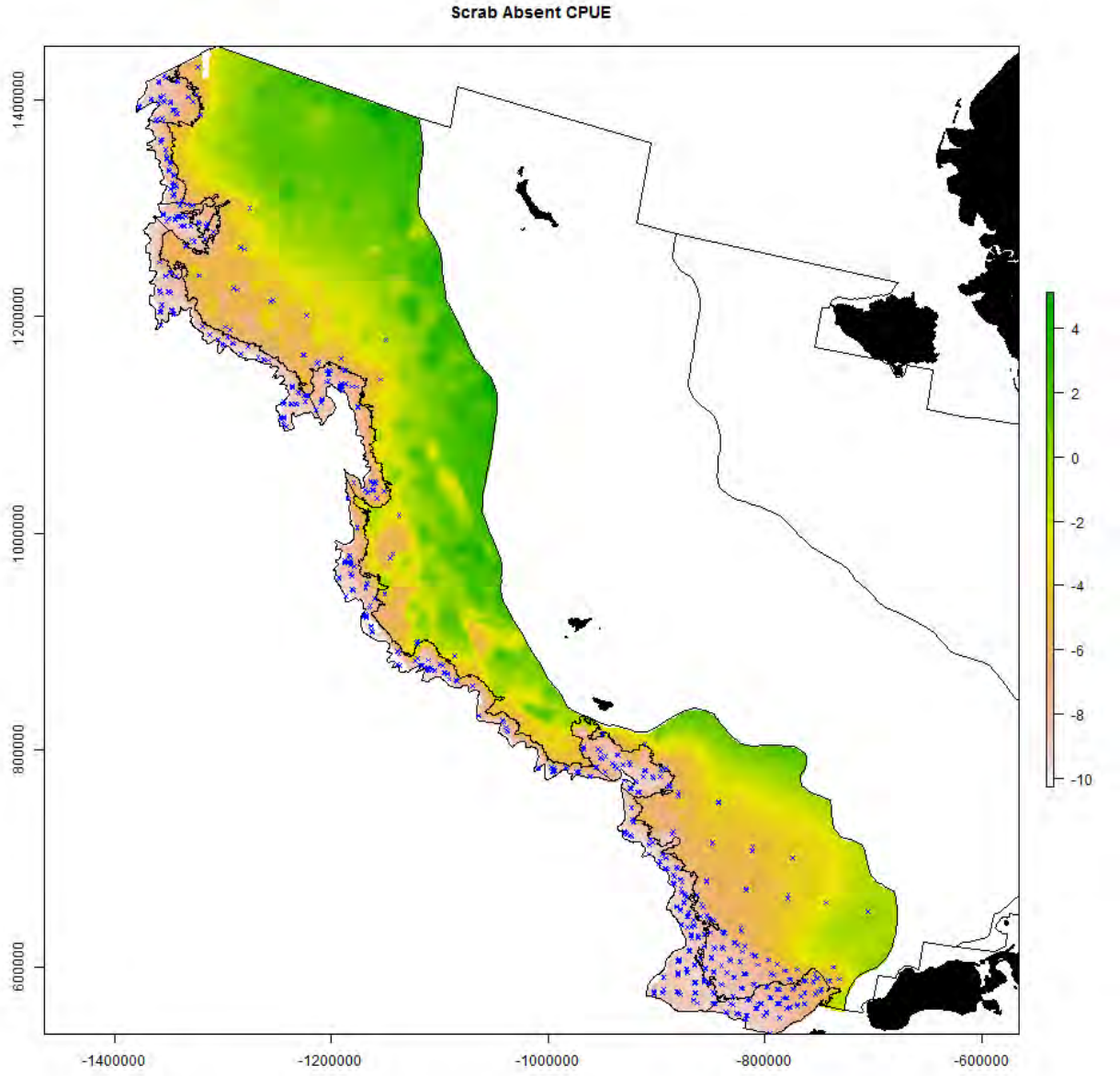
Scrab Absent CPUE
1400000
1200000
1000000
800000
600000
-1400000
-1200000
-1000000
-800000
-600000
4
2
0
-2
-4
-6
-8
-10

1551
1552

S29. Areas identified as “untrawlable” during trawl surveys of the Bering Sea slope (red polygons). In the spatial plots, the x-axis label is easting and the y-axis label is northing and the unit is meters (Alaska Albers Equal Area Conic projection with center latitude = 50° N and center longitude = 154° W).